Micro-Particles as Cellular Delivery Devices

By

Lois Meryl Alexander

Thesis for the Degree of Doctor of Philosophy

UNIVERSITY OF EDINBURGH

COLLEGE OF SCIENCE AND ENGINEERING
SCHOOL OF CHEMISTRY

February 2009

UNIVERSITY OF EDINBURGH

COLLEGE OF SCIENCE AND ENGINEERING
SCHOOL OF CHEMISTRY

Abstract for Doctor of Philosophy

Micro-particles as Cellular Delivery Devices

By Lois Meryl Alexander

Narrowly dispersed amino-functionalised polystyrene microspheres, with a range of diameters, were successfully synthesised *via* emulsion and dispersion polymerisation. Fluorescent labelling allowed cellular translocation to be assessed in a variety of cell lines and was found to be very high, but controllable, whilst exhibiting no detrimental effect on cellular viability. In order to fully determine the mode of microsphere uptake, "beadfected" melanoma (B16F10) cells were studied using both chemical and microscopic methods. Uptake was found to be wholly unreliant upon energetic processes, with microspheres located cytoplasmically and not encapsulated within endosomes, an important characteristic for delivery devices. In order to demonstrate the effective delivery of exogenous cargo mediated by microspheres, short interfering (si)-RNAs were conjugated to beads and investigated for the gene silencing of enhanced green fluorescent protein (EGFP) in cervical cancer (HeLa) and embryonic (E14) stem cells. EGFP knockdown was found to be highly efficient after 48 – 72 hours. Dual-functionalised microspheres displaying a fluorophore (Cy5) and siRNA allowed only those cells beadfected with the delivery vehicle (and thus containing siRNA) to be assessed for EGFP expression, yielding an accurate assessment of microsphere-mediated gene silencing. In addition, by manipulation of the microsphere preparation conditions, micro-doughnuts and paramagnetic microspheres were produced and their cellular uptake assessed. Paramagnetic microspheres were found to enter cells efficiently and were subsequently used to bias the movement of beadfected cells in response to an externally applied magnet, while micro-doughnuts were found to exhibit cell selective properties and were noted to traffic specifically to the liver *in vivo.*

Table of Contents

Declaration of Authorship

I, Lois Alexander, declare that the thesis entitled 'Micro-Particles as Cellular Delivery Devices' and the work presented in it are my own work.

I confirm that:

- This work was done wholly while in the candidature for a research degree under the supervision of Prof. Mark Bradley at the University of Edinburgh;
- Where I have consulted the published work of others, this is always clearly attributed;
- I have acknowledged all main sources of help;
- Where the thesis is based on work done by myself jointly with others, I have made clear exactly what was done by others and what I have contributed myself;
- Parts of this work (see rear of thesis) have been published as:

L. Alexander, R. Sanchez-Martin, M. Bradley, *Bioconj. Chem.,* **2009,** *20*, 422 – 426: Knocking (anti)-sense into cells – The microsphere approach to gene silencing.

L. Alexander, K. Dhaliwal, J. Simpson, M. Bradley, *Chem. Commun.,* **2008,** *30,* 3507 – 3509: Dunking doughnuts into cells – Selective cellular translocation and *in vivo* analysis of polymeric micro-doughnuts.

R. Sanchez-Martin, L. Alexander, M. Bradley, *Ann. N. Y. Acad. Sci.,* **2008,** *1130,* 207 – 217: Multifunctionalized biocompatible microspheres for sensing.

M. Bradley, L. Alexander, R.M. Sanchez-Martin, *J. Fluoresc.,* **2008,** *18,* 733 – 739: Cellular uptake of fluorescent labelled biotin-streptavidin microspheres.

M. Bradley, L. Alexander, K. Duncan, M. Chennaoui, A.C. Jones, R. Sanchez-Martin, *Bioorg. Med. Chem. Lett.,* **2007,** *18,* 313 – 317: pH sensing in living cells using fluorescent microspheres.

Signed:_____

Date:_____

Acknowledgements

Firstly, I would like to thank my supervisor, Professor Mark Bradley, for not only the chance to do a PhD in his group, but also for his continued and steady support over the past 3 – 4 years and for always sparing time to speak to me no matter how busy he was.

A massive thank you goes out to Dr. Rosario Sánchez-Martín for teaching me everything that I know about microspheres and helping me to mould my PhD research. I also thank her for her unconditional support as a friend and for having the same love of chocolate and Sex and The City! I also thank Dr. JuanJo Díaz-Mochón and Dr. Asier Unciti-Broceta for always being there when I needed someone to talk to and offering invaluable advice.

Thank you to all members of the Bradley group (past and present) for providing a fun place to work and for all the great times over the years. In particular, a massive thank you to Adam for the KB chats, for being a true friend and for always making me laugh no matter what. Thank you also to JuanMa for being a great friend and project mate and not minding that I was always borrowing his things! Thank you to my collaborators and the 'Microsphere Consortium'. In particular, I have to say a massive thank you to Dr. Anestis Tsakiridis for always taking the time to chat with me and for giving me invaluable advice and help (and for not minding that I was always stealing his stem cells). A big thank you also to Dr. Josh Brickman who offered the sort of constructive criticism that really helped me develop during my PhD (even if I didn't always appreciate it). I also have to thank Dr. Kev Dhaliwal for being the enthusiasm behind parts of this PhD and for staying optimistic that we would make it back to Europe during the infamous San Diego trip!

A special (but insufficient) thank you goes out to Salvo, for bringing me through the dark days and for all his love, support and continuity during this PhD.

Finally, the biggest thank you goes out to my family (mum, dad, Zoë, Toni, Jason and, most recently, Sophie Bo) for their steadfast support, proof-reading, patience and love that has made it possible for me to get through this PhD with my sanity (mostly) intact!

Abbreviations

Ahx	Aminohexanoic acid
AIBN	Azobisisobutyronitrile
ATP	Adenosine triphosphate
BODIPY	Boron-dipyrromethene
BSA	Bovine serum albumin
C.V	Coefficient of variation
CPP	Cell penetrating peptide
d	Doublet (NMR assignment)
dd	Double Doublet (NMR assignment)
Dde	*N* -(1-(4,4-dimethyl-2,6-dioxocyclohex-1-ylidene)ethyl)
DIC	*N*, *N*-Diisopropylcarbodiimide
DIPEA	Diisopropylethylamine
DMA	Dimethylamiloride
DME	Dimethoxyethane
DMEM	Dulbecco's modified eagle medium
DMF	*N*, *N*-Dimethylformamide
DMSO	Dimethylsulfoxide
DNA	Deoxyribonucleic acid
DOPE	1,2-Dioleoyl-*sn*-glycero-3-phosphoethanolamine
DTT	Dithiothreitol
DVB	Divinylbenzene
EDAC	*N*-(3-Dimethylaminopropyl)-3-ethylcarbodiimide hydrochloride
EDTA	Ethylenedinitrilotetraacetic acid
EDX	Energy dispersive X-ray
EGFP	Enhanced green fluorescent protein
EI	Electron Impact (mass spectrometry)
ES	Electrospray (mass spectrometry)
ES	Embryonic stem cells
FACS	Fluorescence activated cell sorting
FAM	5(6)-Carboxyfluorescein
FBS	Foetal bovine serum
FM4-64	*N*-(3-triethylammoniumpropyl)-4-(6-(4-(diethylamino)phenyl)hexatrienyl)pyridinium dibromide
Fmoc	9*H*-fluoren-9-ylmethoxycarbonyl
FRET	Fluorescence resonance energy transfer
GFP	Green fluorescent protein
GMEM	Glasgow's modified eagle medium
HBSS	Hank's balanced saline solution
HOBt	1-Hydroxybenzotriazole

Hoechst 33342	2'-(4-Ethoxyphenyl)-5-(4-methyl-1-piperazinyl)-2,5'-bi-1*H*-benzimidazole trihydrochloride
HPLC	High pressure liquid chromatography
IgG	Immunoglobulin G
Indo-1	2-[4-(bis(carboxymethyl)amino)-3-[2-[2-(bis(carboxymethyl)amino)-5-methylphenoxy]ethoxy]phenyl]-1H-indole-6-carboxylic acid
IPA	Isopropyl alcohol
IR	Infra-Red
LacCer	Lactosylceramide (*N*-(4,4-difluoro-5,7-dimethyl-4-bora-3a,4a-diaza-*s*-indacene-3-pentanoyl)sphingosyl 1-β-D-lactoside)
LIF	Leukaemia inhibitory factor
m	Multiplet (NMR assignment)
m/z	Mass/charge ratio (mass spectrometry)
MES	2-(*N*-morpholino)ethanesulfonic acid
MNT	Magnetic nanotube
Mp	Melting point
MRI	Magnetic resonance imaging
mRNA	Messenger Ribonucleic acid
MTT	3-(4,5-dimethylthiazol-2-yl)-2,5-diphenyltetrazolium bromide
mβCD	*m*-β-cyclodextrin
NMR	Nuclear magnetic resonance
PAM	Pulminary alveolar macrophages
PBS	Phosphate buffered saline
PEG	Polyethyleneglycol
PI	Propidium iodide
PyBOP	Benzotriazole-1-yloxytrispyrrolidinophosphonium hexafluorophosphate
Rf	Retention factor
RISC	Ribonucleic acid induced silencing complex
RNA	Ribonucleic acid
RNAi	Ribonucleic acid interference
RPMI-1640	Roswell park memorial institute medium
RT	Retention time
R-T	Real-Time
s	Singlet (NMR assignment)
S.D	Standard deviation
S50D	Supelco Discovery
sc	Solid content of suspension
SEM	Scanning electron microscopy
siRNA	Short interfering ribonucleic acid
t	Triplet (NMR assignment)

TAMRA	5-carboxytetramethylrhodamine
TB	Trypan blue
TFA	Trifluoroacetic acid
THF	Tetrahydrofuran
TLC	Thin layer chromatography
UV	Ultraviolet
V-50	2,2'-Azobis-2-methyl propionamide
VBAH	Vinylbenzylamine hydrochloride

Chapter 1: *Introduction*

1.1. The Importance of the Cellular Membrane

The cellular membrane poses a formidable barrier to the intracellular flux of compounds circulating extracellularly and creates an additional complexity in the world of drug design or cellular investigation. The reason for this is due to the selective permeability of the membrane towards compounds, based mainly on ionic charge and hydrophobicity.[1] A typical eukaryotic cell membrane is composed of a lipid bilayer made up of phospholipids, which spontaneously arrange themselves with the polar (phospho) head-group directed towards the exterior and interior aqueous regions of the cell, sandwiching the hydrophobic carbon chains in between.[2] However, the cellular membrane is much more complicated than just a simple bilayer. Dispersed throughout the membrane are various proteins, channels, lipids and carbohydrates (**Figure 1.1**), allowing numerous cellular functions to occur, including cell signalling, adhesion and transport.

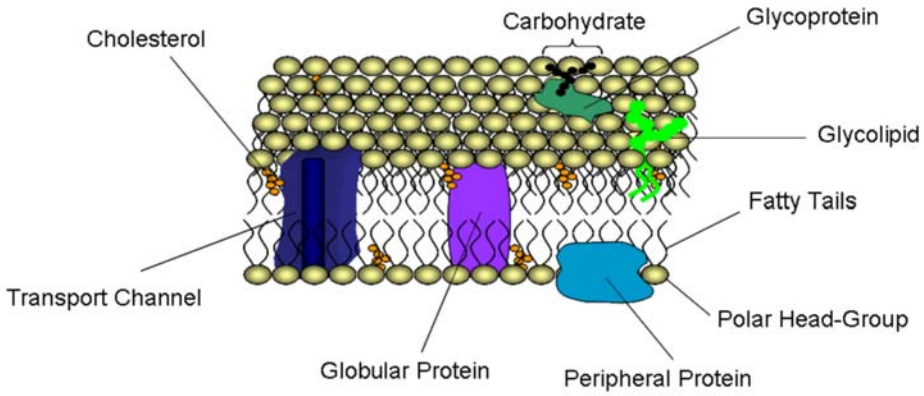

Figure 1.1. The Lipid Bilayer. Pictorial representation of the lipid bilayer, comprising phospho-lipids, proteins, transport channels, cholesterol, carbohydrate chains and glycolipids.

1.2. Cellular Uptake Pathways

1.2.1. Passive Diffusion

For compounds to freely diffuse across the lipid bilayer they should be non-polar or uncharged so as not to interact with the phospho head-groups and to facilitate translocation across the hydrophobic fatty region.[3] A passive diffusive mechanism is not reliant on an energy source and may still occur at low temperatures (**Figure 1.2**). However, due to the strict selective permeability of the membrane many entities are not able to cross passively and require alternative mechanisms. Amino acids, ions, proteins and other bulky materials are examples of compounds which are unable to cross the bilayer in a diffusive manner and rely on ion transport channels or active pathways, such as endocytosis.

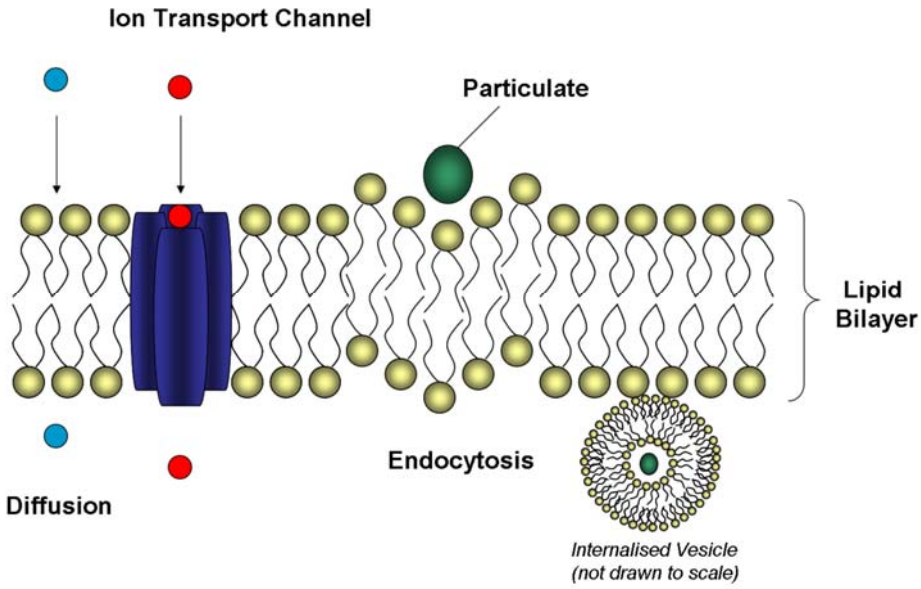

Figure 1.2. Cellular Uptake. Some of the main cellular uptake pathways, including passive diffusion, ion transport channels and endocytosis (not drawn to scale).

1.2.2. Ion Channels

Ion channels are typically voltage or ligand-gated pores in the membrane that allow solutes to travel across their electrochemical gradient (**Figure 1.2**).[4] The 'gate' may be operated by chemical or electrical signals from the cell or by the binding/dissociation of a specific ligand.[5,6] Although this mechanism of cellular

transport is important to ion flux, it is not applicable to many larger macromolecules (e.g. proteins) and these constructs require an alternative uptake pathway.

1.2.3. Endocytosis

Endocytosis is a process by which the material to be internalised is captured within a portion of the cellular membrane that encapsulates the cargo to form a vesicle. Once internalised, the vesicle pinches off internally from the intracellular membrane (**Figure 1.2**). The term 'endocytosis' is a general concept that encompasses several biologically distinct pathways. In fact, it can be broken down into three sub-mechanisms: phagocytosis,[7] pinocytosis[8] and receptor mediated endocytosis.[9]

Phagocytosis is an operation usually seen only in specialist cells known, broadly, as phagocytes. This process involves non-specific endosome formation, where the cell effectively 'eats' the particulate. ***Pinocytosis*** is similar to phagocytosis in as much as it is non-specific vesicular formation and is typically observed in professional cells. However, the vesicles formed are very small and are typically filled with extracellular fluid and, hence, it is sometimes referred to as 'cell drinking'. ***Receptor mediated endocytosis*** applies to the endocytic pathways which rely on the formation of specialist vesicles, for example those coated with a specific protein, and tends to be much faster than either phago- or pinocytosis. These include clathrin-mediated endocytosis[10] and caveolae-mediated endocytosis.[11] Clathrin mediated endocytosis relies on coating of the pits with the protein, clathrin, which is recruited by adapter proteins (e.g. AP2) to the membrane. Clathrin stabilizes deformation of the membrane to allow vesicle budding. As the endosome invaginates, dynamin (a GTPase) polymerises across the top to pinch off the endosome from the membrane allowing it to become internalised (**Figure 1.3**).[12] An example of a construct internalised by this mechanism is the blood plasma protein, transferrin.[13] In the case of caveolae mediated endocytosis, small flask shaped intrusions into the cell membrane form rich in caveolin, which is thought to aid local membrane deformation (**Figure 1.3**), eventually resulting in the formation of a vesicle, which becomes internalised.[14] Lactosylceramide, an important constituent of the plasma membrane, is an example of a compound internalised by caveolae mediated endocytosis.[15]

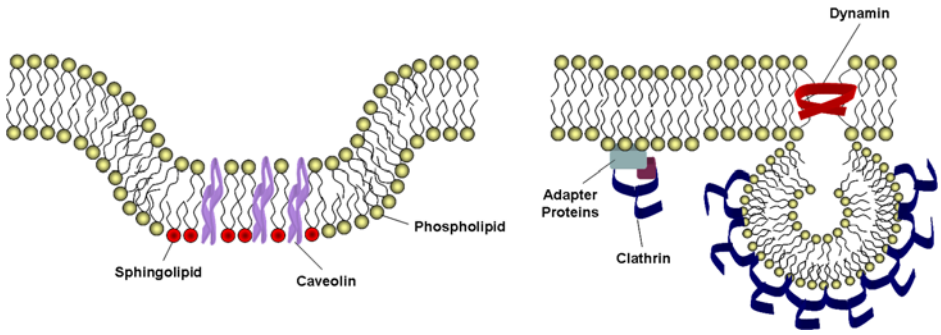

Figure 1.3. Receptor-Mediated Endocytosis. *Left:* Caveolae vesicles rich in caveolin; *Right:* Clathrin mediated vesicle formation (*internalised vesicle is not drawn to scale*).

Common to most forms of endocytosis is energy expenditure and a consequent reliance on an energy source, such as adenosine triphosphate (ATP), which releases energy when it is hydrolysed to adenosine diphosphate (ADP) and adenosine monophosphate (AMP).

It should be noted that particulates internalised by endocytosis still remain 'separated' from the cell's internal environment due to the barrier presented by the endosomal membrane. In addition, endosomes and latterly formed lysosomes have aggressive degradation machinery (in particular, acid hydrolases),[16] which can damage biological cargo and hence endosomal escape is desired when delivering material intracellularly if cytoplasmic localisation is required for function.

1.3. Delivery Methods

Since some exogenous material is unable to enter cells by any of the aforementioned pathways, several methods have been developed for delivering these materials intracellularly. Largely, these methods can be separated into three groups; physical (or mechanical) methods, chemical methods and carrier systems.

1.3.1. Physical and Mechanical Methods

Physical and mechanical methods include electroporation,[17] photoporation[18] and micro-injection[19] and have been used to deliver anything from small drug molecules to DNA.[20, 21] In general, these methods involve making a transient hole in the membrane to facilitate the delivery of compounds which will not cross the membrane

alone. Following permeation, the cell membrane can repair itself; however, physical processes for cellular delivery can be laborious and have a low success rate, meaning it is difficult to translate to high-throughput approaches.[22]

1.3.2. Chemical Methods

Chemical methods work on a similar concept using chemical agents, for example solvents or streptolysin-O,[23] to transiently permeate the membrane. Such methods have been used to deliver proteins intracellularly, but can suffer from cytotoxicity issues.[24] As such, less aggressive techniques have been developed in the form of carrier devices.

1.3.3. Carrier Systems

A diverse range of delivery vessels upon which a cargo can be attached or encapsulated, have been developed and studied immensely. For example, ***Cell Penetrating Peptides*** (CPPs)[25] such as HIV TAT-derived peptides, have been used to deliver an assorted range of cargo from small molecules to bulky proteins.[26] CPPs based on TAT typically have a cationic cluster of 6 arginine residues and 2 lysines in a sequence of 9-10 amino acids, a notable example being GRKKRRQRRR.[27] However, concerns have been raised over the toxicity and metabolic stability of some cell penetrating peptides, which may result in some limitation in their use.[28, 29]

Cationic lipids[30] have been used mostly in the delivery of RNA and DNA[31, 32] and have been commercialised under various trade names including HiPerFect® and Lipofectamine®. They are typically composed of long carbon chain 'tails' with cationic head-groups which, in an aqueous environment, spontaneously organise themselves into DNA containing micelles or lipoplexes in a system that mimics the cell membrane itself. They have been used to efficiently transfect several cell lines, including primary cells.[33] However, they can be toxic and special care must be taken during use to limit undesired effects.[34]

Since the populisation of ***carbon nanotubes*** in 1991,[35] much work has focused on their intracellular use.[36] Thus, they have been used to deliver cell impermeable dyes and siRNA to several cell lines, including primary cells.[37, 38] Although effective, there are several drawbacks associated with their use.

Foremostly, there have been serious concerns over their *in vivo* toxicity, especially so in the case of the larger nanotubes and much confusion has surrounded their biocompatibility.[39] In addition, careful consideration must be made of the functionalisation expressed on the nanotube to facilitate a device which is aqueously soluble with enhanced biocompatibility.[40]

Thus, there is a great need for a delivery vehicle that is stable, non-toxic and easily prepared and functionalised as well as being able to enter a broad range of cells with ease.

1.4. Microspheres

Microspheres have been utilised in research for many years and have wide ranging applications in the biomedical and chemical fields as well as in industry. Their synthesis has been well studied to produce a range of sizes and compositions. For example, in 1986 Tseng *et al.* reported the synthesis of highly uniform polymer particles by a technique known as dispersion polymerisation.[41] Here, they dispersed styrene in ethanol with azo-type initiators and a polymeric stabiliser (polyvinylpyrrolidone, PVP) to produce mono-dispersed spherical latex products in the size range of 1 – 10 μm in diameter. Using a co-polymerisation approach, they were additionally able to easily incorporate a range of functionalisations, including amines, carboxyls and silanes. Following from this, in 1994, Delair *et al.* obtained 200 – 1000 nm latex particles with a highly uniform spherical morphology using emulsion polymerisation.[42] Here styrene was co-polymerised with divinylbenzene, a cross-linking agent which grafts growing polystyrene chains together yielding a final product that was robust and stable (**Figure 1.4**).[43]

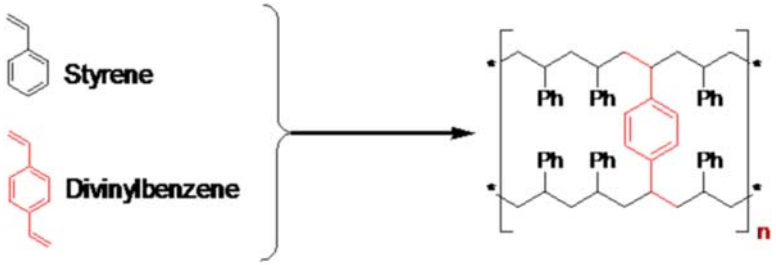

Figure 1.4. DVB Cross-Linking. Co-polymerisation of styrene with divinylbenzene, yielding highly cross-linked stable particles.

Due to the spherical nature of the latex products, they have been termed microspheres and have since been routinely generated using a range of methods. The more common amongst these are suspension, dispersion and emulsion polymerisation. Suspension polymerisation typically produces larger sized microspheres approximately 50 to 500 μm in diameter.[44] This technique involves dispersion of the monomer with a stabiliser in an aqueous solution (for example, water) and the size of the product may be altered by changing the stirring speed. Dispersion polymerisation[45] is a simplistic one-pot method designed to produce 0.5 to 10 μm microspheres and relies on a homogeneous mixture of the monomer, initiator and stabiliser in an organic phase from which the insoluble polymer product can precipitate. Emulsion polymerisation[42] is used to form smaller sized products, approximately $10 – 10^4$ nm in diameter. Here, polymerisation of the monomer occurs within micelles dispersed in an aqueous medium.

Microspheres have previously been used in a diverse range of applications including flow cytometry, markers of phagocytosis and DNA arrays.[46, 47, 48] However, their use as delivery vehicles of therapeutic or investigative cargo in non-phagocytic cells has not been widely studied.

1.5. Aims

It was the aim of this thesis to further develop the construction of microspheres and investigate the methods of their formation by polymerisation. Accordingly, attempts were made to manipulate the microspheres, forming 'magnetic' constructs, which could in-turn be developed as tools for intracellular delivery allowing the biased movement of cells by an externally applied magnetic field.

In turn, it was of interest to explore polystyrene microspheres as vehicles for intracellular delivery to a selection of cell lines and to establish whether microspheres exerted any detrimental cytotoxicity on cells, which could have negative implications on their use as delivery agents. Of particular importance was investigation of the mechanism by which microspheres enter non-phagocytic cells and, in particular, if their internalisation renders them captive within acidic

organelles (e.g. endosomes) or if they are localised cytoplasmically. Non-endosomal capture means that the translation of the delivery device from *in vitro* to *in vivo* use can be simplified as they do not require the application of endosomal disrupting agents and is additionally important to the delivery of many constructs (e.g. enzymes and proteins).[36]

Furthermore, following analysis of microsphere-cell interactions, it was an essential aim to investigate microspheres as delivery agents of a biologically relevant cargo. To this affect, the delivery of siRNA was investigated since it is presently a "hot" area of research and requires cytoplasmic localisation for function and thus will help build on the studies that have previously been performed microspheres.

Chapter 2: *Microspheres as Cellular Delivery Devices*

2.1. Introduction

The appeal of microspheres lies largely in the diverse range of applications these particles have. They are not only used as vehicles for intracellular delivery but also for applications *ex vitro,* for example in investigation of DNA hybridisation (where DNA is coupled to microspheres and anchored to surfaces exhibiting a complementary sequence)[48] or as fluorescent probes in flow cytometry.[47] Furthermore, they are cheap, easy to produce and functionalise, have a long shelf-life and they can be produced from a diverse range of materials and in a multitude of sizes. Their applications in industry range from paints[49] and adhesives[50] to water treatment[51] and, more recently, cosmetics.[52] They are also widely used in many areas of research, for example in catalysis[53] and immunodiagnostics.[54] In terms of intracellular delivery, biodegradable microspheres have been studied more extensively than their bio-stable counterparts,[55] largely due to the applications of biodegradable microspheres in drug delivery, where the delivery device can degrade resulting in a release of an encapsulated drug.[56]

2.1.1. Biodegradable Microspheres

Microspheres can be tailored to biodegrade by the introduction of monomers that will break down under physiological conditions. Examples are lactic acid (giving poly(lactic acid) microspheres) and glycolic acid (giving poly(glycolic acid) microspheres).

2.1.1.2. Preparation

Biodegradable microspheres can be prepared *via* the polymerisation of monomers using suspension, dispersion or emulsion polymerisation to achieve particles of the desired size.[57, 58, 59] However, due to the availability of linear biodegradable polymers, it is some what more common for biodegradable microspheres to be prepared directly from these and there are several methods by which they may be

made. Amongst these are solvent evaporation methods (sometimes called the double emulsion technique) and spray-drying. Solvent evaporation forms microspheres *via* the evaporation of an organic solvent from the linear polymer (oil) droplets and is one of the more extensively studied and used procedures.[60] Firstly, the polymer is added to an organic phase (typically dichloromethane) or melted at high temperatures. Water is added to produce the primary emulsion and the mixture is stirred to produce polymer droplets. This is then added to a larger volume of aqueous medium which contains a stabiliser (for example, polyvinylpyrrolidone) and the mixture is stirred vigorously in order to produce a multiple emulsion. The organic solvent is then evaporated allowing the polymer to harden and precipitate producing microspheres. The microsphere size and porosity can be controlled by alteration of various factors including polymer concentration, temperature and stirring rate with particles from 1 to 100 μm being produced.[61] The attraction of this method is that drug molecules can be added into water during formation of the primary emulsion and become encapsulated within the polymer construct as it hardens, where it may consequently be released as the polymer degrades.[62]

The spray drying technique takes a polymer solution and sprays it through a nozzle producing a fine mist, which as it dries forms microspheres.[63] Plasticisers (e.g. citric acid) are often added to the polymer solution to promote the formation of smooth-surfaced microspheres. Several factors can affect the microsphere diameter, which lies typically in the range of 1 to 10 μm, including the rate of spraying, nozzle size and the drying temperature.

Regardless of method, it is important to choose the appropriate conditions for preparing biodegradable microspheres since the polymer molecular weight, diameter and morphology are all important factors for biodegradability.

2.1.2. Bio-Stable Microspheres

The sensitivity of bio-degradable polymers to aggressive solvents can limit the chemistry that can be performed on the beads and, in addition, they are not particularly suitable as investigative tools where it would be undesirable for the microsphere to degrade, for example as biological sensors. Thus, microspheres

prepared with stable monomers and with cross-linking may be more desirable for some applications.

2.1.2.1. Applications of Bio-Stable Microspheres

A major established application of bio-stable microspheres is the investigation of phagocytic cells by flow cytometry. Bio-stable microspheres can be easily labelled with a fluorophore, yielding a stable fluorescent construct that can allow analysis of phagocytosis by quantitative flow cytometric methods. As such, microspheres have been used to investigate the phagocytic activity of pulmonary alveolar macrophages (PAMs),[64] pinocytosis and phagocytosis in rat peritoneal macrophages[65] and activation of alveolar macrophages.[66] In addition, they have been used as sensors for measuring intracellular calcium levels using Indo-1, a calcium sensitive construct[67] and they have also been applied in the successful measure of intracellular pH utilising the pH sensitive nature of carboxyfluorescein.[68] Using this approach, intracellular pH can be measured accurately over long time periods, which is not possible using alternative methods based on fluorescein diacetate due to cell leakage.[69]

2.1.2.2. Preparation

Several approaches may be adopted to produce bio-stable microspheres and a wide range of monomers are available. Typically, suspension, dispersion and emulsion polymerisation are employed as described previously[42, 70, 71] due to the simple set-up and controllability of the microsphere size and quality by simple measures.

Suspension Polymerisation

Suspension polymerisation typically results in the production of comparatively large microspheres, in excess of approximately 50 μm in diameter, similar to the solvent evaporation method for preparing biodegradable microspheres. In this process, a monomer is dispersed in an aqueous media resulting in the production of monomer droplets. An initiator (which is soluble in the monomer) is added and polymerisation occurs within the monomer droplets resulting in the generation of large polymer

microspheres.[72] The microsphere size can be controlled by varying, for example, the stirring rate.

Suspension polymerisation has been used in the synthesis of sodium polyacrylate microspheres, which is a popular super-absorbent polymer used in nappies.[73] However, the use of suspension polymerisation to prepare microspheres for the bio-medical field and intracellular delivery is limited[74] due to the large diameters of the polymer products and their poly-dispersity. For microspheres relevant to these areas of research, alternative polymerisation methods, including dispersion and emulsion polymerisation, are generally applied.

2.2. Dispersion Polymerisation

Dispersion polymerisation is of particular appeal as it is a simple method where the reagents are mixed in one organic phase and the polymer product is allowed to precipitate from the homogeneous solution over a period of several hours. It gives high conversions and the microspheres are typically narrowly dispersed in size and easily manipulated to give a range of diameters between 0.5 and 10 μm – ideal for biological analysis.[75, 76]

Although the mechanical set-up of a dispersion polymerisation reaction is easy, the mechanism is complex and not well understood. The required monomers and initiator are dispersed in an organic phase containing a stabiliser, for example polyvinylpyrrolidone (PVP). Upon heating, a radical initiator disassociates forming radicals which react with the monomer and polymerisation begins. Initially, there is a rapid nucleation phase forming mono-dispersed nuclei swollen with monomer, short oligomers and initiator radicals.[77] Polymerisation takes place within the swelled monomer droplets since this is where the initiator is soluble. The stabiliser is thought to adsorb to the surface of the nuclei allowing precipitation as mono-dispersed primary particles, which grow by swelling with more monomer or short oligomers to produce microspheres (**Figure 2.1**).[78, 79] Many factors are capable of affecting the size and quality of the polymer product produced, such as the stabiliser molecular weight, temperature, stirring rate and monomer concentration to name but a few (**Figure 2.2**).[80, 81, 82, 83]

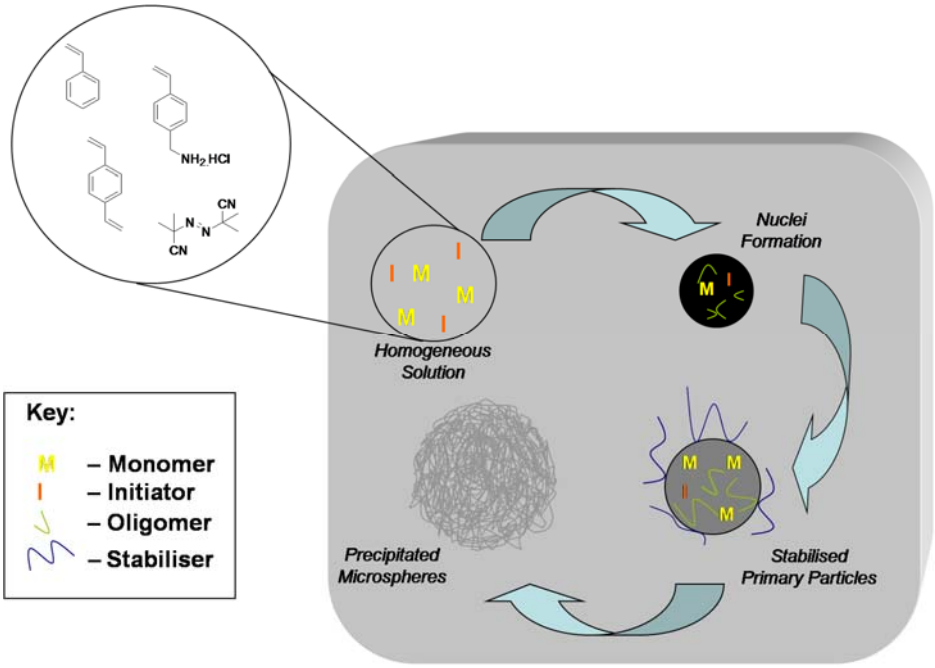

Figure 2.1. Mechanism of Dispersion Polymerisation. Nuclei result in the formation of primary particles which, when appropriately stabilised, precipitate as microspheres.

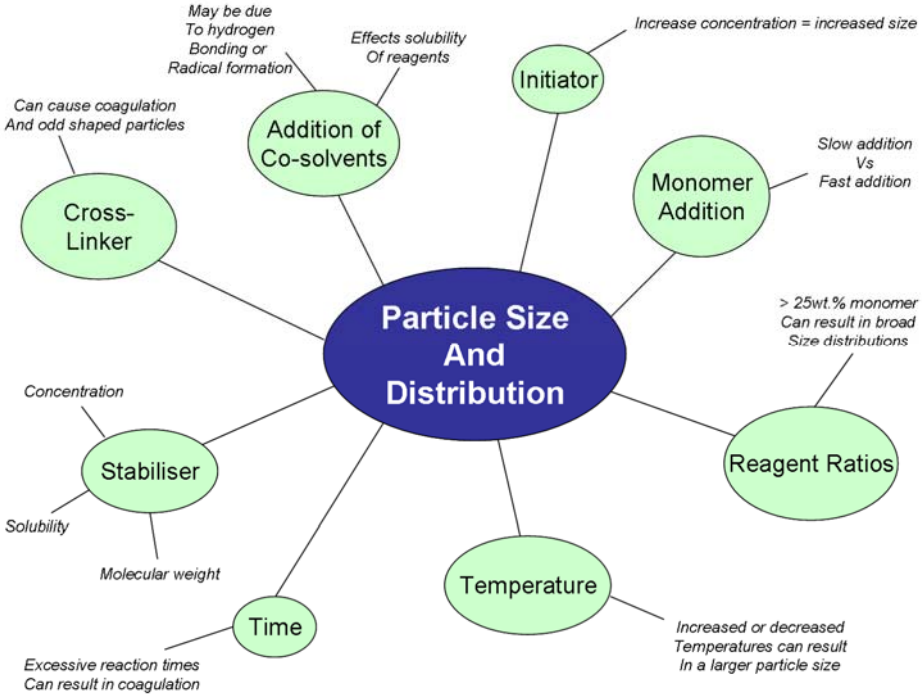

Figure 2.2. Altering the Particle Size. A selection of the many factors which can alter the size, quality and mono-dispersity of the microspheres precipitated from a dispersion polymerisation.[43, 75, 84, 85]

This adaptability makes it all-the-more attractive as it allows the production of a wide range of products with varying diameters using the same simple approach. Dispersion polymerisation was thus investigated in-depth for the production of a range of robust microspheres, for analysis of cellular delivery.

2.2.1. Stabiliser Molecular Weight

An uncomplicated method of altering microsphere size reliably is by consideration of the steric stabiliser used to aid precipitation of the polymer product from solution. Polyvinylpyrrolidone (PVP) is a widely used stabiliser and is available in a range of molecular weights from 1,300,000 to 10,000 Da. During nuclei and primary particle formation hydrophilic PVP chains may graft or adsorb onto the surface of the precipitating particles and offer stabilisation *via* steric interactions with other PVP chains (**Figure 2.3**).

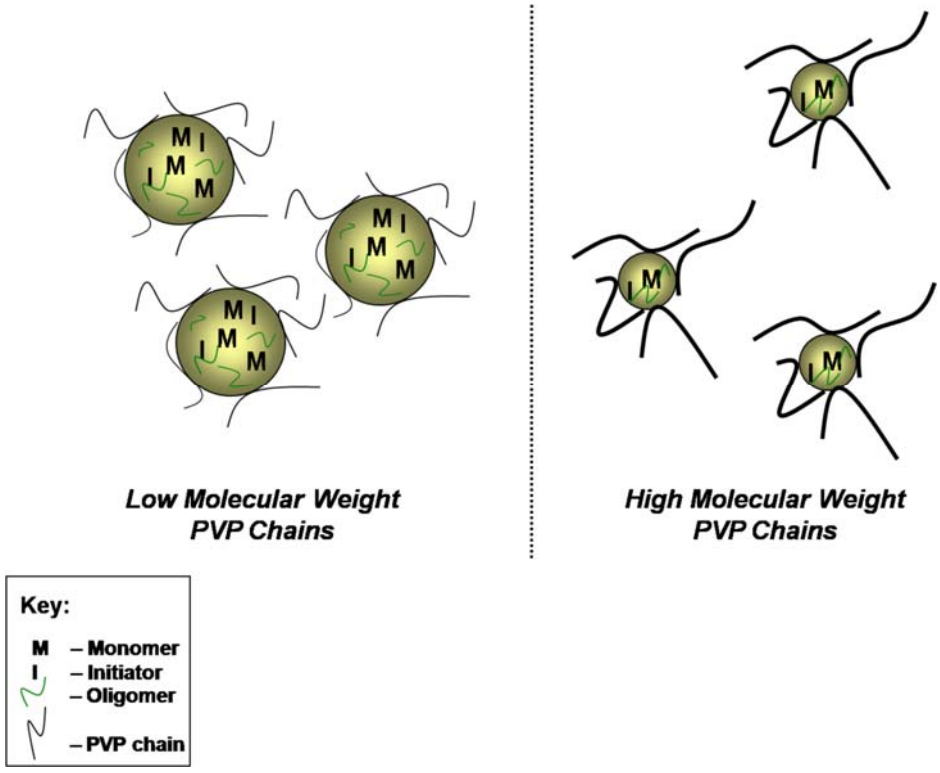

Figure 2.3. Polyvinylpyrrolidone M_w. Microsphere stabilisation by PVP with low molecular weight (e.g. 10,000 Da) and high molecular weight (e.g. 360,000 Da) chains.

Lower molecular weight chains of PVP grafted to the surface of microspheres permit the growth of larger beads as they have a lower degree of steric repulsion than larger molecular weight chains (and thus allow the microsphere to swell with monomer and

oligomer, which polymerise to form a larger sized particle).[86] However, a disadvantage of using low molecular weight chains of PVP is that the stabilisation is less efficient and agglomeration of the microspheres can be a problem.

PVP with molecular weights of 10,000, 29,000, 40,000 and 360,000 Da were used in dispersion polymerisation reactions to investigate the effect of the stabiliser molecular weight. Styrene (**2.4**) was chosen as the main monomer as it is widely available and can be readily polymerised in a free radical manner. To allow production of robust particles a cross-linking agent, *p*-divinylbenzene (DVB) (**2.5**), was used, which effectively ties the polystyrene chains together making the microspheres more stable. Functionalisation was introduced by use of vinylbenzylamine as a hydrochloride salt (VBAH) (**2.3.2**), which was prepared from vinylbenzylchloride (**2.1**) *via* the phthalimide protected analogue (**2.2**) (**Scheme 2.1**) and acidified from the free amine (**2.3.1**).[42] The monomers (styrene, DVB and VBAH) were heated in the presence of a radical initiator, azobisisobutyronitrile (AIBN), to initiate radical formation and the product was precipitated over 18 hours (**Scheme 2.2**).

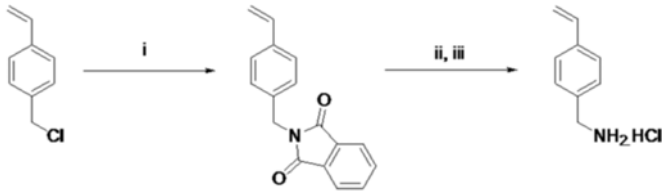

Scheme 2.1. VBAH. Preparation of *p*-vinylbenzylamine.HCl (VBAH) (**2.3.2**) from *p*-vinylbenzylchloride (**2.1**). Free amine, *p*-vinylbenzylamine, is (**2.3.1**).
(i). 1 eq. potassium phthalimide, DMF, 50 ºC, 15 hours; (ii). 2 eq. hydrazine hydrate, ethanol, reflux, 3 hours; (iii). 6N acidic isopropanol (HCl), 0 ºC.

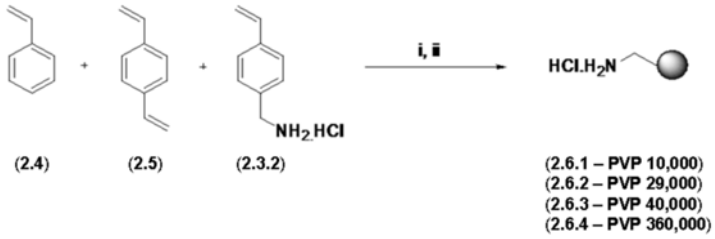

Scheme 2.2. Amino-Microspheres. Preparation of polystyrene latex microspheres (**2.6.1**), (**2.6.2**), (**2.6.3**) and (**2.6.4**) with DVB cross-linking expressing amino functionality prepared *via* dispersion polymerisation with PVP 10,000 – 360,000 Da.

(i). 0.01 eq. AIBN, N_2; (ii). 0.04 eq. PVP (M_w: 10,000 – 360,000 Da), ethanol, 70 ºC, 18 hours.

After precipitation, the microsphere suspension was cooled and washed sequentially (methanol and water) to remove excess reagents.[87] The microsphere diameter was assessed using a technique known as laser diffractometry, which also goes by the names static laser light scattering, Fraunhofer diffraction or Mie scattering.

2.2.1.1. Laser Diffractometry

In laser diffractometry, when light hits a particle a number of events can occur including diffraction, refraction, reflection or absorption. How the light is scattered gives information about the size of the particle that the light interacted with and allows determination of a particle size distribution. If the particle size is larger than the wavelength of the incident of light, then the light will preferentially scatter by diffraction and a laser diffractometer can collect information on the size distribution by detecting light scattered mainly in the forward direction of the sample (**Figure 2.4**). However, if the particle is smaller in diameter than the wavelength of the incident of light then refraction and absorption are the predominant interactions and information on the size of the particle is gathered from light scattered mainly to the sides and backwards of the particle (**Figure 2.4**). A mathematical algorithm allows deduction of a size distribution for the cloud of particles analysed.

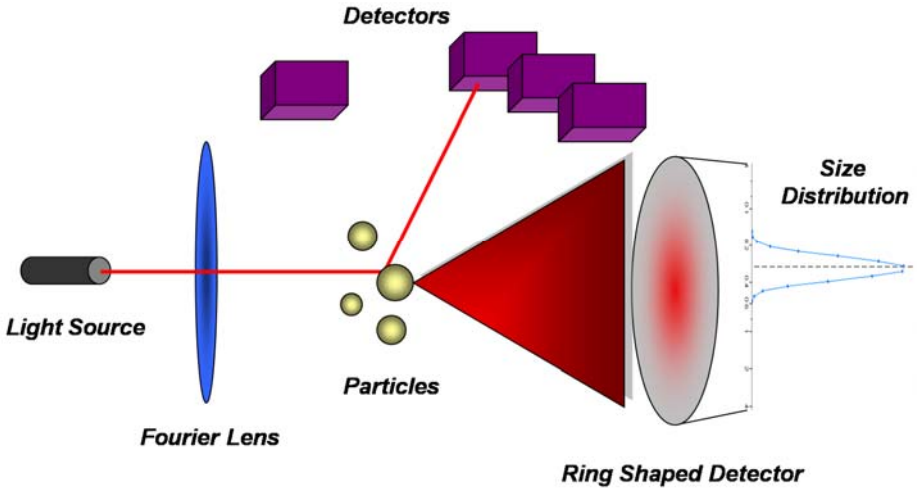

Figure 2.4. Laser Diffractometry. A light source is focused using a Fourier lens and is diffracted, refracted, reflected or absorbed by particles and the information collected from this gives rise to a size distribution profile.

2.2.1.2. Altering PVP Molecular Weight

Polymerisations using PVP with a molecular weight of 10,000 Da often yielded a low viscous suspension (meaning a limited conversion of the reagents) and agglomeration was evident. The mean particle size by laser diffractometry was found to be 3.3 µm (**2.6.1**) (**Figure 2.5b**) but the distribution was poly-dispersed with a coefficient of variation of 79%.

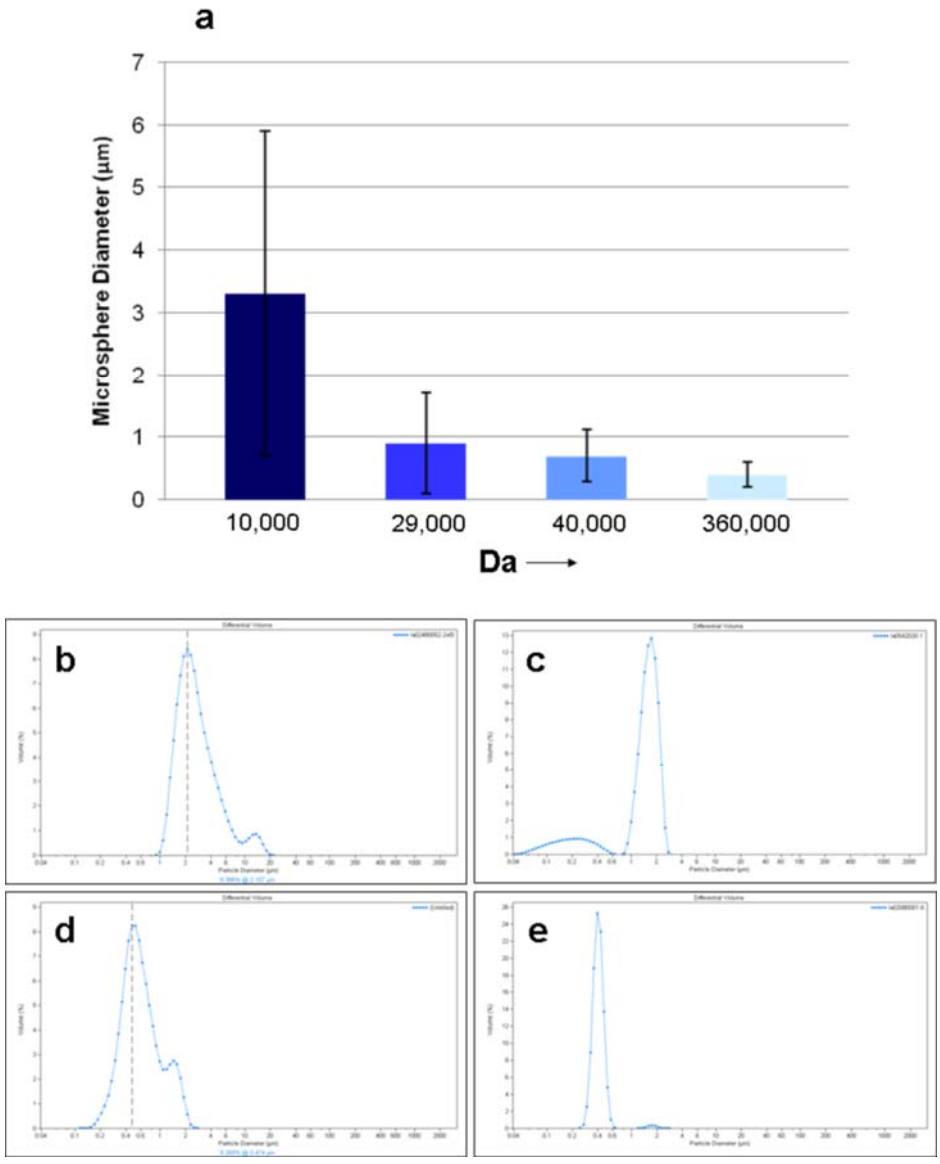

Figure 2.5. Microsphere Diameter with PVP M_w. Laser diffractometry analysis of microspheres **a.** variation of microsphere diameter with PVP molecular weight; **b.** 3.3 µm beads (PVP 10,000 Da, (**2.6.1**)**,** S.D. 2.6 µm, C.V. 79%); **c.** 1.4 µm beads (PVP 29,000 Da, (**2.6.2**)**,** S.D. 0.6 µm, C.V. 44%); **d.** 0.7 µm beads (PVP 40,000 Da, (**2.6.3**)**,** S.D. 0.41 µm, C.V. 59%); **e.** 0.4 µm beads (PVP 360,000 Da, (**2.6.4**)**,** S.D. 0.2 µm, C.V. 39%).

PVP 29,000 Da, as expected with its increased molecular weight, yielded smaller microspheres (1.4 μm) (**2.6.2**) and the suspension appeared more viscous with a good conversion of reagents (**Figure 2.5c**). PVP with a molecular weight of 40,000 Da continued the trend yielding smaller microspheres (**2.6.3**) with a mean diameter of 0.7 μm (**Figure 2.5d**). In the case of PVP 360,000 Da, the mean diameter was found to decrease further to 0.4 μm and, on account of the efficient stabilisation offered by the high molecular weight chains of PVP, little aggregation of the particles was seen and the coefficient of variation decreased to 39% (**2.6.4**) (**Figure 2.5e**). The relationship between PVP molecular weight and the mean diameter of microspheres can be represented in a graphical manner (**Figure 2.5a**), showing not only that larger molecular weights of PVP yield smaller microsphere diameters, but also indicated the narrowing of the size distribution with larger molecular weight PVP (from the error of the distribution).

The quality of the polymer product was additionally assessed by scanning electron microscopy (SEM) (**Figure 2.6**), a microscopic method that scans the surface of a material using a high energy beam of electrons.

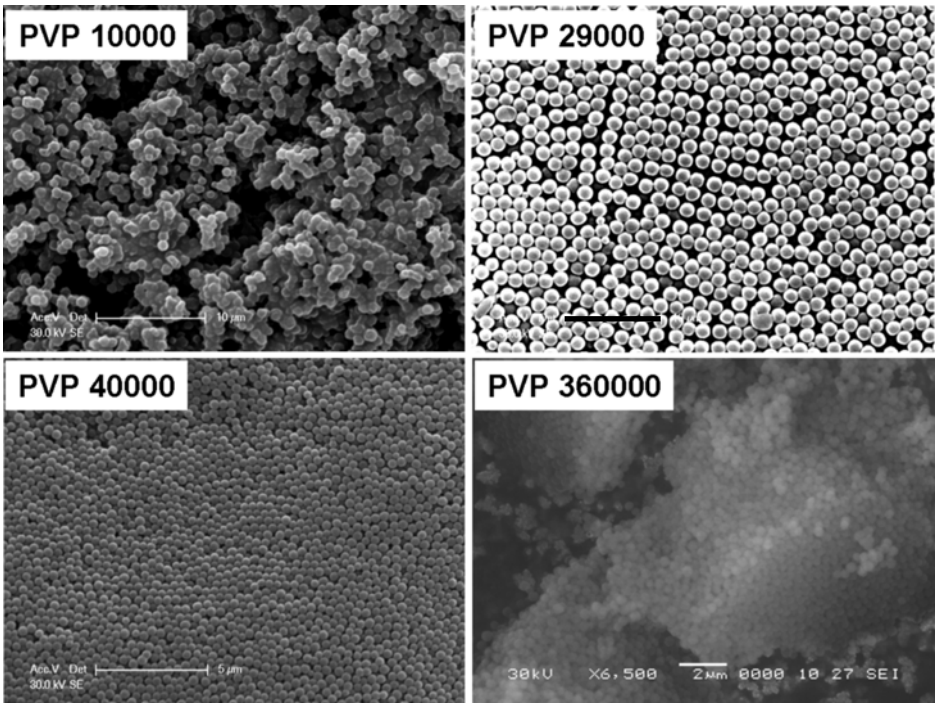

Figure 2.6. Scanning Electron Microscopy. Microspheres prepared from PVP 10,000 Da (**2.6.1**) (Scale bar is 10 μm), 29,000 Da (**2.6.2**) (Scale bar is 10 μm), 40,000 Da (**2.6.3**) (Scale bar is 5 μm) and 360,000 Da (**2.6.4**) (Scale bar is 2 μm).

Microspheres prepared with PVP 10,000 Da were heavily agglomerated, while microspheres prepared with larger molecular weight chains of PVP (≥ 29,000 Da) showed smooth surfaced, evenly sized beads, confirming the results obtained by laser diffractometry.

Many avenues can be approached to increase the efficiency of stabilisation in dispersion polymerisations to produce mono-dispersed microspheres, for example, by alteration of the solubility of PVP. This may be achieved simply and in a subtle manner by alteration of the polymerisation solvent system to increase or decrease the solubility of PVP and thus, increase or decrease effective PVP available for stabilisation.

2.2.2. Stabiliser Solubility

Polyvinylpyrrolidone (**Figure 2.7**) is a hydrophilic stabiliser and polar solvents will result in excellent solubility in solution.

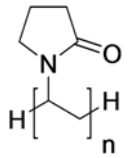

Figure 2.7. Structure of Polyvinylpyrrolidone. The value of *n* is dependent on the molecular weight of the stabiliser.

2.2.2.1. Addition of Water

The obvious choice to increase the polarity of the solvent system is by the addition of water. Thus, deionised water was added at concentrations of 0.5 – 9% to the polymerisation liquor (ethanol) using PVP with a molecular weight of 40,000 Da and the effect on the polymerisation and the product yielded was investigated. Reactions were performed on a Radley carousel to allow 12 reactions to be carried out in parallel with temperature, nitrogen flow rate and stirring speed kept uniform (**Figure 2.8**). At water contents of 0.5 – 5% little change was observed in the size distribution of the population, which was found to be broad with a coefficient of variation of approximately 70% and a mean diameter of 0.7 μm (**Table 2.1**). However, at water contents of between 6 and 8% in ethanol an interesting effect was observed. The diameter of the microspheres, (**2.7.1**), (**2.7.2**) and (**2.7.3**), decreased to 0.4 μm and the size distribution narrowed remarkably giving a coefficient of variation of

approximately 16%, indicating the microspheres were essentially mono-dispersed (**Table 2.1**).

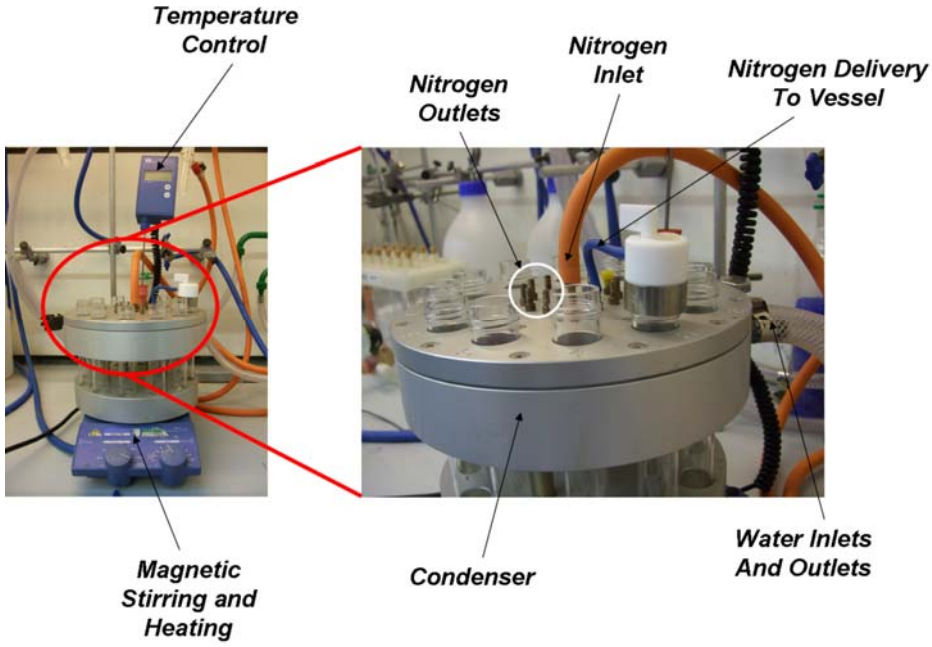

Figure 2.8. Radley Carousel. Stirring rate, temperature and gas flow are kept constant.

% Water Content Added	Mean Diameter (µm)	Coefficient of Variation (%)	Amine Loading (µmol/g)
0.5	0.64	71	22.0
1	0.64	65	14.0
2	0.66	63	16.0
3	0.8	66	11.0
4	0.63	76	15.0
5	0.61	71	16.0
6	0.38	17	28.0
7	0.52	14	29.0
8	0.39	17	16.0
9	19.4	53	23.0

Table 2.1. Addition of Water. Variation of microsphere diameter and amine loading with water content (0.5 – 9%) in ethanol. Amine loading was determined by quantitative ninhydrin analysis on 3 mg of dried microspheres. 6, 7 and 8% water generated (**2.7.1**), (**2.7.2**) and (**2.7.3**) respectively.

Using 7% water in ethanol, a mean diameter of 0.5 µm was achieved and the coefficient of variation was only 14% (**2.7.2**). Importantly, incorporation of the amino functionalised monomer was not detrimentally affected and 29 $\mu molg^{-1}$ of amine was recorded by a quantitative ninhydrin test.[88] Furthermore, (**2.7.2**) appeared

stable in aggressive solvents, such as DMF and had a smooth even surface and regular shape (**Figure 2.9**).

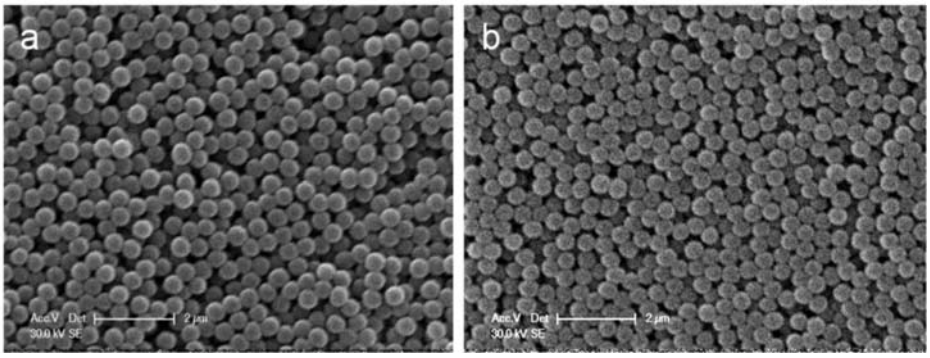

Figure 2.9. Scanning Electron Microscopy. a. 0.5 μm microspheres formed from 7% water in ethanol (**2.7.2**) (Scale bar is 2 μm); **b.** 0.5 μm microspheres formed from 7% water in ethanol and treated for 18 hours with dimethylformamide (DMF) (Scale bar is 2 μm).

Using the optimum content of 7% water (which resulted in the most narrowly dispersed product), the effect of water addition on other molecular weights of PVP (10,000 – 360,000 Da) was investigated and is summarised in **Table 2.2**, where a decrease in microsphere size was generally noted.

PVP M_w (Da)	*Diameter (μm)*	*Coefficient of Variation (%)*	*Amine Loading (μmolg^{-1})*
10,000	6.9	112	15.0
29,000	0.4	40	5.5
360,000	0.3	18	16.0

Table 2.2. Water Addition with PVP M_w. The effect of the addition of 7% water to polymerisations performed in ethanol using PVP with molecular weights of 10,000, 29,000 and 360,000 Da.

This trend suggests that water aids the solubility of PVP making available a greater effective concentration of PVP and thus resulting in a greater stabilisation effect, yielding smaller sized microspheres with a more narrow distribution. However, it was noted that for low molecular weights of PVP (M_w 10,000 Da), the addition of 7% water resulted in a more poly-dispersed product, although the reason for this is unknown.

2.2.2.2. Addition of n-Butanol

The success of influencing microsphere diameter and dispersity by the addition of water encouraged the investigation of alternative solvents. Thus, the effect of adding small contributions (0.5 – 10%) of *n*-butanol to ethanol was investigated and the results are summarised by **Table 2.3**. Incorporations of 2, 4 and 9% *n*-butanol to ethanol (shown in red) resulted in a narrowing of the size distribution of the microsphere product (from a coefficient of variation of 59% (for **2.6.3**) to 13 - 14%). However, it did not significantly result in an increase or decrease in the microsphere diameter, which remained at 0.7 – 0.8 µm. The quality of the polymer product yielded from a reaction containing 2% *n*-butanol was assessed by SEM (**Figure 2.10**). The microspheres (**2.8**) appeared spherical and evenly sized with a narrow size distribution, confirming the results obtained by laser diffractometry.

% n-Butanol Added	Mean Diameter (µm)	Coefficient of Variation (%)	Amine Loading (µmol/g)
0.5	0.8	24	7.8
1	0.6	22	16.3
2	0.7	13	8.7
3	0.4	20	15.2
4	0.8	13	9.4
5	0.9	85	15.7
6	0.9	29	5.7
7	0.7	35	9.9
8	0.8	22	6.4
9	0.7	14	6.5
10	0.8	26	5.6

Table 2.3. Addition of *n*-Butanol. Variation of microsphere diameter and amine loading with *n*-butanol content (0.5 – 10%) in ethanol. 2% *n*-butanol generated (**2.8**).

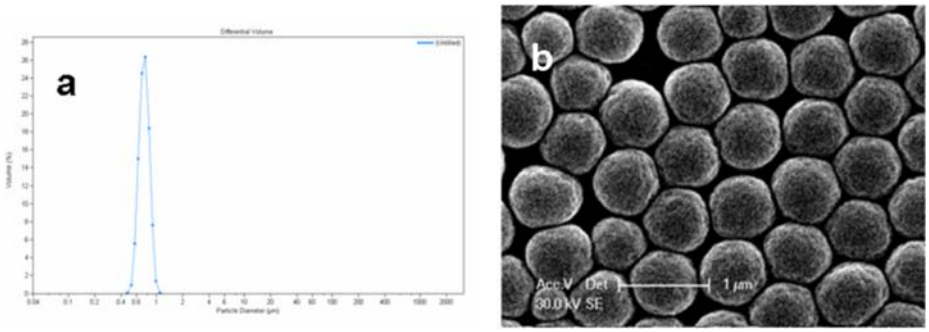

Figure 2.10. Effect of *n*-Butanol. a. Laser diffractometry analysis of microspheres (**2.8**), giving a

size of 0.7 µm (S.D. 0.09 µm, C.V. 13.2%); **b.** Scanning Electron Microscopy of microspheres prepared by dispersion polymerisation in ethanol with 2% *n*-butanol (Scale bar is 1 µm).

2.2.2.3. Addition of 1,2-Dimethoxyethane

To alter the microsphere diameter more dramatically the addition of 1,2-dimethoxyethane (1,2-DME), which is much less polar than ethanol and is not a good solvent for PVP solubility, was investigated (**Table 2.4**). In general, addition of 1,2-DME resulted in agglomeration and large particle size distributions as evidenced by laser diffractometry (**Figure 2.11a**). However, addition of 2% 1,2-DME resulted in an increase in the microsphere diameter to 1.4 µm, without a significant broadening of the size distribution (**Figure 2.11b**). SEM confirmed microspheres (**2.9**) were evenly sized and had smooth surfaces (**Figure 2.12**).

% DME Added	*Mean Diameter (µm)*	*Coefficient of Variation (%)*	*Amine Loading (µmol/g)*
0.5	8.5	98	11.5
1	4.6	107	9.1
2	1.4	31	5.0
3	22.0	59	11.0
4	25.0	67	29.0
5	3.1	77	27.3
6	3.0	129	28.1
7	14.4	80	14.8
8	1.2	62	15.2
9	13.1	120	15.7
10	1.5	40	27.9

Table 2.4. Addition of DME. Variation of microsphere diameter and amine loading with *1,2*-dimethoxyethane content (0.5 – 10%) in ethanol. 2% *1,2*-DME generated (**2.9**)**.**

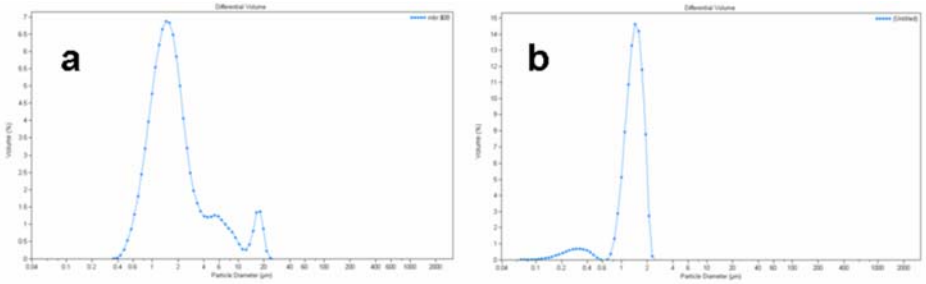

Figure 2.11. Laser diffractometry. Histograms of **a.** 3 µm microspheres prepared with 6% 1,2-DME

in ethanol showing coagulation (S.D. 3.9 µm, C.V. 129%); **b.** 1.4 µm microspheres prepared with 2% 1,2-DME in ethanol (**2.9**) (S.D. 0.4 µm, C.V. 31%).

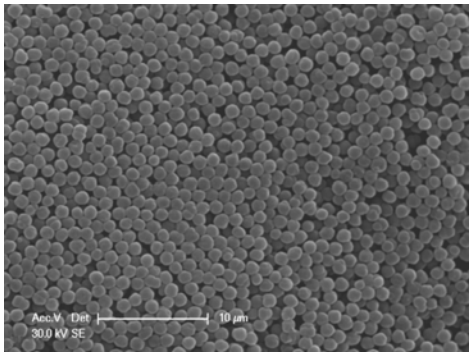

Figure 2.12. Scanning Electron Microscopy. 1.4 µm microspheres (**2.9**) prepared from 2% 1,2-DME in ethanol (Scale bar is 10 µm).

Presumably, the coagulation noted with the addition of 1,2-DME was directly related to a decrease in the polarity of the solvent and a subsequent decrease in PVP solubility affording less efficient stabilisation of the microspheres.

2.2.2.4. Addition of Toluene

To facilitate further increases in microsphere diameter, investigation was made into the addition of toluene, a non-polar solvent. As with 1,2-DME, addition of toluene largely resulted in the agglomeration of the polymer product (**Table 2.5**). However, addition of 4% toluene gave narrowly dispersed 1.8 µm microspheres (**2.10**) as shown by laser diffractometry and confirmed by SEM (**Figure 2.13**).

% Toluene Added	*Mean Diameter (µm)*	*Coefficient of Variation (%)*	*Amine Loading (µmol/g)*
0.5	11.9	119	37.9
1	1.9	106	20.7
2	1.5	99	26.2
3	19.1	52	13.1
4	1.8	16	6.7
5	3.4	142	12.4
6	1.4	90	38.7
7	11.8	107	40.5
8	1.0	43	26.1
9	4.5	98	38.3
10	27.1	127	28.4

Table 2.5. Addition of Toluene. Variation of microsphere diameter and amine loading with toluene

content (0.5 – 10%) in ethanol. 4% toluene generated (**2.10**).

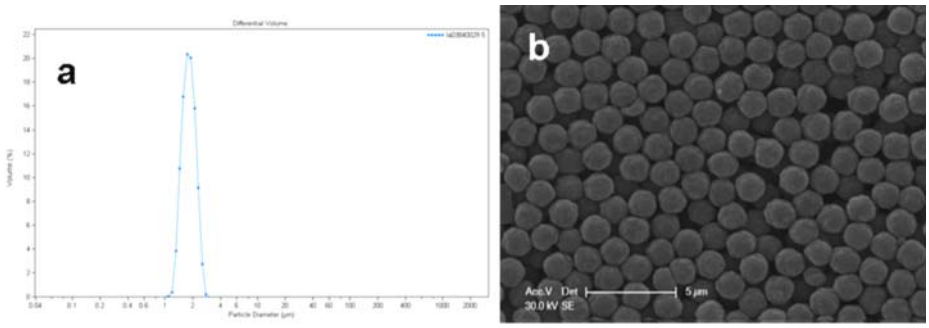

Figure 2.13. Effect of Toluene. a. Laser diffractometry of microspheres (**2.10**), giving a size of 1.8 µm (S.D. 0.3 µm, C.V. 16.1%); **b.** Scanning Electron Microscopy of microspheres (**2.10**) prepared by dispersion polymerisation from 4% toluene in ethanol (Scale bar is 5 µm).

2.2.2.5. Conclusions on Stabiliser Solubility

Addition of small percentages of co-solvents to the ethanol base solvent in the dispersion polymerisation of styrene, DVB and VBAH in the presence of PVP has successfully resulted in the production of microspheres from 0.4 – 1.8 µm in diameter. All the microspheres exhibited the incorporation of the amine functionality and had even spherical morphologies. Although the mechanism of dispersion polymerisation is not well understood, this demonstrates that small, simple changes to the reaction media content can have a reliable yet dramatic effect and may easily achieve a multitude of microsphere diameters.

2.3. Emulsion Polymerisation

Emulsion polymerisation typically results in the preparation of particles less than 0.5 µm in diameter. As such, small sized particles for cellular investigations were prepared by an emulsifier-free emulsion polymerisation procedure as has been previously reported.[42]

Emulsion polymerisation is a reasonably well studied and widely applied procedure for the production of a range of polymers, including synthetic rubbers and latex paints.[89, 90, 91] The mechanism by which emulsion polymerisation results in the production of a polymer precipitate was first established in the 1940s[92, 93] and has recently been re-evaluated by the help of computer simulations.[94] Simplistically, the

process of emulsion polymerisation can be divided into 3 main stages; firstly, an emulsion is formed with the monomer in an aqueous solution containing a surfactant, resulting in the production of large micelles into which the monomer can diffuse. A water-soluble initiator is added and is able to react with monomer in the micelles (**Figure 2.14,** Interval 1). During heating, the monomer polymerises producing a polymer particle, resulting in a system that contains both monomer droplets (monomer not contained within micelles) and early polymer particles (**Figure 2.14,** Interval 2). In the last stage of the emulsion polymerisation, monomer from the excess monomer droplets diffuses into the polymer particles, where it may react with initiator resulting in further oligomeric chains (**Figure 2.14,** Interval 3) and a final microsphere product.

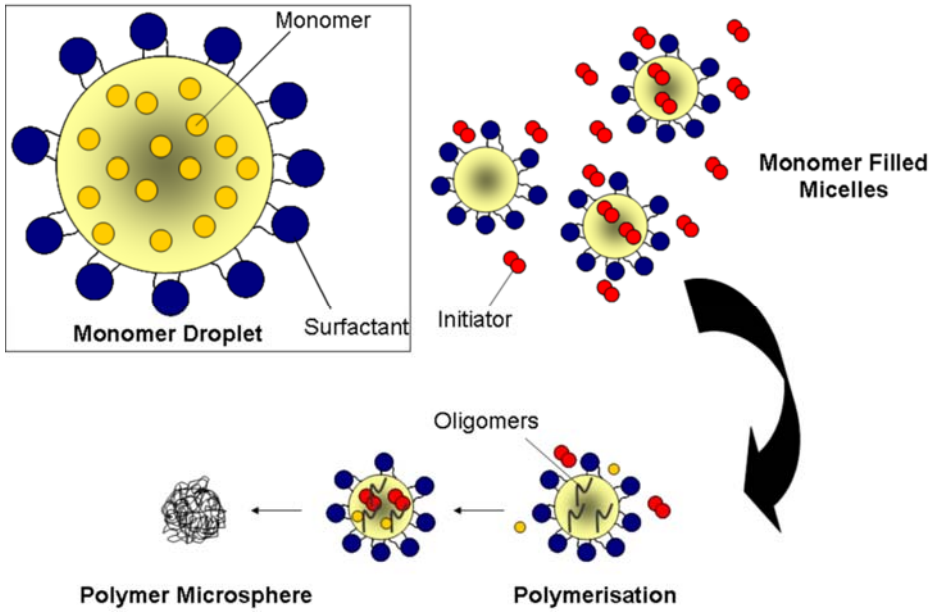

Figure 2.14. Emulsion polymerisation. Summary of the 3 stages: micelle formation, polymerisation and precipitation.

In the production of nanometer sized microspheres, the main monomer (styrene), the cross-linking agent (DVB) and the functionalised co-monomer (VBAH) were added to boiled nitrogen-bubbled water with magnesium sulphate, as a form of stabiliser. After 30 minutes at 80 ºC, water-soluble radical initiator, 2,2'-Azobis-2-methyl propionamide (V-50), was added and the resulting emulsion was stirred for 1 hour producing 0.1 µm microspheres (**2.11**) or 2 hours producing 0.2 µm

microspheres (**2.12**) (**Scheme 2.3**). Microspheres were sized by laser diffractometry (**Figure 2.15**) and 0.2 µm microspheres were additionally evaluated by SEM (**Figure 2.16**).

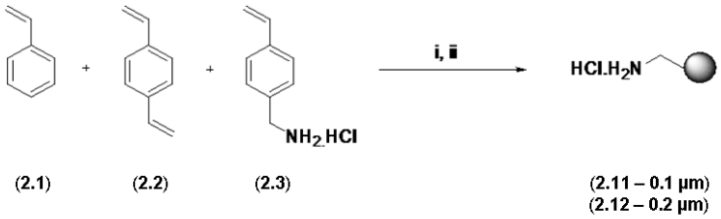

Scheme 2.3. Microspheres. Production of microspheres, (**2.11**) and (**2.12**), by emulsion polymerisation.
(i). 0.004 eq. $MgSO_4$, water, 80 ºC, 30 min; (ii). 0.005 eq. V-50, water, 80 ºC, 1 – 2 h.

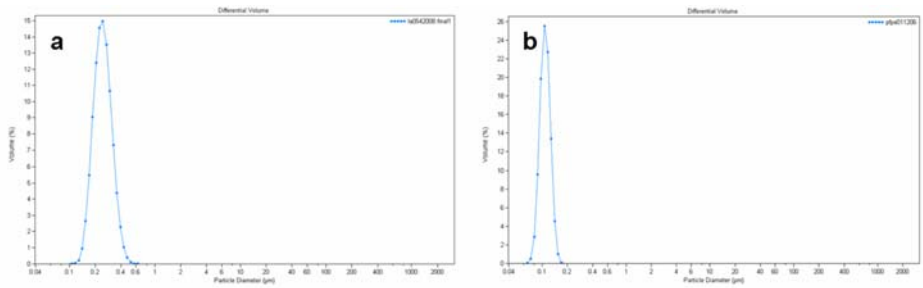

Figure 2.15. Laser Diffractometry. Histograms of microspheres prepared by emulsion polymerisation, giving **a.** 0.2 µm microspheres (**2.12**) (S.D. 60 nm, C.V. 25%); **b.** 0.1 µm microspheres (**2.11**) (S.D. 15 nm, C.V. 14%).

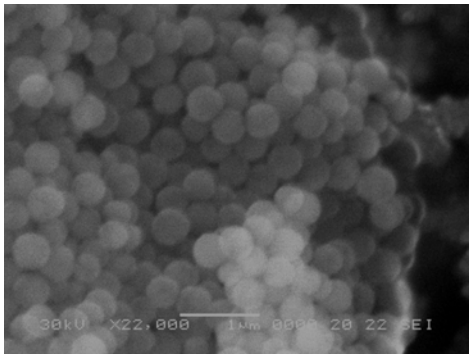

Figure 2.16. Scanning Electron Microscopy. 0.2 µm microspheres (**2.12**) prepared by dispersion polymerisation (Scale bar is 1 µm).

As **Figure 2.15** shows, the microspheres (**2.11**) and (**2.12**) were narrowly dispersed and **Figure 2.16** indicates that 0.2 µm microspheres had smooth, spherical morphologies.

Thus, using dispersion and emulsion polymerisation a selection of microspheres have been prepared from 0.1 μm up to 2 μm, which all exhibit a narrow size distribution and have smooth spherical morphologies. Microspheres in this size range will have particular applications for intracellular studies, for example in delivery and cellular investigations.

2.4. Cellular Uptake

The use of polymer microspheres for intracellular studies is not a novel technique. In fact, they are well established tools.[47] However, their intracellular use in non-phagocytic cells is not well documented. As such, it was of interest to study the uptake of a selection of polystyrene microspheres (0.2, 0.5 and 2 μm), prepared as above, in a range of cell lines (**Table 2.6**) at varying incubation times. Cells which grow in adhesion and suspension as well as mouse, human and embryonic stem cells were studied.

Cell Line	***Cell Type***	***Comments***
B16F10	Mouse melanoma cells	Epithelial-like, adherent
E14TG2a	Mouse stem cells (E14)	Lymphocyte-like, adherent
HEK293T	Human embryonic kidney cells	Epithelial-like, adherent
HeLa	Human cervical cancer cells	Epithelial-like, adherent
Jurkat	Human T cells from blood	Lymphocyte-like, suspension
K562	Chronic myelogenous leukemia cells	Lymphoblast-like, suspension
L929	Mouse fibroblast cells	Adherent
RAW264	Mouse macrophage	Phagocytotic, adherent

Table 2.6. Cell Lines. Established cell lines investigated for microsphere uptake, including mouse/human adherent and suspension cells and mouse stem cells.

2.4.1. Preparation of Fluorescent Microspheres

In order to study the uptake of microspheres in cells it was necessary to couple a fluorophore to the beads so they can be seen intracellularly by standard microscopy or cytometry methods. To this affect, a selection of amino-functionalised polystyrene microspheres (0.2, 0.5 and 2 μm, (**2.12**), (**2.7.2**) and (**2.10**) respectively) were linked covalently to 5(6)-carboxyfluorescein *via* an aminohexanoic spacer unit (**Scheme 2.4**).

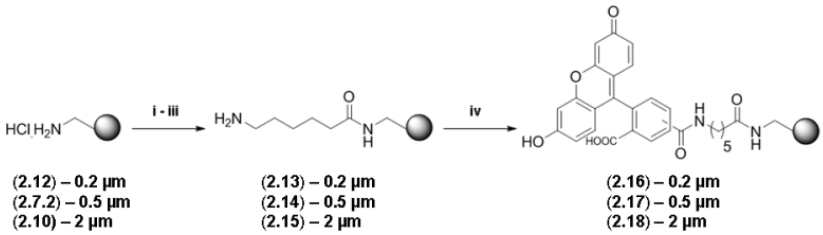

Scheme 2.4. FAM-Microspheres. Preparation of 0.2, 0.5 and 2 µm 5(6)-carboxyfluorescein microspheres (**2.16**), (**2.17**) and (**2.18**) *via* aminohexanoic microspheres (**2.13**), (**2.14**) and (**2.15**).
(i). 1 N NaOH; (ii). 10 eq. Fmoc-Ahx-OH, 10 eq. HOBt, 10 eq. DIC, DMF, 18 h, 25 ºC; (iii). 20% piperidine/DMF; (iv). 10 eq. 5(6)-carboxyfluorescein, 10 eq. PyBOP, 10 eq. HOBt, 10 eq. DIPEA, 18 h, 25 ºC.

The use of the hexanoic spacer unit was for two reasons. Firstly, incorporation of a spacer lessens steric repulsions between the bulky dye molecules and amino residues embedded within the entangled polymeric chains. Secondly, use of some spacer units can result in enhanced biocompatibility and can aid the interactions between microspheres and cell surfaces.[95] Carboxyfluorescein was successfully coupled to all sizes of microspheres and they were confirmed to be fluorescent by fluorescence-based flow cytometry (**Figure 2.17**), compared to uncoupled microspheres.

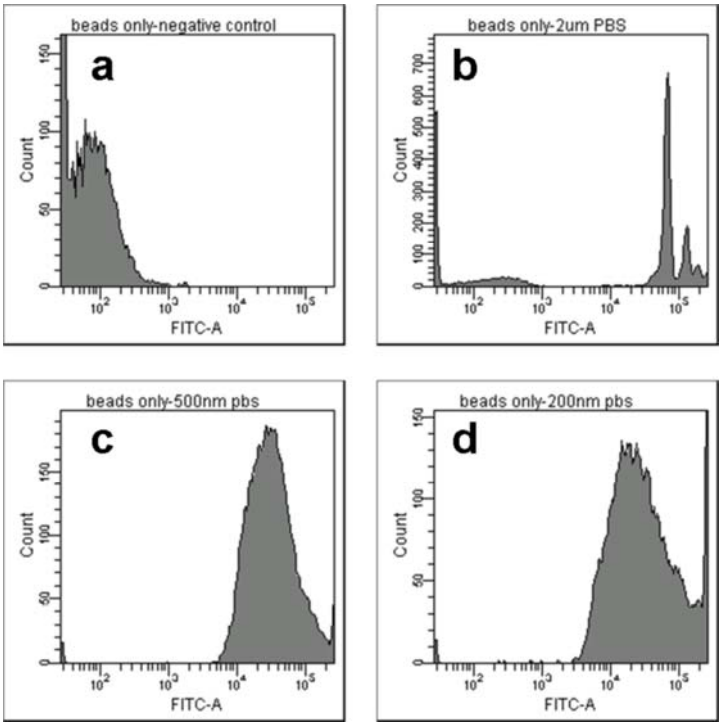

Figure 2.17. Flow Cytometry. a. uncoupled non-fluorescent microspheres; **b.** 2 µm (**2.18**); **c.** 0.5 µm (**2.17**); and **d.** 0.2 µm (**2.16**) fluorescein microspheres (excitation: 488 nm, emission 515 – 545 nm).

Adaptation of the microspheres making them fluorescent allows not only for microspheres which have been internalised by cells to be examined by microscopy, but also allows for quantitative techniques, such as flow cytometry to measure the percentage of cells which have been "beadfected" by fluorescent microspheres.

2.4.2. Flow Cytometry

Fluorescence-based flow cytometric techniques allow for the high-throughput quantification of cellular fluorescence and can analyse several thousand cells per second. The technique works by passing the cells in a stream of droplets (where one droplet contains, approximately, one cell) through a series of lasers, which excite the fluorophore present. Emission from the fluorescent compound is collected by a detector and relayed to a computer.

More specifically, techniques like Fluorescence Activated Cell Sorting (FACS) allow for cell populations to be sorted based on their fluorescent output (**Figure 2.18**).

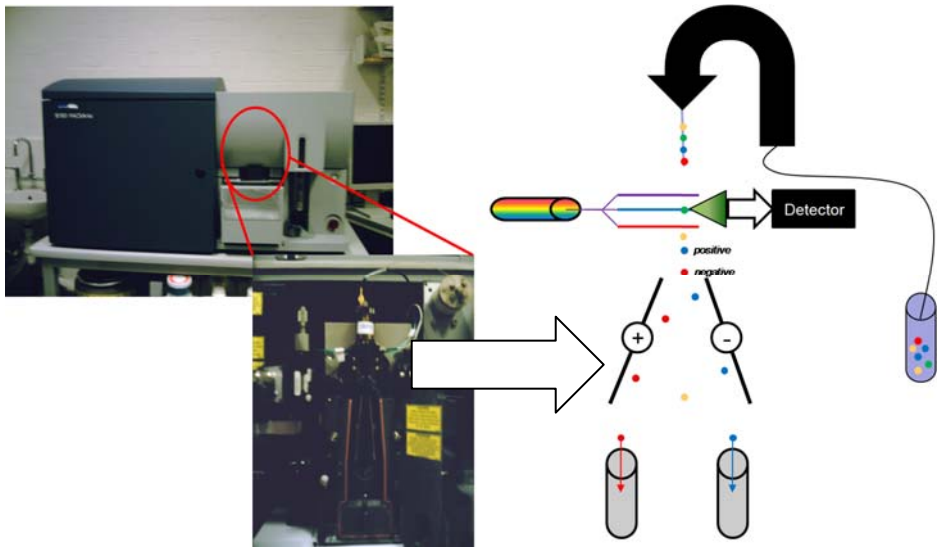

Figure 2.18. Fluorescence Activated Cell Sorting (FACS). Cells are passed in a stream of droplets through a series of lasers. They can be charged positive or negative dependent on their fluorescent output and sorted *via* charged deflection plates. Instrument shown is a BD Bioscience FACAria and the inset image shows the deflection plates and sorting chamber.

Here, the droplets are charged positive or negative dependent on their fluorescence (or lack of fluorescence) and they may then be deflected into a collection chamber

via charged deflection plates. This allows pure populations to be isolated and analysed.

0.2, 0.5 and 2 μm fluorescein microspheres, (**2.16**), (**2.17**) and (**2.18**), were incubated with human erythroleukemic (K562) cells, mouse (E14) stem cells, mouse fibroblast (L929) cells, human cervical cancer (HeLa) cells, human embryonic kidney (HEK293T) cells, mouse melanoma (B16F10) cells, human Jurkat T-cells and mouse macrophage (RAW264) cells to study cellular uptake. Incubations were run over 6 – 24 hours at a constant microsphere concentration of 86 μg/mL (**Graph 2.2**), to establish cell line dependence on uptake and how microsphere diameter affects internalisation. Uptake was found to be high across all cell lines analysed and was dependent on incubation time with, expectedly, longer incubation times resulting in higher uptakes. In addition, smaller sized microspheres (0.2 μm (**2.16**) and 0.5 μm (**2.17**)) were found, in general, to enter cells more rapidly than the larger 2 μm microspheres (**2.18**). However, this result may be expected for steric reasons, as a 2 μm bead has a volume up to 100 times that of a 0.2 μm microsphere. In addition, microspheres showed good uptake in both suspension (K562 and Jurkat) and adherent cells, showing microspheres are able to enter a range of cell lines cultured in diverse ways. Unsurprisingly, RAW264 cells were seen to ingest a high number of microspheres as they are a professional phagocyte cell type (**Figure 2.19**). In this cell line, over-loading was noted to be a problem and incubations had to be strictly controlled (*via* microsphere concentration and incubation time). Additionally, HEK293T cells also showed impressive uptake, as has been previously reported,[95] with beadfection more than 90% after 24 hours using smaller sized microspheres, (**2.16**) and (**2.17**). In addition, cancer cells (B16F10, HeLa and K562), which can traditionally be more difficult to deliver external cargo to, efficiently took up microspheres with uptake approaching 95% after 24 hours using, in particular, 0.2 μm microspheres.

In addition, the beadfected cells were assessed for their fluorescence intensity after 24 hours and compared to one another to evaluate which cells took up the highest number of microspheres (**Graph 2.3**).

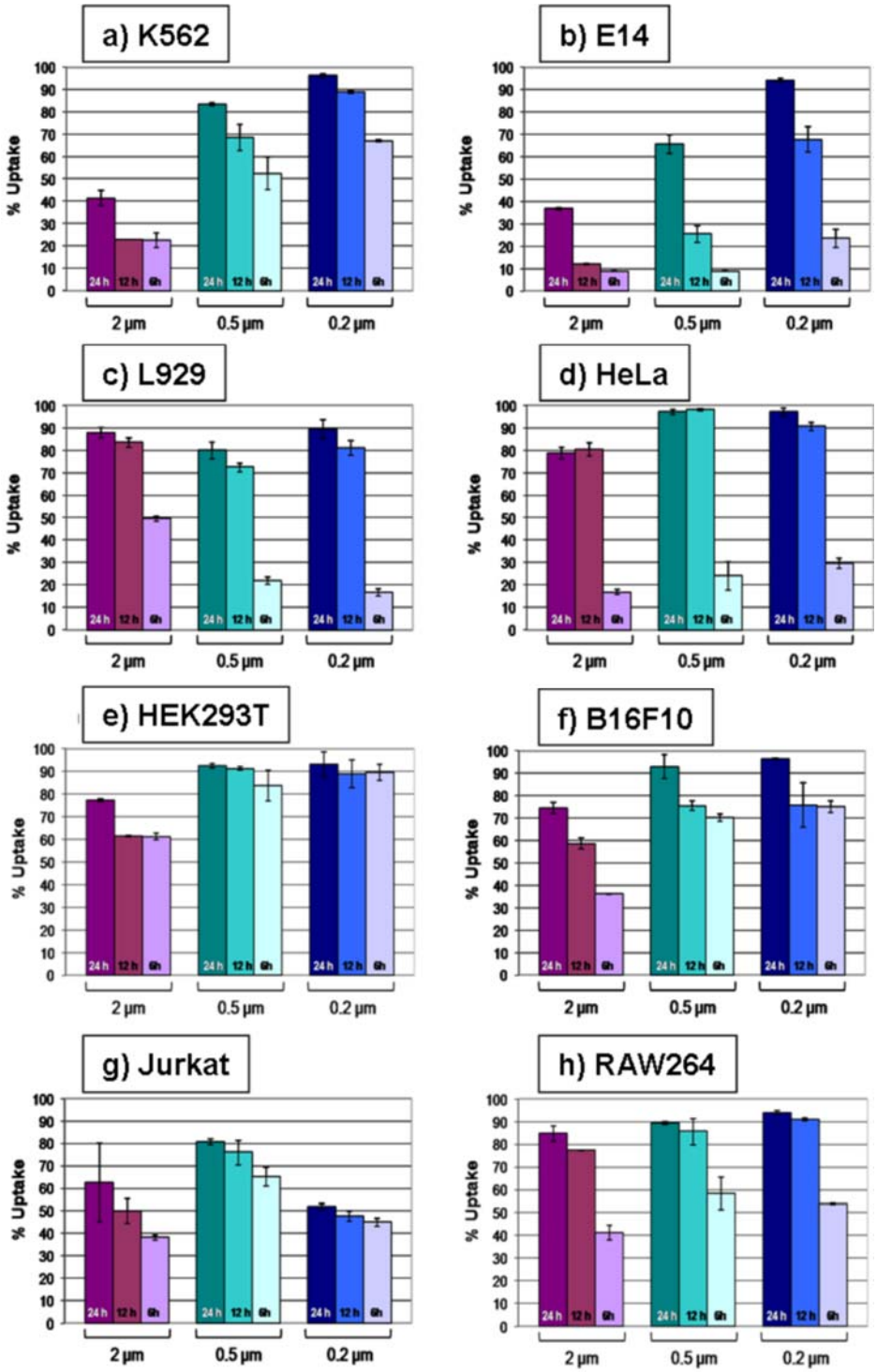

Graph 2.2. Uptake of fluorescein microspheres. 0.2 (**2.16**), 0.5 (**2.17**) and 2 µm (**2.18**) uptake by **a)** K562; **b)** E14; **c)** L929; **d)** HeLa; **e)** HEK293T; **f)** B16F10; **g)** Jurkat and **h)** RAW264 cells after 6, 12 and 24 h incubations. % uptake was measured as the % of cells with a fluorescent emission exceeding untreated control cells, which were taken as 0% uptake. Microsphere concentration was 86 µg/mL.

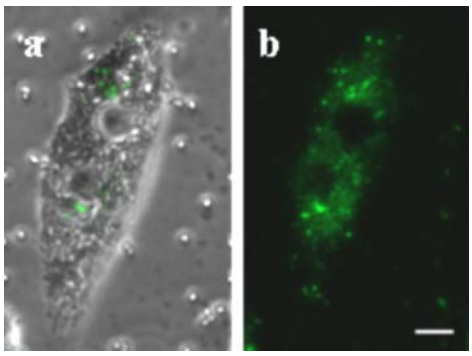

Figure 2.19. Cellular Over-Loading. Microscopy of 0.5 µm fluorescein microspheres (**2.17**) (86 µg/mL) by RAW264 cells after 24 hours. **a.** Phase contrast image; **b.** Fluorescence image (microspheres in green). Scale bar is 50 µm.

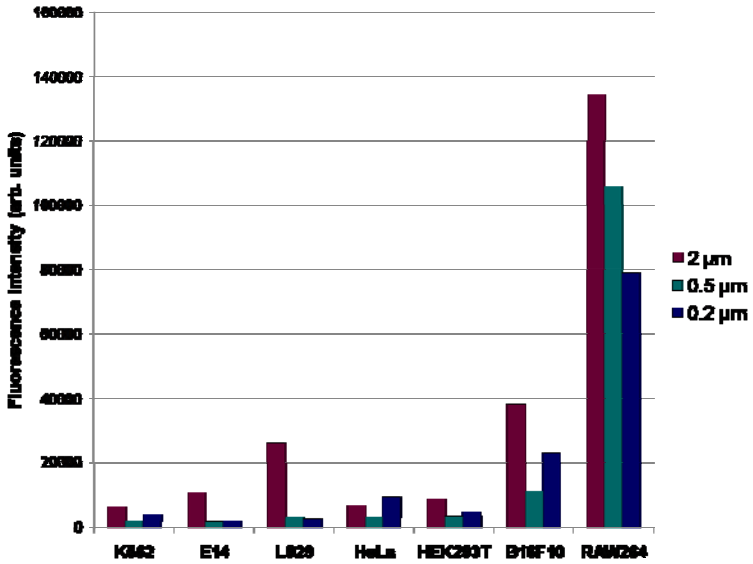

Graph 2.3. Fluorescence Intensity. Intensity of cells (arbitrary units) beadfected with 2, 0.5 or 0.2 µm fluorescein microspheres (86 µg/mL) after 24 hours.

As expected, RAW264 mouse macrophage cells took up the highest number of all microsphere sizes and thus were the most fluorescent. However, most other cell types showed comparable fluorescence suggesting they ingested similar numbers of microspheres.

Uptake of the microspheres was confirmed by pseudo-confocal microscopy (**Figure 2.20**), showing B16F10 cells as a representative example stained with an actin filament specific dye based on phalloidin and a nuclei specific stain.

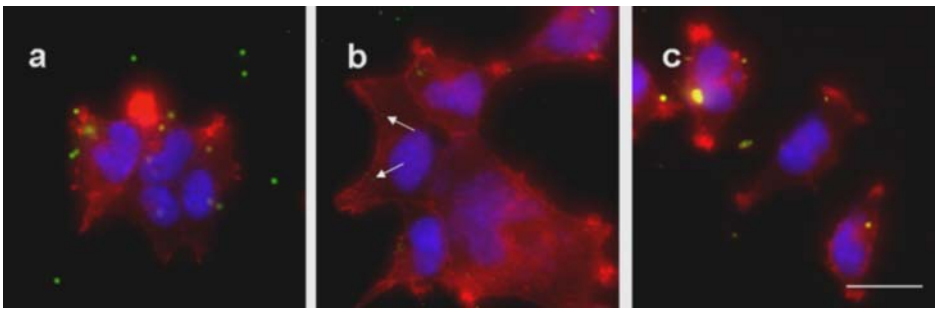

Figure 2.20. Microscopy of Uptake. B16F10 cells labelled with AlexaFluor-568 phalloidin (actin filaments) and Hoechst 33342 (nuclei) with **a.** Fluorescein labelled 2 µm microspheres, (**2.18**); **b.** Fluorescein labelled 0.5 µm microspheres, (**2.17**); **c.** Fluorescein labelled 0.2 µm microspheres, (**2.16**). Scale bar is 25 µm. Images collected after 12 hours (microsphere concentration of 86 µg/mL).

2.4.3. Microscopy

Confocal microscopy works by imaging cells in slices whereby, at any one time, only one slice (or 'Z-slice') of the cell can be seen, as all light that is not in focus is eliminated using a pin-hole system (**Figure 2.21**). The slices can then be stacked and reconstructed to generate a 3-D model.

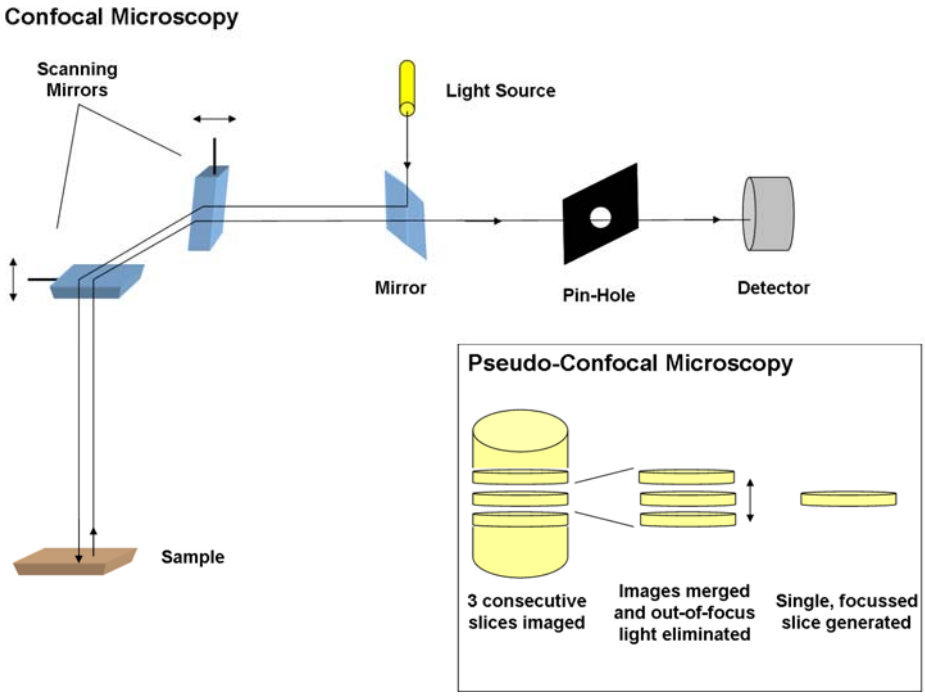

Figure 2.21. Confocal and Pseudo-Confocal Microscopy. These techniques work by eliminating out-of-focus light from an image.

Pseudo-confocal microscopy works in a similar manner, whereby 3 images are taken of closely associated Z-slices within a cell. The 3 images are then combined and out-of-focus light is eliminated using a computer-based algorithm, generating one image of a single section of a cell (**Figure 2.21**, *inset*). Similar to confocal microscopy, pseudo-confocal microscopy can be used to generate a 3-D model of the imaged material. As such, it allows microspheres inside and outside the cell to be distinguished.

2.4.4. Embryonic Stem Cells

Embryonic stem cells are an undifferentiated cell line, which can be indefinitely maintained in *in vitro* cultures.[96, 97] Their importance in research is related to their ability to differentiate into all cell types (**Figure 2.22**).[98] However, in general, delivery of cargo intracellularly to stem cells has been hindered by poor uptake and, in some cases, extensive cytotoxicity.[99, 100]

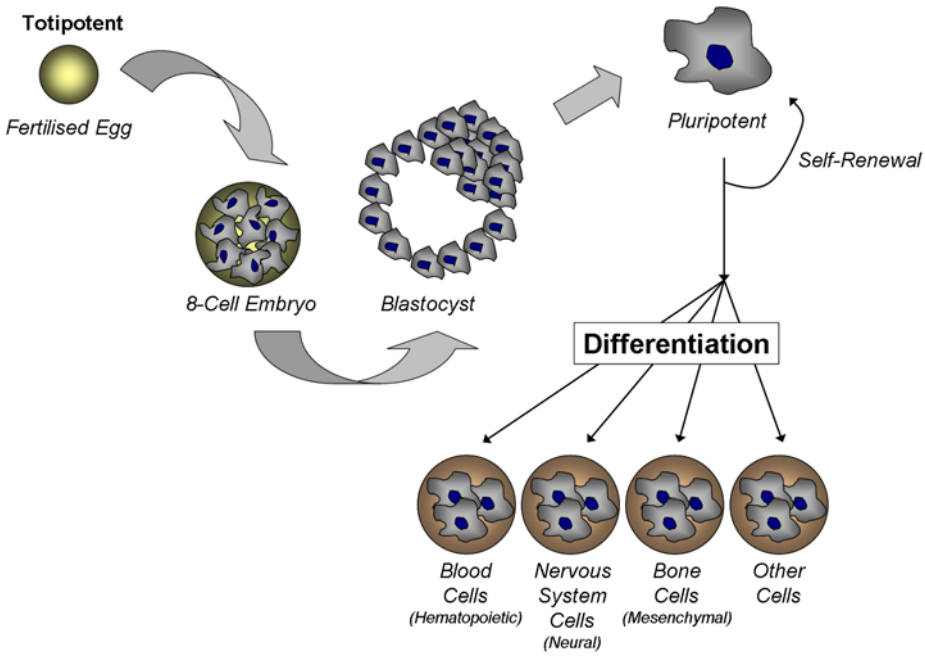

Figure 2.22. ES Cells. Embryonic stem cells can differentiate into all lineages of both the foetus and the adult.

In contrast, embryonic stem cells (E14TG2a or E14) showed good uptake of 0.2 µm and 0.5 µm microspheres (90 and 70% respectively after 24 hours) (**Figure 2.23**). Although, it should be noted that uptake was relatively poor at short incubation times

suggesting microspheres require longer times to efficiently enter stem cells. In addition, E14 cells did not efficiently take up the larger 2 µm microspheres (35% after 24 hours). However, given the typically smaller size of stem cells in comparison to some transformed cell lines (which can be up to 70 µm in diameter), it may not be surprising that E14 cells were less capable of taking up these larger particles.

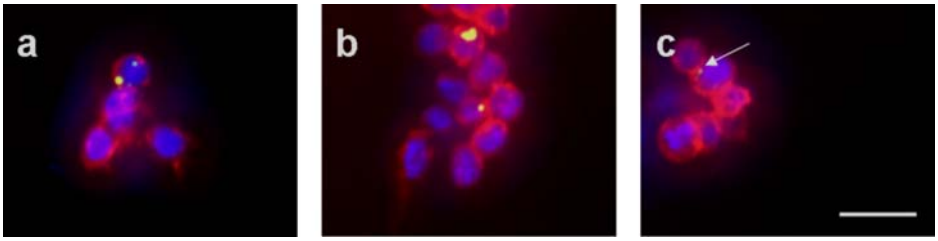

Figure 2.23. Microscopy of ES Cells. E14 incubated with **a.** 2 µm fluorescein microspheres (**2.18**); **b.** 0.5 µm fluorescein microspheres, (**2.17**), and **c.** 0.2 µm fluorescein microspheres, (**2.16**). Actin filaments stained with AlexaFluor-568 phalloidin and nuclei with Hoechst 33342. Images collected after 12 hours (microsphere concentration 86 µg/mL). Scale bar is 50 µm.

2.4.5. Concentration Dependence

Analysis was additionally made of the concentration dependence of uptake by adding varying concentrations (30 – 60 µg/mL) of 0.2, 0.5 and 2 µm microspheres to B16F10, HeLa and HEK293T cells. Uptake analysis was performed after 24 hours and the results are summarised by **Graph 2.4**. As may be expected, lower concentrations of microspheres (of all sizes) yielded lower uptake than higher concentrations. However, it must be noted that microspheres, even at low concentrations, are in great excess over cells (up to nearly 3 million times) (**Table 2.7**). Such an excess means that varied concentrations may have a lesser effect on cellular uptake than perhaps might be expected, due to saturation.

Diameter (µm)	*Microspheres/mL*	*Microspheres/cell*
2	2.4×10^{8}	2800
0.5	1.5×10^{10}	175000
0.2	2.4×10^{11}	2800000

Table 2.7. Microspheres per Cell. Number of microspheres per mL and per cell under typical culture conditions, based on a concentration of 86,000 cells/mL.

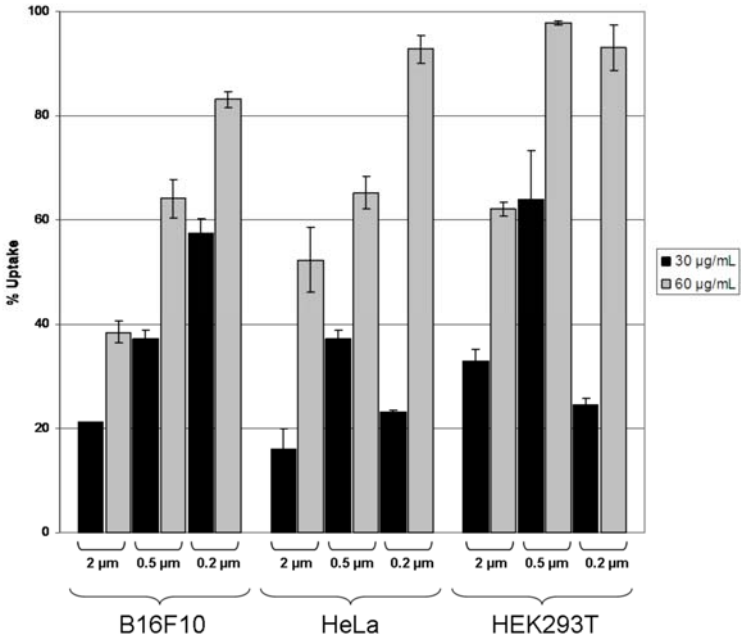

Graph 2.4. Concentration Dependence. Uptake of 0.2 (**2.16**), 0.5 (**2.17**) and 2 µm (**2.18**) microspheres after 24 hours in B16F10, HeLa and HEK293T cells at concentrations of 30 and 60 µg/mL.

2.4.6. Extracellular Quenching

In order to distinguish between internalised microspheres and those on the extracellular membrane of cells, flow cytometry was performed in a solution designed to quench any extracellular fluorescence associated with the fluorescein microspheres (0.2% trypan blue/Hank's Balanced Saline Solution (HBSS)). Trypan blue is an intercalating dye (excitation ~ 520 nm and emission ~ 650 nm), which is unable to translocate the membrane of healthy cells (**Figure 2.24**).

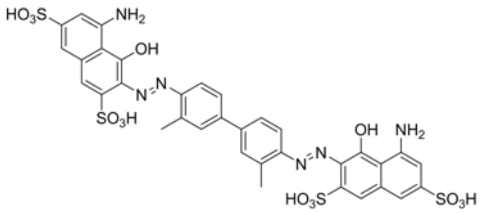

Figure 2.24. Trypan Blue. Structure of intercalating dye, trypan blue.

Instead it coats the extracellular membrane of the cell and any fluorescein-like fluorophores on the exterior cellular membrane can be quenched in a Fluorescence Resonance Energy Transfer (FRET)-like system (**Figure 2.25**).[101]

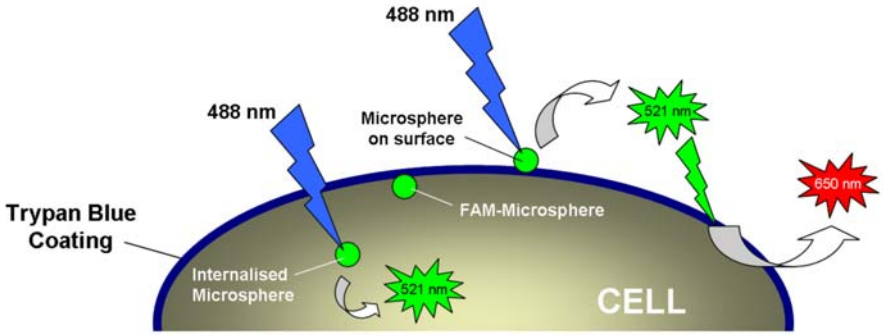

Figure 2.25. Extracellular Quenching. Fluorescein-like fluorophores can be quenched by trypan blue in a FRET system.

In order to assess the extracellular quenching ability of trypan blue, B16F10 mouse melanoma cells were incubated with fluorescein microspheres (0.2, 0.5 and 2 µm) for periods between 10 minutes and 24 hours. Cellular uptake was assessed by flow cytometry in 0.2% trypan blue/HBSS (pH 7.4) and in a control solution of 2% foetal calf serum (FCS) in Phosphate Buffered Saline (PBS, pH 7.4), which will not offer any quenching of extracellular fluorescence. The results are summarised by **Graph 2.5a-c** and **Figure 2.26**.

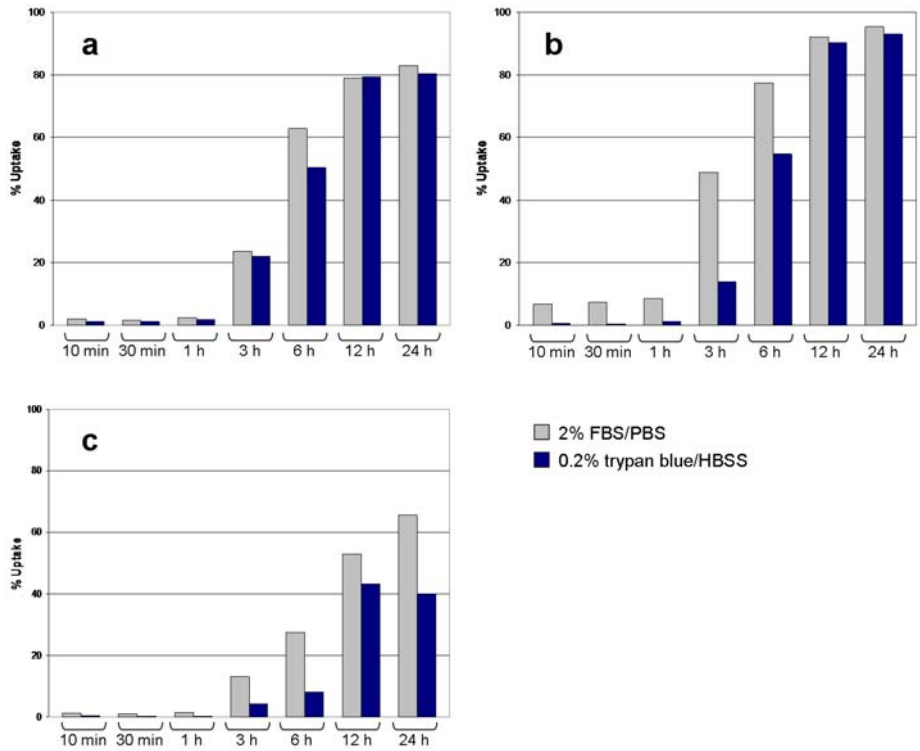

Graph 2.5. Extracellular Quenching. Flow cytometric analysis of cellular uptake in B16F10 after 10 minutes – 24 hours, analysed in 2% FBS/PBS or 0.2% trypan blue/HBSS with **a.** 2 µm fluorescein

microspheres (**2.18**); **b.** 0.5 µm fluorescein microspheres (**2.17**); **c.** 0.2 µm fluorescein microspheres (**2.16**). Microsphere concentration was 86 µg/mL.

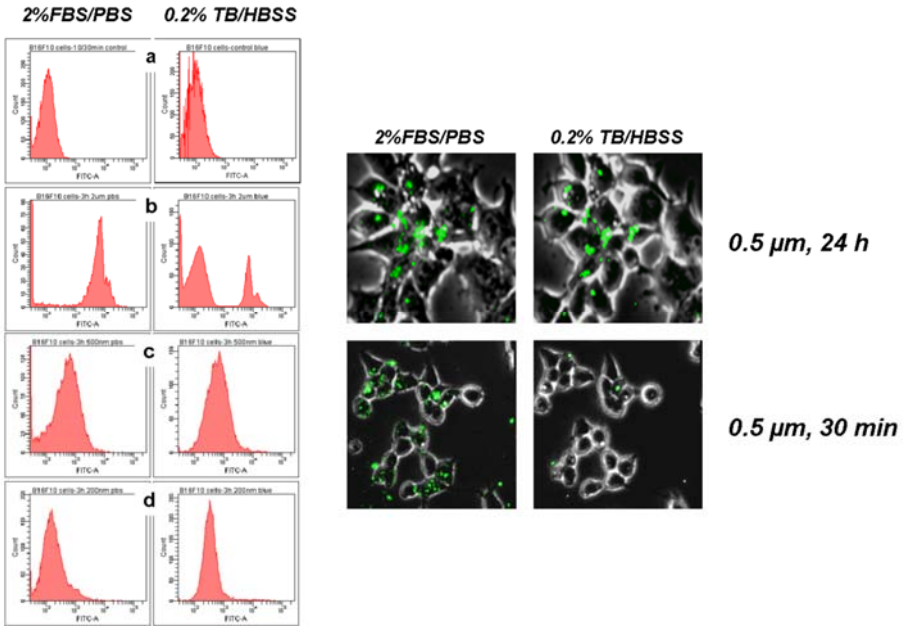

Figure 2.26. Extracellular Quenching. *Left:* Flow cytometry histograms in 2% FBS/PBS or 0.2% TB/HBSS after 6 hours of **a.** un-beadfected control cells; **b.** cells beadfected by 2 µm fluorescein microspheres (**2.18**); **c.** cells beadfected by 0.5 µm fluorescein microspheres (**2.17**); **d.** cells beadfected by 0.2 µm fluorescein microspheres (**2.16**). *Right:* Microscopy of B16F10 cells beadfected with 0.5 µm fluorescein microspheres (**2.17**) after 24 hours and 30 minutes in 2% FBS/PBS and 0.2% TB/HBSS.

At short incubation times (*ca* 10 minutes to 1 hour), microspheres in suspension have not yet settled on the cells (which grow in adhesion) and as such, there is little difference between the cellular uptake of the microspheres in the quenching and non-quenching solutions. However, after 3 hours significant differences are observed in the uptake of microspheres 0.2 and 0.5 µm in diameter indicating efficient quenching with the trypan blue solution. After 3 hours, the uptake differed by as much as 35% using 0.5 µm microspheres and further differences were seen after 6 hours. After prolonged incubation times (12 – 24 hours), cellular uptake in the quenching and non-quenching solution began to equalise again, indicating that the majority of the microspheres on the surface of the cells have been ingested. This was confirmed by microscopy (**Figure 2.26**, *right*), where images were collected in the control solution (2% FBS/PBS) and in trypan blue/HBSS. After 30 minutes, vast differences were

seen between quenched and unquenched cells (**Figure 2.26**, *right bottom*), indicating that the majority of the microspheres were extracellular. However, after 24 hours less difference was noted (**Figure 2.26**, *right top*), indicating that microspheres had been internalised and corroborating the results achieved by flow cytometry.

However, 2 μm microspheres showed similar uptakes in the control solution and in the trypan blue quenching solution, even at short incubation times. The reason for this may be two-fold. Either the 2 μm microspheres rapidly enter cells upon contact, meaning they are all intracellular and cannot be quenched by trypan blue or it may be indicative of the larger size of the 2 μm microsphere not being efficiently quenched. Given the previous findings indicating that 2 μm microspheres enter cells slower than the smaller beads, the latter explanation may be more appropriate.

2.4.7. Definable Loadings

An additional advantage that microspheres exhibit over alternative delivery methods is that defined cellular loadings could be achieved with, in particular, the 2 μm microspheres (**2.18**). Definite cell populations containing 1 bead, 2 beads and 3 beads could be distinguished by flow cytometry (**Figure 2.27**) and the cell populations could be easily sorted obtaining pure populations of specific loadings. The benefit of this is that by alteration of the microsphere concentration and incubation time, a definable and known loading can be achieved. This means that the concentration of cargo per cell can be controlled in an efficient and simple manner.

2.4.8. Culture Requirements

Some cellular delivery devices (e.g. cationic lipids) require special culture conditions for their efficient intracellular translocation, such as serum-free conditions or antibiotic-free media.[102] Not only does this add a complexity to experiments, but it can also have a detrimental effect on the cell cultures. In contrast, microspheres were seen to enter cells under normal (serum-supplemented) culture conditions making their use uncomplicated and also demonstrating possible translation *in vivo*, where tolerance of serum is essential.[103] To demonstrate that the uptake of microspheres was not affected by serum, a selection of cells were studied for their uptake under serum-supplemented and serum-free conditions (**Table 2.8**).

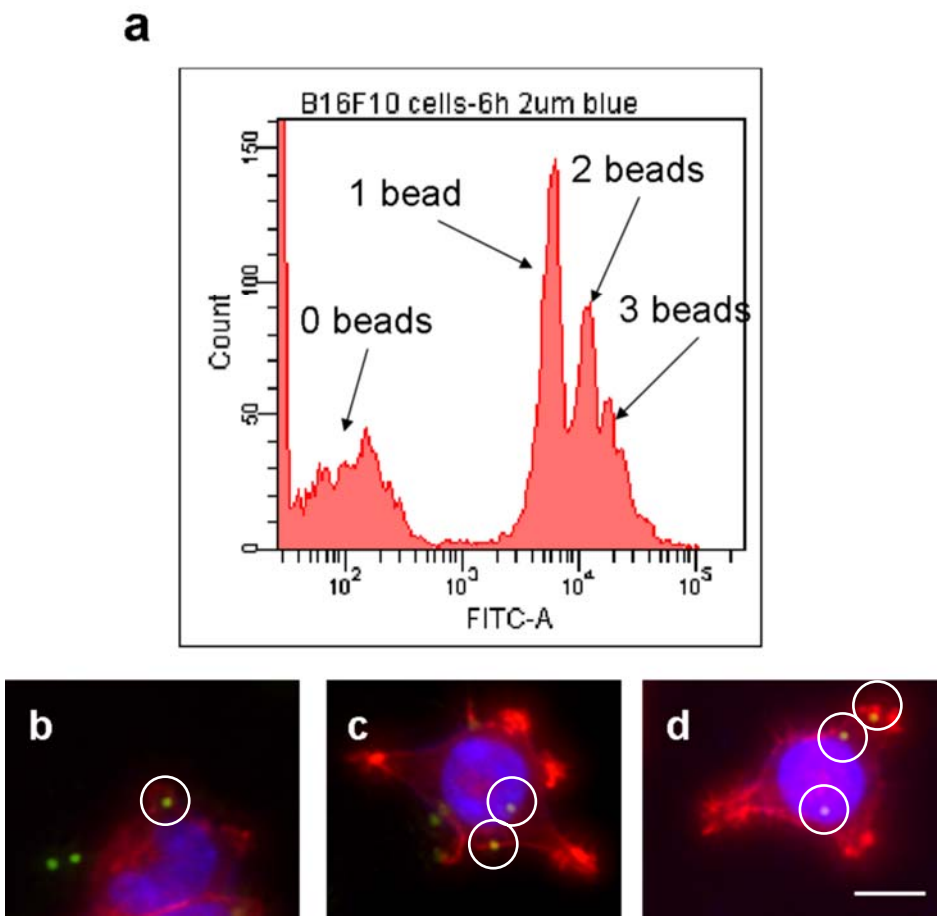

Figure 2.27. Definable Cellular Loadings. B16F10 cells incubated with 2 µm fluorescein microspheres, **a.** Flow cytometric histogram after 6 hours; **b – d.** Microscopy following sorting, where **b.** shows one bead/cell; **c.** shows two beads/cell; **d.** shows three beads/cell.

The uptake of microspheres was not seen to dramatically increase or decrease when cultured in complete or serum-free media, demonstrating microsphere indifference to varied culture conditions.

Cell Line	*Uptake in Complete Media (%) after 6 h (left) and 24 h (right)*						*Uptake in Serum-Free Media (%) after 6 h (left) and 24 h (right)*					
	2 µm		*0.5 µm*		*0.2 µm*		*2 µm*		*0.5 µm*		*0.2 µm*	
B16F10	36	75	71	97	75	96	23	56	56	100	11	62
K562	23	42	58	83	67	96	24	49	72	99	54	74
L929	50	88	23	83	17	89	14	47	37	81	18	58

Table 2.8. Serum-Free *vs* Serum-Supplemented. Uptake of 0.2 µm (**2.16**), 0.5 µm (**2.17**) and 2 µm (**2.18**) fluorescein microspheres in B16F10, K562 and L929 cells in complete media and serum-free media after 6 and 24 hours. Microsphere concentration 86 µg/mL.

2.5. Toxicity

The uptake of 0.2, 0.5 and 2 μm microspheres has been seen in a variety of cell lines and was found to be high but controllable. However, it is vital that microspheres do not exhibit cytotoxicity in these cells if they are to be applied as delivery devices. In order to examine this, MTT assays[104] were used to assess cellular viability in the presence and absence of 0.2 μm (**2.16**), 0.5 μm (**2.17**) and 2 μm (**2.18**) fluorescein microspheres. MTT assays use 3-(4,5-dimethylthiazol-2-yl)-2,5-diphenyltetrazolium bromide, a tetrazole which is converted by healthy cells to purple formazan crystals. Once dissolved, the absorbance of the formazan produced can be measured (λ = 570 nm) and related to the cellular viability (taking untreated control cells as 100 % viable). **Graph 2.6** summarises the cellular viability of E14, HeLa, HEK293T, B16F10, K562, L929 and Jurkat cells treated with 0.2, 0.5 and 2 μm microspheres at concentrations of 75 and 150 μg/mL. No substantial cytotoxicity was noted in any cell line using any size of microsphere at the concentrations tested (viability was over 70% in all cases and was generally more than 90%). However, HEK293T cells were noted to be more sensitive to microspheres than the other cell lines. This is likely due to over-loading of the cells by microspheres rather than toxicity inherent of the particles themselves, as uptake of the beads was noted to be rapid and high (approaching 90% after 6 hours) in this cell line. A separate control was established where microspheres alone were incubated in the presence of MTT to show that microspheres are unable to convert yellow MTT to the purple formazan crystals.[39]

2.6. In Vivo

As has been previously seen with some forms of nanotube, even when cytotoxicity is not evident *in vitro*, toxicity can still occur *in vivo* as the biological system is much more complex. As such, it was of interest to examine the affect of microspheres in the animal model and, in particular, to evaluate toxicity. Consequently, a 6 week old mouse was given an intravenous tail vein injection of 0.5 μm Cy7 coupled microspheres and the subject was then imaged after 6 hours (**Figure 2.28**).

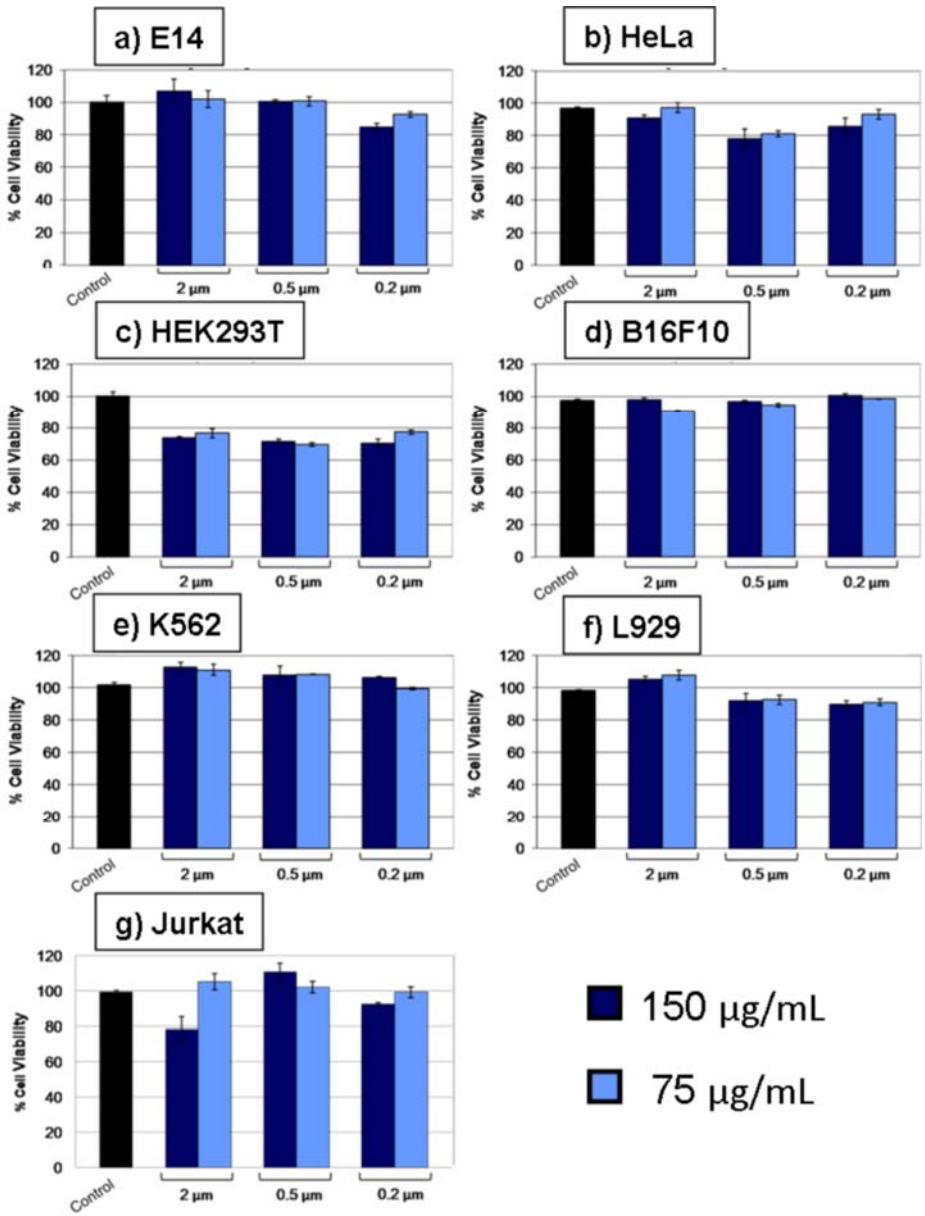

Graph 2.6. Cellular Viability. a) E14; **b)** HeLa; **c)** HEK293T; **d)** B16F10; **e)** K562; **f)** L929 and **g)** Jurkat cells in the presence of 75 and 150 µg/mL 0.2, 0.5 and 2 µm fluorescein labelled microspheres, (**2.16**), (**2.17**) and (**2.18**) respectively, assessed for viability by MTT assay. 'Control' (*black*) indicates untreated cells, assumed to be 100% viable. Analysis was performed after 24 hours.

Microspheres were found in the lung, liver and spleen but no adverse effects were noted in the animal, even after prolonged time periods. These results demonstrate that microspheres can be considered biocompatible.

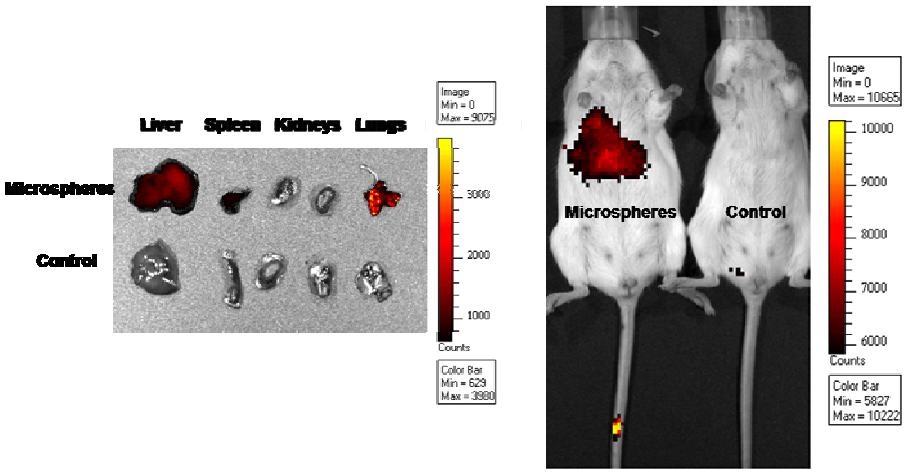

Figure 2.28. ***In Vivo.*** *Right:* A 6 week old mouse following intravenous tail vein injection of Cy7-coupled 0.5 μm microspheres (imaged after 6 hours, shown on the left – control animal, with no injection, shown on right); *Left:* Excised organs, showing microspheres in the lung, liver and spleen.

2.7. Conclusions

0.2, 0.5 and 2 μm microspheres have been prepared by emulsion and dispersion polymerisation and characterised by laser diffractometry and SEM. In particular, alteration of the conditions employed in the dispersion polymerisation of styrene, divinylbenzene and vinylbenzylamine in an alcoholic media generated microspheres with a wide range of controllable diameters from 0.4 μm up to 2 μm.

In addition, the polymer products were shown to be evenly sized with smooth, spherical morphologies and subsequently, the uptake of the microspheres was demonstrated in a wide range of cell lines, including mouse stem cells, suspension and adherent cell lines of both murine and human species. Uptake was found to be good over all lineages investigated and was additionally found to be not only cell line dependent, but also dependent on the microsphere diameter, concentration and the incubation time. MTT assays confirmed that the microspheres did not detrimentally affect cell viability at the concentrations analysed, demonstrating the micro-beads as efficient biocompatible cellular delivery devices.

Chapter 3: *Like Hot Bullets into Butter?*

3.1. Introduction

As described in ***Chapter 1***, permeability of the cellular membrane is strictly regulated and vital for cell survival.[105] In order for a molecule to passively diffuse across the lipid bilayer it must fulfil stringent criteria in terms of its molecular weight and solubility.[1] As such, many compounds are unable to enter cells under passive conditions and instead rely on energetic uptake mechanisms. Endocytosis is a general term for a number of cellular uptake pathways that include phagocytosis,[8] pinocytosis[7] and receptor mediated endocytosis.[9] These pathways are reliant upon an energy source[106] and result in vesicular formation around the cargo, which is subsequently internalised. As a consequence of endocytosis, the cargo is trapped within an acidic organelle (~ pH 5 - 6) known as an endosome, receptosome, phagosome or coated vesicle, dependent on the nature of the endocytosis and its cellular location (**Figure 3.1**).

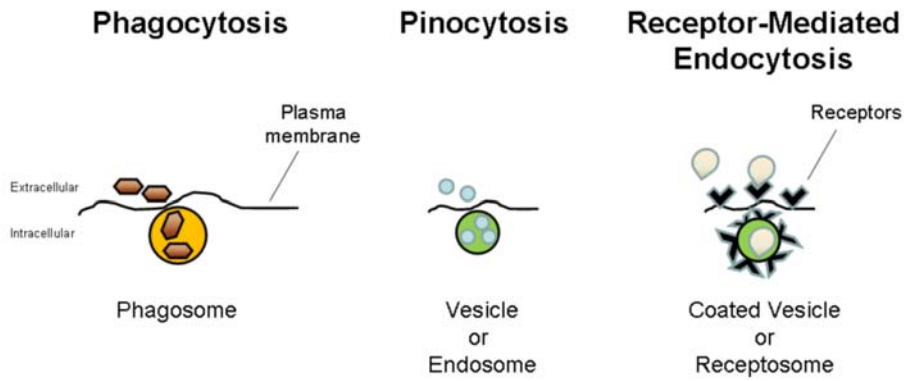

Figure 3.1. Endocytosis. Active uptake pathways can result in the cargo being trapped in phagosomes (*left*), endosomes (*middle*) or coated vesicles (*right*).[7, 8, 9]

The acidity of the vesicle is required for function of the degradative enzymes present within it and is maintained *via* proton pumps on the vesicular membrane. If a cargo is unable to escape the endosomal compartment then it will be trafficked from early endosomes to late endosomes and eventually to lysosomes, which have aggressive

degradation machinery, for example acid hydrolases (including nucleases and proteases) specifically capable of degrading a range of foreign materials.[16] For a cellular delivery device to be considered successful, its cargo must escape from the endosomal environment and be released cytoplasmically. Often, endosomal disrupting agents, such as chloroquine (a mild base, which accumulates in the acidic endosomes causing swelling and destabilisation), are required to force early release of the cargo from the endosome.[36] In the case of some delivery agents, such as some cationic lipids, they contain a component that facilitates release from the endosome. For example, dioleoylphosphatidylethanolamine (DOPE)[107] is thought to act *via* fusion of the lipid with the endosomal wall to facilitate release of the cargo cytoplasmically and is thus described to be "fusogenic".[108] Clearly, if a delivery vehicle requires the application of endosomal disrupting agents in order for the cargo to be delivered cytoplasmically, its use *in vivo* may be limited. As such, it was important to fully understand the mechanism of entry by which microspheres enter cells so as to fully appreciate the possible spectrum of their applications.

3.2. Microsphere Uptake

Despite the reasonably widespread intracellular use of microspheres, their mechanism of uptake by non-phagocytic cells is not well understood and detailed studies regarding their cellular uptake are limited.[109] In general, two main uptake mechanisms may be considered; active endocytic processes[110] and/or passive diffusive mechanisms.[111] Insertion into the lipid bilayer and diffusion to the intracellular environment has previously been suggested for carbon nanotubes[112, 113] after finding sodium azide (which interferes with the mitochondrial production of ATP, the main energy source for endocytosis) had a limited effect on uptake. Endocytosis as a mechanism for microsphere uptake has been supported by findings using commercially available microspheres.[109, 110, 114] However, this form of uptake does not explain how microspheres can be successfully used as pH and calcium sensors,[67, 68] which require cytoplasmic localisation for function. Furthermore, the results obtained from studies on microsphere uptake are highly variant due to

differences in experimental set-up, cell type, bead composition and functionality amongst other things, which often lead to contradictory results.

Following on from observations that microspheres with sizes between 0.2 and 2 μm are highly efficiently taken up by a diverse range of cell types it became increasingly important to understand how they entered cells. Consequently, it was the ambition of this chapter, to deduce the mechanism of intracellular uptake of 0.2, 0.5 and 2 μm amino functionalised polystyrene microspheres into cells using a number of techniques, both chemical and microscopy-based.

3.3. Chemical Inhibition of Uptake

The use of chemical inhibitors to selectively block endocytic pathways has been widely applied in uptake studies and successfully used to realise the mechanism of cellular entry for cationic lipids and carbon nanotubes.[35, 110] Chemical modulators of cellular uptake are simple to apply to cells and affordable (in comparison to more expensive antibodies for receptor staining). However, many of the inhibitors are organic compounds insoluble in water and often require solvation in aggressive and cytotoxic solvents, such as dimethylsulfoxide (DMSO) or methanol. As a result, the use of a chemical blockade can result in unwanted toxicity, which can complicate and confuse results.[115] However, at appropriate doses and with appropriate controls, chemical inhibitors can be used without significant cellular damage.

3.3.1. General Energy Dependence Blockade

Adenosine triphosphate (ATP) is used by the cell as an energy source for many endocytosis-mediated uptake processes[106] and sodium azide is a general inhibitor of most energy dependent mechanisms within the cell[116] (including endocytosis) as it inhibits the production of ATP by interfering with ATP hydrolase in the mitochodria.[117] With low doses and short pre-incubation times required in order to observe inhibition,[118] sodium azide presents itself as an excellent candidate for initial investigation of microsphere uptake. In order to first establish an appropriate dosage, mouse melanoma B16F10 cells were pre-incubated with 20 mM sodium azide for 1 hour prior to the addition of positive controls, known to be ingested by energy-

dependent mechanisms to establish that the concentration of sodium azide was sufficient to block endocytosis. Lactosylceramide (LacCer), an important constituent of the plasma membrane, is widely accepted to be internalised by caveolae-mediated endocytosis[15] and blood plasma protein, transferrin, is known to enter cells *via* the clathrin-mediated pathway.[13] As such, BODIPY FL C_5-LacCer and FITC-conjugated transferrin were incubated with sodium azide treated B16F10 cells and their uptake analysed by flow cytometry after 2 hours (**Graph 3.1**). Externally bound transferrin was removed by an acidic wash (pH 5.0)[119] and externally bound LacCer was removed by washing cells with 1% bovine serum albumin (BSA) in PBS.[120]

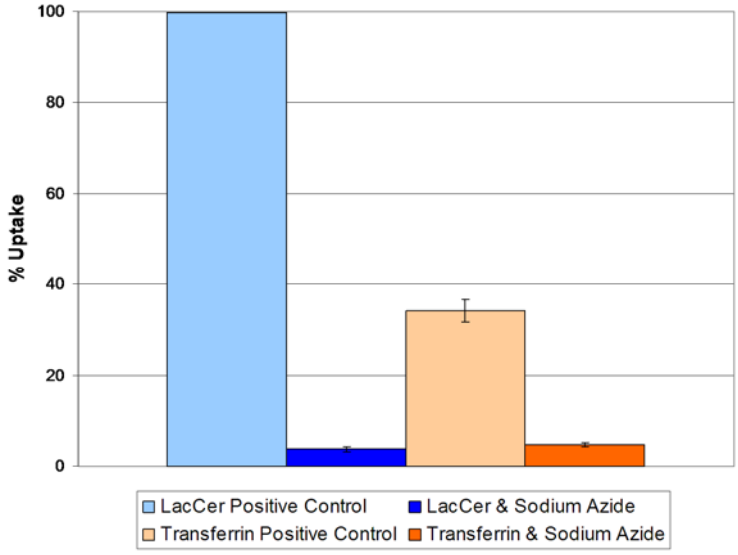

Graph 3.1. Positive Controls. Inhibition of LacCer (5 µM) and transferrin (70 µg/mL) uptake in B16F10 cells following treatment with 20 mM sodium azide.

20 mM sodium azide was sufficient to cause an 86% reduction in transferrin uptake and a 96% decrease in LacCer uptake in B16F10 mouse melanoma cells. Thus, B16F10, human embryonic kidney (HEK293T) cells, human cervical cancer (HeLa) cells and mouse fibroblast (L929) cells were pre-incubated with 20 mM sodium azide prior to the addition of 0.2, 0.5 or 2 µm fluorescein labelled microspheres, (**2.16**), (**2.17**) and (**2.18**) respectively. In addition, mouse embryonic stem (E14) cells were treated with sodium azide to assess the energy dependence on beadfections in stem cells. Uptake was assessed after 3 hours in 0.2% trypan blue in Hank's Balanced Saline Solution (HBSS), which is a well documented quencher of

extracellular fluorescence associated to fluorescein-like fluorophores (***Chapter 2***)[101, 121] and the results are summarised in **Graphs 3.2a-e**.

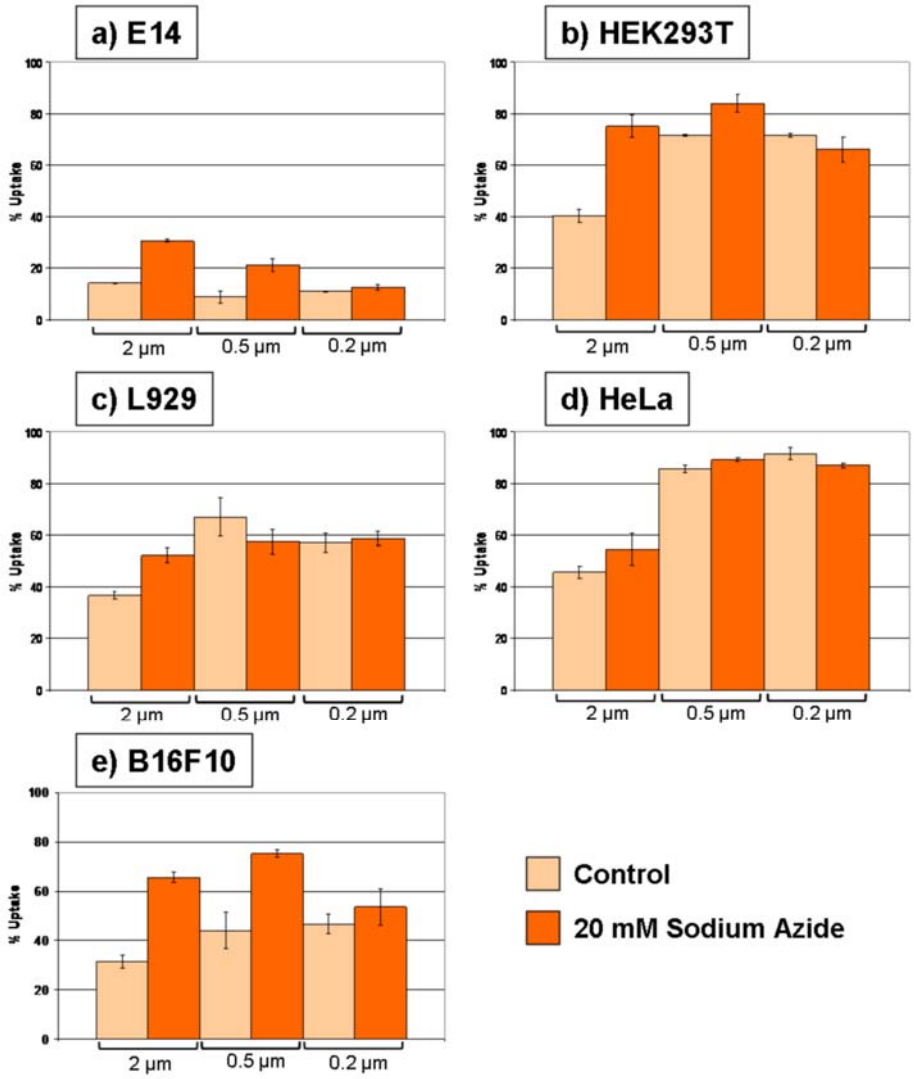

Graph 3.2. Effect of Sodium Azide. Uptake of 2, 0.5 and 0.2 µm fluorescein microspheres under ATP depletion by 20 mM sodium azide in **a)** E14 mES; **b)** HEK293T; **c)** L929; **d)** HeLa and **e)** B16F10 cells.

At concentrations of sodium azide that resulted in almost complete inhibition of transferrin and LacCer endocytosis, microsphere uptake was still prevalent in all the cell lines analysed and was virtually indistinguishable from control cells treated with microspheres in the absence of sodium azide. Indeed, in some cells (e.g. E14 cells) uptake was even mildly increased. This was confirmed by microscopy, showing B16F10 cells in **Figure 3.2** as a representative example.

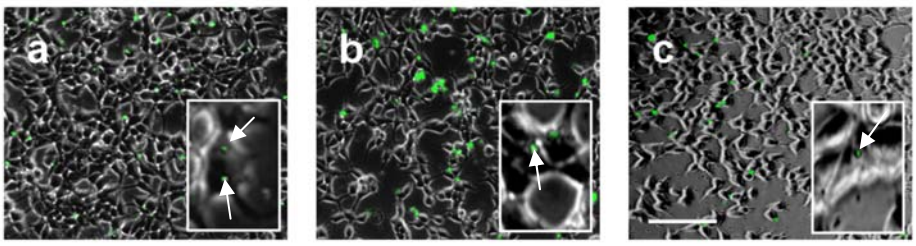

Figure 3.2. Microscopy of Sodium Azide Treated Cells. Pseudo confocal optical slices of B16F10 cells pre-treated with 20 mM sodium azide and beadfected (86 µg/mL) for 3 hours with **a.** 2 µm; **b.** 0.5 µm and **c.** 0.2 µm fluorescein microspheres. Scale bar is 400 µm. Inset images are 4× magnification.

This suggests that, in all the cell lines studied, the mechanism by which microspheres of 2, 0.5 and 0.2 µm diameter enter cells is not dependent on ATP as an energy source. In consideration that endocytosis is an energy-dependent process, it additionally suggests that the microspheres are not ingested by endocytosis, a finding that is supported by the use of microspheres in intracellular sensing studies. However, a more detailed evaluation was required before an energy dependent mechanism could be wholly discounted.

Since all the cell lines analysed for the uptake of microspheres under ATP depletion showed no significant changes in uptake levels at concentrations which near fully blocked transferrin and LacCer ingestion, one cell line was selected for a more detailed analysis of microsphere uptake. B16F10 mouse melanoma cells were selected as they are well studied and durable as well as having efficient uptake of 2, 0.5 and 0.2 µm microspheres after short incubation times.

3.3.2. Toxicity Assays of Chemically Treated Cells

In consideration that toxicity associated with the use of chemical inhibitors can confuse the results obtained from an uptake study (as during cell death the membrane can become permeable allowing cellular influx of foreign material, e.g. microspheres), it was important to establish cellular viability following treatment with chemical modulators (**Graph 3.3**).

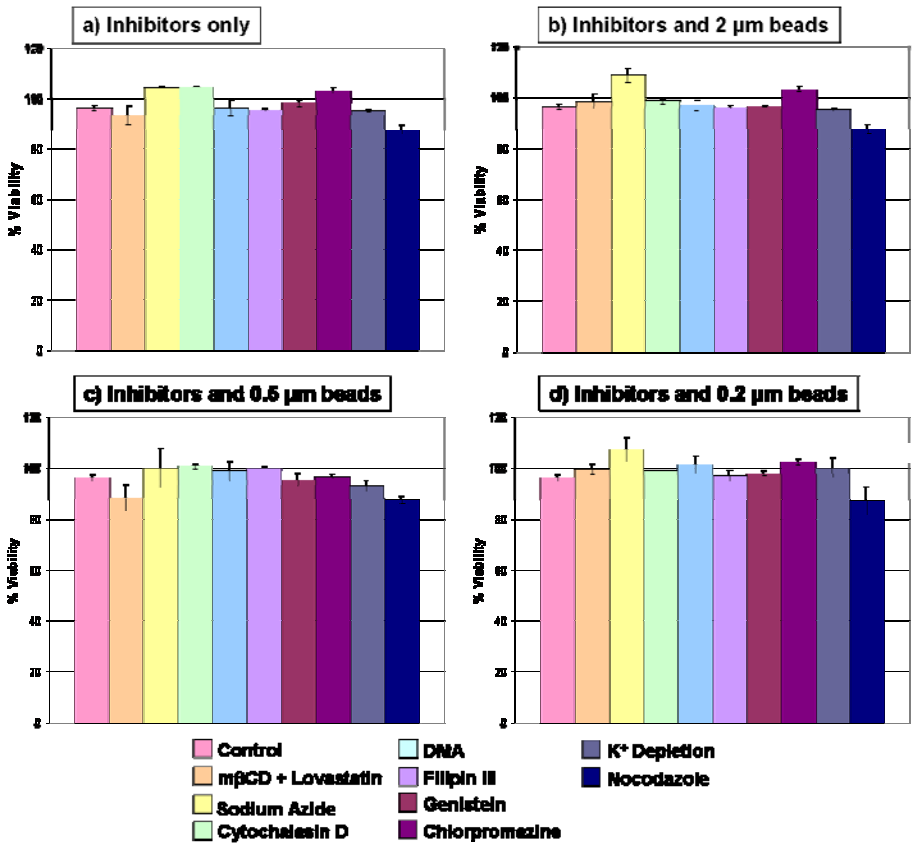

Graph 3.3. Cellular Viability of Chemically Treated Cells. MTT assay results in B16F10 cells with **a)** Chemical inhibitors only (after 1 hour); **b – d)** Chemical inhibitors followed by microspheres **b)** 2 µm microspheres; **c)** 0.5 µm microspheres; **d)** 0.2 µm microspheres. The concentrations of chemical inhibitor used were those used in uptake assays. Microsphere concentration was 86 µg/mL. 'Control' refers to untreated cells.

B16F10 cells were found to be resilient to the addition of a variety of chemical inhibitors (targeting membrane cholesterol levels, caveolae and clathrin-mediated endocytosis and macropinocytosis), even following incubation with microspheres. The viability was more than 80% by MTT assay in all cases demonstrating that cellular function was reasonably unaffected by the addition of chemical inhibitors at the concentrations required to provide a blockade on energy-dependent processes. This demonstrated that microsphere uptake following chemical modulation of endocytosis was not due to membrane fragility or permeability associated to toxicity.

3.3.3. Cholesterol Dependence

Cholesterol is an important constituent of the cellular membrane that is often summoned during endocytosis and is considered to be vital to most endocytic

mechanisms.[122] Inhibitors which can remove and/or inhibit the production of cholesterol include mβ-cyclodextrin (mβCD), which binds strongly to cholesterol present in the cellular membrane and removes it from the cell[123] and lovastatin, which prevents the formation of new cholesterol by inhibiting 3-hydroxy-3-methyl-glutaryl-CoA reductase (HMG-CoA reductase).[124] As such, B16F10 mouse melanoma cells were pre-incubated with 10 mM mβCD and 1 μg/mL lovastatin (concentrations that were sufficient to block the uptake of transferrin and LacCer, **Graph 3.4**) for 1 hour prior to the addition of microspheres.

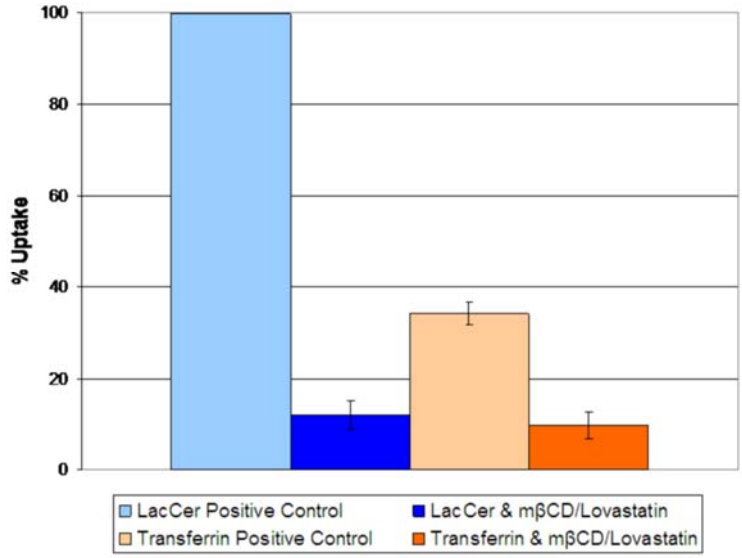

Graph 3.4. Positive Controls. Inhibition of LacCer (5 μM) and transferrin (70 μg/mL) uptake by B16F10 cells following treatment with 10 mM mβCD and 1 μg/mL lovastatin.

After 3 hours incubation with beads, uptake was assessed by flow cytometry in 0.2% trypan blue (**Figure 3.3**). At concentrations that significantly inhibited the uptake of transferrin and LacCer controls, no significant decreases in uptake could be observed for the microspheres, suggesting that uptake was not reliant on cholesterol mobility in B16F10 cells.

3.3.4. Caveolae-Mediated Endocytosis

Following from the findings that ATP depletion and cholesterol inhibition/sequestering failed to inhibit the uptake of microspheres in B16F10 cells, more specific analysis was made of individual endocytic mechanisms.

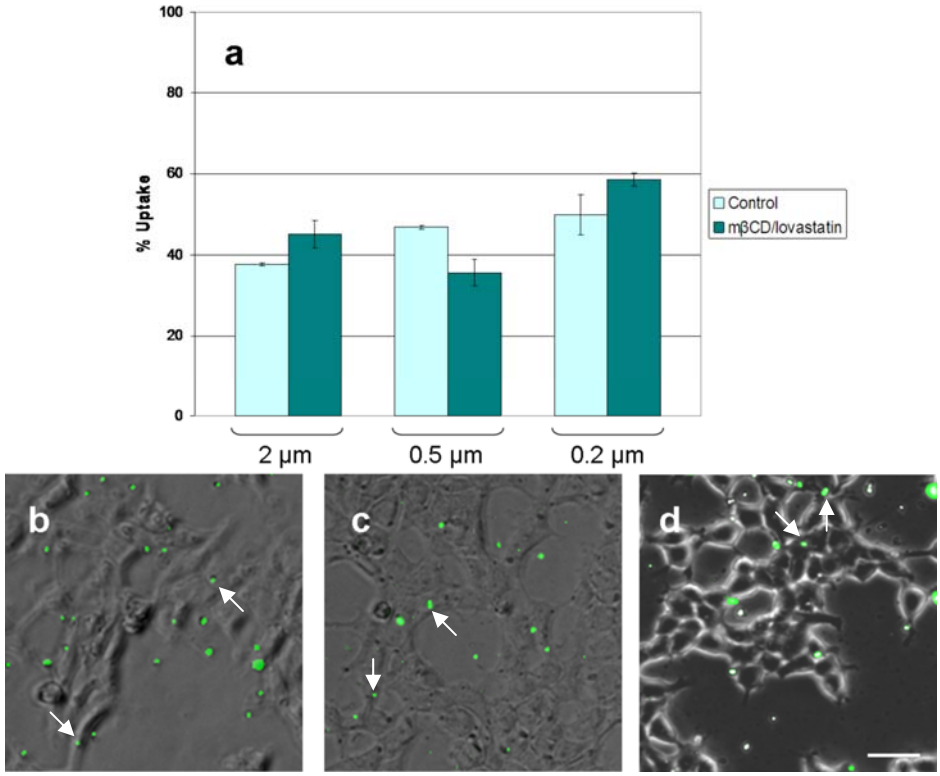

Figure 3.3. Effect of Cholesterol Depletion. B16F10 cells pre-treated with 10 mM mβCD and 1 µg/mL lovastatin. *Top:* **a**. Uptake of 2, 0.5 and 0.2 µm fluorescein microspheres (86 µg/mL) by flow cytometry; *Bottom:* Pseudo-confocal microscopy of B16F10 cells under cholesterol depletion with **b.** 2 µm; **c.** 0.5 µm and **d.** 0.2 µm fluorescein microspheres. Analysis was made after 3 hours. Scale bar is 50 µm.

Caveolae mediated endocytosis results in the formation of flask-shaped invaginations into the lipid bilayer lined with the protein, caveolin.[14] It can be selectively blocked with filipin III and genistein,[125, 126] which sequester cholesterol from lipid rafts (which are essential for caveolae formation) and inhibit a tyrosine kinase (which is required to phosphorylate the proteins involved in caveolae formation) respectively. In order to establish the appropriate concentrations which result in the near-complete inhibition of caveolae-mediated endocytosis, B16F10 cells were pre-treated with a range of concentrations of filipin III and genistein followed by the addition of BODIPY-labeled LacCer (known to be ingested by this mechanism), with analysis by flow cytometry (**Graph 3.5**). Concentrations of 5 µg/mL filipin III and 200 µM genistein resulted in an approximate 97% reduction in uptake of LacCer.

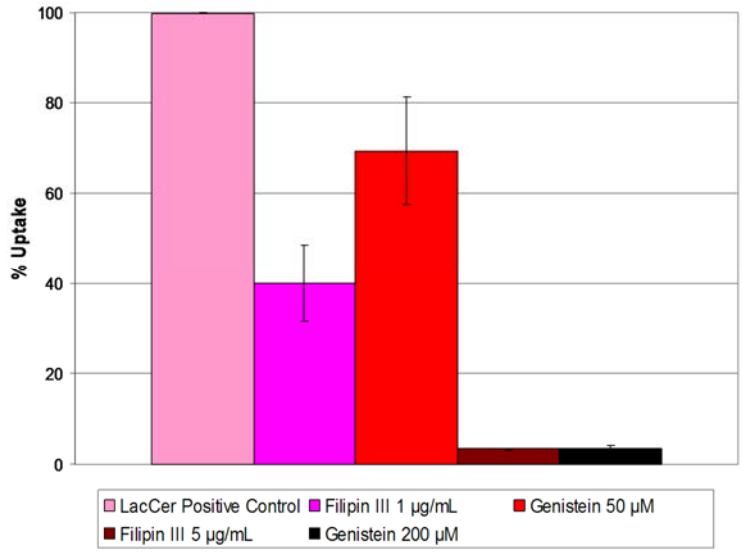

Graph 3.5. Lactosylceramide Control for Caveolae-Mediated Endocytosis. Uptake of BODIPY-LacCer (5 µM) after 2 hours in B16F10 cells with caveolae inhibition by filipin III (1 – 5 µg/mL) or genistein (50 – 200 µM).

As such, cells were pre-treated with the inhibitors for 1 hour prior to the addition of 2, 0.5 and 0.2 µm fluorescein labelled microspheres and flow cytometric analysis (**Figure 3.4,** *top*). However, microsphere uptake was unaffected by the inhibition of caveolae-mediated endocytosis at concentrations which resulted in the near-complete inhibition of LacCer uptake. Microscopic examination (**Figure 3.4,** *bottom*) was carried out to confirm microsphere uptake under caveolae-mediated endocytosis inhibition. These results suggest endocytosis linked to caveolae is not responsible for microsphere uptake, confirming the results achieved with sodium azide and mβCD/lovastatin.

3.3.5. Clathrin-Mediated Endocytosis

In consideration that caveolae invaginations into the cellular membrane are only 50 – 100 nm in diameter[127] it may not be surprising that microspheres, which are 4 to 40 times larger than these regions, are not ingested *via* this mechanism. As such, clathrin-mediated endocytosis, which can result in the formation of larger sized vesicles largely dependent on the diameter of the cargo,[12] was investigated. Clathrin-mediated endocytosis is inhibited by treatment with chlorpromazine[128] and by incubating cells under potassium free conditions.[10]

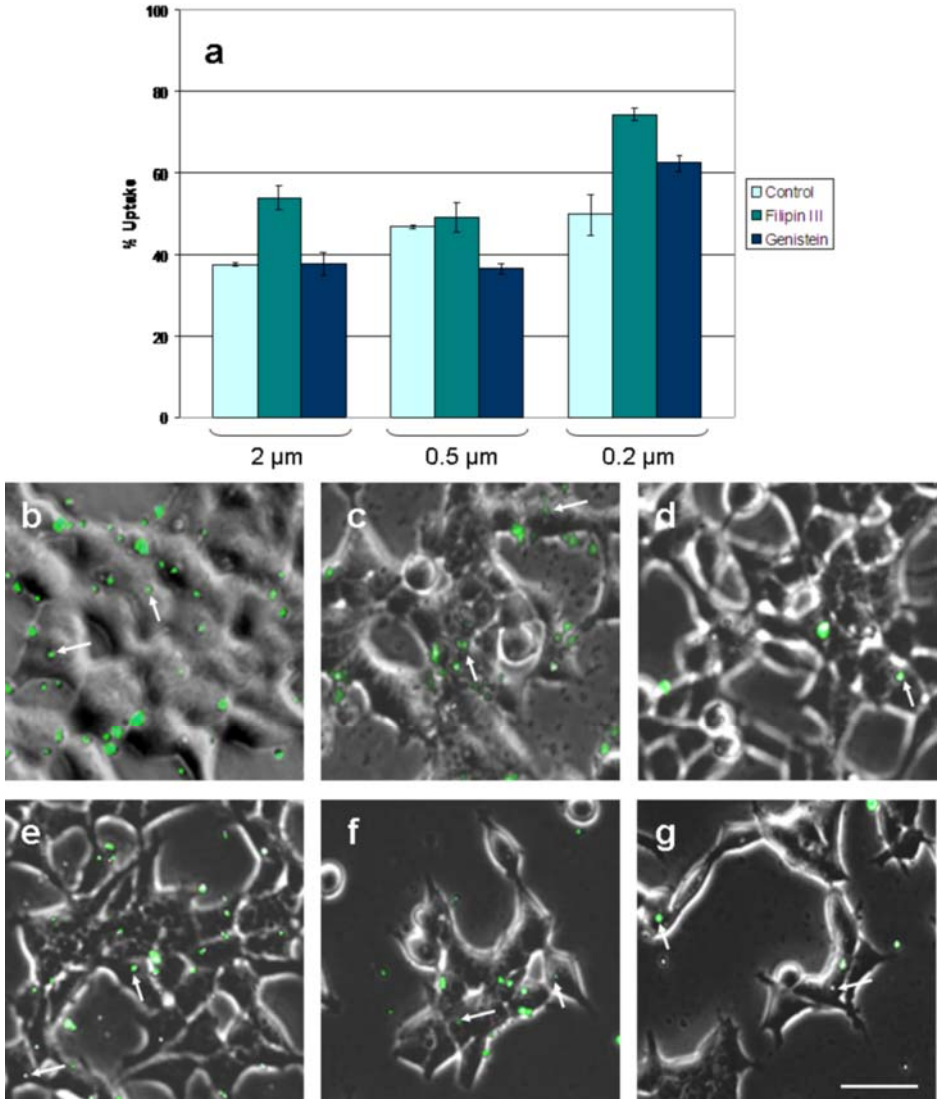

Figure 3.4. Effect of Caveolae Depletion. B16F10 cells pre-treated with 200 µM genistein and 5 µg/mL filipin III. *Top:* **a.** Uptake of 2, 0.5 and 0.2 µm fluorescein microspheres (86 µg/mL) by flow cytometry; *Bottom:* Pseudo-confocal microscopy of B16F10 cells under caveolae-mediated endocytosis inhibition with **b.** genistein and 2 µm; **c.** genistein and 0.5 µm; **d.** genistein and 0.2 µm; **e.** filipin III and 2 µm; **f.** filipin III and 0.5 µm and **g.** filipin III and 0.2 µm fluorescein microspheres. Analysis was made after 3 hours. Scale bar is 100 µm.

Chlorpromazine and potassium depletion are known to disrupt the clathrin-mediated pathway by preventing coated pit assembly. Again, flow cytometric analysis was used to determine the appropriate concentrations of chlorpromazine-mediated inhibition using FITC-conjugated transferrin (**Graph 3.6**).

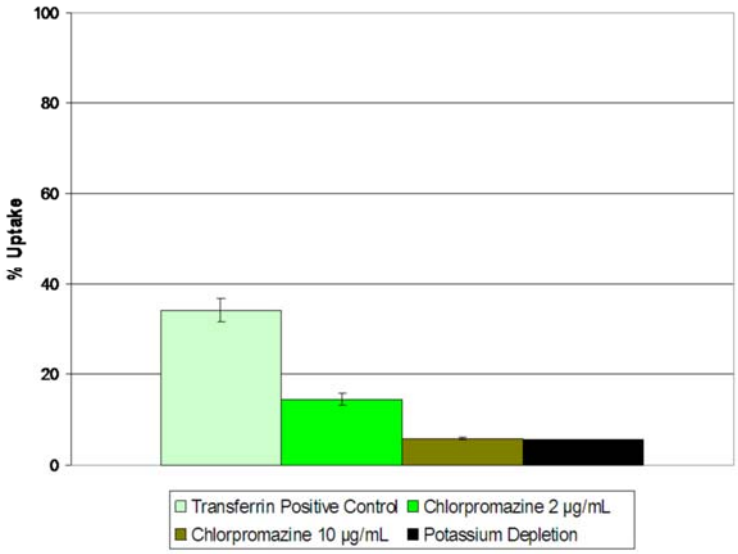

Graph 3.6. Transferrin Control for Clathrin-Mediated Endocytosis. Uptake of FITC-transferrin (70 µg/mL) after 2 hours in B16F10 cells with clathrin inhibition by chlorpromazine (2 – 10 µg/mL) or potassium depleted conditions.

As such, B16F10 cells were grown under potassium-free conditions (see Experimental for details) or treated with 10 µg/mL chlorpromazine (which resulted in an 86% reduction in transferrin uptake) for 1 hour prior to the addition of 2, 0.5 and 0.2 µm microspheres. Analysis of uptake was *via* flow cytometry (**Figure 3.5,** *top*) in a trypan blue quenching solution. At concentrations which significantly inhibited transferrin uptake, microsphere entry into cells was virtually indistinguishable from controls where beads were incubated with cells in the absence of chlorpromazine or under potassium-supplemented conditions. Microscopy (**Figure 3.5,** *bottom*) confirmed microsphere uptake, establishing that clathrin mediated endocytosis is unlikely to be responsible for the ingestion of microspheres into cells.

3.3.6. Microtubule Polymerisation

Lipid raft mediated uptake and intracellular vesicular trafficking is thought to be dependent upon microtubule polymerisation and is known to be blocked by nocodazole.[129] It was of interest as to what effect microtubules have on the uptake and transport of microspheres.

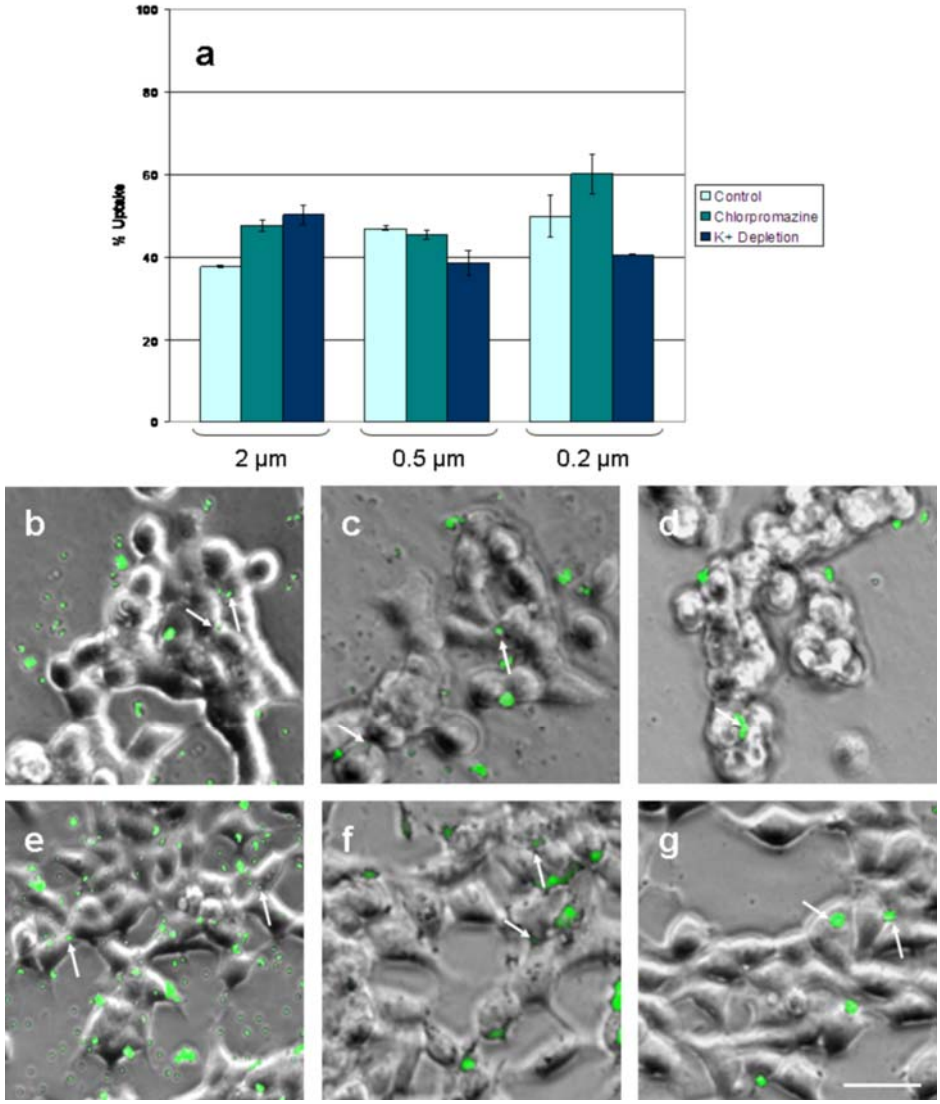

Figure 3.5. Effect of Clathrin Depletion. B16F10 cells pre-treated with 10 µg/mL chlorpromazine or potassium depletion. *Top:* **a.** Uptake of 2, 0.5 and 0.2 µm fluorescein microspheres (86 µg/mL) by flow cytometry; *Bottom:* Pseudo-confocal microscopy of B16F10 cells under clathrin-mediated endocytosis inhibition with **b.** chlorpromazine and 2 µm; **c.** chlorpromazine and 0.5 µm; **d.** chlorpromazine and 0.2 µm; **e.** potassium depletion and 2 µm; **f.** potassium depletion and 0.5 µm and **g.** potassium depletion and 0.2 µm fluorescein microspheres. Analysis was made after 3 hours. Scale bar is 100 µm.

As such B16F10 cells were pre-incubated with 10 µg/mL nocodazole before the introduction of fluorescein microspheres. Uptake was analysed by flow cytometry and is summarised by **Figure 3.6**.

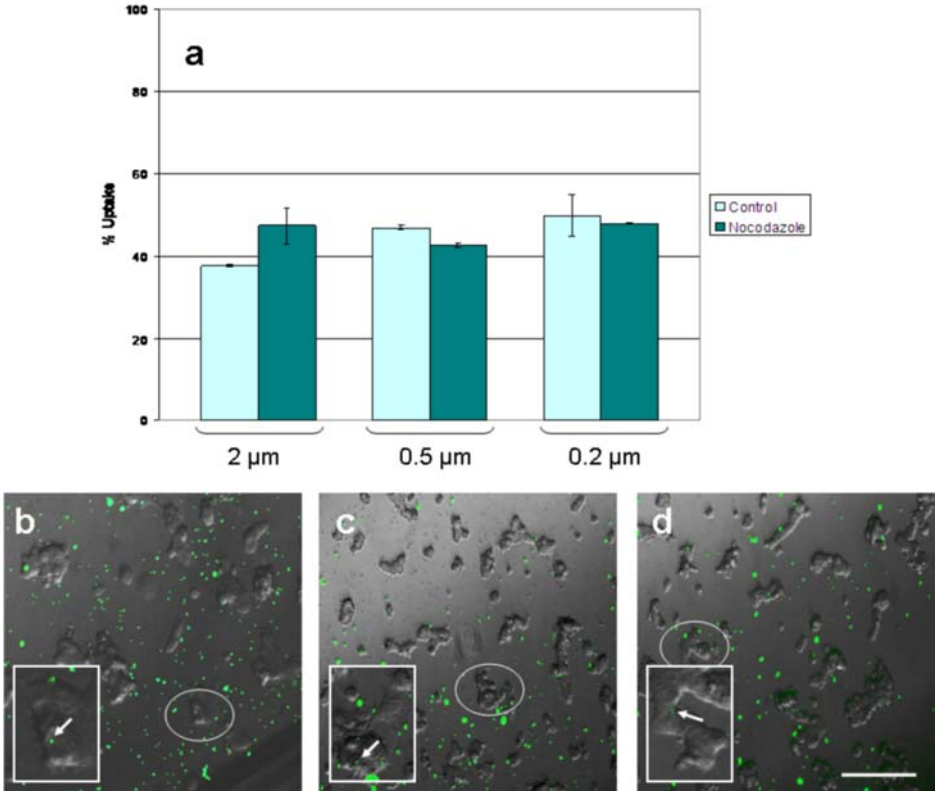

Figure 3.6. Effect of Nocodazole. B16F10 cells pre-treated with 10 µg/mL nocodazole. *Top:* **a.** Uptake of 2, 0.5 and 0.2 µm fluorescein microspheres (86 µg/mL) by flow cytometry; *Bottom:* Pseudo-confocal microscopy of B16F10 cells under microtubule polymerisation inhibition with **b.** 2 µm; **c.** 0.5 µm; **d.** 0.2 µm fluorescein microspheres. Scale bar is 200 µm. Inset images are a 4× magnification and analysis was performed after 3 hours.

Inhibition *via* nocodazole had little effect on microsphere uptake, suggesting microtubule polymerisation and lipid raft mediated uptake are not fundamental to either the interaction of the microspheres with the cellular membrane or the passage of the microspheres across the lipid bilayer. Microscopy confirmed microsphere uptake (**Figure 3.6,** *bottom*) and taken together, these results further confirm that endocytosis is unlikely to be the mechanism by which microspheres are internalised within B16F10 mouse melanoma cells.

3.3.7. Macropinocytosis

Specific endocytosis pathways associated to caveolin or clathrin appear not to be responsible for microsphere uptake. Thus, it was of interest to examine a non-specific endocytic pathway, such as macropinocytosis, whereby a ruffling-like

procedure by the cell membrane results in the formation of a vesicle, which may subsequently be internalised.[130] Macropinocytosis can be blocked by incubation of cells with cytochalasin D[131] and dimethylamiloride (DMA).[132] Cytochalasin D interferes with F-actin elongation and consequently prevents the non-specific membrane ruffling that accounts for macropinocytosis. Whereas DMA is an inhibitor of Na^+/H^+ exchange, which influences the sodium ion concentration important to the stimulation of cells to undergo macropinocytosis.

Thus, B16F10 cells were incubated with 10 μM cytochalasin D and DMA prior to the addition of 0.2, 0.5 and 2 μm microspheres and flow cytometric analysis (**Figure 3.7,** *top*) was performed to assess uptake. In the case of DMA, no significant reduction in microsphere uptake was observed and microscopy confirmed uptake (**Figure 3.7,** *bottom*). However, a contradictory result was obtained with cytochalasin D. In this case, over all microsphere diameters, a decrease in uptake was observed. This equated to a 26 – 63% reduction, dependent on the microsphere size. 0.5 μm microspheres showed the greatest decrease in uptake going from 47% uptake in 3 hours to just over 17% under cytochalasin D conditions. Both 2 μm and 0.2 μm microspheres saw a decrease of 26% under cytochalasin D conditions.

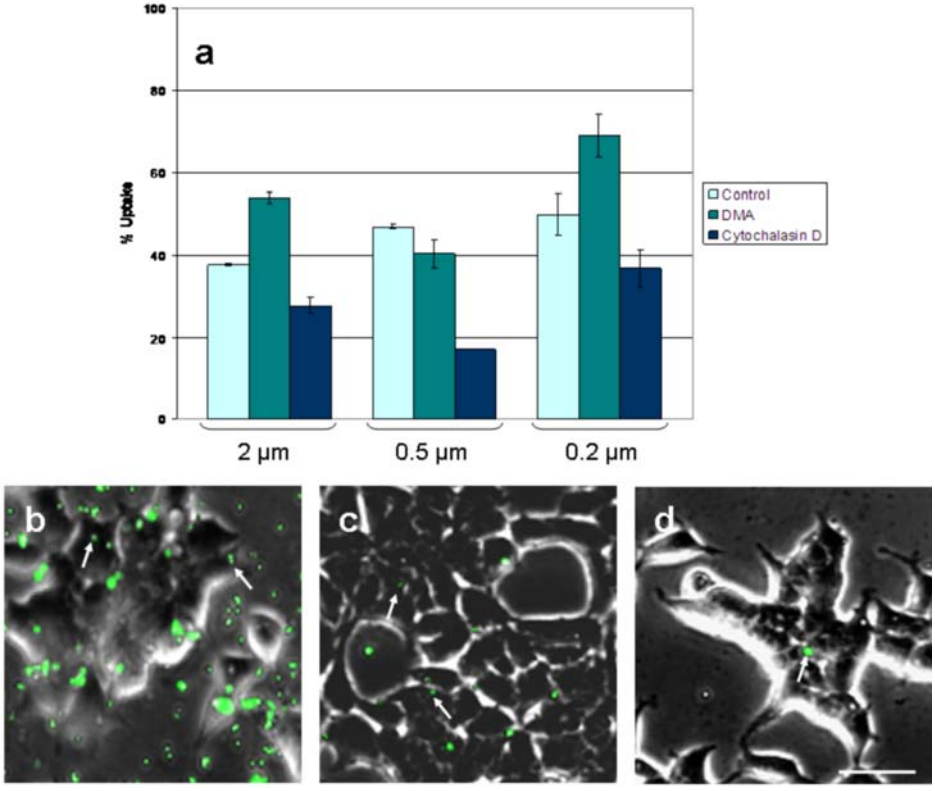

Figure 3.7. Effect of Macropinocytosis Inhibition. B16F10 cells pre-treated with 10 μM

cytochalasin D or 10 μM dimethylamiloride (DMA). *Top:* **a.** Uptake of 2, 0.5 and 0.2 μm fluorescein microspheres (86 μg/mL) by flow cytometry; *Bottom:* Pseudo-confocal microscopy of B16F10 cells under dimethylamiloride-mediated inhibition of macropinocytosis with **b.** 2 μm; **c.** 0.5 μm; **d.** 0.2 μm fluorescein microspheres. Analysis was performed after 3 hours. Scale bar is 100 μm.

Microscopy, with staining of the actin filaments (which are degraded by incubation with cytochalasin D)[133] with AlexaFluor-568 phalloidin,[134] confirmed disruption of the actin cytoskeleton and lack of microsphere uptake in cells pre-treated with cytochalasin D (**Figure 3.8**).

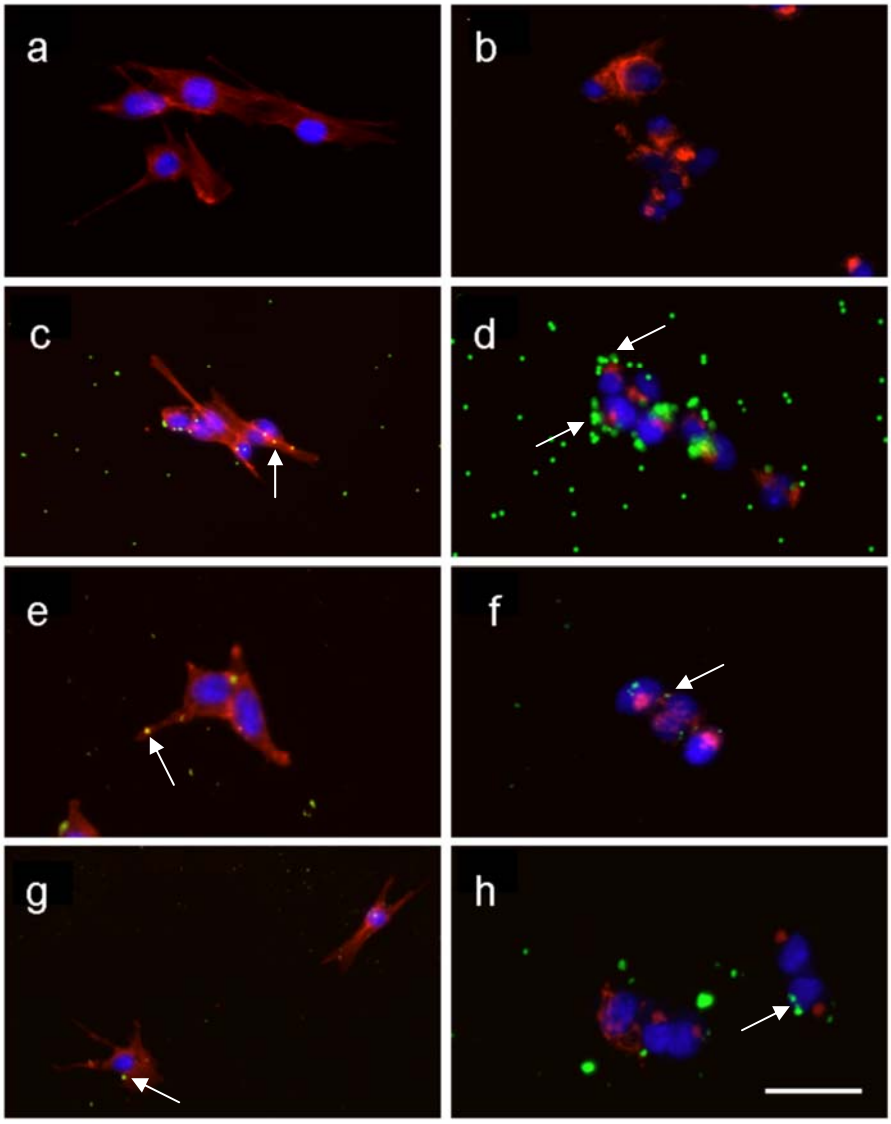

Figure 3.8. Microscopy of Cytochalasin D Treated Cells. B16F10 cells incubated under standard incubation conditions (**a, c, e** and **g**) and in the presence of cytochalasin D (**b, d, f** and **h**). **a**. and **b**. are control cells with no microspheres; **c**. and **d**. are with 2 μm FAM-beads; **e**. and **f**. are with 0.5 μm FAM-beads; **g**. and **h**. are with 0.2 μm FAM-beads. Actin filaments are stained with AlexaFluor 568-

phalloidin and the cell nuclei are stained with Hoechst 33342. Microsphere concentrations was 86 µg/mL and analysis was performed after 3 hours. Scale bar is 140 µm.

Instead, the microspheres appeared clustered around the extracellular membrane of the cell, unable to cross to the intracellular environment. Cytochalasin D non-specifically interferes with the polymerisation of actin, resulting in degradation. F-Actin is an important protein involved in many transport processes and is a fundamental constituent of the cytoskeleton.[135] Degradation may consequently have a negative impact on the cellular architecture, which may be important for microsphere uptake, for example in the interaction of microspheres with the cellular membrane.

In consideration that dimethylamiloride, sodium azide and cholesterol inhibitors failed to decrease microsphere uptake it is unlikely that the results achieved with cytochalasin D are due to direct inhibition of macropinocytosis. Furthermore, macropinocytosis is an uptake mechanism seen mostly in professional phagocytic cells (which B16F10 are not). In addition to this, membrane ruffling resulting in macropinocytosis is seen mostly in the uptake of solutes and is improbable for large particulates such as microspheres.[129, 136]

To further elucidate this finding, non-specific membrane ruffling was also disfavoured by allowing cells to grow to 100% confluency (which disfavours membrane ruffling through steric effects)[137] before addition of fluorescent microspheres. Flow cytometry was used to determine microsphere uptake and a control was established with cells at 50% confluency (**Graph 3.7**).

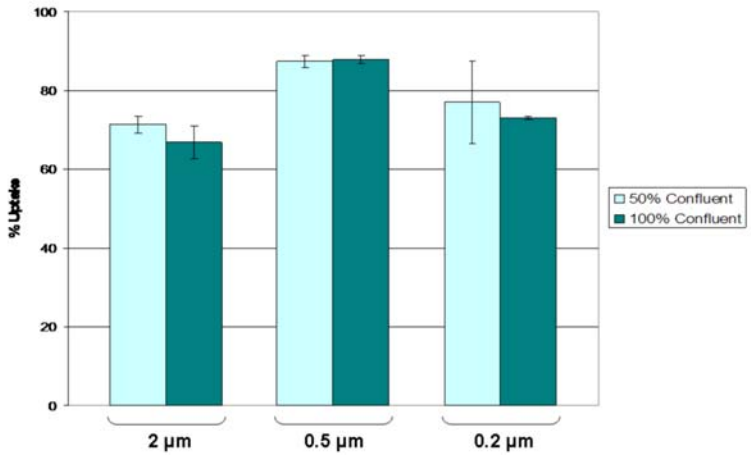

Graph 3.7. Effect of Membrane Ruffling. 2, 0.5 and 0.2 µm microsphere uptake in B16F10 cells

after 6 hours grown to 100% confluency (control is 50% confluency). Microsphere concentration was 86 μg/mL for 100% confluency or 43 μg/mL for 50% confluent cells.

Microsphere uptake was not affected by cell confluency, further suggesting that the non-specific membrane ruffling that may account for macropinocytosis is not responsible for microsphere intake into cells. This strongly suggests that the decreases in uptake observed after pre-incubation with cytochalasin D were due to a possible interference with the cellular cytoskeleton, which may result in a poorer interaction of the microspheres with the cell or may hinder the passage of microspheres across the bilayer.

3.4. Temperature Dependence of Uptake

Low temperatures have a substantial effect on cellular uptake processes. For example, energy dependent pathways are generally considered to be "blocked" by temperatures considerably lower than those found in normal incubations (as cellular reactions start to slow down).[138] In addition, hardening of the lipid bilayer at lowered temperatures will slow some passive diffusive mechanisms due to the increased viscosity of the membrane.[139] Accordingly, it was of interest to investigate the temperature dependence on microsphere uptake and, thus, B16F10 cells were incubated at 37, 20 and 4 ºC and entry of microspheres into the cells assessed after 3 hours by flow cytometry and microscopy (see **Figure 3.9**). In all cases, uptake was dramatically lowered at 20 °C and the effect was even more pronounced at 4 °C. **Figure 3.9** (*far bottom*) shows microspheres anchored to the extracellular regions of the cell but not yet in the intracellular environment. In consideration that general and specific endocytosis inhibitors failed to decrease uptake, it is likely that this reduction in uptake is due to hardening of the lipid bilayer and a decrease in membrane fluidity.

These results suggest a plausible mechanism of microsphere uptake may be that the bead anchors to the extracellular matrix through ionic (due to the amino functionality) or hydrophobic (due to the polystyrene matrix) interactions and, after a period of time dependent upon the microsphere diameter, sinks into the bilayer and

makes its passage to the intracellular region. Such a mechanism would not be reliant upon ATP, cholesterol or vesicle formation associated to endocytosis but would require membrane fluidity and, in the initial stages, would rely on an intact cytoskeleton for efficient microsphere-cell contact.

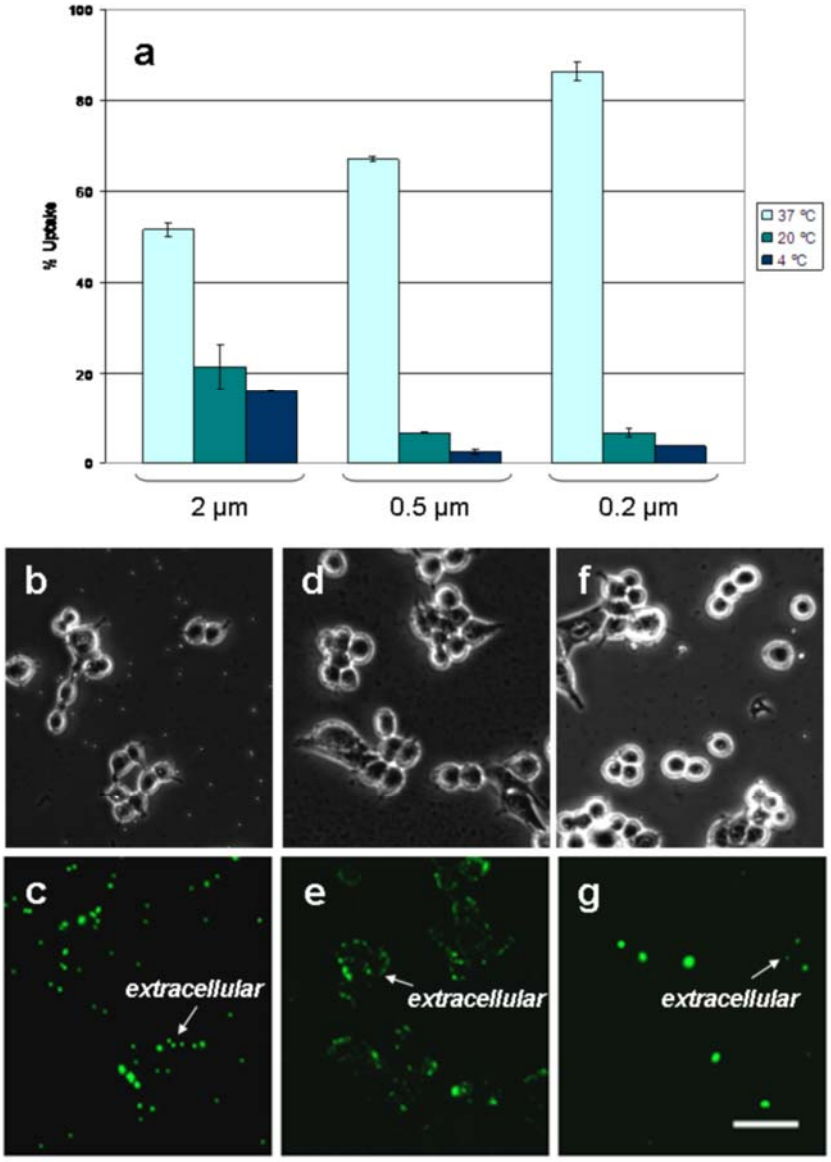

Figure 3.9. Effect of Temperature. Beadfections (86 µg/mL) in B16F10 cells after 3 hours. **a.** Uptake of 0.2, 0.5 and 2 µm fluorescein microspheres at 37, 20 and 4 ºC by flow cytometry. *Bottom:* Pseudo-confocal microscopy at 20 ºC with **b./c.** 2 µm; **d./e.** 0.5 µm; and **f./g.** 0.2 µm fluorescein microspheres. **b**, **d** and **f** are brightfield images and **c**, **e** and **g** are fluorescence images, showing microspheres in green. Scale bar is 100 µm.

3.5. Scanning Electron Microscopy

In order to further study the interaction of microspheres with the extracellular membrane of cells, scanning electron microscopy (SEM) was performed on B16F10 mouse melanoma cells incubated with unlabelled 2 µm microspheres (**2.10**) for 2 - 24 hours (**Figure 3.10**).[140] After 2 hours, the microspheres were seen anchored to the membrane of the cell. It is unlikely that microspheres just settle on the cell (as cells were subjected to extensive washing during SEM preparation, see Experimental for details) and so it is proposed that they "adhere" to the cell by some sort of ionic (as microspheres are amino functionalised) or hydrophobic interactions (as microspheres are composed of polystyrene chains).

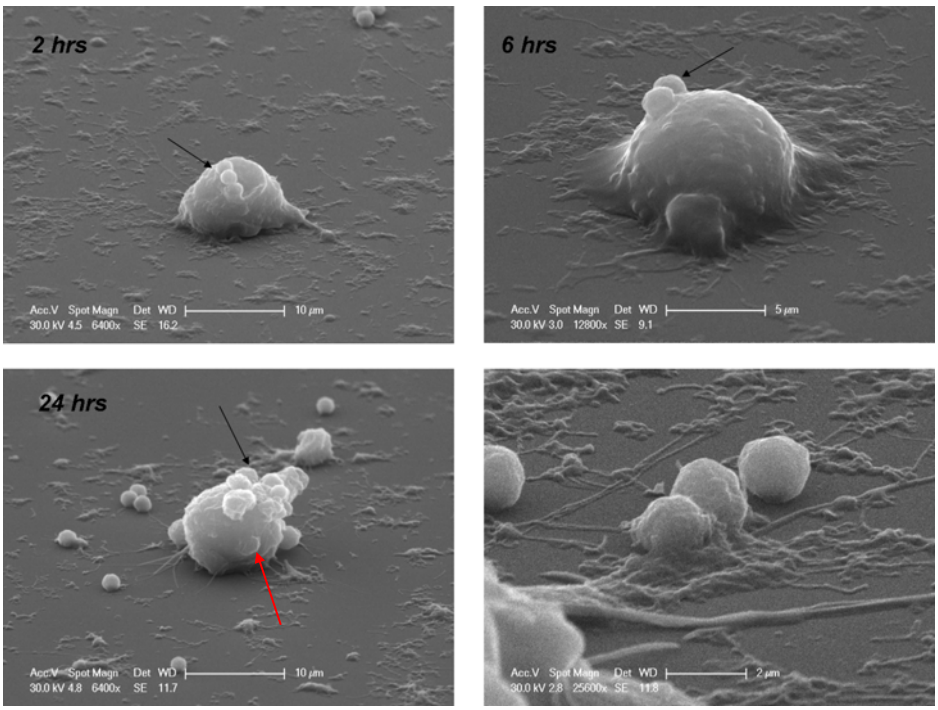

Figure 3.10. Scanning Electron Microscopy. Images of B16F10 cells incubated with 2 µm microspheres (*black arrows*) for 2 hours (*top left*) (scale bar is 10 µm), 6 hours (*top right*) (scale bar is 5 µm) and 24 hours (*bottom left*) (scale bar is 10 µm). Microspheres are shown in the bottom right panel (scale bar is 2 µm). Microsphere concentration was 86 µg/mL.

However, after 6 hours, the microspheres appear not only anchored to the cell but also appear to be grafted on (possibly coated by serum proteins). In addition, the microspheres appear to be "seeping" through the membrane of the cell and there is

no appearance of membrane ruffling or vesicular formation around the microspheres. At 24 hours, the microspheres appear clearly distorted with possible serum proteins grafted over their surface making their inherent spherical structure almost unrecognisable. Again, microspheres are seen seeping into the cell (*red arrow*) without the appearance of a vesicle around the beads. **Figure 3.10** additionally shows microspheres not associated to the cell (*bottom right panel*), but associated to possible serum proteins, which appear to be grafting to the beads. These serum proteins (which aid the adhesion of cells to a biocompatible surface) may be aiding the adhesion of polystyrene microspheres to the cell, which may ultimately allow the microsphere to make its passage across the lipid bilayer. However, this explanation does not explain why microspheres enter cells efficiently under serum-free conditions and indicates that the circumstances under which microspheres and cells interact is a complex event.

3.6. Endosomal and Lysosomal Markers

Although chemical inhibition of endocytic pathways had little effect on microsphere uptake, it is difficult to wholly rule out this mechanism without further evidence. FM4-64 is a commercially available lipophilic styryl dye, which through anchorage into the lipid bilayer labels the membrane of the cell and any subsequently formed endosomal compartments.[141]

B16F10 mouse melanoma cells were pre-incubated with FM4-64 followed by 0.5 μm fluorescein microspheres and real-time confocal analysis was carried out over a period of 30 minutes (see Supporting Information on CD for the movie and **Figure 3.11**). Initially, three microspheres can be seen anchored to the extracellular membrane of the cell (**Figure 3.11 a** and **b**) and after repeated re-orientation of their alignment into a "spear-like" arrangement, the microspheres (still associated to one another) cross the lipid bilayer rapidly without any appearance of an enclosed endosome (**Figure 3.11 c** and **d**). It was noted, however, that there was some membrane (or possibly FM4-64 stain) associated to the microspheres on one side. After 21 minutes incubation (**Figure 3.11 e**), the microspheres entered the cytoplasmic region of the cell causing a certain degree of membrane disruption. As

the microspheres entered the cytoplasmic region they move freely around and within 7 minutes the associated membrane stain was largely lost (**Figure 3.11 f**).

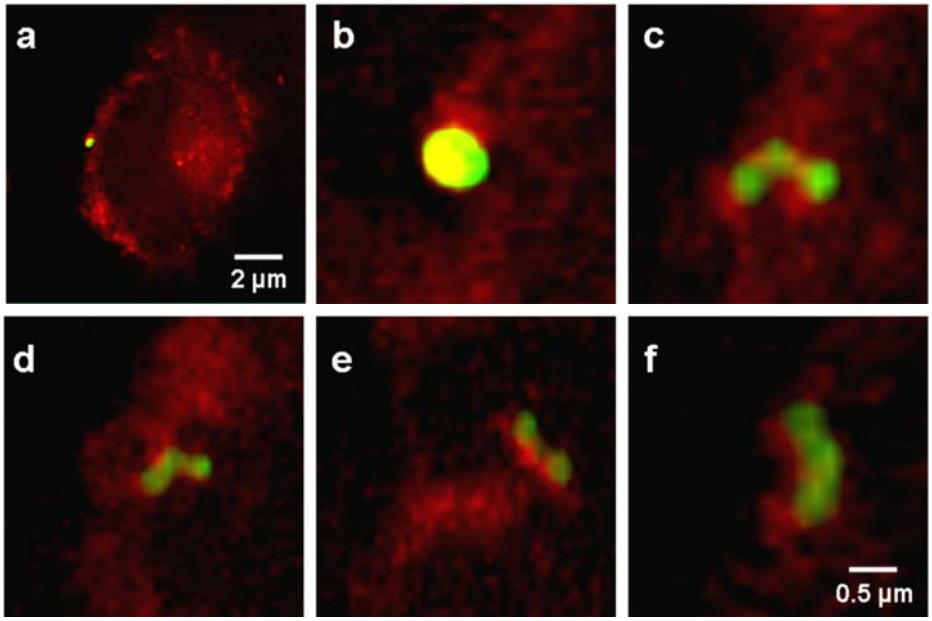

Figure 3.11. FM4-64 Staining. Real time confocal microscopy of a B16F10 cell stained with FM4-64 incubated with 0.5 µm fluorescein microspheres: **a**. time = 0 minutes, microspheres anchored extracellularly; **b**. time = 0 minutes, enlarged image; **c**. time = 4.5 minutes, microspheres rearrange alignment; **d**. time = 15 minutes, microspheres pass the bilayer; **e**. time = 21 minutes, microspheres cause membrane disruption; **f**. time = 30 minutes, microspheres are cytoplasmic.

This confirms that this is unlikely to be any classic endosomal localisation and is instead most likely some dislodged membrane, which during passage of the microspheres across the dye stained lipid bilayer has associated to the beads.

To further demonstrate the lack of endosomal or lysosomal compartmentalisation of the microspheres within cells, B16F10 cells were treated with LysoTracker Red, a stain capable of marking acidic organelles,[142] following incubation with 2, 0.5 and 0.2 µm Cy5 microspheres (**Figure 3.12** and **Scheme 3.1**).

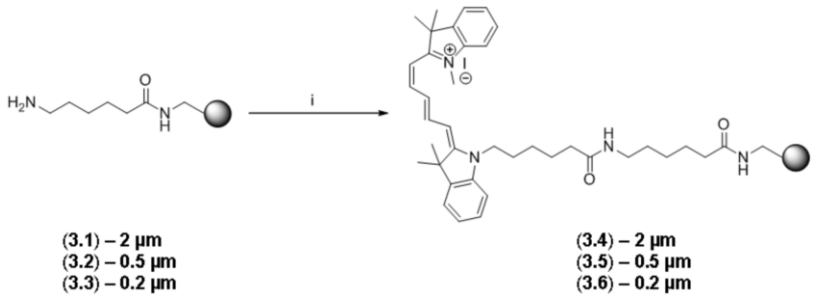

Scheme 3.1. Cy5-Microspheres. Production of Cy5 microspheres, (**3.4**), (**3.5**) and (**3.6**)**,** from

aminohexanoic microspheres, (**3.1**), (**3.2**) and (**3.3**).

(i). 10 eq. Carboxy-Cyanine5 (Cy5), 10 eq. HOBt, 10 eq. PyBOP, 10 eq. DIPEA, DMF, 18 h, 25 ºC.

Positive controls were established in a similar manner with LacCer and transferrin, which show co-localisation (yellow/orange colour, **Figure 3.12**) since they are known to be ingested by endocytosis. In contrast, there was no evident co-localisation between microspheres and endosomes/lysosomes using any size microsphere. This was confirmed also in HEK293T, HeLa and E14 cells (**Figure 3.13**). The lack of co-localisation with endosomal and lysosomal stains strongly supports a passive mechanism, whereby microspheres are attracted to the cell and anchor to the extracellular matrix of the membrane. Following a period of time where microspheres appear to re-orientate themselves they rapidly, without an energy requirement, cross the bilayer resulting in a small amount of membrane disruption which is rapidly recovered.

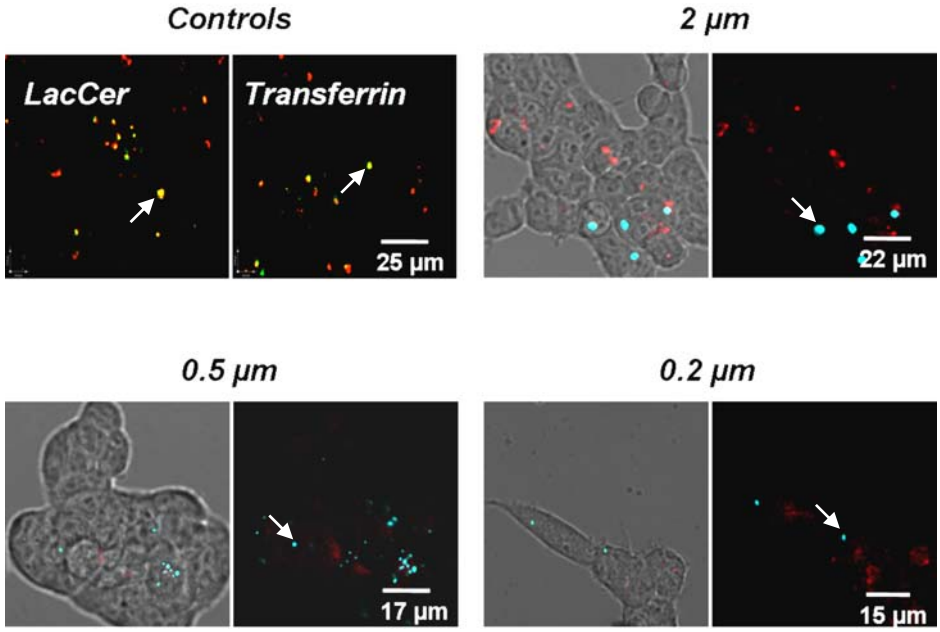

Figure 3.12. LysoTracker Red. B16F10 cells incubated with Cy5 labelled 2 µm, 0.5 µm and 0.2 µm microspheres (*cyan*, 86 µg/mL) followed by LysoTracker Red (*red*). Controls were established with BODIPY-LacCer and FITC-transferrin (*top left* and *right*) (co-localisation = *yellow/orange*).

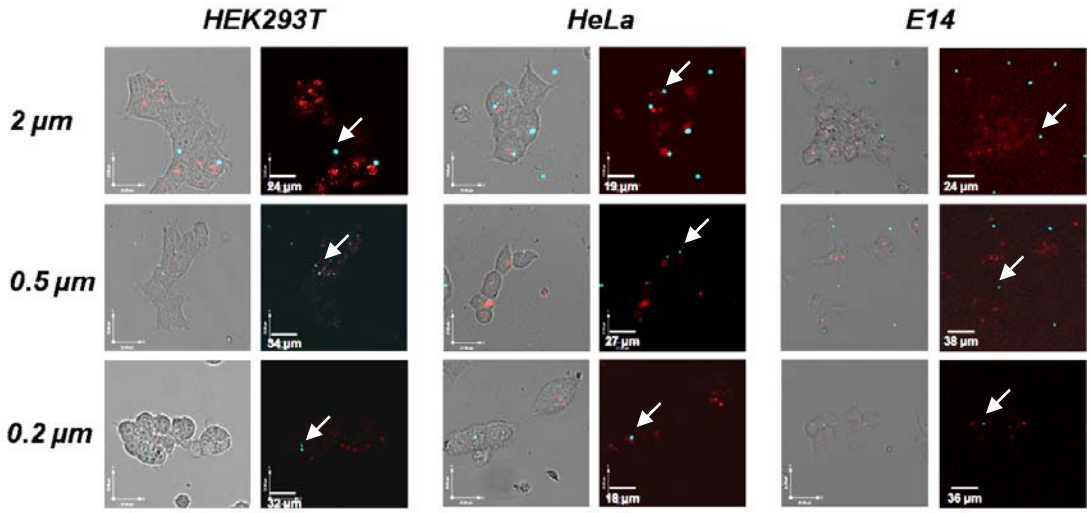

Figure 3.13. LysoTracker Red. HEK293T, HeLa and E14 cells treated with LysoTracker Red following 2, 0.5 or 0.2 µm Cy5 labelled microspheres (86 µg/mL).

3.7. Membrane Leakage

In the hypothesised mechanism, microspheres anchor to the extracellular membrane of the cell and force a hole in the membrane that allows the bead to passively pass through the lipid bilayer into the intracellular environment (**Figure 3.14**).

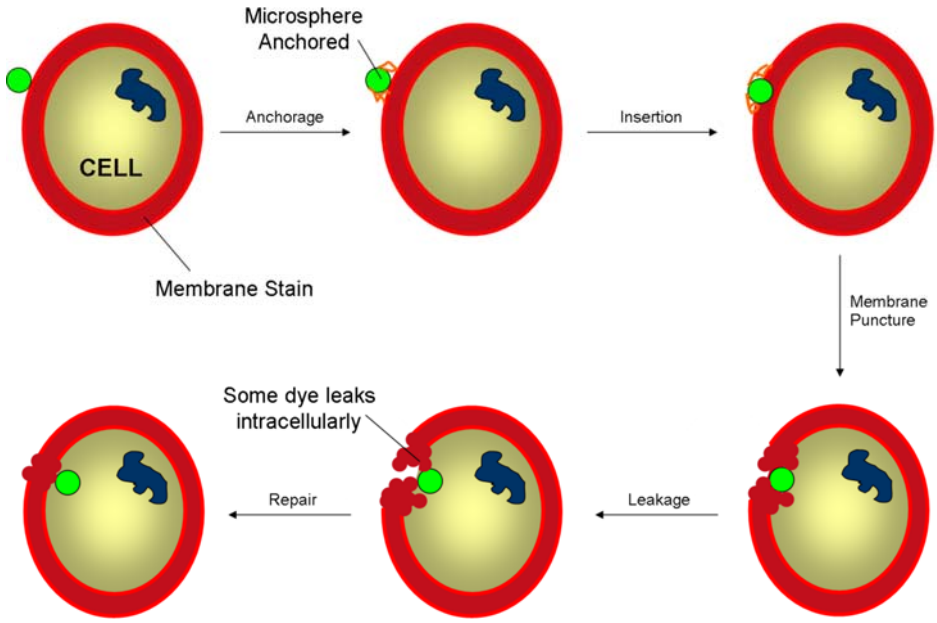

Figure 3.14. Anchor-Mediated Uptake. Hypothesised uptake mechanism of microspheres.

The membrane disruption caused by the bead passage is then rapidly recovered, restoring the cellular membrane to normal. Extensive studies of microsphere toxicity by MTT assay and by gene expression profiling[143] suggests limited toxicity, confirming that the disruption caused likely repairs very rapidly and does no lasting damage to the cell.

3.7.1. Propidium Iodide

If the microspheres do enter by this proposed mechanism, it is likely that an amount of membrane leakage occurs as the beads passage across. In order to analyse this effect, microspheres were incubated with HEK293T, B16F10, HeLa and L929 cells in the presence of propidium iodide (PI), an intercalating dye (**Figure 3.15**) often used in toxicity assays.[144]

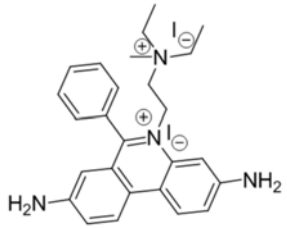

Figure 3.15. Propidium Iodide. Structure of intercalating dye, propidium iodide (PI).

Propidium iodide is inherently fluorescent (emission maxima: 620 nm), but its fluorescence is increased 30 – 40 fold when it intercalates into DNA in the nucleus.[145] However, propidium iodide is unable to cross the cellular membrane of healthy cells. It is only able to translocate the lipid bilayer when the cellular membrane becomes 'leaky' – for example in unhealthy, dying cells (hence its use in toxicity assays). Leakage of the membrane to propidium iodide may be induced by the influx of microspheres if the beads puncture a small hole in the lipid bilayer while crossing the cellular membrane. As such, Cy5 labelled microspheres were incubated with cells in the presence of propidium iodide for 3 hours. Flow cytometry was then used to select only the beadfected cells (based on the Cy5 fluorescence) and the propidium iodide staining of these cells was analysed (control cells were treated for 3 hours with propidium iodide, but without microspheres to give the background levels of staining). In order to exclude toxicity as the cause resulting in the influx of propidium iodide to beadfected cells, a control was establish where cells were

incubated with Cy5 microspheres for 3 hours followed by propidium iodide for 30 minutes, in a manner traditionally applied in toxicity assays. In addition, to exclude the possibility that the microspheres swell with propidium iodide to facilitate its intracellular delivery, microspheres were incubated with propidium iodide alone and the fluorescence of the microspheres assessed. Fluorescence emission associated to propidium iodide could not be found co-localised with the microspheres, suggesting it is not possible for the microspheres to either adsorb or swell with this compound. Instead, in all cases, introduction of the microspheres resulted in increased leakage to propidium iodide and was found to be cell line and bead size dependent (**Graph 3.8** and **Figure 3.16**).

HeLa and L929 cells showed the greatest increases in propidium iodide staining under bead treatment, while the fluorescence intensities of propidium iodide in HEK293T and B16F10 beadfected cells were less. The reason for this may be that the "puncture" made by the microspheres was repaired more rapidly in HEK293T and B16F10 cells than in HeLa or L929 cells, allowing less leakage.

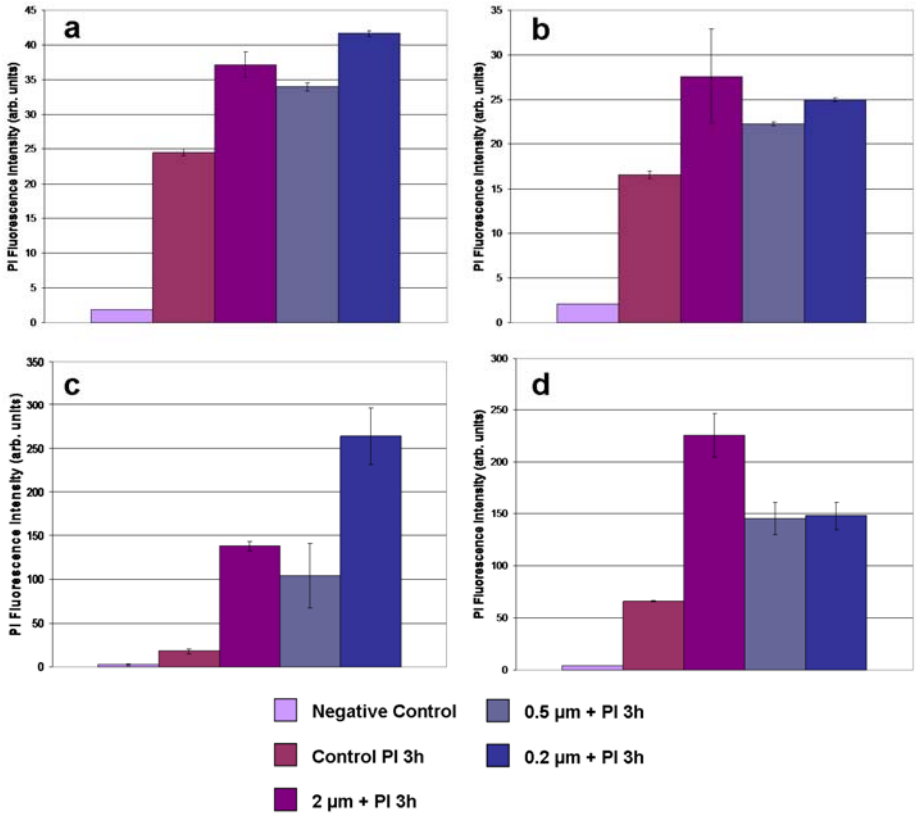

Graph 3.8. Leakage of Propidium Iodide into Beadfected Cells. a. HEK293T cells; **b.** B16F10 cells; **c.** HeLa cells and **d.** L929 cells. 'Negative control' refers to untreated cells; 'Control PI 3h'

refers to un-beadfected control cells treated with propidium iodide (PI) for 3 hours; '2 µm + PI 3h' refers to cells treated with 2 µm Cy5 microspheres together with propidium iodide for 3 hours; '0.5 µm + PI 3h' refers to cells treated with 0.5 µm Cy5 microspheres together with propidium iodide for 3 hours; '0.2 µm + PI 3h' refers to cells treated with 0.2 µm Cy5 microspheres together with propidium iodide for 3 hours. Microsphere concentration was 86 µg/mL; PI concentration was 14 µg/mL.

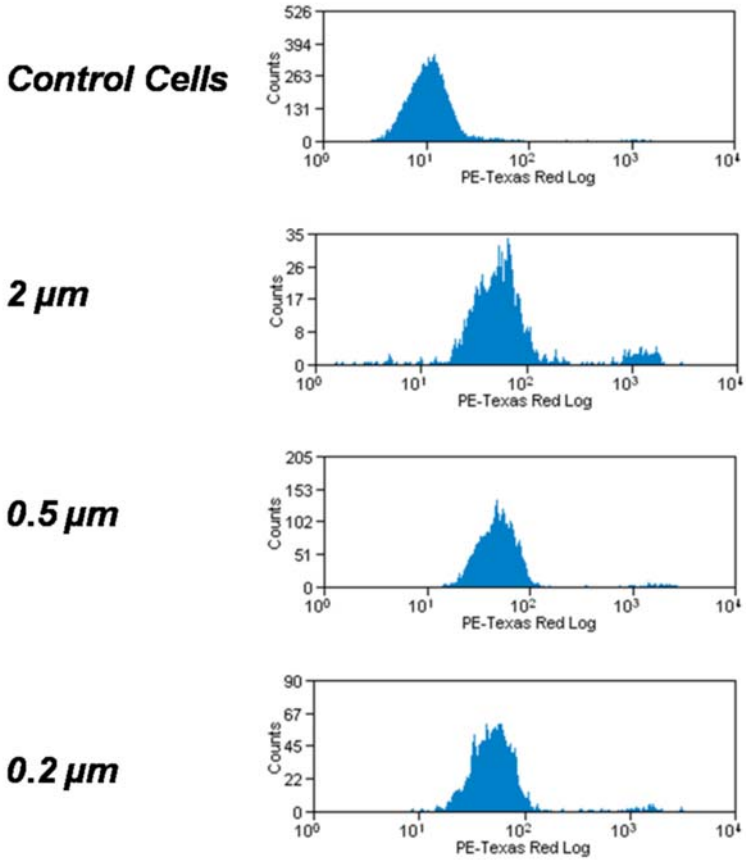

Figure 3.16. Propidium Iodide Leakage. Flow cytometry histograms of the propidium iodide fluorescence in control cells (treated only with PI) and cells treated with 2, 0.5 and 0.2 µm Cy5 labelled microspheres (86 µg/mL) together with propidium iodide (14 µg/mL). 'PE-Texas Red' shows PI fluorescence.

In order to demonstrate that this increased fluorescence associated to propidium iodide influx was not possible with an endocytic mechanism of uptake, a further control was established using LacCer. BODIPY-LacCer was incubated with HeLa cells in the presence of propidium iodide for 3 hours before flow cytometry to assess the PI fluorescence intensity of those cells containing LacCer compared to control cells (treated with PI in the absence of LacCer). The results are summarized by

Graph 3.9 and show that there was no increase in the fluorescence intensity of propidium iodide in cells when they were treated with LacCer from control cells not treated with LacCer. Thus, endocytosis does not result in leakage of propidium iodide into the cell.

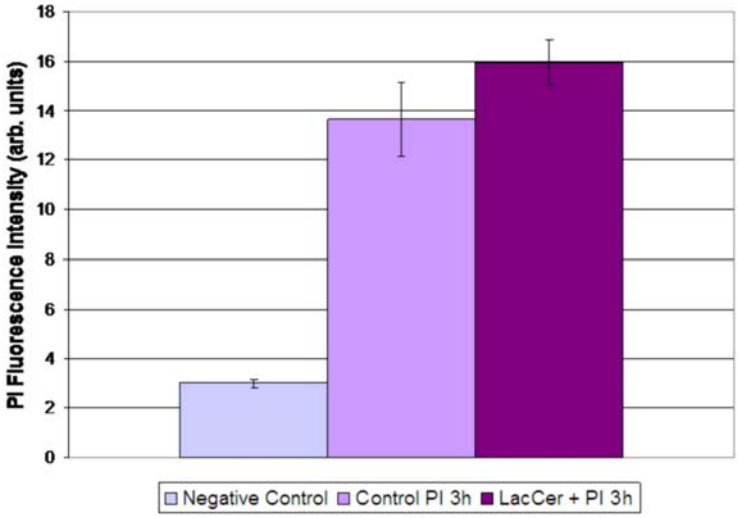

Graph 3.9. Negative Control. Leakage of HeLa cells to propidium iodide (PI) (14 μg/mL) induced by the endocytosis of LacCer (5 μM).

If propidium iodide is cytoplasmic when it enters the cell (as it would be for microsphere-induced leakage), it will traffic to the nucleus and intercalate with DNA resulting in an intense fluorescent signal. As such, microscopy was performed (**Figure 3.17**) to deduce if this was the case for microspheres and it was evident that the propidium iodide stain had reached the nucleus and had intercalated with DNA resulting in an intense fluorescence output.

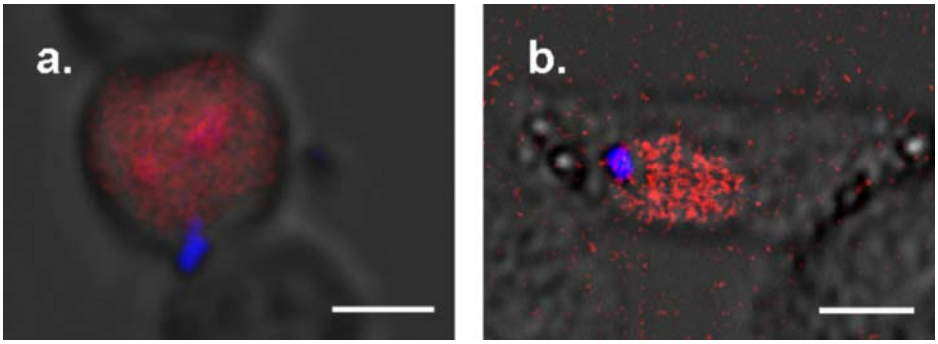

Figure 3.17. Propidium Iodide Microscopy. Propidium iodide (*red*) leakage into cells with 2 μm Cy5 microspheres (*blue*). **a.** HeLa cells (scale bar is 12 μm); **b.** L929 cells (scale bar is 9 μm). Microscopy performed after 3 hours.

3.7.2. Trypan Blue

To further prove membrane leakage due to the transient puncture of microspheres, the experiment was repeated using trypan blue, another intercalating dye, which is unable to translocate the cell membrane[146] (**Graph 3.10 – 3.11** and **Figure 3.18**). When cells were incubated with microspheres and trypan blue, increases in fluorescence were observed as with propidium iodide (most notably so in HeLa cells) (**Graph 3.11**), further suggesting that microspheres facilitate trypan blue leakage into cells by causing a transient "puncture" of the cell membrane. As with propidium iodide, trypan blue localisation in the nucleus was confirmed by microscopy (**Figure 3.19**) demonstrating that, upon its intracellular entry, trypan blue must have been cytoplasmic. In addition, LacCer, known to be ingested by caveolae-mediated endocytosis, was not able to facilitate trypan blue leakage into cells, showing that endocytosis-like mechanisms can not account for this transient, non-toxic membrane permeability as induced by microspheres.

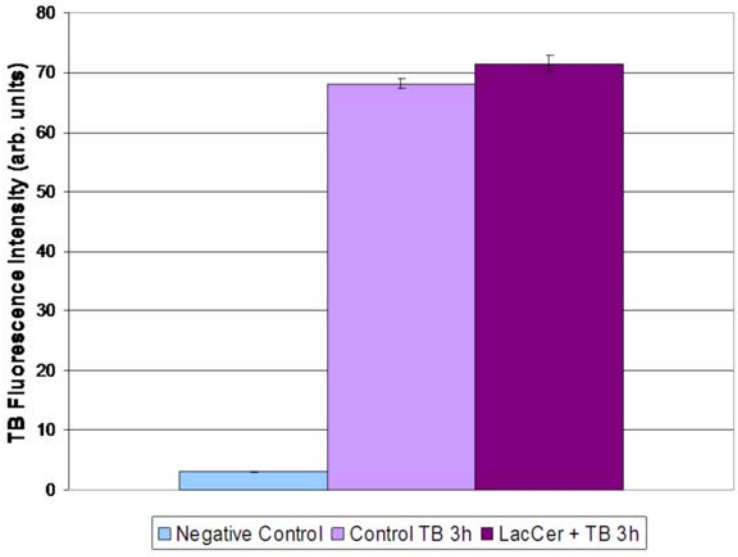

Graph 3.10. Negative Control. Leakage of HeLa cells to trypan blue (TB, 6 μg/mL) induced by the endocytosis of LacCer (5 μM).

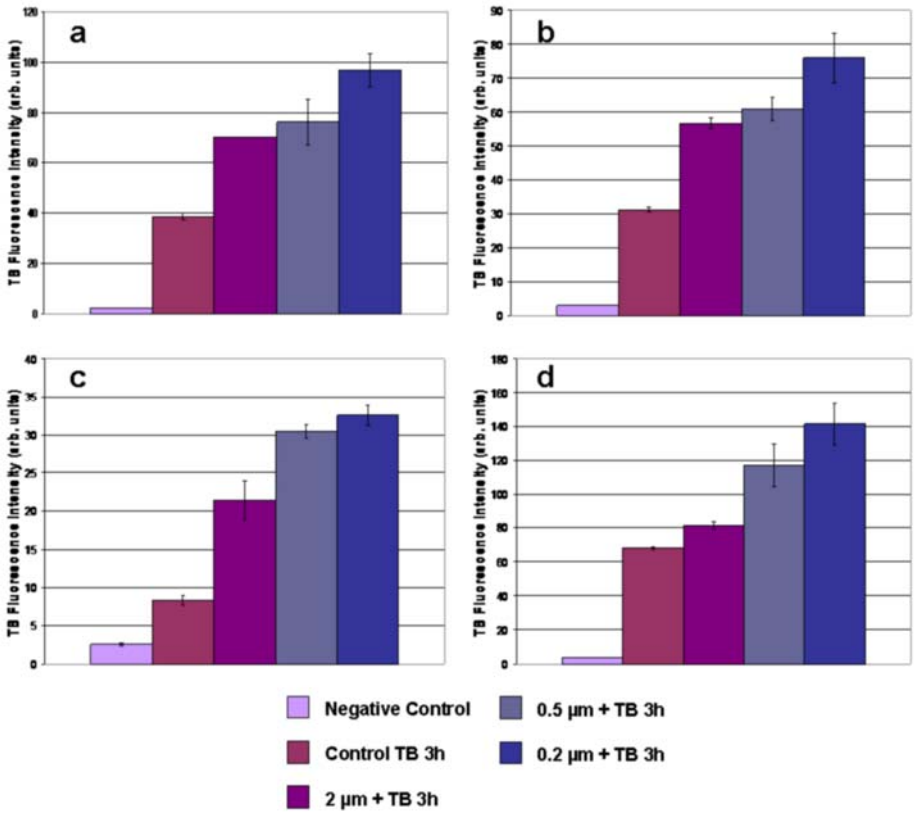

Graph 3.11. Leakage of Trypan Blue into Beadfected Cells. a. HEK293T cells; **b.** B16F10 cells; **c.** HeLa cells and **d.** L929 cells. 'Negative control' refers to untreated cells; 'Control TB 3h' refers to un-beadfected control cells treated with trypan blue (TB) for 3 hours; '2 µm + TB 3h' refers to cells treated with 2 µm Cy5 microspheres together with trypan blue for 3 hours; '0.5 µm + TB 3h' refers to cells treated with 0.5 µm Cy5 microspheres together with trypan blue for 3 hours; '0.2 µm + TB 3h' refers to cells treated with 0.2 µm Cy5 microspheres together trypan blue for 3 hours. Microsphere concentration was 86 µg/mL; TB concentration was 6 µg/mL.

These results strongly support a mechanism whereby microspheres puncture a small hole in the membrane as they passively pass across the lipid bilayer to the intracellular environment. However, the puncture is transient, heals rapidly and does not appear to have a detrimental effect on the cellular viability or membrane permeability.

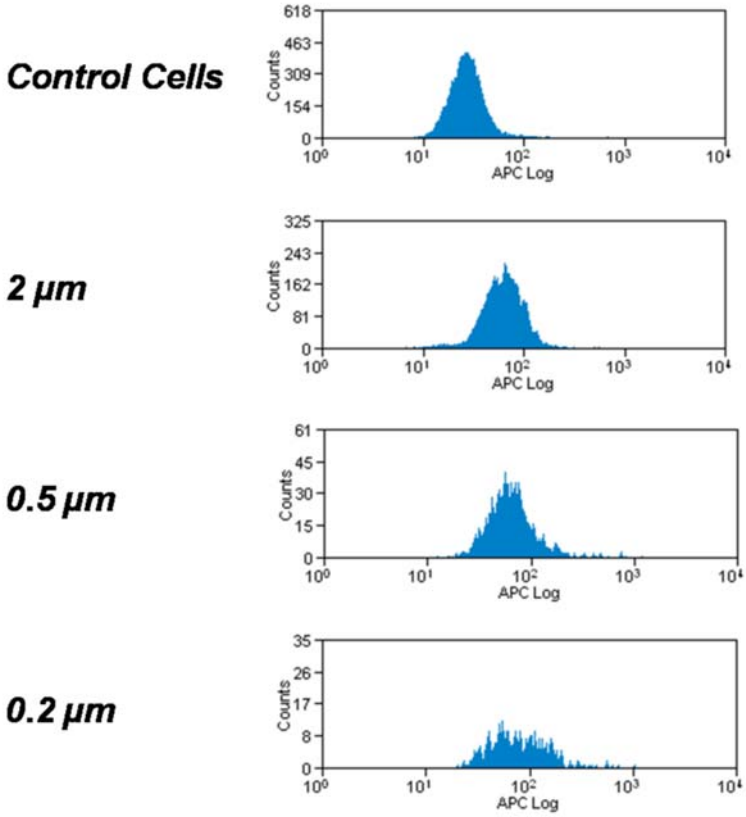

Figure 3.18. Trypan Blue. Flow cytometry histograms of the trypan blue fluorescence in control cells (treated with TB only) and cells treated with 2, 0.5 and 0.2 µm fluorescein labelled microspheres (86 µg/mL). TB concentration was 6 µg/mL. 'APC' shows TB fluorescence.

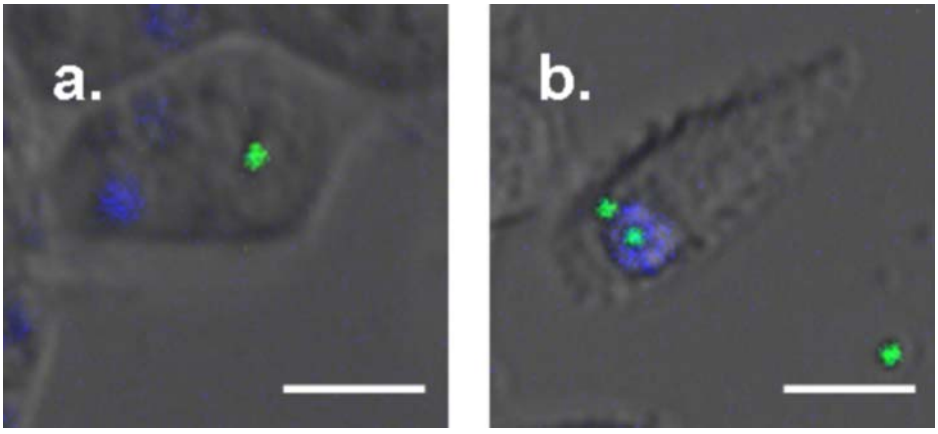

Figure 3.19. Microscopy. Trypan blue (*blue*) leakage into cells with 2 µm FAM-microspheres (*green*). **a.** HeLa cells (scale bar is 13 µm); **b.** L929 cells (scale bar is 14 µm). Microscopy performed after 3 hours.

3.8. Conclusions

The mechanism by which non-phagocytic cells take up polymer microspheres is not well understood. Here, energy dependent endocytic mechanisms have been evaluated using chemical and microscopic techniques. 0.2, 0.5 and 2 μm microspheres were not found to be dependent on ATP or cholesterol and were not inhibited by a specific chemical blockade on caveolae or clathrin-mediated endocytosis. Furthermore, staining with endosomal/lysosomal markers (LysoTracker and FM4-64) showed no co-localisation with microspheres. This evidence strongly suggests that microspheres were ingested by a passive mechanism, whereby microspheres anchor to the extracellular matrix of cells before transiently puncturing the membrane to facilitate bead entry. As such, membrane leakage was assessed and evidenced by the influx of membrane impermeable intercalating dyes (propidium iodide and trypan blue) associated to the puncturing of the cell bilayer by the passive entry of microspheres.

This result, whereby microspheres are determined to be cytoplasmic and not trapped within endosomes, widens the possible applications that microspheres may have (for example, in the delivery of cargo which requires cytoplasmic localization).

Chapter 4: *When David Moves Goliath*

4.1. Introduction

A major advantage of microspheres is their ability to enter a wide range of cell lines with high efficiency.[95] To further the use of microspheres in the bio-medical field, it would be of interest to develop microspheres which target specific organs *in vivo*, or which may allow cellular separations in a facile and rapid manner.

Magnetic nanoparticles have been extensively studied in the biomedical and biochemical fields and they have a vast range of possible applications ranging from drug delivery to biosensors to Magnetic Resonance Imaging (MRI) contrast agents.[147, 148, 149] Often iron oxide nanoparticles are used, however their use can be limited by lack of sufficient functionalisation and limited control over the particle size.[150] However, their incorporation into functionalisable constructs has greatly enhanced their use. For example, in 2005 silica nanotubes were prepared containing an inner layer of magnetite (Fe_3O_4) with encapsulated human IgG,[151] which successfully separated anti-human IgG from anti-bovine IgG. Also in 2005, magnetic nanowires were bound to the extracellular matrix of NIH-3T3 mouse fibroblast cells *via* integrins facilitating their phagocytosis. Subsequently, the intracellular wires were used to bias the movement of a population of cells in response to an externally applied magnetic field, so as to align cells in an array format demonstrating the affectivity of magnetic nanodevices in cellular manipulations.[152]

The introduction of magnetic metal oxides within polymer spheres is something that has been reasonably well studied since they were first introduced in the 1970s.[153, 154, 155] Similar to magnetic nanotubes (MNTs), paramagnetic materials enclosed within the polymer shell renders the entire microsphere paramagnetic and able to respond to an externally applied magnetic field. However, these particles have the advantage over MNTs of being easily functionalised and the size distribution can be controlled, producing a range of narrowly dispersed particle sizes.[156, 157] Indeed, magnetic microspheres have already been used in a number of applications within the bio-medical research field, in bioassays amongst other

applications.[158, 159, 160] They have additionally been commercialised in, for example, Magnetic Cell Sorting (MACS).[161] In this technique, cells expressing an antigen are incubated with MACS® MicroBeads, which are small (50 nm) biodegradable superparamagnetic particles functionalised with the corresponding antibody. Thus, the MicroBeads anchor to the cell *via* an antigen/antibody interaction. The cells are then passed in a stream through a column transversing a powerful magnet, which positively selects those cells anchored to magnetic MicroBeads. Cells which are not labelled with MicroBeads are washed through the column, thus separating the cell populations. This technique can result in population purities of up to 95%[162] and can be fully automated, sorting approximately 10 million cells per second.

4.1.1. Preparation

In the past, chemical metal deposition, suspension and emulsion polymerisation have been amongst the methods employed for the preparation of magnetic microspheres.[163, 164, 165] Famously, Ugelstad and co-workers[166] developed a procedure which has led to the now commercially available DynaBeads. However, this method requires a multi-step approach and can be complicated and lengthy in nature. As such, alternative methods have been sought for the production of magnetically manipulable microspheres.

4.2. Dispersion Polymerisation

Dispersion polymerisation presents a one-step procedure allowing the formation of mono-dispersed particles between 0.3 and 10 μm in diameter, while the introduction of metal oxide nanopowders in the dispersion allows the generation of magnetic particles.[167] The high conversions obtained and the ease of manipulation of dispersion polymerisation makes it attractive as a method for preparing magnetic beads. However, it is well recorded that the introduction of foreign materials (e.g. iron oxide) into a polymerisation mixture can cause a disruption in the mechanism by which dispersion polymerisation occurs.[160, 168, 169] As such, agglomeration or highly dispersed particles can result since mono-dispersity is heavily reliant on a rapid nucleation period,[170] with which the iron oxide may interfere.[171, 172, 173, 174]

As a result, polystyrene microspheres encapsulating iron oxide were prepared by a dispersion polymerisation approach and labelled with a fluorophore to allow intracellular uptake to be followed by fluorescence-based flow cytometry techniques, as with the non-magnetic microspheres discussed in ***Chapters 2*** and ***3***.

4.2.1. 0.3 μm Paramagnetic Microspheres

Small sized cross-linked polystyrene microspheres encapsulating maghemite nanopowder (Fe_2O_3) were produced from a dispersion polymerisation procedure, disbanding iron oxide in aqueous ethanol with PVP (M_w 360,000 Da), as shown in **Scheme 4.1**.

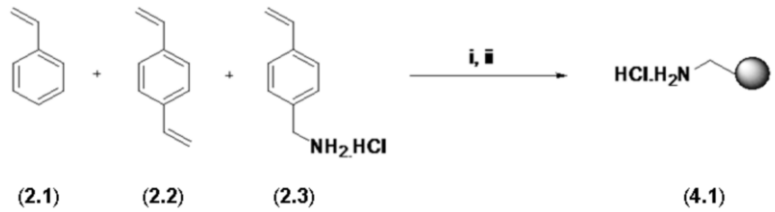

Scheme 4.1. Magnetic Microspheres. Preparation of polystyrene microspheres (**4.1**), containing iron oxide nanopowder *via* dispersion polymerisation.
(i). 0.01 eq. AIBN, N_2; (ii). 0.04 eq. PVP (M_w: 360,000), 2 wt.% Fe_2O_3, ethanol:water (97:3), 70 ºC, 18 hours.

The maghemite nanopowder contained particulates less than 50 nm in diameter and the solid required initial dispersion within the polymerisation mixture by sonication prior to the addition of the monomers to promote an even dispersion. High molecular weight PVP was used to promote the uniform precipitation of not only small sized polymer microspheres, but also efficiently stabilised, narrowly dispersed beads from the alcoholic media.

Under these conditions, 0.3 μm paramagnetic microspheres (**4.1**) were produced (**Figure 4.1**).

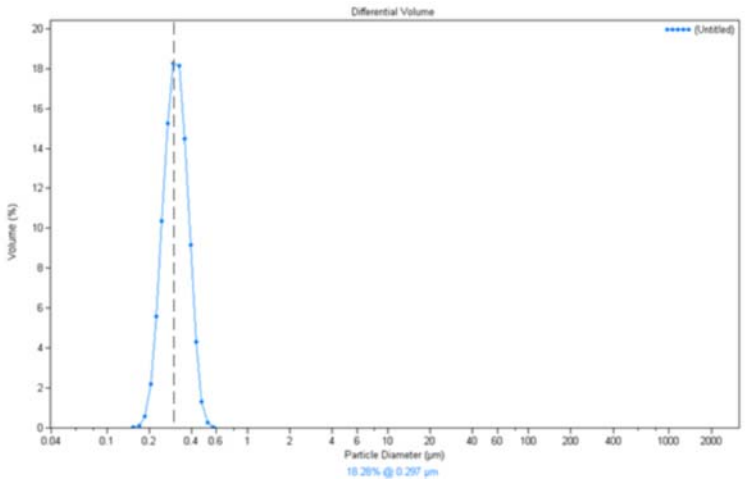

Figure 4.1. Laser Diffractometry Analysis. 0.3 µm paramagnetic microspheres (**4.1**) (S.D: 0.06 µm; C.V. 19.1%).

Microspheres were noted to be narrowly dispersed with a coefficient of variation of 19%. Scanning electron microscopy of the microspheres (**Figure 4.2**) showed they were spherical with a smooth surface. Iron oxide was not extensively evident on the surface of the microspheres,[167] suggesting it was mostly encapsulated within the polymer matrix. To ensure there was no free iron oxide present, paramagnetic beads were treated with dilute hydrochloric acid (2 M) and washed sequentially with water.[169] In addition, prior to analysis, microspheres were purified by magnetic sublimation to remove microspheres which had not encapsulated iron oxide.

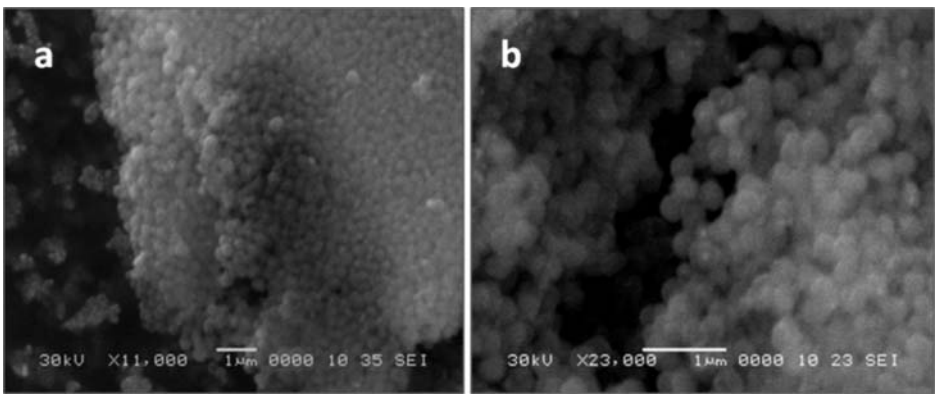

Figure 4.2. Scanning Electron Microscopy. 0.3 µm paramagnetic microspheres (**4.1**). **a.** *en masse*; **b.** 2× magnification of *en masse* image. Scale bars are 1 µm.

In order to determine the quantity of iron oxide captured within the microspheres, a technique known as Energy Dispersive X-Ray (EDX) analysis was performed (**Figure 4.3**).

4.2.1.1. Energy Dispersive X-Ray Analysis

This technique can be used in conjunction with SEM analysis on dried, carbon- or gold-coated samples. In EDX, an electron beam is aimed at the surface of a sample and this results in the emission of X-Rays from the material. The energy of the X-Rays emitted from the sample is dependent on the material itself and can allow the detection of not only the elements present, but their relative abundance in the material. However, it should be noted that, in general, EDX is not a sensitive enough technique to be able to detect elements below an atomic number of approximately eleven.

EDX analysis of 0.3 µm paramagnetic microspheres yielded an iron concentration of 3.7 wt.% of the microsphere bulk (**Graph 4.1**). This suggests that for every mg of microspheres there is approximately 37 µg of iron or 0.5 femto-grams per microsphere (one microsphere weighs approximately 14 femto-grams).

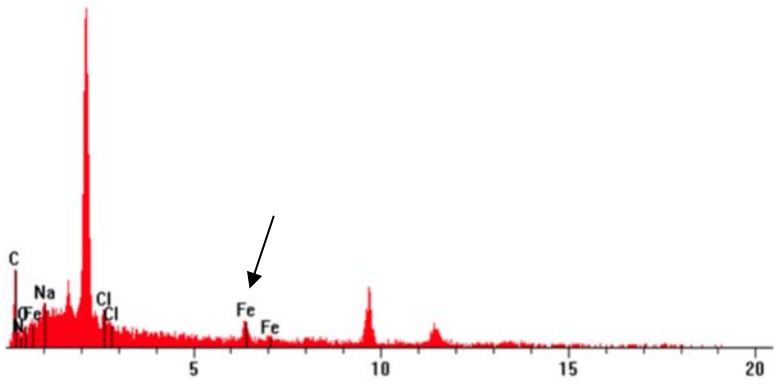

Figure 4.3. EDX Analysis. 0.3 µm paramagnetic microspheres (**4.1**) identifying the incorporation of iron within the microspheres at 3.7 wt.% (x-axis values in keV).

To qualitatively assess the properties of the paramagnetic microspheres in response to an externally applied field, 0.3 µm microspheres (**4.1**) were seated in a neodymium magnetic separator (**Figure 4.4**) (neodymium magnets are lightweight yet powerful magnets typically composed of neodymium, iron and boron).

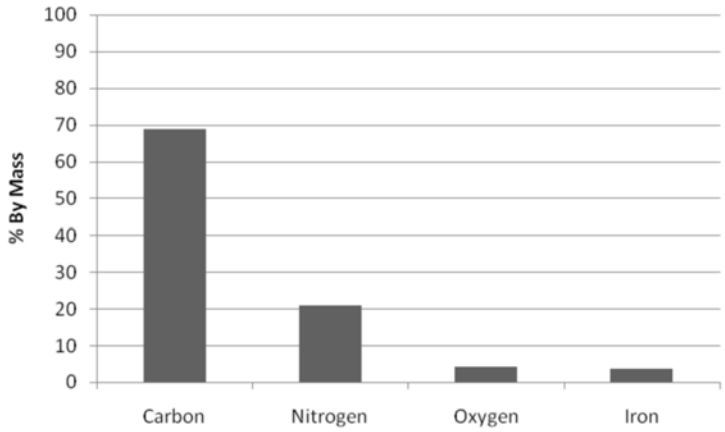

Graph 4.1. Quantitative Energy Dispersive X-Ray. 0.3 μm paramagnetic microspheres (**4.1**) (Carbon: 68.7, Nitrogen: 21.0, Oxygen: 4.2, Iron: 3.7). Elemental analysis gave Carbon: 91%, Hydrogen: 8%, Nitrogen: 0.6%.

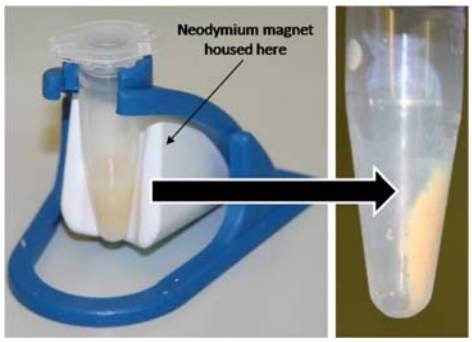

Figure 4.4. Magnetic Sublimation. 0.3 μm paramagnetic microspheres (**4.1**) respond to an external magnetic field generated by a neodymium magnetic separator.

Within 30 seconds, all magnetic particles moved in response to the applied magnetic field demonstrating that the encapsulated magnetic material within the polymer constructs renders the entire device paramagnetic and able to respond rapidly to an externally applied field over short distances (*ca* 1 cm).

4.2.1.2. Magnetic Hysteresis

Encapsulation of iron oxide within the polymer construct may alter the magnetic properties of the paramagnetic material (maghemite). To ensure that the iron oxide microspheres behaved in a similar manner to free un-encapsulated iron oxide nanopowder, magnetic hysteresis analysis was performed. Magnetic hysteresis is the phenomenon that occurs when a magnetic field is applied to a ferri- or ferro-

magnetic material. Initially, the atomic dipoles will align with the field and when the field is subsequently removed some of the alignment is retained by the sample, which may be said to have become "magnetised" (**Figure 4.5**). The magnetic field strength that has been retained by the sample is known as the "remanence" and, if a sample is behaving in a magnetically consistent fashion, the remanence will be constant (at constant field strength). In the case of paramagnetic and superparamagnetic samples, remanence is not observed as the material is unable to retain a magnetic field.

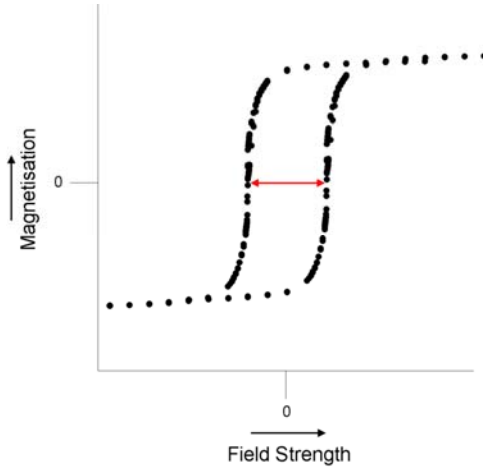

Figure 4.5. Remanence. Magnetic hysteresis loop analysis of a ferri- or ferro-magnetic material, showing "magnetisation". *Red arrow* indicates the magnetic field retained by the sample (the remanence).

Magnetic hysteresis analysis (**Graph 4.2**) confirmed the microspheres exhibited the desired paramagnetic properties (no magnetic field was retained by the sample) as compared to free iron oxide nanopowder as the magnetic hysteresis curves are virtually indistinguishable. This confirms that the magnetic properties of iron oxide (maghemite) are unaffected by its encapsulation within a polymeric shell.

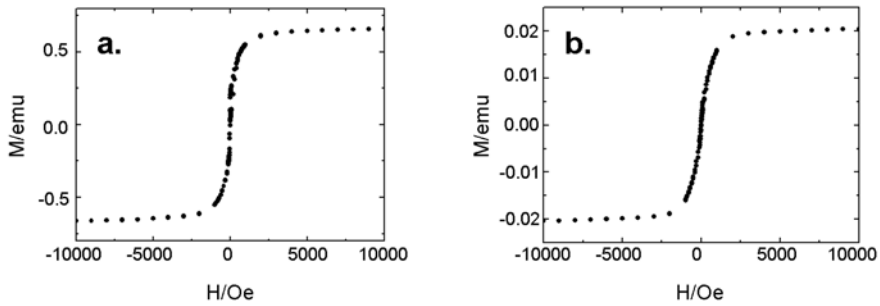

Graph 4.2. Magnetic Hysteresis Analysis. a. Iron oxide nanopowder; **b.** 0.3 μm paramagnetic microspheres (**4.1**). Analysis run at 300 K. 'M' indicates the magnetic flux density and 'H' indicates the magnetic field strength.

4.2.2. Effect of PVP Molecular Weight

Following the production of narrowly dispersed 0.3 μm paramagnetic microspheres (**4.1**) it was of interest to produce a range of bead sizes. Investigation centred on what effect lowering the molecular weight of PVP would have on the resulting paramagnetic microspheres. In the case of non-magnetic microspheres (***Chapter 2***), lowering the PVP molecular weight resulted in larger particles.[78, 79, 80] As such, the PVP molecular weight was reduced to 40,000 Da and the effect on the diameter and dispersity of the polymer product was examined by laser diffractometry analysis (**Figure 4.6**) and SEM (**Figure 4.7**).

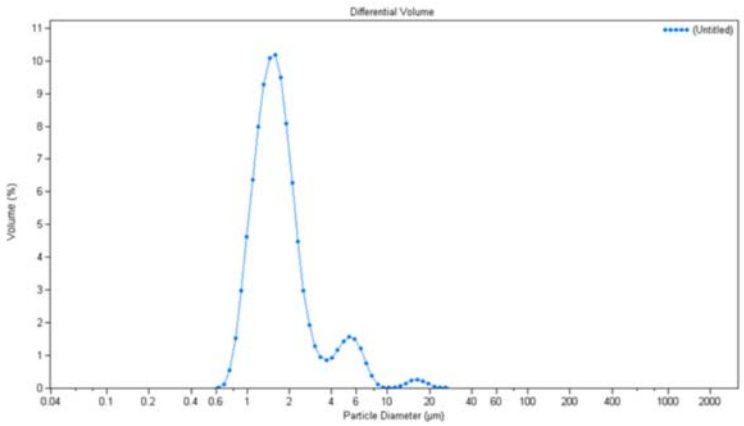

Figure 4.6. Laser Diffractometry Analysis. 2 μm paramagnetic microspheres (**4.2**) (S.D: 1.97 μm; C.V. 91.5%).

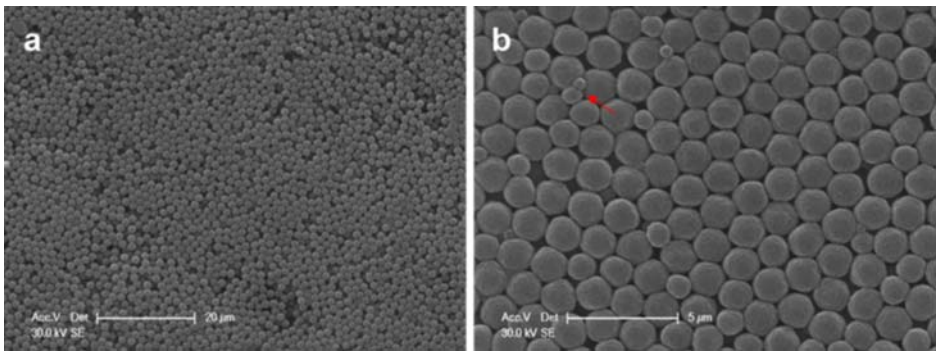

Figure 4.7. Scanning Electron Microscopy. Images of 2 µm paramagnetic microspheres (**4.2**). **a.** *en masse* (scale bar is 20 µm); **b.** 4× magnification of *en masse* image. *Red arrow* shows poly-dispersity (scale bar is 5 µm).

The mean diameter of microspheres was found to have increased to 2 µm but the population dispersity was also seen to spread (C.V. 92%), with agglomeration resulting in secondary peaks by laser diffractometry.

However, the product was noted to be spherical by SEM (**Figure 4.7**) and of a mostly even size. Interestingly, the microspheres exhibited a slightly rough surface indicating that iron oxide deposits were likely coating the microsphere, as well as being encapsulated. In order to quantitatively confirm iron oxide encapsulation, EDX analysis was performed (**Figure 4.8, Graph 4.4**) and showed a 1.8 wt.% incorporation of iron.

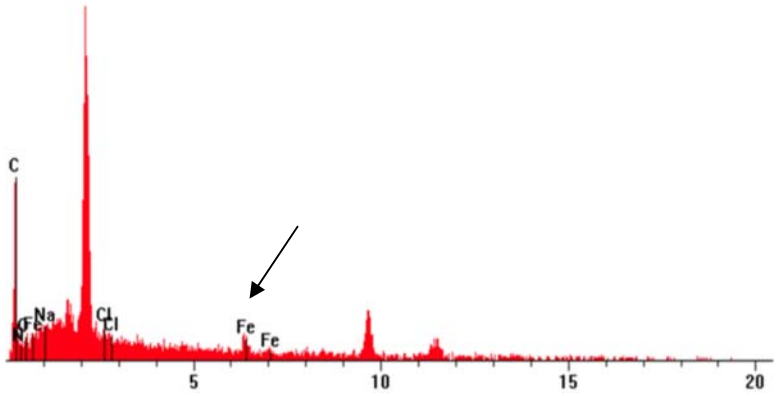

Figure 4.8. EDX Analysis. 2 µm paramagnetic microspheres (**4.2**) identifying the incorporation of iron within the microspheres at 1.8 wt.% (x-axis values in keV).

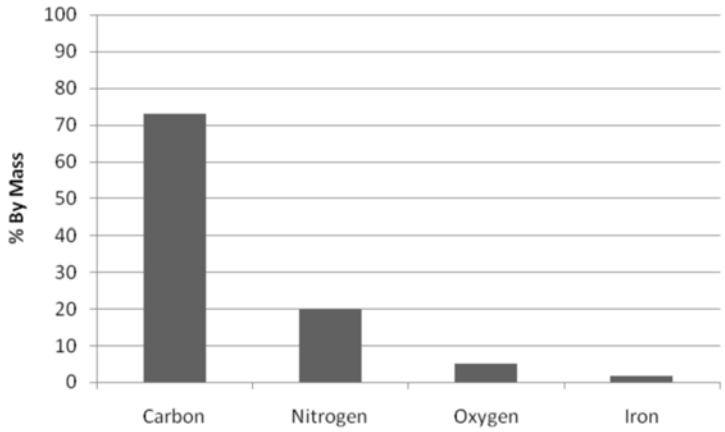

Graph 4.4. Quantitative Energy Dispersive X-Ray. 2 μm paramagnetic microspheres (**4.2**) (Carbon: 73.1, Nitrogen: 19.8, Oxygen: 5.0, Iron: 1.8). Elemental analysis gave Carbon: 62% Hydrogen: 3% Nitrogen: 0.3%.

Incorporation of DVB[175, 176] may have led to the evidenced poly-dispersity, where several small sized microspheres were observed (**Figure 4.7,** *red arrow*). This effect is thought to be due to the continuous second nucleation period occurring due to the prolonged period of time required for DVB cross-linked primary particles to form and fully mature.[177] This may be worsened by the use of iron oxide nanopowders in the dispersion leading to poly-dispersed microspheres.

4.2.3. Effect of Divinylbenzene

In order to produce a larger sized paramagnetic polymer product with a more even size distribution, a procedure previously developed by Zhang and co-workers[177] whereby DVB addition was made after the period of nucleation, was adopted. It is considered that the final size and quality of the polymer product which precipitates from the reaction mixture is decided in the early stages of the polymerisation, during the nucleation period. If the kinetics of the nucleation period are fast, the polymer product is more likely to be mono-dispersed.[176] Introduction of DVB and iron oxide into the polymerisation is thought to slow the kinetics of the nucleation period and may, thus, result in poly-dispersed microspheres.[175, 176, 177] However, if for example, DVB, is added after the nucleation period then cross-linking can still be achieved and a substantially detrimental effect on the dispersity of the polymer particles may be avoided. Using this "post-addition" method with PVP 40,000, 1.6 μm paramagnetic

microspheres (**4.3**) were precipitated from the reaction as found by laser diffractometry (**Figure 4.9**).

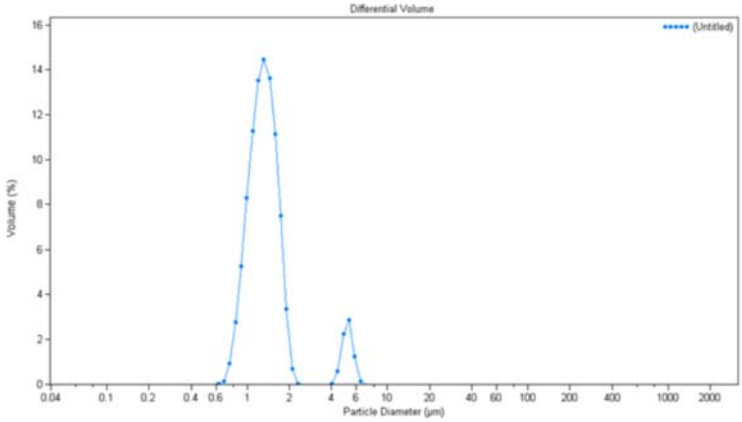

Figure 4.9. Laser Diffractometry Analysis. 1.6 µm paramagnetic microspheres (**4.3**) (S.D: 1.05 µm; C.V. 65.6%).

A peak 4 times the mean microsphere diameter was noted and is considered to be the aggregation of 3 – 4 microspheres, a probable direct result of the paramagnetic nature of the beads. SEM confirmed a regular size distribution (**Figure 4.10**) and also indicated a surface coating of iron oxide (evidenced by the furry nature of the microspheres). However, in this case, the iron oxide deposits appeared more substantial, as 'lumps' on the microsphere surface (**Figure 4.10,** *red arrow*). This phenomenon has previously been reported by Pich *et al.*[178] as "pickering" on the surface of poly(styrene/acetoacetoxyethyl methacrylate) microspheres enriched with iron oxide. Taking into consideration that microspheres have an amino functionality, it is additionally conceivable that this is forming a complex with the iron resulting in a surface coating.

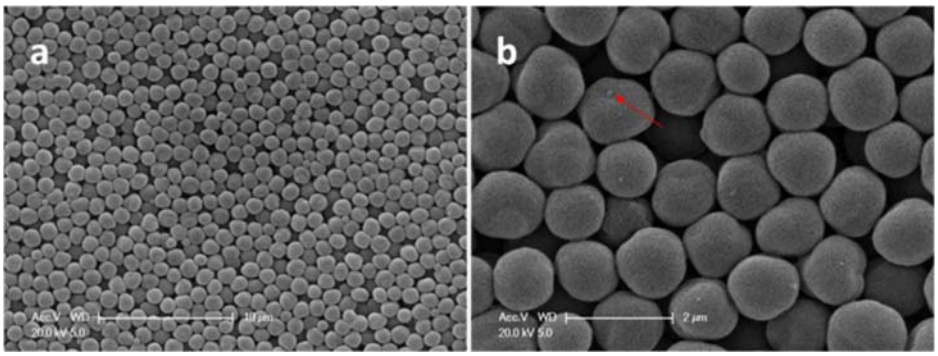

Figure 4.10. Scanning Electron Microscopy. Images of 1.6 µm paramagnetic microspheres (**4.3**). **a.** *en*

masse (scale bar is 10 µm); **b.** 5× magnification of *en masse* image (*Red arrow* shows a slight surface coating of iron oxide and 'pickering') (scale bar is 2 µm).

EDX analysis of the microspheres (**Figure 4.11, Graph 4.5**) confirmed the presence of iron, indicating its incorporation within the microspheres at 0.4 wt.%.

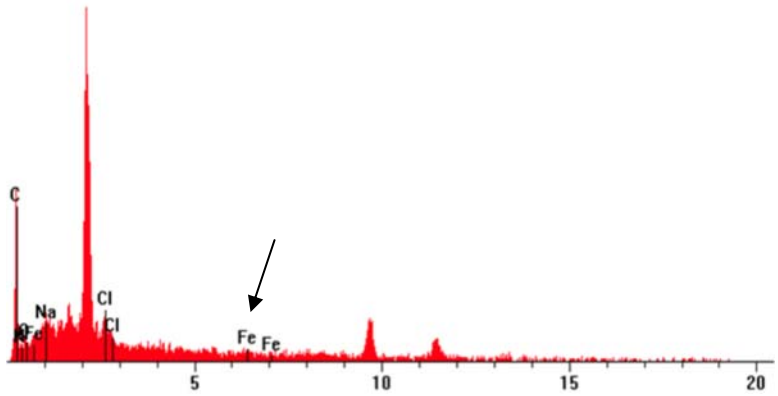

Figure 4.11. EDX Analysis. 1.6 µm paramagnetic microspheres (**4.3**) identifying the incorporation of iron within the microspheres at 0.4 wt.% (x-axis values in keV).

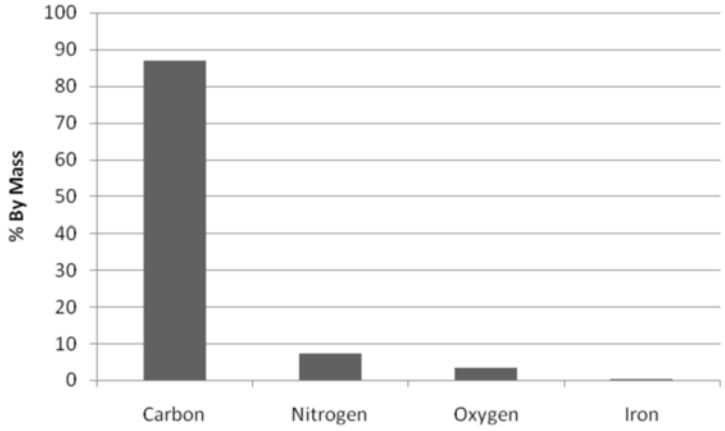

Graph 4.5. Quantitative Energy Dispersive X-Ray. 1.6 µm paramagnetic microspheres (**4.3**) (Carbon: 86.8, Nitrogen: 7.3, Oxygen: 3.4, Iron: 0.4). Elemental analysis gave Carbon: 91% Hydrogen: 8% Nitrogen: 0.5%.

Using dispersion polymerisation, a range of paramagnetic microspheres have been prepared with diameters between 0.3 and 2 µm with amino functionalities and DVB cross-linking. EDX has been used to confirm the presence of iron within the constructs and was found to be between 0.4 – 4 wt.%. In addition, SEM was used to show that the microspheres had even, spherical morphologies. Furthermore,

magnetic hysteresis analysis was used to confirm that iron oxide trapped within the microspheres retained its paramagnetic behaviour.

4.3. Cellular Uptake

To fully appreciate the use of magnetic microspheres as cellular delivery devices, it was of interest to study the cellular uptake of these beads in a range of cell lines and to examine how well tolerated the particles were by cytotoxicity assays.

As such, 0.3, 1.6 and 2 μm paramagnetic microspheres, (**4.1**), (**4.3**) and (**4.2**) respectively, were labelled with carboxyfluorescein *via* an aminohexanoic spacer unit rendering the microspheres fluorescent, yielding (**4.7**) (0.3 μm), (**4.8**) (1.6 μm) and (**4.9**) (2 μm). This allowed quantification of cellular uptake *via* fluorescence-based flow cytometric methods (**Graph 4.6**). Uptake was analysed in mouse melanoma (B16F10), E14 mouse stem cells, human embryonic kidney (HEK293T), human cervical cancer (HeLa), human erythroleukemic (K562) and mouse fibroblast (L929) cells after 6, 12 and 24 hours incubation (analysis was performed in 0.2% trypan blue to quench extracellular fluorescence). Similar to non-magnetic microspheres, cellular uptake was found to be cell line, bead size and incubation time dependent. Unsurprisingly, incubating the cells with the paramagnetic microspheres for 24 hours resulted in the highest uptake and was typically over 70%. K562 erythroleukemic cells showed the highest uptake over all bead sizes and HEK293T cells also showed a good uptake. In general, 2 and 0.3 μm microspheres tended to show a higher uptake than 1.6 μm microspheres. However, the differences in uptake between the varyingly sized microspheres were minimal, with all the beads showing a reasonable uptake, which was additionally confirmed by microscopy (**Figure 4.12**).

Mouse embryonic stem cells showed a good uptake of paramagnetic microspheres after 24 hours, particularly of the smaller sized beads (~ 90%), as seen with the non-magnetic microspheres.

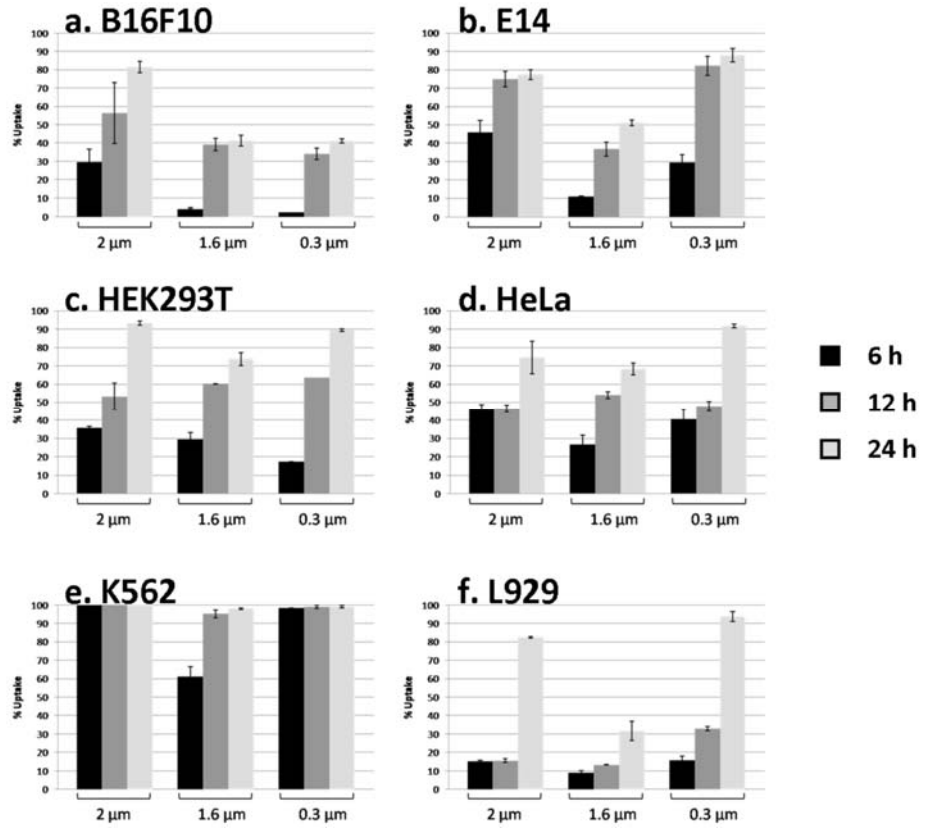

Graph 4.6. Cellular Uptake. 2, 1.6 and 0.3 µm paramagnetic fluorescein microsphere beadfections after 6, 12 and 24 hours by **a.** B16F10; **b.** E14 mES; **c.** HEK293T; **d.** HeLa; **e.** K562 and **f.** L929 cells. Microsphere concentration was 86 µg/mL.

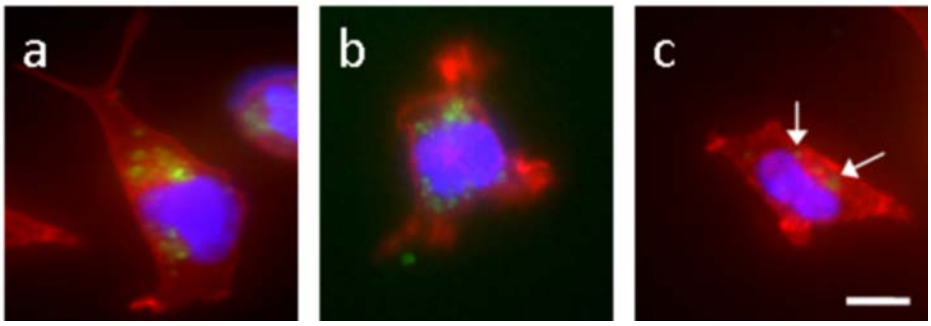

Figure 4.12. Microscopy of Beadfected HeLa Cells. After 12 hours beadfection stained with AlexaFluor-568 phalloidin (actin filaments) and Hoechst 33342 (nuclei). **a.** 2 µm (**4.9**); **b.** 1.6 µm (**4.8**) and **c.** 0.3 µm (**4.7**) fluorescein labelled paramagnetic microspheres. Scale bar is 15 µm.

4.4. Toxicity

Following from the successful uptake of paramagnetic microspheres in a range of cell

lines, it became important to analyse cellular viability following beadfection to examine whether the microspheres exerted any toxicity. To this end, MTT assays were carried out on beadfected and untreated control cells (**Graph 4.7**).

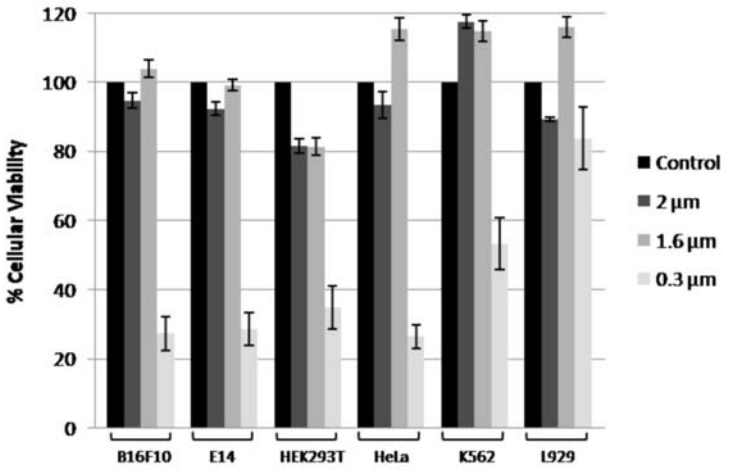

Graph 4.7. Cellular Viability. MTT assays in B16F10, E14, HEK293T, HeLa, K562 and L929 cells with 2, 1.6 and 0.3 µm paramagnetic microspheres. 'Control' is untreated cells assumed to be 100% viable. Microsphere concentration was 86 µg/mL and MTTs were performed after 24 h.

2 and 1.6 µm paramagnetic microspheres showed no substantial toxicity in any of the cell lines analysed, even with more sensitive cell lines (e.g. E14 or HEK293T), with over 80% viability in all cases. In contrast, 0.3 µm paramagnetic microspheres showed substantial toxicity (less than 50% viability) in all cell lines except L929 cells (where cell viability was over 80%). These smaller magnetic beads may exert their toxicity by over-loading the cell with iron oxide (0.3 µm paramagnetic microspheres had the highest iron content by weight) as they showed the highest uptake in many of the cell lines, especially after shorter time periods. Unfortunately, this toxicity limits their further use as intracellular delivery agents.

4.5. Biased Cellular Movement

It was of great interest to investigate whether, once internalised within cells, the magnetic beads could be used to bias cellular movement. The mass of a single, or even a cluster of microspheres is much less than the mass of a cell, so it would be a remarkable accomplishment if a microsphere could facilitate the biased movement of a

cell up to 150 times its volume (the volume of a 2 μm microsphere is approximately 3.4×10^{-14} L, the volume of a cell is approximately 5.0×10^{-12} L).[179]

As such, 2 μm paramagnetic beads (which had good uptake and no toxicity) labelled with fluorescein were incubated with HEK293T cells over 24 hours and the beadfected cells were sorted from non-beadfected cells using fluorescence activated cell sorting to collect a pure population of "mag-fected" cells containing paramagnetic microspheres. The 'magnetic' cells were then incubated over a neodymium magnet (**Figure 4.13**) and the cells assessed for their position with regards to the magnet. Cells were noted to have trafficked close to the position of the magnet and had adhered in a close formation around it (resulting in a higher density of cells close to the magnet). In contrast, very few cells adhered at further distances from the magnet (more than 2 cm) indicating that the majority of the mag-fected cell population had trafficked close to the magnet.

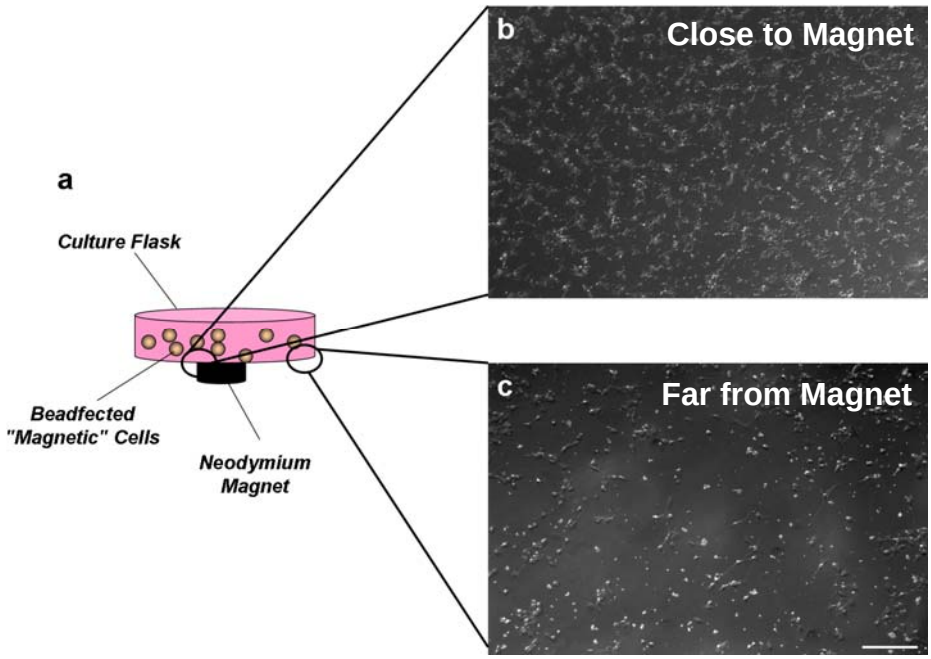

Figure 4.13. Biased Cellular Movement. 'Magnetic' cells were incubated over a neodymium magnet (**a**) in order to assess how cells react to an external magnetic field *in vitro.* **b.** Analysis of cells close to the magnet (< 5 mm); **c.** Analysis of cells far from the magnet (> 2 cm). Scale bar is 500 μm.

Furthermore, 'magnetic' cells sorted *via* their beadfection with fluorescently tagged magnetic microspheres were collected from suspension and exposed to an external magnetic field *en masse*. Their movement in response to the magnetic field was

recorded and is shown in **Figure 4.14** and **4.15** and in the Supplementary Information (real-time movie on CD). Within 1 minute, the cells (from an originally homogeneously dispersed suspension) (**Figure 4.15,** *top left panel*) localised to the magnet (**Figure 4.15,** *bottom left panel*) demonstrating that paramagnetic microspheres internalised within cells have the power to bias the movement of cells towards an externally applied magnetic field.

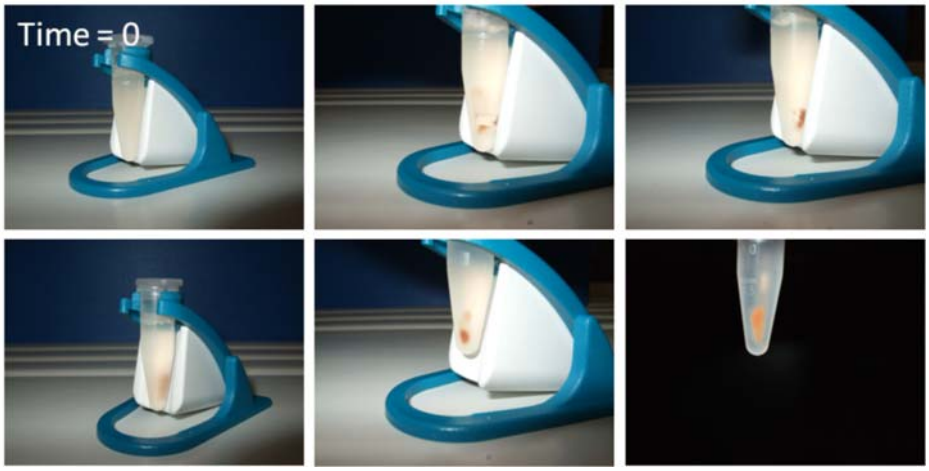

Figure 4.14. Real-Time. Biased movement of HEK293T cells mag-fected with 2 µm paramagnetic microspheres with time (left to right).

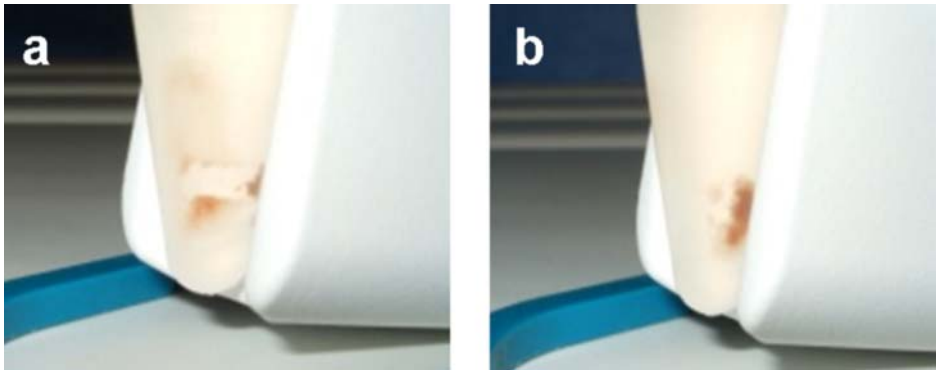

Figure 4.15. Magnetic Cells. a. From a homogeneous solution "mag-fected" cells being to aggregate and are attracted to the external magnet; **b.** "Mag-fected" cells cluster at the external magnet.

Furthermore, no evidence could be found of microspheres leaving the cell when the magnetic field was applied and the cells could be repeatedly moved in response to the magnetic field. This result demonstrates that not only do magnetic microspheres efficiently enter cells, but they are additionally capable of "magnetising" the cell and

allowing its movement in response to a magnetic field, despite its comparatively small size.

4.6. Conclusions

Magnetically susceptible microspheres in the size range of 0.3 – 2 μm have been produced by a dispersion polymerisation procedure. Size variation was achieved by alteration of the stabiliser molecular weight and the monomer addition procedure. Incorporation of 4-vinylbenzylamine.HCl allowed production of amino functionalised microspheres and the use of divinylbenzene provided highly cross-linked microspheres that were stable in several solvents including DMF and DMSO. This allowed the microspheres to be fluorescently labelled with carboxyfluorescein, which allowed their intracellular translocation to be followed by flow cytometry and microscopy. The uptake of paramagnetic microspheres was successful in all the cell lines investigated, which included standard suspension and adherent cells and mouse embryonic stem cells. The larger sized microspheres (2 and 1.6 μm) did not negatively affect cell viability. However, 0.3 μm beads were noted to detrimentally affect cell viability. HEK293T cells were mag-fected with 2 μm paramagnetic microspheres and the movement of the cells was biased by the application of an external magnetic field. The cells responded rapidly and significantly to the magnetic field demonstrating the power microspheres have to move cells many times larger than themselves. Such particles could have a range of applications in the fields of cell purification and site specific targeting.

Chapter 5: *Dunking Doughnuts into Cells*

5.1. Introduction

Small mono-disperse particles have previously been demonstrated to have a range of applications in the biomedical and biochemical fields, such as in DNA sequencing,[180, 181] cellular analysis, biochemical reaction multiplexing[95] as well as carriers of *in vitro* cellular sensors.[67] Many methods may be employed to prepare microspheres, however, dispersion polymerisation (although complicated to fully appreciate mechanistically) is perhaps the most easy to manipulate by varying the polymerisation conditions. For example, the solubility of the steric stabiliser (e.g. PVP) may be altered by the addition of polar and non-polar solvents to the alcoholic base media or by the reaction temperature and stirring speeds.[95, 42, 43, 71] In ***Chapter 2***, the addition of water in ethanol facilitated the production of 0.4 – 0.5 μm microspheres, whereas addition of toluene resulted in the formation of 1.8 μm microspheres. This ease of "manipulability" together with the ability to form mono-dispersed particles and the typically excellent yields and conversions obtained[75, 76] makes dispersion polymerisation a particularly attractive method for preparing polymeric materials. Following the successful variation of microsphere diameter by the introduction of co-solvents, further investigations allowed the effect of alternative solvents on the size and morphology of the polymer particles produced to be investigated.

5.2. The Effect of Co-Solvents

Although its effect on the mechanism of dispersion polymerisation is not fully understood, it may be hypothesised that the addition of polar and non-polar co-solvents may facilitate an increase or decrease in the solubility of the stabiliser, PVP. As a consequence, this may have an enhancing or reducing effect on particle stabilisation, resulting in the production of varyingly sized microspheres and, under the addition of some solvents, particles with morphological abnormalities.

5.2.1. Addition of Diethylketone

The addition of 2% *n*-butanol was shown to result in the production of narrowly dispersed 0.7 µm microspheres (***Chapter 2***). As such, alternative solvents with comparable polarity were investigated, such as diethylketone. Polymerisations were carried out, as described in ***Chapter 2***, using styrene, DVB, VBAH and AIBN with PVP as a stabiliser. Under these conditions with 2% diethylketone, laser diffractometry indicated the precipitation of particles of 2.3 µm (**5.1**) in diameter with a coefficient of variance of 40% (2% *n*-butanol in ethanol gave microspheres with a C.V. of 13%) (**Figure 5.1**). SEM confirmed the particle size (**Figure 5.2**) but additionally indicated that some of the 'microspheres' prepared by this method had an unusual structure and appeared heavily swollen and dimpled (**Figure 5.2,** *red arrow*). These unusual structures were found amongst a sea of seemingly normal yet poly-dispersed microspheres.

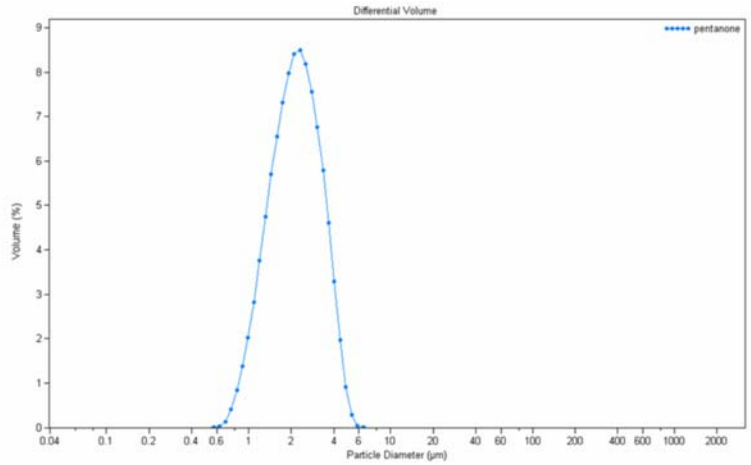

Figure 5.1. Laser Diffractometry. Histogram of 2.3 µm microspheres (**5.1**) prepared by dispersion polymerisation in 2% diethylketone in ethanol (S.D. 0.9 µm, C.V. 39.8%).

There was no obvious reason for the production of these particles and their mechanism of formation was not fully understood. It appeared that normal microspheres were capable of forming under these conditions (**Figure 5.2,** *yellow arrow*), but the polymerisation mixture also facilitated the production of large swollen (possibly hollow) microspheres, which (under their own weight) appeared to collapse, resulting in a dimpled morphology.

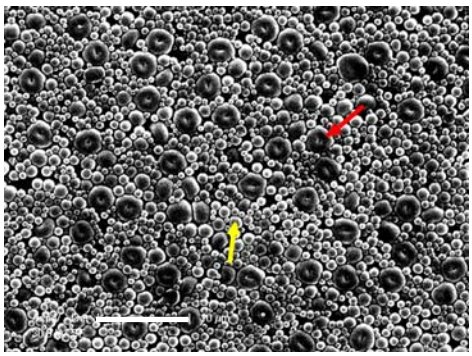

Figure 5.2. Scanning Electron Microscopy. (**5.1**) prepared by dispersion polymerisation in 2% diethylketone in ethanol. Scale bar is 10 µm. *Red arrow* shows dimpled micro-particles; *Yellow arrow* shows polydispersed microspheres.

The unusual result obtained from adding diethylketone to the polymerisation mixture prompted the investigation of further solvents and consideration of how they could affect the product morphology.

5.2.2. Addition of Isopropyl Alcohol

With the addition of 2% IPA to ethanol, laser diffractometry indicated the production of narrowly dispersed 1.8 µm microspheres (**5.2**) (**Figure 5.3**). However, in contrast, SEM analysis showed the production of poly-dispersed, irregularly shaped, swollen and dimpled microspheres (**Figure 5.4**).

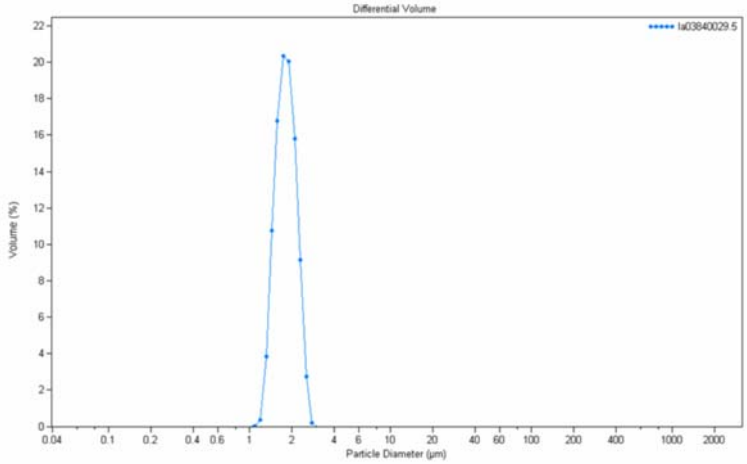

Figure 5.3. Laser Diffractometry. Histogram of 1.8 µm microspheres prepared by dispersion polymerisation with 2% IPA in ethanol (**5.2**) (S.D. 0.28 µm, C.V. 15.8%).

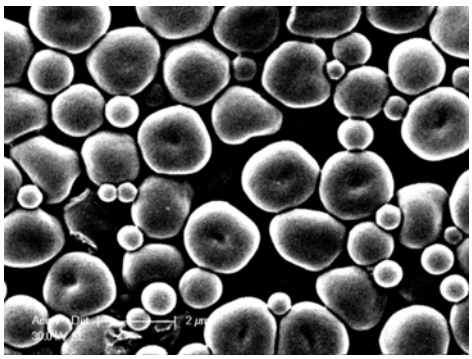

Figure 5.4. Scanning Electron Microscopy. Microspheres prepared by dispersion polymerisation in 2% IPA in ethanol (**5.2**). Scale bar is 2 μm.

In this instance, the size distribution information from the laser diffractometry of microspheres in solution and that from a vacuum dried sample of the microspheres prepared for SEM did not match. This result may suggest that, similar to diethylketone, the addition of IPA to the polymerisation mixture interferes with the production of robust microspheres. As such, the microspheres may swell with fluid and upon drying under vacuum collapse in on themselves (under their own weight). This may be correlated to the dimpled nature of the microspheres using diethylketone or IPA. The occurrence of this perhaps suggests that the 'microspheres' are extensively porous or possibly even hollow (or swollen with fluid).

5.2.3. Addition of Tetrahydrofuran

Further study was made using tetrahydrofuran (THF), which is less polar than diethylketone and IPA. Accordingly, 5% THF in ethanol resulted in 1.6 μm microspheres (**5.3**) by laser diffractometry (**Figure 5.5**), which were subsequently determined by SEM (**Figure 5.6**) to be a poly-dispersed array of microspheres and unusually shaped particles. In this case, polymer constructs exhibiting a central hole were noted to be amongst the array of microspheres, although they were a minority population. Their diameter was found to be approximately 3 μm by SEM and the size of the central hole was approximately 1 μm. In addition, swollen, dimpled microspheres were also noted to be present, similar to those formed from the addition of IPA and diethylketone.

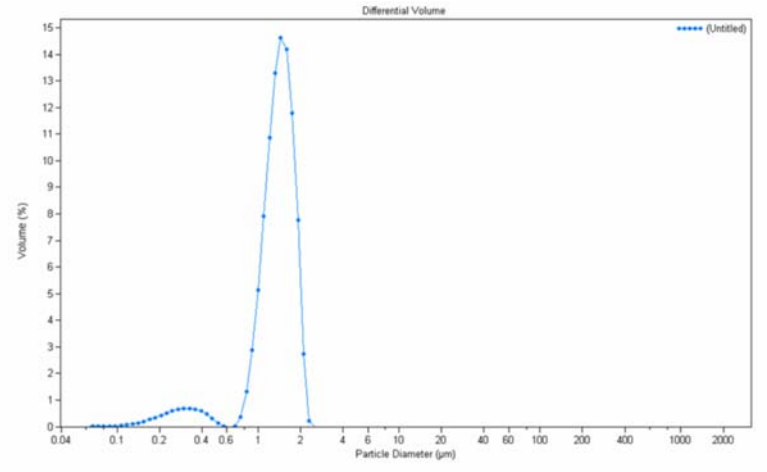

Figure 5.5. Laser Diffractometry. Histogram of 1.6 µm microspheres prepared by dispersion polymerisation in 5% THF in ethanol (**5.3**) (S.D. 0.3 µm, C.V. 21%).

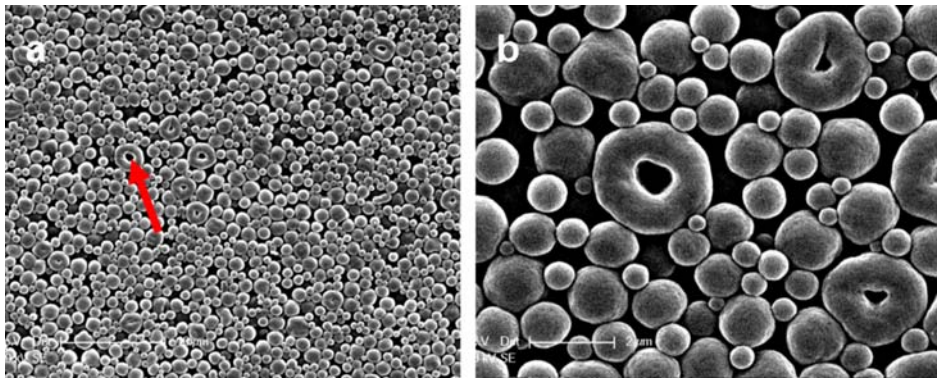

Figure 5.6. Scanning Electron Microscopy. Microspheres prepared by dispersion polymerisation in 5% THF in ethanol (**5.3**). **a.** *en masse*. *Red arrow* shows doughnut-like structures. Scale bar is 10 µm; **b**. 10× magnification of *en masse* image. Scale bar is 2 µm.

This may substantiate that, during drying under vacuum, swollen microspheres become unstable and collapse inward under their own weight generating, initially, dimpled microspheres and finally yielding a "micro-doughnut" morphology. Indeed this hypothesis was corroborated by analysing the particle diameter *via* laser diffractometry following vacuum drying, where a widely poly-dispersed distribution was recorded.

5.3. Addition of 1,4-Dioxane

Varying the solvent in which dispersion polymerisation occurs has been shown to have a profound effect on not only the size, but also the quality and shape of the polymer product precipitated. As such, the effect that an additional solvent, 1,4-dioxane, had on the polymer product was investigated adding 0.5 – 10% to ethanol. This resulted in the production of varyingly sized particles from 1.2 – 9.1 µm in diameter, (**5.4**) **–** (**5.14**), as found by laser diffractometry (**Figure 5.7**). Interestingly, SEM analysis of particles prepared with 5% 1,4-dioxane in ethanol revealed the production of particles with a uniform doughnut-like morphology (**5.9**) (**Figure 5.8**).

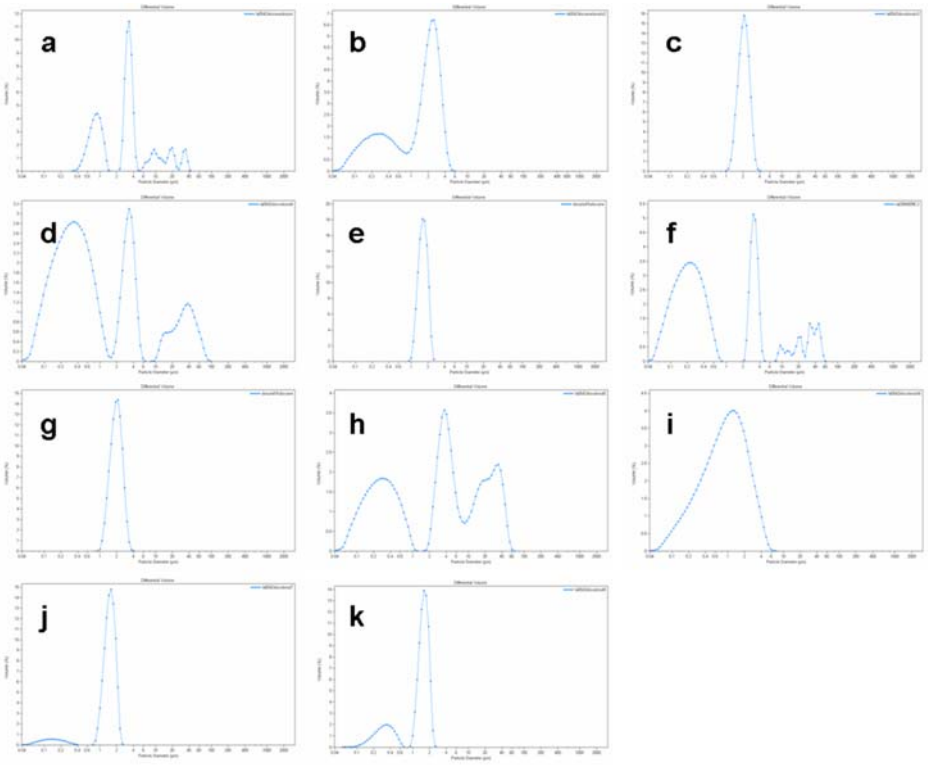

Figure 5.7. Laser Diffractometry. Histograms of microspheres, (**5.4**) **–** (**5.14**), prepared with **a.** 0.5% (**5.4**) (mean 5.5 µm, S.D. 7.8 µm, C.V. 141%); **b.** 1% (**5.5**) (mean 1.7 µm, S.D. 1.2 µm, C.V. 71%); **c.** 2% (**5.6**) (mean 2.1 µm, S.D. 0.5 µm, C.V. 22%); **d.** 3% (**5.7**) (mean 6.3 µm, S.D. 13.7 µm, C.V. 218%); **e.** 4% (**5.8**) (mean 1.6 µm, S.D. 0.3 µm, C.V. 18%); **f.** 5% (**5.9**) (mean 4.8 µm, S.D. 10.8 µm, C.V. 227%); **g.** 6% (**5.10**) (mean 2.0 µm, S.D. 0.5 µm, C.V. 24%); **h.** 7% (**5.11**) (mean 9.1 µm, S.D. 12.5 µm, C.V. 137%); **i.** 8% (**5.12**) (mean 1.2 µm, S.D. 1.0 µm, C.V. 83%); **j.** 9% (**5.13**) (mean 1.4 µm, S.D. 0.5 µm, C.V. 34%) and **k.** 10% (**5.14**) (mean 1.3 µm, S.D. 0.6 µm, C.V. 46%) 1,4-dioxane in ethanol.

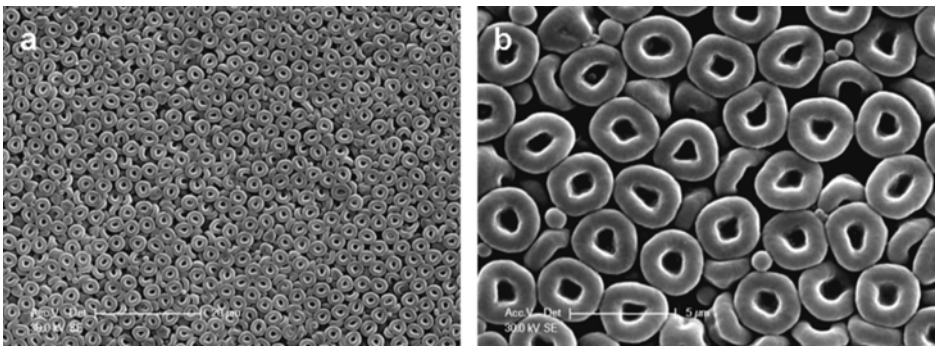

Figure 5.8. Scanning Electron Microscopy. Micro-doughnuts prepared with 5% 1,4-dioxane (**5.9**). **a.** *en masse* micro-doughnuts. Scale bar is 20 μm; **b.** 4× magnification of *en masse* image. Scale bar is 5 μm.

Other percentages of 1,4-dioxane resulted in the production of poly-dispersed microspheres (**Figure 5.9**), except, 7% 1,4-dioxane in ethanol, which also resulted in the formation of micro-doughnuts (**5.11**). However, in this instance, the micro-doughnuts were produced alongside poly-dispersed microspheres.

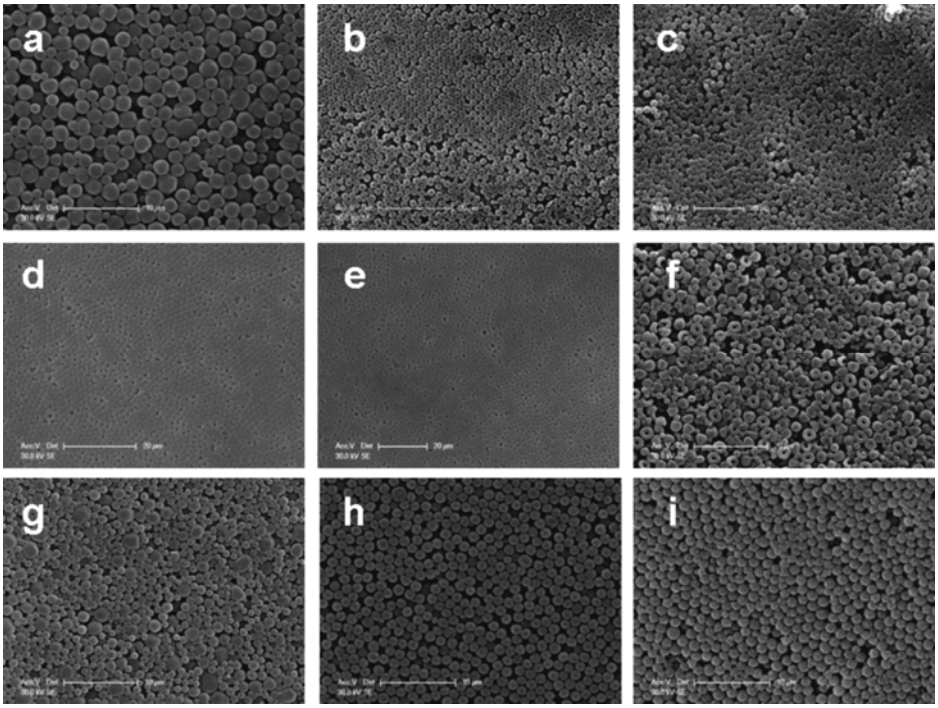

Figure 5.9. Scanning Electron Microscopy. (**5.4**) **–** (**5.8**) and (**5.10**) **–** (**5.14**), prepared with 1,4-dioxane as the co-solvent. **a.** 0.5% (scale bar is 10 μm); **b.** 1% (scale bar is 20 μm); **c.** 2% (scale bar is 20 μm); **d.** 3% (scale bar is 20 μm); **e.** 4% (scale bar is 20 μm); **f.** 6% (scale bar is 20 μm); **g.** 7% (scale bar is 20 μm); **h.** 8% (scale bar is 10 μm); **i.** 9% (scale bar is 10 μm) and **j.** 10% (scale bar is 10 μm) 1,4-dioxane in ethanol.

5.3.1. Micro-Doughnuts

By SEM the micro-doughnuts were found to be 3 µm in diameter with a 1 µm central hole, a result corroborated by laser diffractometry analysis, where a sharp peak was present at 3 µm (**Figure 5.7 f**). This suggests that, unlike diethylketone, IPA and THF (where the in-solution laser diffractometry analysis did not support the vacuum-dried SEM analysis), the micro-doughnuts were stable in solution and formed during the polymerisation process (or upon cooling of the reaction mixture) rather than being formed during vacuum drying. This was confirmed, examining the micro-doughnuts in solution by microscopy.

Although the mechanism by which the micro-doughnuts form is not fully understood, it appears that not only the solvent plays a crucial role in their formation.

5.3.2. Divinylbenzene

Divinylbenzene exhibits its cross-linking activity by anchoring the growing polystyrene chains together resulting in 'hardening' of the particle and rendering it more stable (**Scheme 5.1**). This allows reactions to be performed on the particles in aggressive solvents, such as DMF.

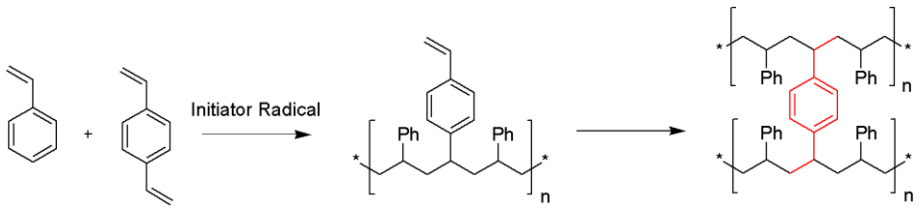

Scheme 5.1. DVB Cross-Linking. Divinylbenzene anchors polystyrene chains together, generating stable microspheres.

To prevent the premature polymerisation of DVB, it is packaged with an inhibitor (in this case, 4-*tert*-butylcatechol at 1000 ppm), which may be removed by sequential washing with 25% sodium hydroxide and water, resulting in a colour change of the DVB solution from clear colourless to bright yellow. However, it was noted that, over a period of several months storage (at 4 ºC), the yellow colour subsided, giving a pale straw colour (**Figure 5.10,** *right*). In order for micro-doughnuts to form, 5% 1,4-dioxane had to be used in combination with "aged" DVB (pale straw colour).

Figure 5.10. Divinylbenzene. DVB containing t-butylcatechol (*left*); DVB freshly washed free of t-butylcatechol (*middle*); DVB washed free of t-butylcatechol and stored at 4 ºC for > 1 month (*right*).

When dioxane is used with freshly washed DVB, poly-dispersed microspheres resulted (**Figure 5.11a**). If DVB was not added to the polymerisation mixture, microspheres precipitated (**Figure 5.11b**).

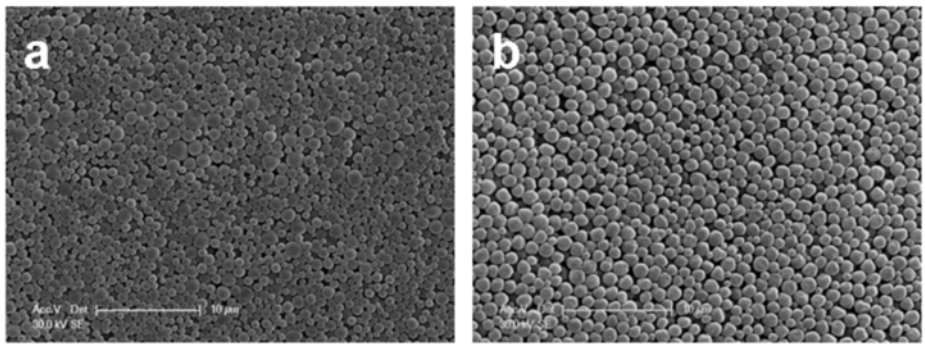

Figure 5.11. Scanning Electron Microscopy. Microspheres prepared with **a.** 5% 1,4-dioxane and freshly washed DVB; **b.** 5% 1,4-dioxane but in the absence of DVB. Scale bars are 10 µm.

To investigate the differences between the DVB solutions shown in **Figure 5.10**, DVB containing 4-*tert*-butylcatechol, DVB freshly washed free of 4-*tert*-butylcatechol and the DVB used to prepare micro-doughnuts were analysed and compared by HPLC and NMR. Interestingly, NMR showed that the DVB solutions were indistinguishable. However, HPLC analysis of the DVB solutions showed an impurity peak present in DVB used to prepare micro-doughnuts (retention time: 3.8 minutes), which was not extensively present in either freshly washed DVB or DVB containing 4-*tert*-butylcatechol (**Figure 5.12c,** *black arrow*). However, it is unclear what this contaminant is, since it was not significant enough to be detected by NMR and thus is unlikely to be due to short chain DVB oligomers.

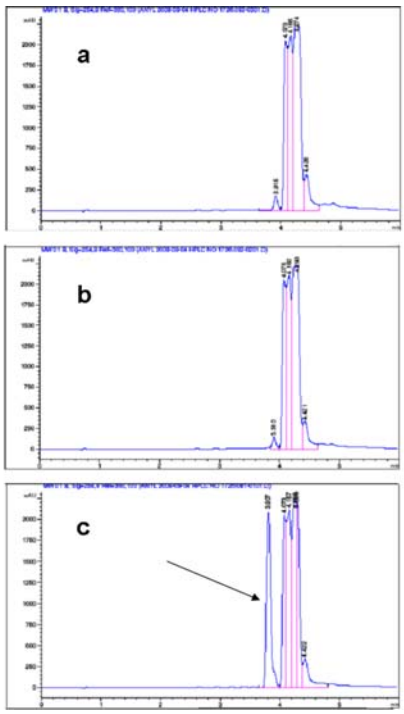

Figure 5.12. HPLC Analysis. a. DVB containing t-butylcatechol; **b.** DVB freshly washed with 25% NaOH/water; **c.** DVB washed with 25% NaOH/water and stored at 4 ºC for > 1 month. λ = 254 nm.

5.3.3. Mechanism of Micro-Doughnut Formation

As with diethylketone, IPA and THF, it is plausible that microspheres originally precipitate from the homogeneous solution. However, the microspheres may have inefficient cross-linking from DVB and thus begin to swell with solvent. As they distend they may become unstable, unable to support their own weight. As this occurs, the microsphere may collapse inward resulting in at first a dimpled morphology and subsequently a ring-shaped structure. This theory is supported by the presence of unusually shaped particles, which appear as elongated micro-doughnuts (**Figure 5.13**).

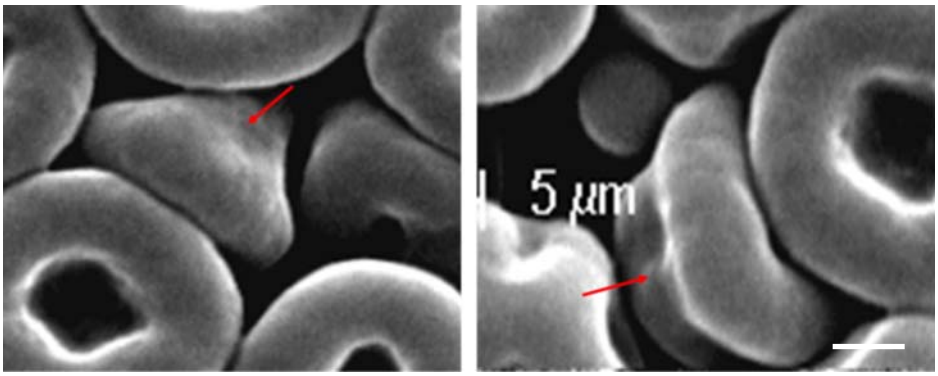

Figure 5.13. Scanning Electron Microscopy. Elongated doughnuts (*red arrows*). Scale bar is 1 µm.

Doughnut-like structures have previously been generated using a number of techniques, such as electrohydrodynamic atomization or the so-called "breath figure" technique.[182, 183, 184, 185] Electrohydrodynamic atomization (EHDA) is largely an electrospray technique, whereby a high voltage is applied to a nozzle through which a solution is pumped. At the tip of the nozzle a liquid cone is generated, from which mono-dispersed droplets are released. The diameter of the droplets (and thus of the final product) are dependent on many factors, including the density and the conductivity of the pumped fluid.[186] In the 'breath figure' technique, which is applied to the production of porous constructs, water micro-droplets are condensed onto a solution surface containing polymers. The polymers present in this cast solution then precipitate around the water droplets generating honeycomb-like structures.[187] However, in both these techniques the doughnut-like particles were typically generated within a sea of other particles and were non-homogeneous in size and shape. Using dispersion polymerisation the doughnut products were mono-dispersed and the shape was highly uniform.

5.3.4. Preparation of Fluorescent Micro-Doughnuts

Micro-doughnuts incorporated vinylbenzylamine giving an amine loading of 9.6 $\mu molg^{-1}$ and allowed labelling of the micro-doughnuts with a fluorophore (**Scheme 5.2**).

Scheme 5.2. FAM-Doughnuts. Labelling of amino micro-doughnuts (**5.9**) with fluorescein (**5.16**) *via* an aminohexanoic analogue (**5.15**).
(i). 10 eq. Fmoc-Ahx-OH, 10 eq. HOBt, 10 eq. DIC, DMF, 10 minutes, 25 ºC, 18 h; (ii). 20% piperidine/DMF; (iii). 10 eq. 5(6)-carboxyfluorescein, 10 eq. PyBOP, 10 eq. HOBt, 10 eq. DIPEA, 1 minute, 25 ºC 18 h.

Fluorescein micro-doughnuts (**5.16**) were analysed by confocal microscopy to establish if the 1 μm central hole transversed the particle or if it was merely a surface defect (**Figure 5.14** and the Supplementary Information on CD for

movie). This established not only that the micro-doughnut hole translocated the entire construct but it also confirmed that labelling of the micro-doughnut with fluorescein transversed the entire particle and was not just surface bound. This indicated the chemical accessibility of amino functionalities throughout the entire micro-doughnut. It additionally demonstrated the stability of the micro-doughnuts, since coupling reactions were performed in DMF.

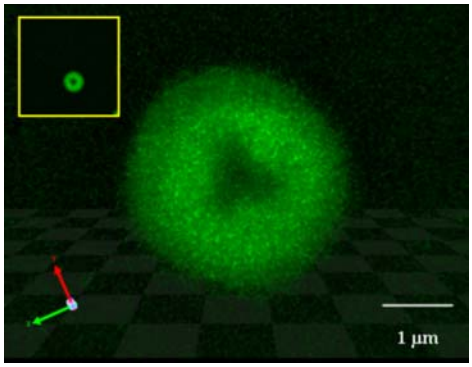

Figure 5.14. Confocal Microscopy. 3-D reconstruction of a fluorescein micro-doughnut (**5.16**).

5.4. Cellular Uptake

Microspheres exhibited highly efficient cellular uptake in a number of cell lines, including stem cells (***Chapter 3***). It was therefore of interest to examine what affect the doughnut-like morphology would have on cellular uptake. As such, carboxyfluorescein labelled micro-doughnuts (**5.16**) were incubated with a variety of mammalian cells (mouse fibroblast (L929) cells, mouse macrophage (RAW264) cells, human embryonic kidney (HEK293T) cells, human cervical cancer (HeLa) cells, mouse melanoma (B16F10) cells, erythroleukemic (K562) cells and mouse stem cells (E14)) for 6, 12 and 24 hours at a concentration of 86 µg/mL (analogous to the concentration of microspheres used in a typical uptake analysis). Uptake was quantified by flow cytometry using 0.2% trypan blue to quench extracellular fluorescence[110] thus ensuring that only those particles that entered the cells were detected. The results have been summarised by **Graph 5.1** and interestingly, uptake was found to vary widely between the cell lines with only RAW264 macrophages, HEK293T and L929 cells showing a reasonable uptake of micro-doughnuts (93 – 33% after 24 hours). Furthermore, in general the uptake of micro-doughnuts in cells

was lower than microspheres. For example, the uptake of micro-doughnuts in HEK293T cells after 24 hours was found to be 50%, however, the uptake of microspheres (at the same mass/mL and after the same incubation time) was generally more than 90%. However, analogous to microspheres, it was found to be incubation time and concentration dependent (**Graph 5.2**).

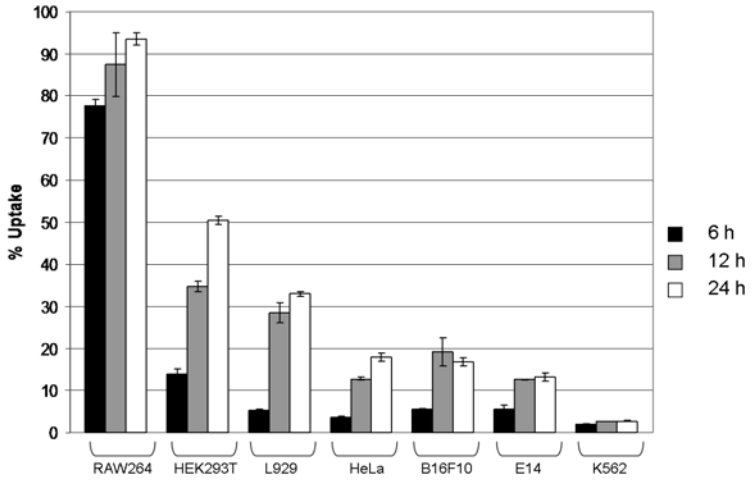

Graph 5.1. Doughnut-Fection. Uptake of (**5.16**) by L929, RAW264, HEK293T, HeLa, B16F10, K562 and E14 cells after 6, 12 and 24 at 86 µg/mL.

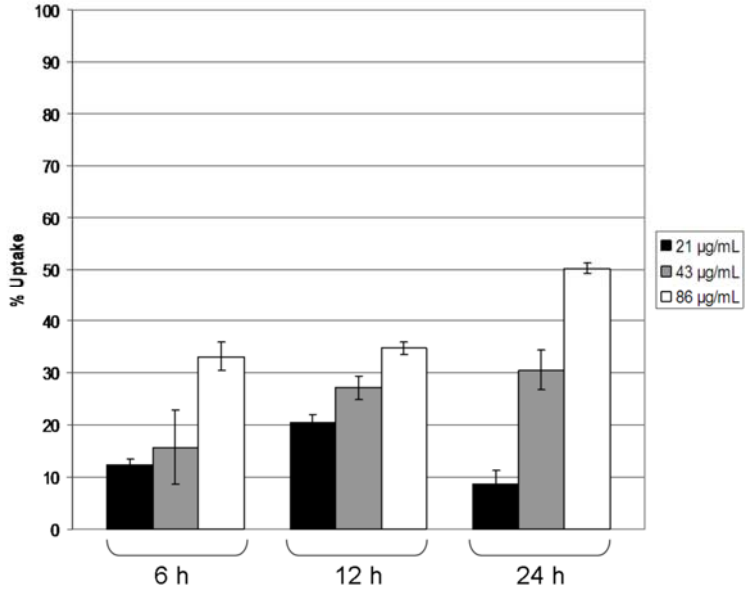

Graph 5.2. Concentration Dependence. Uptake of fluorescein micro-doughnuts (**5.16**) in HEK293T cells as a function of time (6 – 24h) and concentration (21 – 86 µg/mL).

As with microspheres, it should be noted that micro-doughnuts were in great excess over cells (approximately 3000:1) and altering the concentration of micro-doughnuts

present does not have as substantial an effect as may be at first expected, as it is already at a near-saturation level.

Internalisation was additionally confirmed by pseudo-confocal microscopy and a representative example of RAW264 cells is shown in **Figure 5.15**, where cellular appetite for the doughnuts was excessive. This resulted in over-loading of the cells (**Figure 5.15b-c**) due to the active phagocytic nature of RAW264 cells, unless highly controlled concentrations were used (**Figure 5.15a**).

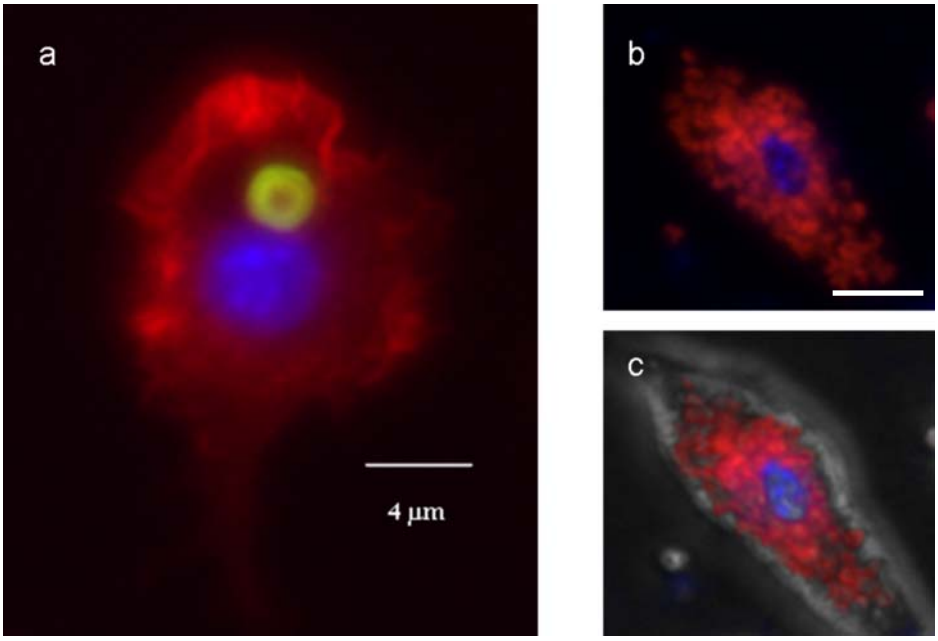

Figure 5.15. Excessive Consumption? Uptake of micro-doughnuts by RAW264 cells **a.** fluorescein micro-doughnut (**5.16**) in RAW264 cell stained with AlexaFluor568-phalloidin (actin filaments) and Hoechst 33342 (nucleus). Microscopy was performed after 3 hours (21 µg/mL); *Right:* RAW264 cell heavily laden with Rhodamine B labelled micro-doughnuts (**5.17**) (shown in red) (scale bar is 20 µm) **b.** Fluorescence image only; **c.** Fluorescence image merge with brightfield. Microscopy performed after 24 hours (86 µg/mL).

5.5. Toxicity

As shown in **Figure 5.15**, RAW264 cells ingested large quantities of micro-doughnuts resulting in cellular over-loading. In RAW264 cells, this type of uptake is understandable as they are a phagocytic cell line 'designed' to ingest and degrade foreign materials. However, it is vital that micro-doughnuts taken up by cells do not

cause detrimental cytotoxicity if they are to be applied as cellular delivery/tracking devices. To this affect, MTT assays were carried out on "doughnut-fected" cells (**Graph 5.3**) to establish cellular viability.

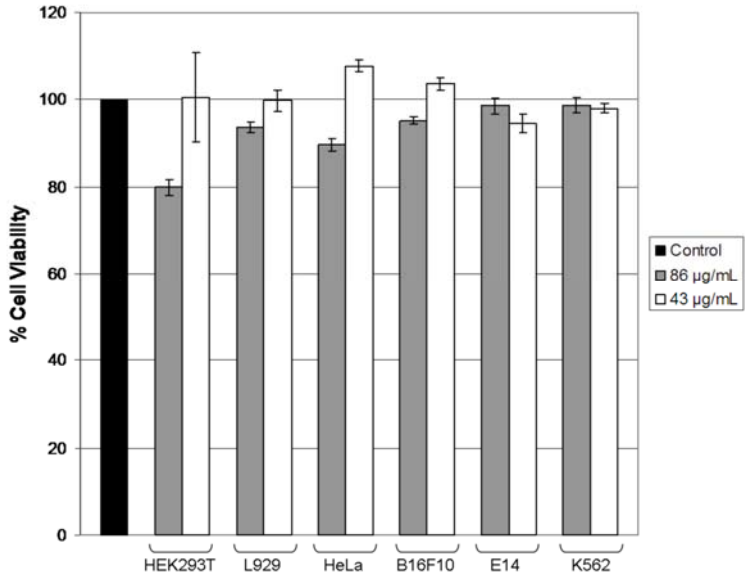

Graph 5.3. Cellular Viability. MTT viability assays of dough-fected cells, compared to untreated control cells assumed to be 100% viable ('Control'). Analysis was performed after 24 h.

Micro-doughnuts did not cause any cytotoxicity *in vitro* and cellular viability was more than 80% in all cases and was more commonly found to be more than 90%.

5.6. Cell Specificity

During these investigations, an interesting pattern was noted in the cellular uptake of micro-doughnuts. Where microspheres are largely indiscriminate, entering most cell lines with high efficiency, micro-doughnuts seemed to be more cell line specific. They were seen to enter macrophage cells (RAW264), human embryonic kidney cells (HEK293T) and mouse fibroblast cells (L929) with good efficiency but their uptake in HeLa, B16F10, E14 and K562 cells was poor (< 20%).

The differences in uptake of micro-doughnuts and microspheres (0.5 and 2 µm) in a range of cell lines are summarised by **Graph 5.4**. Although the microspheres showed little discrimination in terms of cellular uptake, the doughnuts were much more selective.

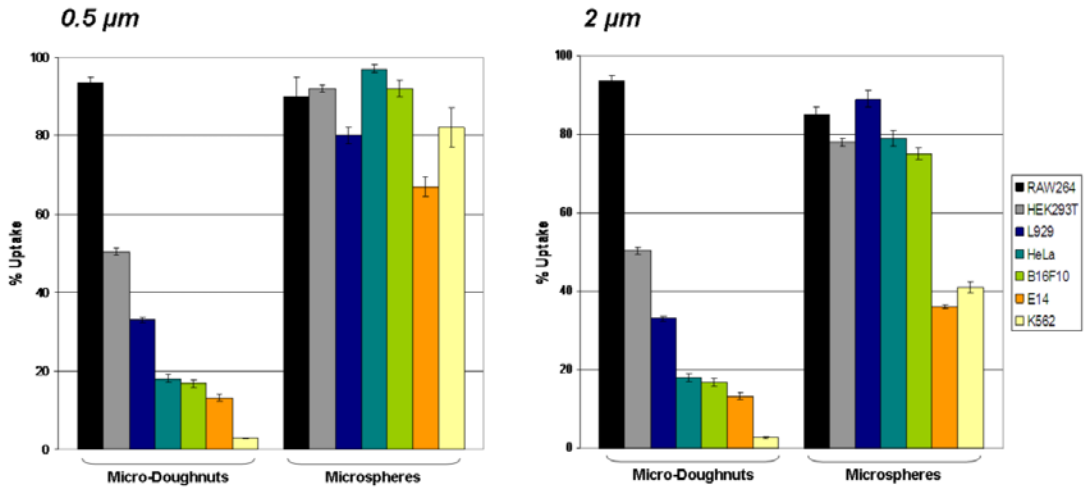

Graph 5.4. Microsphere *vs* Micro-Doughnut. Uptake of micro-doughnuts *vs* (*left*) 0.5 µm microspheres and (*right*) 2 µm microspheres as determined by flow cytometry in RAW264, HEK293T, L929, HeLa, B16F10, E14 and K562 cells. A concentration of 86 µg/mL (micro-doughnuts and microspheres) was used and uptake measured after 24 h.

To illustrate this discrimination a multiplexing experiment was established, where cells were beadfected with fluorescently labelled microspheres so that different cells could be discriminated based on their fluorescent read-out (**Figure 5.16**). Thus, HEK293T cells were "beadfected" with Cy5 labelled microspheres and B16F10 cells with dansyl labelled microspheres. The cells were mixed and re-grown over 24 hours. Rhodamine B labelled micro-doughnuts (**5.17**) were added to the mixed cell culture and after 24 hours, flow cytometry was performed to ascertain which cell line contained micro-doughnuts based on the fluorescent 'tracking' microspheres. A control was established whereby fluorescein microspheres were added to mixed cell cultures to establish the difference in uptake between the two cell lines in competition for an additional microsphere. No specificity was noted for this microsphere, with approximately 70 – 80% uptake in each case (**Figure 5.17**), demonstrating that HEK293T and B16F10 cells had the same capability of taking up additional beads when in competition.

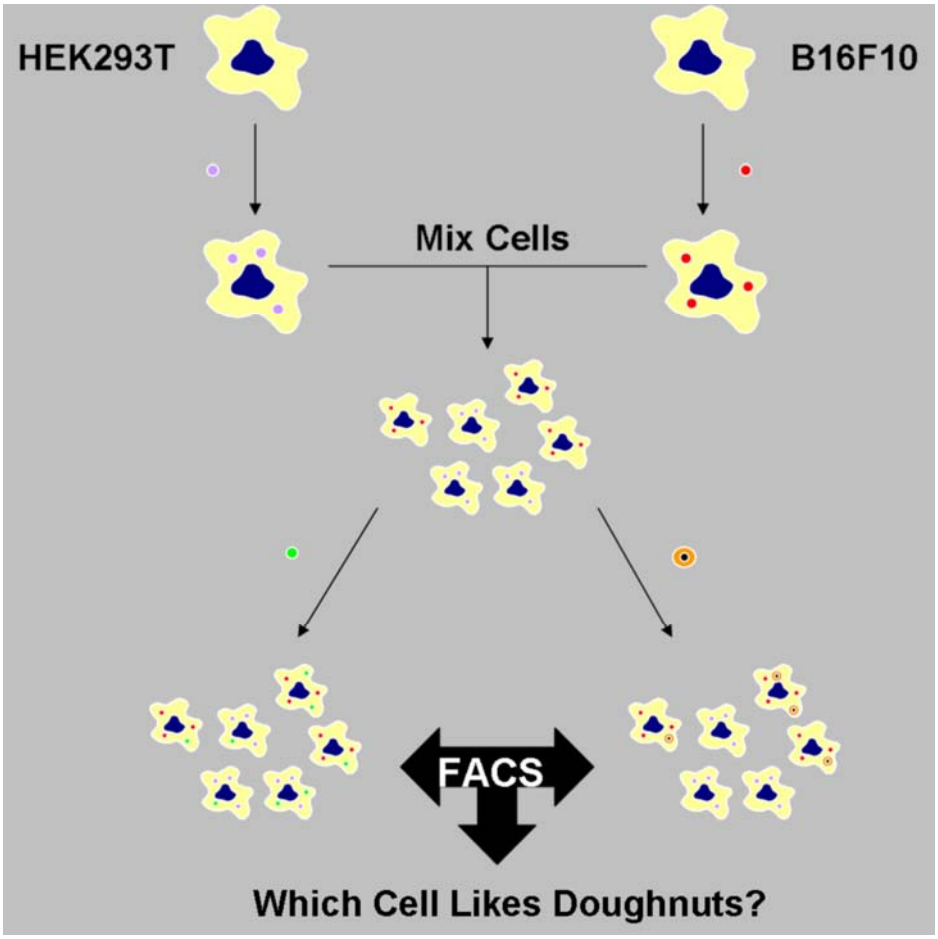

Figure 5.16. Multiplexing. Cells in competition for micro-doughnuts: HEK293T *vs* B16F10.

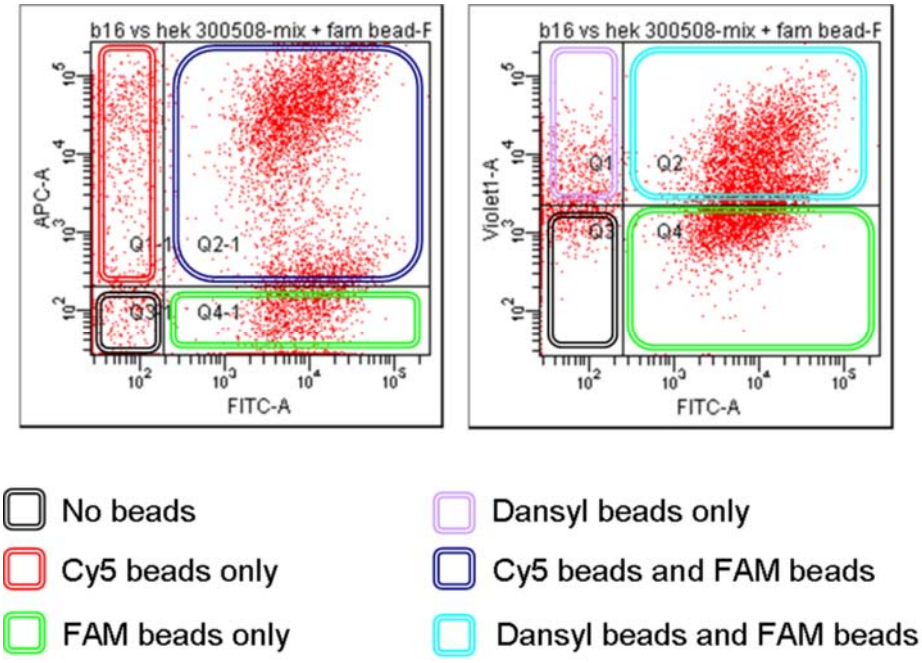

Figure 5.17. Microsphere Multiplexing. FACS histograms of mixed cell cultures beadfected with a fluorescein microsphere. *Left:* HEK293T cells showed 72% ± 0.1% uptake of the fluorescein bead

('APC-A' = Cy5 fluorescence, 'FITC-A' = fluorescein fluorescence); *Right:* B16F10 cells showed 78% ± 2% uptake of the fluorescein bead ('Violet1-A' = dansyl fluorescence).

However, in the case of the uptake of micro-doughnuts, HEK293T cells overwhelmingly took up these particles (42% of cells were "doughnut-fected") preferentially over B16F10 cells (13% of cells were doughnut-fected) (**Figure 5.18**).

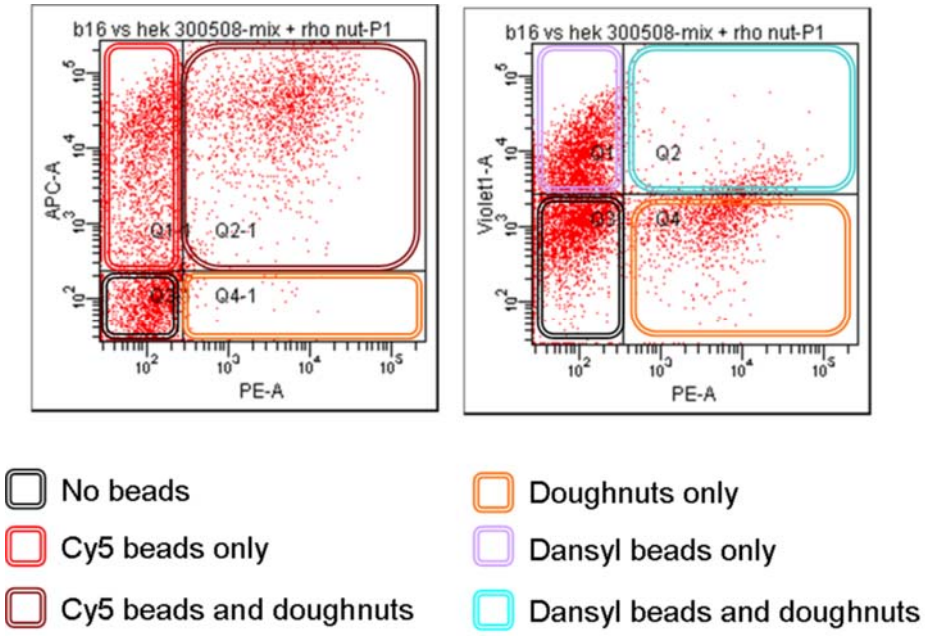

Figure 5.18. Doughnut Multiplexing. FACS histogram of mixed cell cultures incubated with rhodamine micro-doughnuts. *Left:* HEK293T cells showed a doughnut uptake of 42% ± 3%; *Right:* B16F10 cells showed a doughnut uptake of 13% ± 0.5%. 'PE-A' = rhodamine B fluorescence.

This result was confirmed by microscopy (**Figure 5.19**), where HEK293T cells beadfected with Cy5 microspheres (blue) were seen to have taken up the micro-doughnuts (red), whereas B16F10 cells with dansyl microspheres (yellow) were not seen to contain micro-doughnuts.

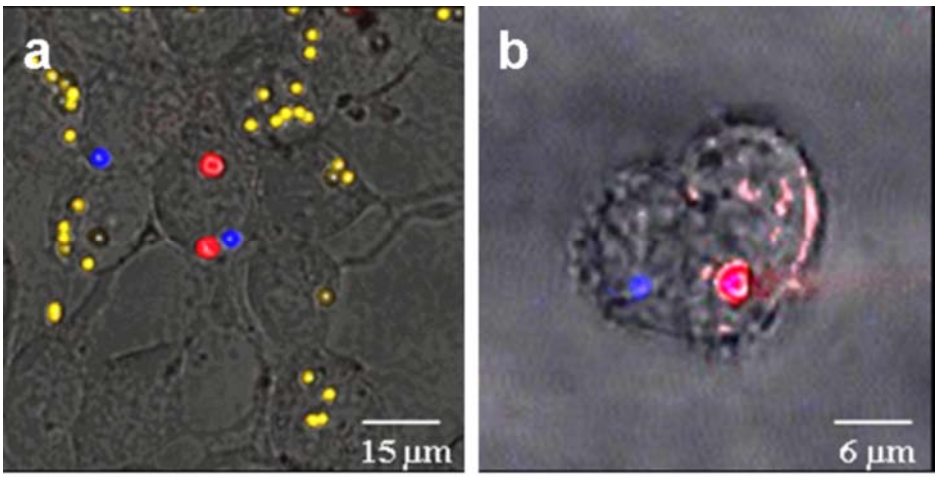

Figure 5.19. Preferential Doughnut-Fection. a. B16F10 cells beadfected with dansyl microspheres (*yellow*) and HEK293T cells beadfected with Cy5 beads (*blue*) and "doughnut-fected" with rhodamine B doughnuts (*red*); **b.** HEK293T cell co-labelled with a Cy5 bead (*blue*) and rhodamine B doughnut (*red*).

This cell specific uptake opens up extremely interesting avenues in the fields of cell separation and site specific targeting and addresses the lack of specificity microspheres have with respect to their entry into cells.

5.7. In Vivo

Even when cell specificity can be demonstrated *in vitro,* the situation in the animal model is much more complex. As such, results obtained in cell cultures can vary widely from those obtained *in vivo.* It was therefore important to investigate if the cell specificity noted in *in vitro* cell cultures was conserved *in vivo.* As such, the *in vivo* fate of Cy7 labelled micro-doughnuts (**Scheme 5.3**) was determined after intravenous injection (tail vein injection, 30 µg) into a 6 week old mouse (all animal experiments were undertaken by Dr. Kev Dhaliwal with an approved licence from the Animal Scientific Procedure Division of the Home Office, London, U.K.).

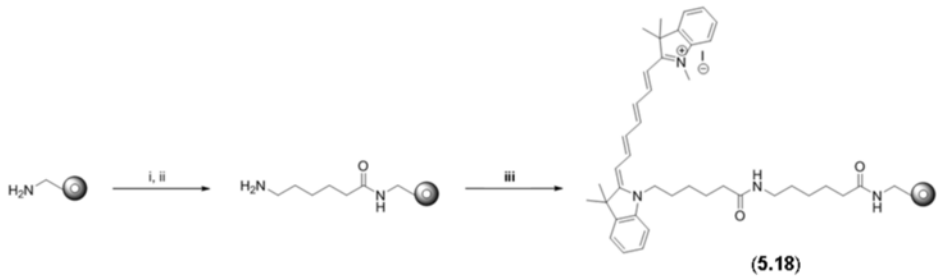

Scheme 5.3. Cy7-Doughnuts. Preparation of Cy7 micro-doughnuts (**5.18**) *via* the aminohexanoic counterpart.
(i). 10 eq. Fmoc-Ahx-OH, 10 eq. HOBt, 10 eq. DIC, DMF, 10 minutes,18 h, 25 ºC; (ii). 20% piperidine/DMF; (iii). 10 eq. Carboxy-Cy7, 10 eq. HOBt, 10 eq. PyBOP, 10 eq. DIPEA, DMF, 18 h, 25 ºC.

After 4 hours, the doughnuts were detected solely in the liver region (**Figure 5.22**) and not in other organs. Presumably, cells circling in the bloodstream (macrophages) took up the micro-doughnuts which were then trafficked to the liver, where they became localised. This may be an attempt to detoxify the blood of foreign material, whereby phagocytic cells are activated to ingest the micro-doughnuts and then transport them to the liver in an attempt to degrade them.

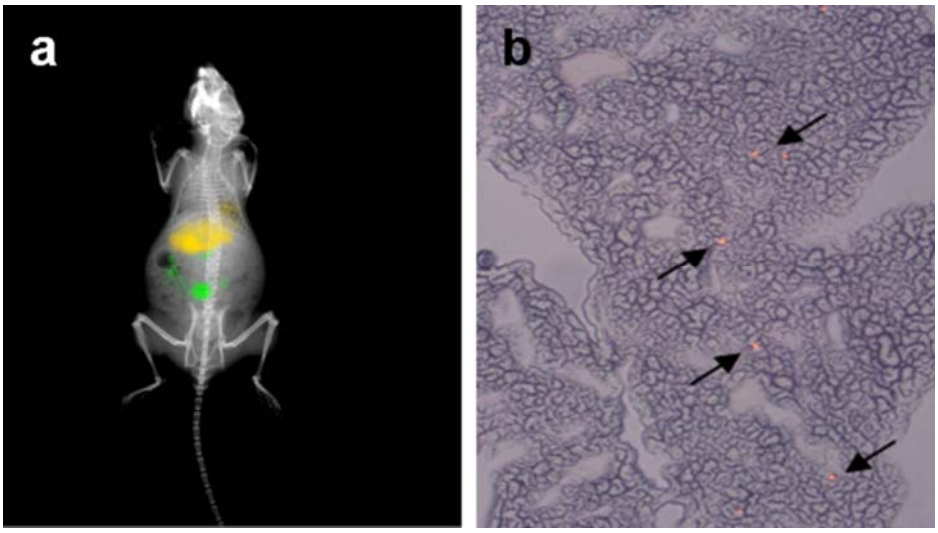

Figure 5.20. *In Vivo.* a. Optical whole body image of Cy7 labelled doughnuts (*yellow*) in the liver. Food (chlorophyll - *green*) is shown in the gut; **b.** Histology on cryostat sections of the liver showing rhodamine B doughnuts (*red, black arrows*) in the liver parenchyma.

As was found in ***Chapter 2***, microspheres were found dispersed in the liver, spleen and lungs following intravenous injection and were unable to show selectivity for any specific organ. The specificity of micro-doughnuts for the liver opens up the opportunity to use these particles in therapy for conditions that affect the liver (for example liver disease) as therapeutics can be selectively delivered to the area of need. Perhaps more importantly, no adverse effects were observed in the animal following injection.

In order to determine the location of the micro-doughnuts within the liver, histology was performed showing that the doughnuts were within the liver parenchyma (**Figure 5.20**), or the main body of the liver. This result is consistent with the micro-doughnuts trafficking to the liver as a result of being ingested by cells present in the bloodstream.

5.8. Conclusions

In conclusion, polymeric composites with an unusual structure were produced *via* the dispersion polymerisation of styrene in 5% dioxane in ethanol, with accessible amino functionalities distributed throughout the doughnut matrix. Their selective cellular uptake has been demonstrated in a variety of cell lines and, when in competition, their selectivity for one cell line over another is clear. Additionally, their selective nature was demonstrated *in vivo*, where intravenously injected micro-doughnuts were noted to localise specifically in the liver suggesting they are ingested by circulating cells and trafficked there using the cell almost as a Trojan horse. More importantly, they were not seen to exhibit any toxic effects in the animal model. This demonstrates that micro-doughnuts could have applications in site-specific delivery, as selective cell tags or could even be applied in cellular separations.

However, it must be noted that micro-doughnuts form under extremely specific conditions, which makes manipulation of their size, shape or composition difficult.

Chapter 6: *Knocking Anti-Sense into Cells*

6.1. Introduction

Microspheres (0.2 – 2 μm) have been shown to rapidly and efficiently enter a range of cell lines, including stem cells (***Chapter 2***) and their uptake has been established to not be an energy dependent process. Furthermore, the microspheres are not seen trapped within endosomes (***Chapter 3***) and instead exhibit cytoplasmic localisation which is beneficial for several reasons. Firstly, cargo which becomes trapped within endosomes can be trafficked to acidic lysosomes, which have aggressive equipment (e.g. nucleases and proteases) that can result in the degradation of the cargo. As such, for many delivery devices to function, they require administration of endosomal disrupting agents. Secondly, some specific cargos, for example enzymes or siRNA, require cytoplasmic localisation for function.[188]

6.1.1. The RNAi Pathway

siRNA (short interfering RNA or small interfering RNA) are short (typically 18 – 21 nucleotides long) double stranded pieces of RNA. They are produced naturally and are involved in a pathway known as RNA interference (RNAi).[189, 190] Since its discovery in the 1990s[191] interest has grown exponentially due to the applications it may have in the biomedical field, for example in the silencing of genes that are known to cause a diseased state.

The RNAi pathway starts with cytoplasmic double stranded siRNA forming a construct with a multi-protein unit forming a complex known as the RNA-Induced Silencing Complex or, more commonly, RISC.[192] Although it is not fully understood it is considered that the RISC facilitates the dissociation of the double stranded siRNA and the sense strand (the anti-guide or passenger strand) may then be degraded by the RISC.[193] Thus, the protein together with the anti-sense strand of the siRNA (the guide strand) forms an activated RNA-Induced Silencing Complex, which seeks out endogenous mRNA with a complementary sequence to the guide strand (**Figure 6.1**). When the mRNA hybridises with the anti-sense siRNA strand a

chain of events are triggered which results in the degradation of the mRNA strand, possibly by a type of RNase.[194]

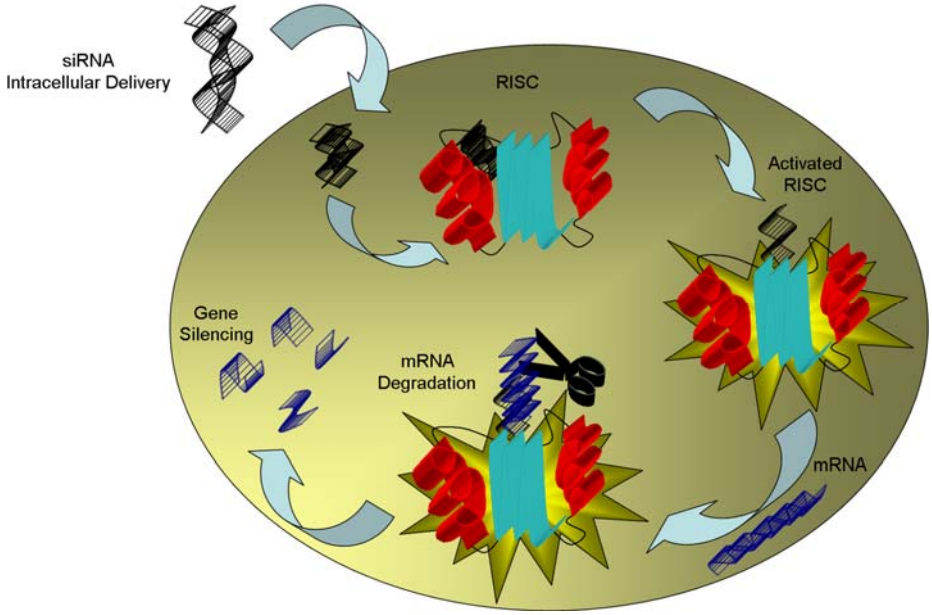

Figure 6.1. RNAi. The RNA Interference pathway.

As a consequence, the protein which is coded for by the mRNA is not made and there is a decrease in its concentration (described as knockdown or gene silencing). Under conditions where a gene is responsible for causing the diseased-state, the degradation capability of siRNA may be harnessed as a therapy.[195, 196]

6.1.2. Delivery of Therapeutic siRNA

Non-natural siRNA is not able to translocate the cellular membrane itself due to the negative charge associated to the phosphate backbone (**Figure 6.2**) and thus requires a delivery vehicle. Although viral approaches[197] have been shown to be widely effective, safety implications rule out their wide spread use. The most commonly used viruses are adenoviruses, lentiviruses and retroviruses. Adenoviruses are DNA viruses capable of entering a wide range of mammalian cells *via* their interaction with the coxsackie adenovirus receptor (CAR) followed by integrin mediated endocytosis. It then traffics to the nucleus where its DNA becomes expressed. Lentiviruses and retroviruses are positive-strand RNA viruses that are capable of integrating their genome into the host chromosomes. Again, these viruses are capable of entering an extensive range of mammalian cells.

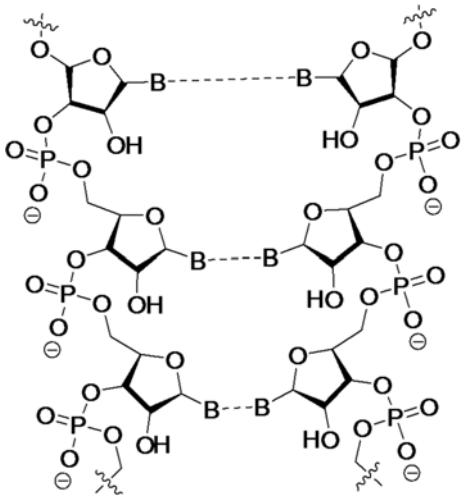

Figure 6.2. siRNA. Example structure of double stranded siRNA with a negatively charged phosphate backbone. 'B' = nucleobase.

Non-viral vectors have also been investigated; amongst these are cationic lipids and carbon nanotubes.[198, 199] Cationic lipids have subsequently been commercialised under a variety of names, including Lipofectamine™ and HiPerFect™. However, they can require specialist transfection conditions (for example, serum-free and antibiotic-free) and care must be taken to avoid substantial cytotoxicity.[102] Carbon nanotubes have successfully been used to perform *in vitro* gene silencing in a number of cell lines including primary human T cells, where they were employed in the knockdown of CXCR4 and CR4 receptors.[198] However, there are questions related to the toxicity of carbon nanotubes,[39] they can be problematic to functionalise[200] and they are widely considered to be internalised by endocytosis meaning endosomal disrupting agents must be employed in order to release the siRNA to the cytoplasmic region before it is degraded in the endosome/lysosome.[36]

To research further into the range of therapeutic applications siRNA can have, there is a greater need for an efficient, non-toxic delivery device that can facilitate the cytoplasmic delivery of siRNA.

6.2. Microspheres as Delivery Devices of siRNA

Microspheres have previously been demonstrated as efficient delivery agents of biological cargos, including sensors, proteins and dye molecules.[67, 68] As well as

having high uptake efficiency in a wide range of cells, they also have been shown to be non-toxic at appropriate concentrations[95] and may be easily functionalised. These traits make microspheres particularly applicable to siRNA delivery.

6.2.1. Enhanced Green Fluorescent Protein

An easily measurable and well studied knockdown target is enhanced Green Fluorescent Protein (EGFP). Transformed cell lines, for example human cervical cancer (HeLa) cells, can be easily genetically modified to code for the permanent production of GFP, which renders the cells fluorescent (excitation at 488 nm, emission at 509 nm). Silencing of the gene which codes for the production of GFP can be easily quantified by flow cytometry and visualised by microscopy, making it an easily validated target.

In order to study microsphere mediated EGFP silencing, a number of siRNA sequences were first generated, which should facilitate silencing of the gene responsible for the production of GFP in both HeLa and ES cells (**Figure 6.4**).[201, 202]

GFP Sequence	*Sense (5' → 3')*	*Anti-Sense (5' → 3')*
GFP-1	GCU GAC CCU GAA GUU CAU CUU	GAU GAA CUU CAG GGU CAG CUU
GFP-2	CGA GCA CGA CUU CUU CAA GUU	CUU GAA GAA GUC GUG CUG CUU
GFP-3	GCA AGC UGA CCC UGA AGU UCA UUU	AUG AAC UUC AGG GUC AGC UUG CUU

Figure 6.4. siRNA Sequences. Silencing of the EGFP gene with homologous siRNA sequences (target sequence: 5'-GCU GAC CCU GAA GUU CAU-3').[203]

In order to establish which of the 3 sequences facilitated efficient GFP silencing, human cervical cancer cells permanently expressing EGFP (HeLa-EGFP) were transfected with the 3 sequences using the commercially available transfection agent, Lipofectamine™ 2000 (**Graph 6.1**). Sequence GFP-1 delivered the most efficient gene silencing (48% maximal) and was thus employed in further studies.

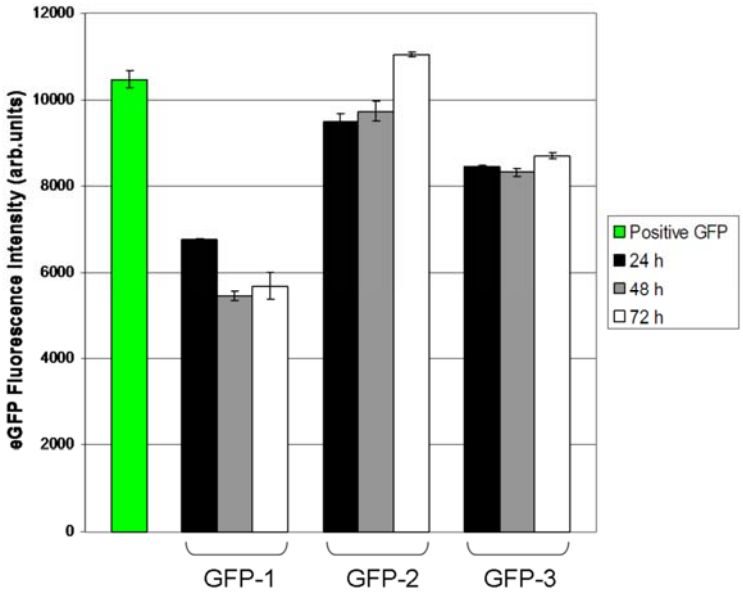

Graph 6.1. Lipofection. Silencing of EGFP in HeLa-EGFP cells using siRNA (GFP-1, GFP-2, GFP-3, 20 pmol) transfected with Lipofectamine™ 2000. Positive GFP refers to untreated HeLa-EGFP cells (average fluorescence over 72 hours).

6.2.2. siRNA Coupling to Microspheres

6.2.2.1. Fluorescently Labelled siRNA

In order to facilitate the linkage of siRNA (GFP-1) to microspheres and to quantitate this coupling, siRNA functionalised with an amino residue on the 5' end of the sense strand (passenger strand) and a TAMRA fluorophore (excitation at 542 nm, emision at 568 nm) on the 5' anti-sense strand was adopted and coupled to 2, 0.5 and 0.2 μm polystyrene microspheres using standard solid phase techniques (**Scheme 6.1**). Using fluorescently labelled siRNA allowed the success of coupling to be measured by flow cytometry (**Figure 6.3**) and was found to be successful for 0.5 and 0.2 μm microspheres. However, it was not possible to couple siRNA efficiently to 2 μm microspheres despite repeated attempts. It is unclear why siRNA did not couple well to the larger sized microspheres, which were shown to be of good quality by SEM (***Chapter 2***) and had an amine loading of 6.7 $\mu molg^{-1}$ by quantitative ninhydrin test, sufficient for significant siRNA loading.

An additional advantage of using fluorescent siRNA is that the approximate loading of siRNA per microsphere could be calculated by analysis of the supernatant from the coupling by fluorescence spectrofluorimetry.

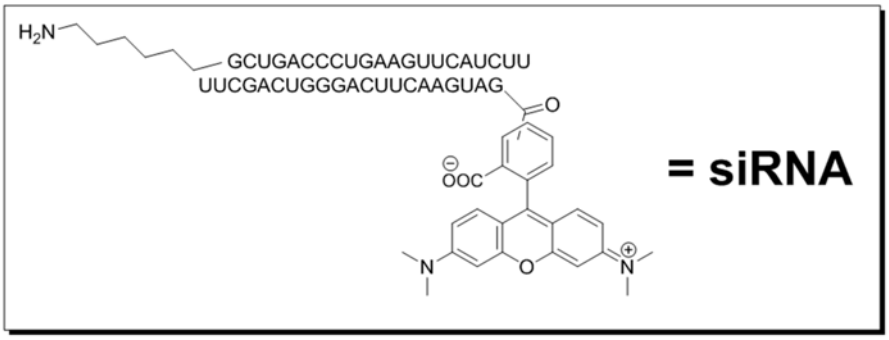

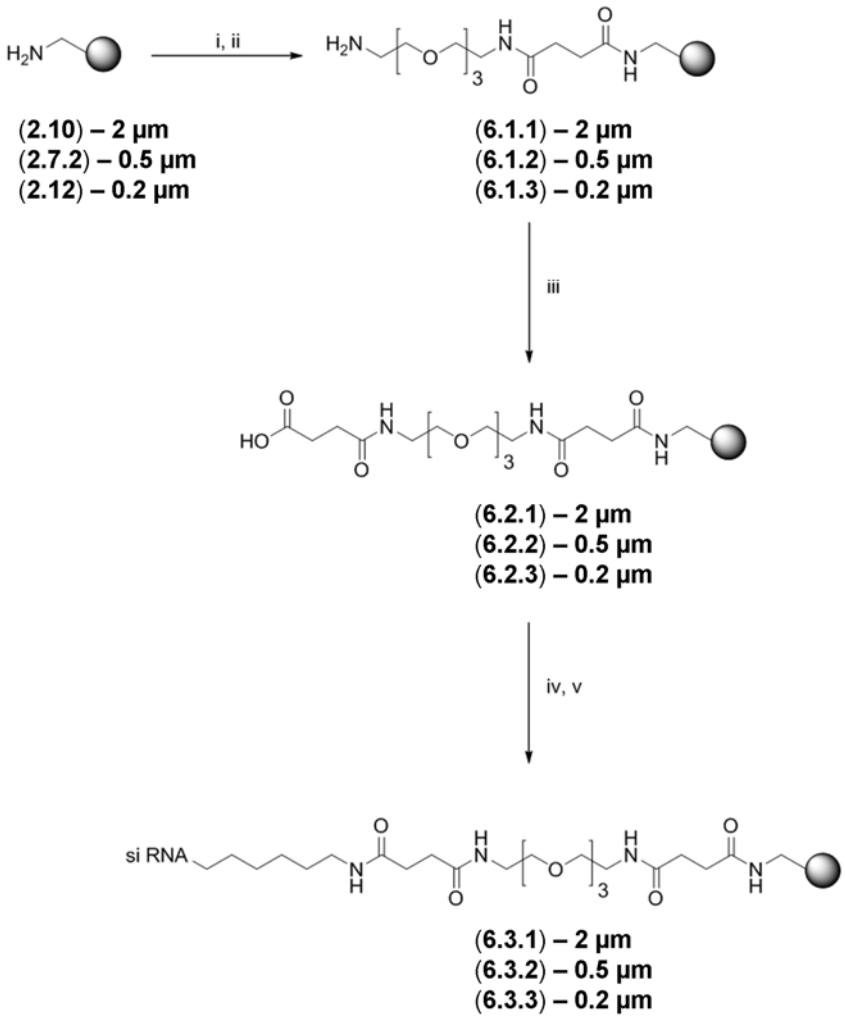

Scheme 6.1. siRNA Microspheres. Coupling of siRNA to 2 µm (**2.10**), 0.5 µm (**2.7.2**) and 0.2 µm (**2.12**) microspheres *via* a non-cleavable succinic linkage, yielding (**6.3.1**), (**6.3.2**) and (**6.3.3**).
(i). 10 eq. Fmoc-PEG-OH, 10 eq. HOBt, 10 eq. DIC, DMF, 18 h, 25 ºC; (ii). 20% piperidine/DMF, 3 × 20 min, 25 ºC; (iii). 10 eq. Succinic anhydride, 10 eq. DIPEA, DMF, 18 h, 25 ºC; (iv). 10 eq. EDAC, MES (pH 5.5), 2 h, 25 ºC; (v). TAMRA labelled *or* unlabelled amino-siRNA, sterile RNase Free water, 24 h, 25 ºC.

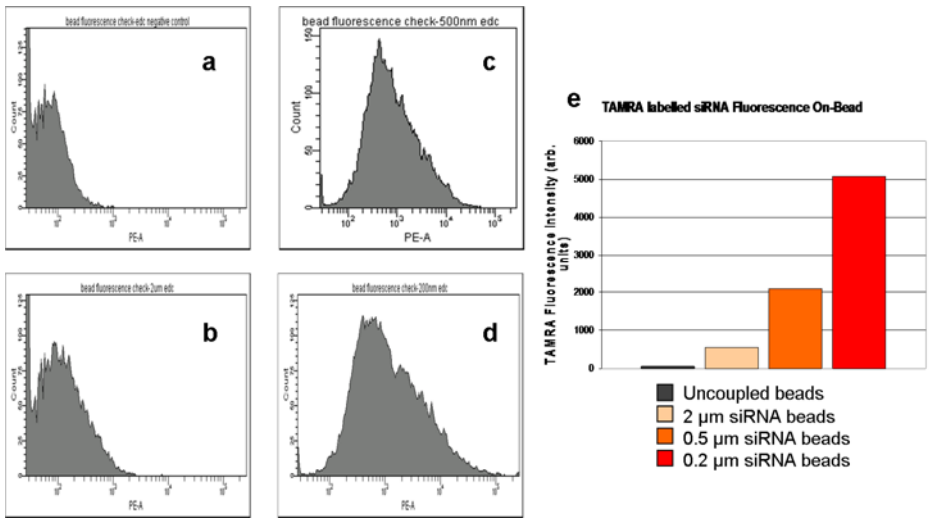

Figure 6.3. siRNA Coupling to Microspheres. *Left:* FACS histograms of **a.** uncoupled control microspheres; **b.** 2 µm-TAMRA siRNA microspheres (**6.3.1**); **c.** 0.5 µm-TAMRA siRNA microspheres (**6.3.2**); **d.** 0.2 µm-TAMRA siRNA microspheres (**6.3.3**) ('PE-A' refers to TAMRA fluorescence); *Right:* **e.** TAMRA fluorescence intensity as found by flow cytometry.

As such, the supernatant from siRNA/microsphere couplings (which contained residual TAMRA labelled siRNA not coupled to the 0.2 and 0.5 µm microspheres) was analysed by spectrofluorimetry and compared to calibration samples of known siRNA concentrations. Thus, the quantity of siRNA coupled to the microspheres was calculated.

0.2 µm siRNA Microspheres

The supernatant resulting from the coupling of TAMRA-siRNA to 0.2 µm microspheres was analysed and the emission maximum recorded at 580 nm. The fluorescence emission obtained correlated to 40 pico-mol of siRNA that was *not* coupled to microspheres. The quantity of siRNA originally added to 0.2 µm microspheres was 1 nmol, which indicates that 0.96 nmol of siRNA was successfully coupled to the microspheres. The beads have a solid content in solution of 3% (30 mg/mL) and 3 mg were used in the coupling of siRNA (or 7.2×10^{11} beads, based on a number of particles per gram[204] of 2.4×10^{14}). Hence, it can be established that there was 1.3×10^{-21} mol of siRNA per bead and this relates to 783 chains of siRNA per microsphere. Using 86 µg/mL of 0.2 µm microspheres in cell experiments, this would give a siRNA concentration of 28 nM per culture (see Experimental for details). If one microsphere entered a cell (assuming an intracellular volume of 5000

μ^3)[179] and released all the on-bead siRNA cytoplasmically, this would yield an intracellular concentration of 0.3 nM siRNA. Given that the RNAi pathway is catalytic (one guide strand can facilitate the degradation of many mRNA strands) this is an excellent intracellular concentration.

0.5 µm siRNA Microspheres

In a similar manner, the quantity of siRNA on 0.5 µm microspheres was calculated and gave 13,244 chains of siRNA per microsphere and a siRNA culture concentration of 28 nM. If one 0.5 µm microsphere entered a cell and released all the on-bead siRNA, this would yield an intracellular concentration of 4 nM. Although this is more than 10 times more than that of 0.2 µm microspheres, it must be noted that less 0.5 µm microspheres enter a typical cell than 0.2 µm beads.

6.2.3. On-Bead siRNA Stability

A further advantage of using TAMRA labelled siRNA in the microsphere couplings was that the fluorescent label could be used to study the siRNA stability under varying culture conditions by flow cytometry. As such, 0.2 and 0.5 µm TAMRA siRNA microspheres were incubated (37 ºC) for between 30 minutes and 24 hours in Phosphate Buffered Saline (PBS, pH 7.4), complete culture media (supplemented with 10% foetal bovine serum and 100 units/mL penicillin and streptomycin) and serum-free culture media. Fluorescence was measured by flow cytometry and compared to an untreated control sample (**Figure 6.4** and **Graph 6.2**). TAMRA labelled siRNA microspheres were stable under all conditions, except serum supplemented culture conditions. Under these circumstances, the siRNA appeared degraded after as little as 30 minutes. In contrast, serum-free conditions provided a stable environment for the siRNA microspheres, even after 24 hours.

It is not surprising that siRNA microspheres were not stable under serum-supplemented conditions. Foetal bovine serum (FBS) contains a range of nucleases capable of resulting in the degradation of sensitive RNAs and, since the microsphere does not offer any physical protection for the siRNA, it is unsurprising that it becomes degraded. This result indicates that microspheres should be incubated with

cells under serum-free conditions during gene silencing experiments to prevent the premature degradation of siRNA.

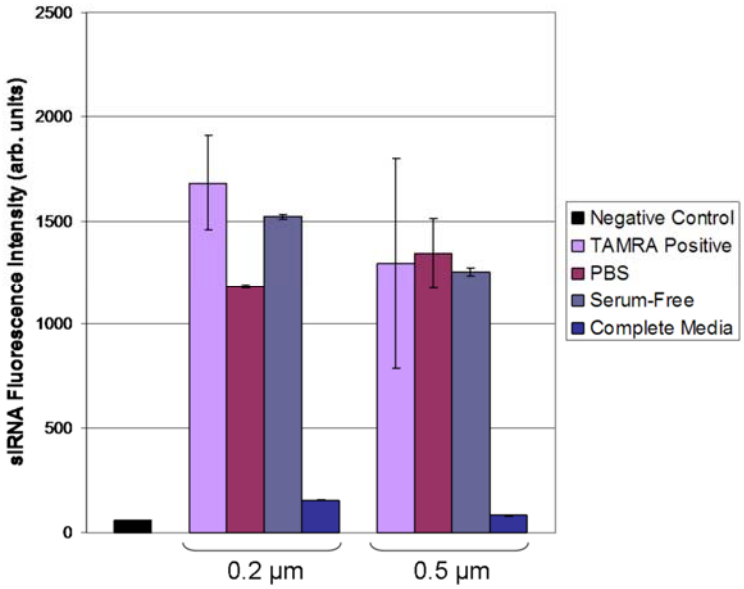

Graph 6.2. siRNA On-Bead Stability. 0.2 and 0.5 µm TAMRA siRNA microspheres (**6.3.3** and **6.3.2** respectively) after 24 hour treatment with PBS, complete media and serum-free media at 37 ºC as found by flow cytometry. 'Negative Control' is uncoupled microspheres; 'TAMRA Positive' are untreated 0.2 and 0.5 µm microspheres coupled with TAMRA siRNA.

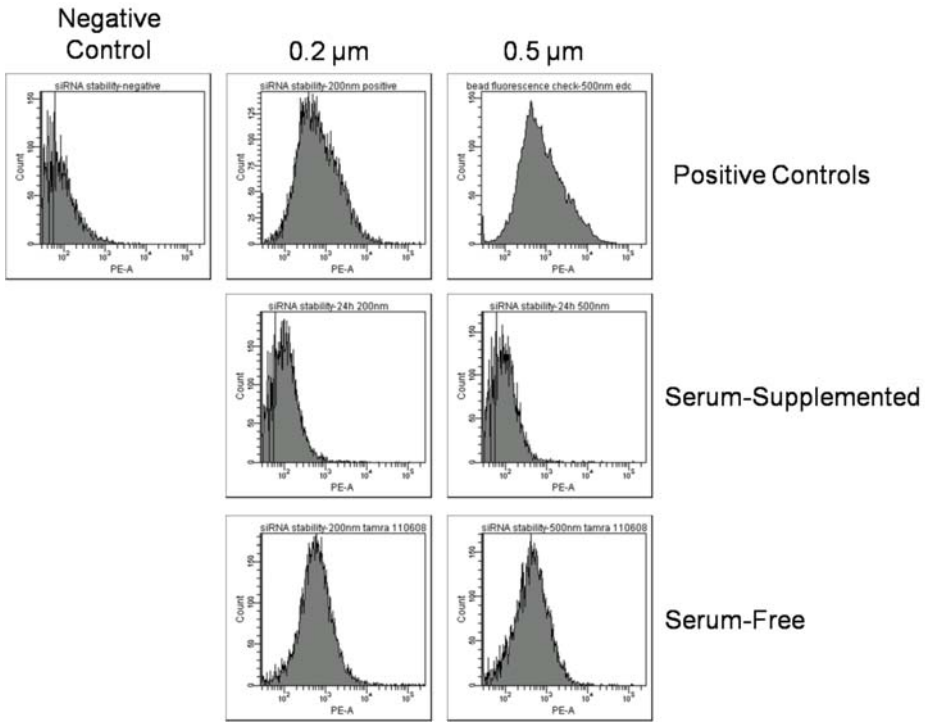

Figure 6.4. siRNA On-Bead Stability. Flow cytometry histograms of 0.2 and 0.5 µm TAMRA siRNA microspheres ((**6.3.3**) and (**6.3.2**) respectively) after 24 hour treatment with complete media

and serum-free media at 37 ºC. 'Positive Controls' are 0.2 and 0.5 µm microspheres coupled to TAMRA siRNA and untreated; 'Negative Control' refers to uncoupled microspheres.

6.2.4. Microsphere Mediated Delivery of siRNA

6.2.4.1. Non-Cleavable Linkages

TAMRA-labelled siRNA was coupled to microspheres *via* a non-cleavable amide linkage for reasons of stability. However, modification of siRNA with a fluorophore (in particular when it is incorporated into the anti-sense strand) can result in a poor knockdown efficiency when compared to the non-fluorescent counterparts, as was found lipofecting HeLa-EGFP cells with labelled and unlabelled GFP-1 siRNA and making analysis after 72 hours by flow cytometry (**Graph 6.3**).[205]

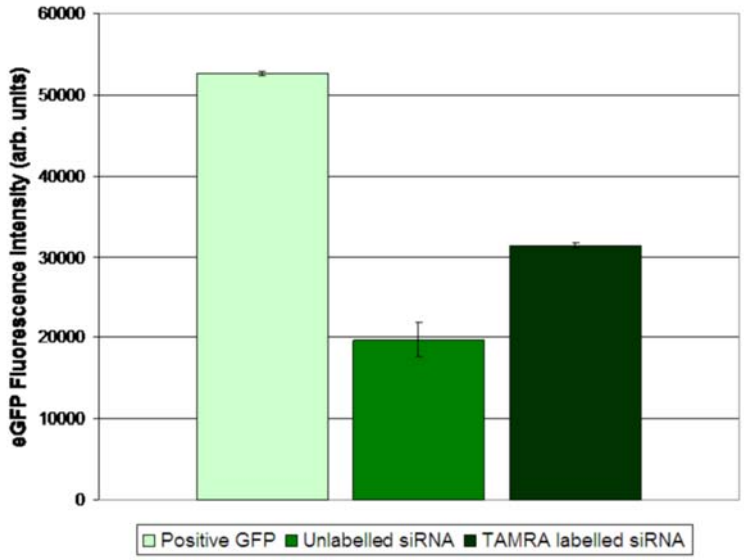

Graph 6.3. TAMRA-siRNA. Gene silencing with fluorescent and non-fluorescent GFP-1 (28 nM) transfected into HeLa-EGFP cells by Lipofectamine™ 2000. Analysis performed after 72 hours. 'Positive GFP' refers to untreated HeLa-EGFP control cells.

For this reason, non-fluorescent siRNA was coupled to 0.2 and 0.5 µm microspheres in the same manner as the TAMRA labelled siRNA (**Scheme 6.1**).

6.2.4.2. Cleavable Linkages

It is not well established whether siRNA needs to be freed from its delivery device in order to function efficiently. As such, an alternative linkage was additionally used, whereby siRNA was coupled to the microspheres *via* a disulphide linker, which could be cleaved intracellularly by endogenous glutathione (**Scheme 6.2**).

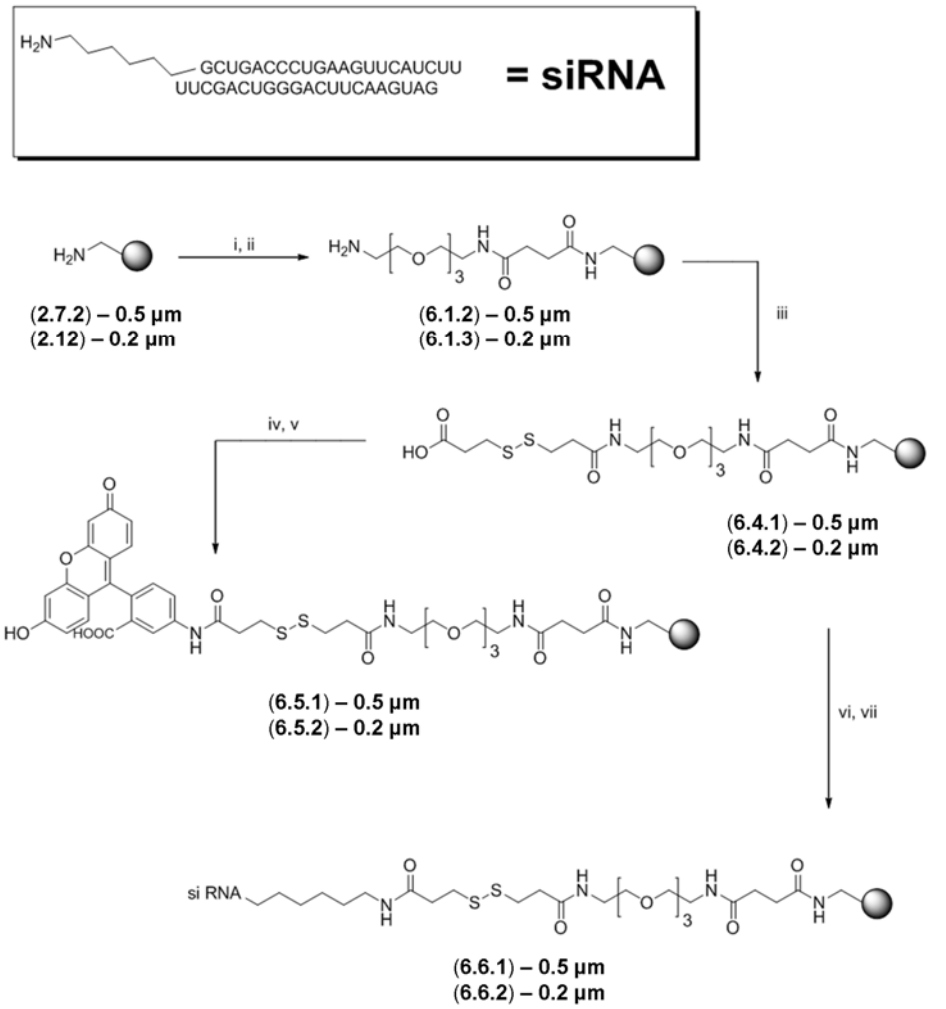

Scheme 6.2. Cleavable siRNA and FAM Microspheres. Coupling of siRNA and fluorescein to 0.2 and 0.5 µm microspheres *via* a cleavable disulphide linkage, yielding (**6.5.1**)/(**6.5.2**) – (**6.6.1**)/(**6.6.2**). (i). 10 eq. Fmoc-PEG-OH, 10 eq. HOBt, 10 eq. DIC, DMF, 18 h, 25 ºC; (ii). 20% piperidine/DMF, 3 × 20 min, 25 ºC; (iii). 10 eq. Dithiodipropionic acid, 10 eq. HOBt, 10 eq. DIC, DMF, 18 h, 25 ºC; (iv). 10 eq. HOBt, 10 eq. DIC, DMF, 2 h, 25 ºC; (v). 10 eq. Fluoresceinamine, DMF, 18 h, 25 ºC; (vi). 10 eq. EDAC, MES (pH 5.5), 2 h, 25 ºC; (vii). amino-siRNA, sterile RNase Free water, 24 h, 25 ºC.

In order to establish the cleavage of the disulphide linker, fluorescein was coupled to 0.2 and 0.5 µm microspheres, yielding (**6.5.2**) and (**6.5.1**) respectively. (**6.5.2**) and (**6.5.1**) were subsequently treated with 10 mM dithiothreitol (DTT) or glutathione *ex vitro* (**Figure 6.5** and **Graph 6.4**). After 1 hour treatment with DTT, the fluorescence associated with fluorescein decreased by 55% on 0.5 µm microspheres and 75% on 0.2 µm microspheres. Use of glutathione facilitated a decrease in fluorescence intensity of 50% on 0.5 µm microspheres and 60% on 0.2 µm microspheres after 1 hour. After 24 hours, the fluorescence intensity had decreased to a base value that

likely related to the cleavage of all the fluorescein from the surface of the microspheres.

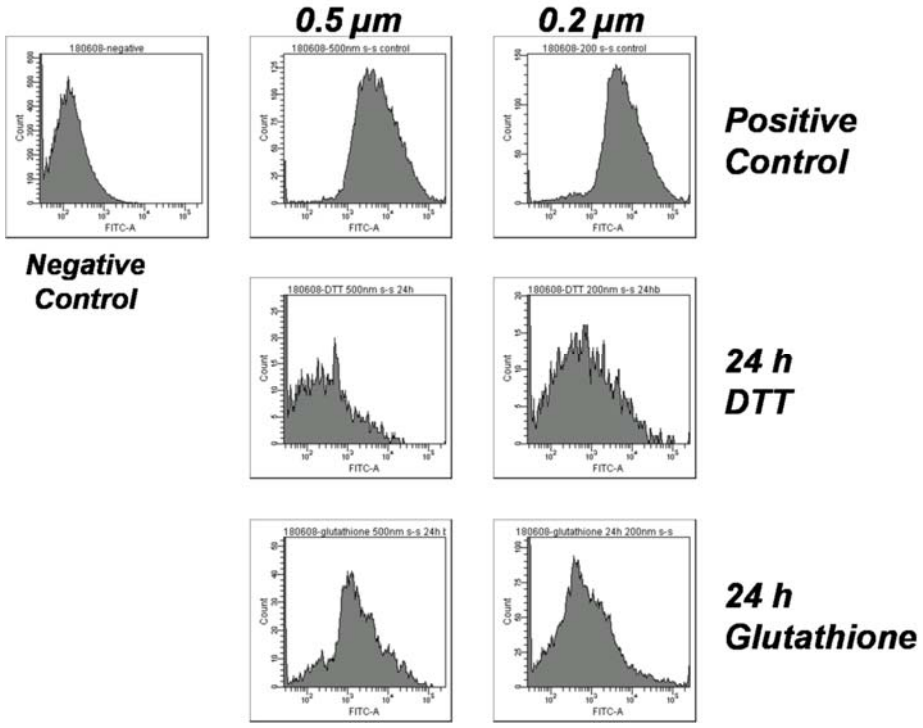

Figure 6.5. Disulphide Cleavage. FACS histograms of 0.2 and 0.5 µm fluorescein microspheres ((**6.5.2**) and (**6.5.1**) respectively) treated with DTT and glutathione (10 mM) for 24 h. 'Positive Control' refers to FAM-coupled untreated microspheres; 'Negative Control' refers to uncoupled microspheres.

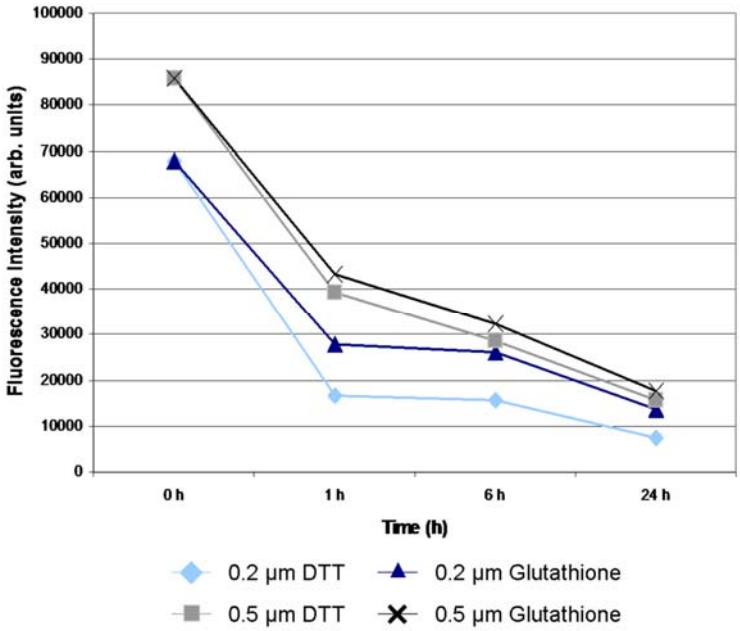

Graph 6.4. Disulphide Cleavage. Dissociation of fluorescein from 0.2 and 0.5 µm disulphide

microspheres ((**6.5.2**) and (**6.5.1**) respectively) by treatment with 10 mM DTT or 10 mM glutathione in PBS, after 1, 6 and 24 hours. Under the same conditions succinic-FAM microspheres retained their fluorescence.

In order to study the cleavage of the disulphide linkage *in vitro*, HeLa cells were beadfected with 0.2 (**6.5.2**) and 0.5 μm (**6.5.1**) disulphide-FAM microspheres and intracellular cleavage was assessed by microscopy (**Figure 6.6**). The fluorescein dye originally associated to microspheres was noted to be dispersed within the cytoplasmic region of the cell, indicating the successful dissociation of fluorescein from the microspheres indicative of disulphide cleavage. In contrast, microspheres linked to fluorescein *via* a non-cleavable succinic linkage ((**6.7.1**) and (**6.7.2**)) (**Scheme 6.3**) showed a localisation of fluorescence associated with the microspheres and not dispersed within the cell (**Figure 6.7**).

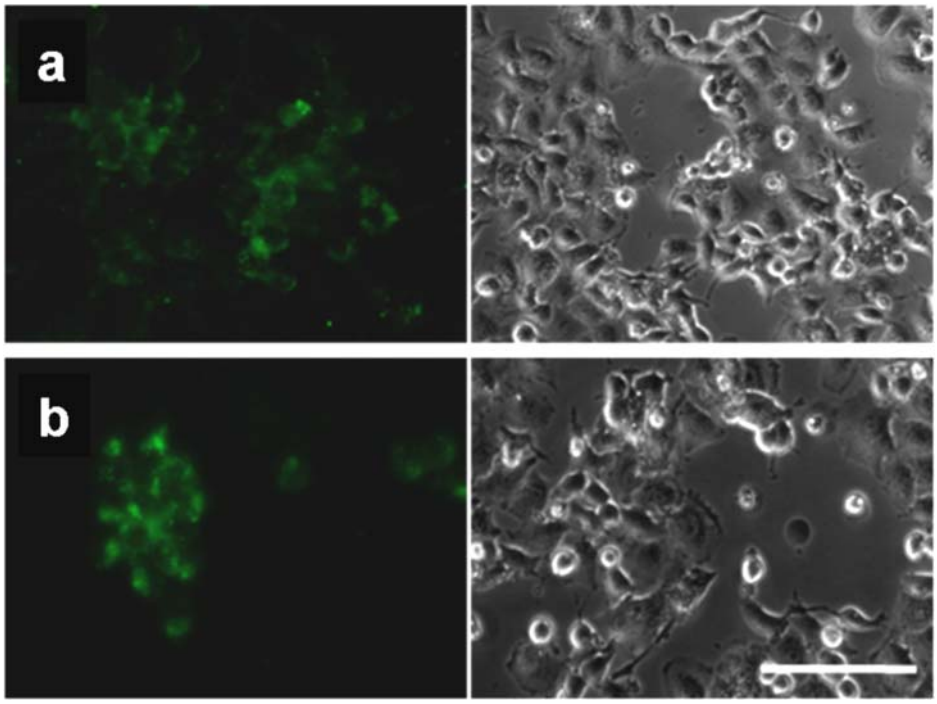

Figure 6.6. Microscopy of Disulphide Cleavage. a. 0.2 μm (**6.5.2**) and **b.** 0.5 μm (**6.5.1**) disulphide-FAM microspheres (86 μg/mL) in HeLa cells after 12 hours. *Left* are fluorescence images showing dye dispersion into the cell cytoplasm; *Right* are brightfield images showing cell location. Scale bar is 100 μm.

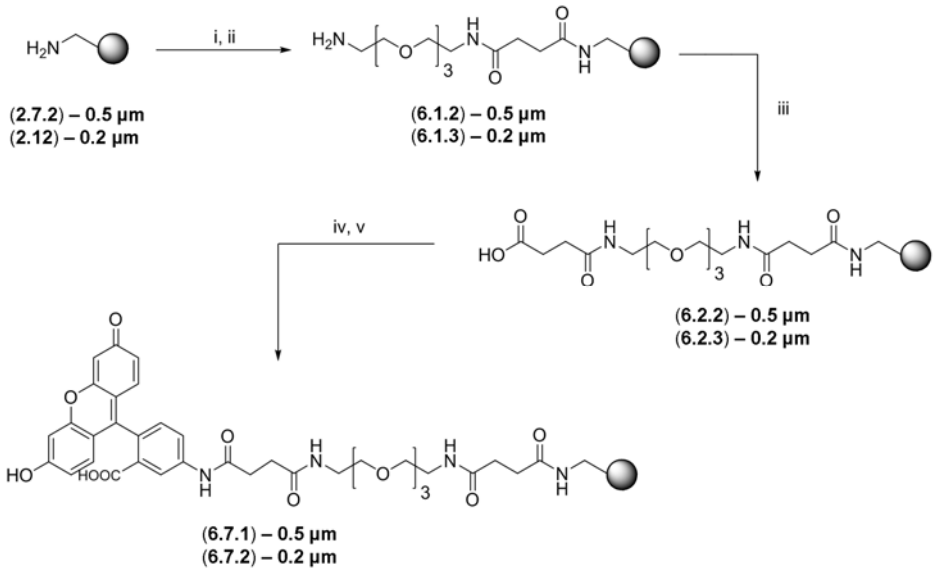

Scheme 6.3. Succinic-FAM Microspheres. Coupling of fluorescein to microspheres, *via* a non-cleavable amide linkage yielding (**6.7.1**) and (**6.7.2**).
(i). 10 eq. Fmoc-PEG-OH, 10 eq. HOBt, 10 eq. DIC, DMF, 18 h, 25 ºC; (ii). 20% piperidine/DMF, 3 × 20 min, 25 ºC; (iii). 10 eq. Succinic anhydride, 10 eq. DIPEA, DMF, 18 h, 25 ºC; (iv). 10 eq. HOBt, 10 eq. DIC, DMF, 2 h, 25 ºC; (v). 10 eq. Fluoresceinamine, DMF, 18 h, 25 ºC.

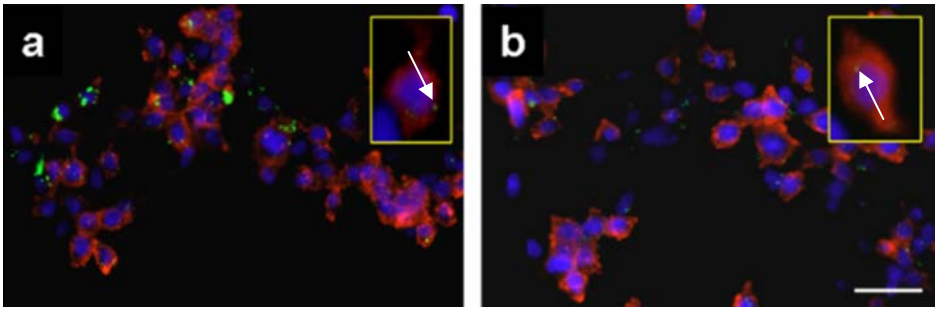

Figure 6.7. Microscopy of Non-Cleavable Microspheres. a. 0.5 µm (**6.7.1**) and **b.** 0.2 µm (**6.7.2**) (86 µg/mL) uptake by HeLa cells after 12 hours. Actin filaments are labelled with AlexaFluor-568 phalloidin and nuclei are stained with Hoechst 33342. Scale bar is 100 µm. Inset images are a 4× magnification.

6.3. Toxicity of Microspheres for siRNA Delivery

One major problem associated with some cellular delivery agents is cytotoxicity, with concerns over liposome transfection agents and carbon nanotubes. As such, it was important to establish that siRNA microspheres do not cause toxicity in cells over the incubation periods required for gene silencing experiments (72 hours)

(**Graph 6.5**). As such, MTT assays were used to show that no detrimental cytotoxicity was evident in either HeLa or E14 cells beadfected with 0.2 or 0.5 µm amide (succinic) or disulphide microspheres and cellular viability was >80% in all cases, even after 72 hours, indicating the applicability of microspheres to gene silencing experiments when long incubations are typically required to observe silencing.

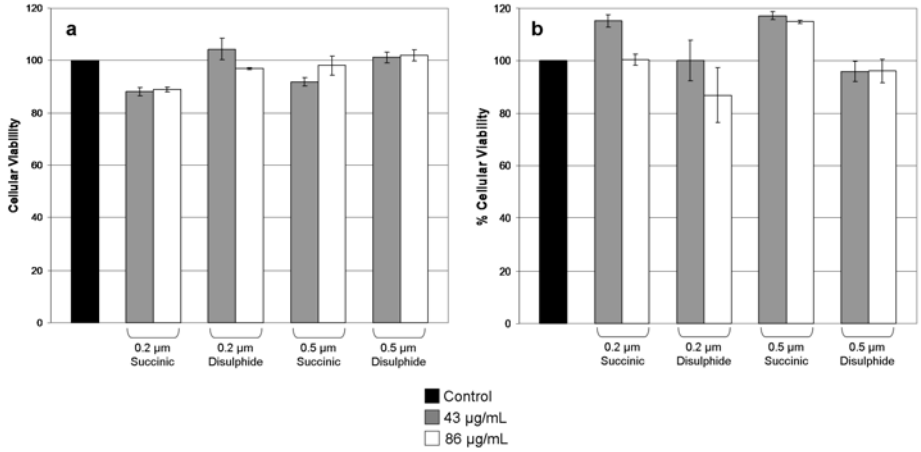

Graph 6.5. Cellular viability. a. HeLa and **b.** E14 cells beadfected (43 and 86 µg/mL) for 72 hours with siRNA microspheres (**6.3.2**), (**6.3.3**), (**6.6.1**) and (**6.6.2**) and analysed by MTT assay. 'Control' indicates untreated.

6.4. Gene Silencing of EGFP in HeLa Cells

6.4.1. Beadfection of HeLa Cells with *Labelled* siRNA

Following the successful linkage of TAMRA-labelled siRNA to 0.5 and 0.2 µm microspheres ((**6.3.2**) and (**6.3.3**) respectively) its *in vitro* fate was studied. As such, HeLa-EGFP cells were incubated with siRNA microspheres and analysed for GFP expression by flow cytometry and microscopy (**Figure 6.8 – 6.10**). After 24 hours, some cells containing siRNA microspheres appeared decreased in EGFP fluorescence (**Figure 6.8,** *white arrows*) and siRNA beads could be observed as localised fluorescent points. However, after 48 – 72 hours the TAMRA labelled siRNA, which was originally localised on the microsphere, appeared dispersed into the cell and the microspheres no longer appeared extensively fluorescent (**Figure 6.9**). This may suggest that the anti-sense strand (which is TAMRA labelled) has

become disassociated from the sense strand (and, thus disengaged from the microsphere). This is possibly facilitated by the interaction of the on-bead siRNA with the RISC.

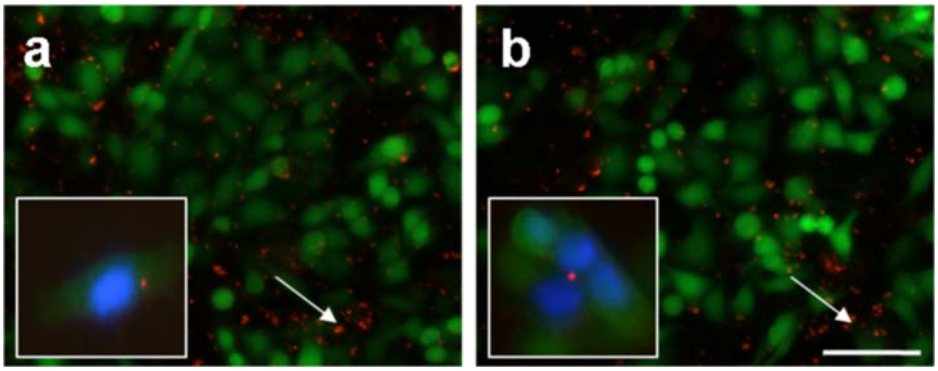

Figure 6.8. Microscopy of TAMRA-siRNA Microspheres. a. 0.2 µm (**6.3.3**) TAMRA siRNA microspheres after 24 h; **b.** 0.5 µm (**6.3.2**) TAMRA siRNA microspheres after 24 h. Scale bar is 200 µm. Inset is 5× magnification. Microsphere concentration was 86 µg/mL.

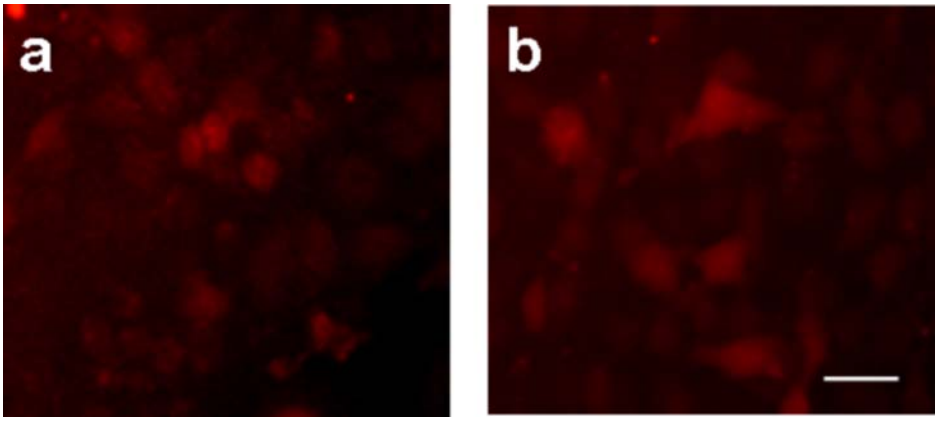

Figure 6.9. siRNA Release. Microscopy of HeLa-EGFP cells beadfected with **a.** 0.5 µm (**6.3.2**) TAMRA siRNA microspheres after 72 h; **b.** 0.2 µm (**6.3.3**) TAMRA siRNA microspheres after 72 h. Scale bar is 50 µm. Microsphere concentration was 86 µg/mL.

Quantitative analysis by flow cytometry showed silencing of EGFP in HeLa cells after 48 hours using 0.2 (**6.3.3**) and 0.5 µm (**6.3.2**) microspheres linked to TAMRA-labelled siRNA and the GFP intensity was reduced by 47% and 65% respectively. This result indicates that a cleavable linker is not essential to EGFP silencing as the RISC appears to be capable of selecting the anti-sense siRNA and unwinding it from the sense strand, which is covalently coupled to the microsphere.

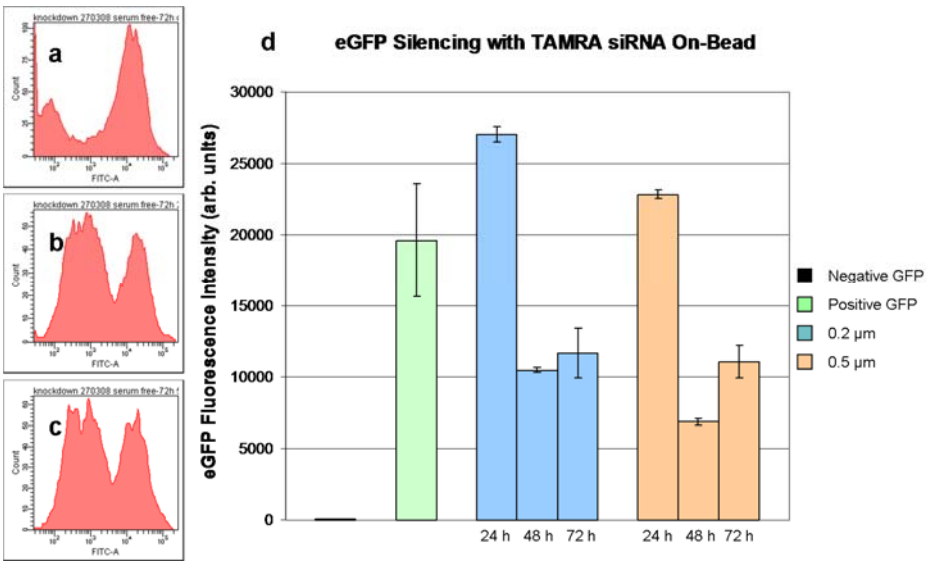

Figure 6.10. Gene Silencing with TAMRA-siRNA Microspheres. *Left:* Flow cytometry histograms after 72 hours **a.** untreated control cells; **b.** cells treated with 0.5 µm (**6.3.2**) TAMRA siRNA microspheres; **c.** cells treated with 0.2 µm (**6.3.3**) TAMRA siRNA microspheres; **d.** Decrease in EGFP fluorescence intensity after 24, 48 and 72 hours as analysed by flow cytometry, following treatment with 0.5 (**6.3.2**) or 0.2 µm (**6.3.3**) TAMRA siRNA microspheres. Microspheres were added to give a siRNA concentration of 28 nM (86 µg/mL microspheres). 'Negative GFP' are untreated HeLa cells; 'Positive GFP' are untreated HeLa-EGFP cells.

6.4.2. Beadfection of HeLa Cells with *Unlabelled* siRNA

As discussed, siRNA that is fluorescently labelled does not generally offer as an efficient gene silencing as non-fluorescent siRNA. As such, EGFP silencing in HeLa cells was repeated with non-fluorescent siRNA linked to 0.2 and 0.5 µm microspheres *via* disulphide ((**6.6.2**) and (**6.6.1**) respectively) and non-cleavable (succinic) linkers ((**6.3.3**) and (**6.3.2**) respectively). Analysis was made by flow cytometry and microscopy over 24 – 72 hours (**Graph 6.6** and **Figure 6.11 – 6.12**). No significant gene silencing was noted after 24 hours, however, after 48 hours a knockdown of 80 – 90% was noted in cells incubated with siRNA microspheres. After 72 hours this was increased to 90 – 93%. No significant differences could be seen between the amide and disulphide linkages. This suggests that, in this case, cleavage of the double strand from the microsphere was not required and the RISC may facilitate the release of the guide strand (which is not covalently linked to the microsphere), as seen with TAMRA-siRNA microspheres.

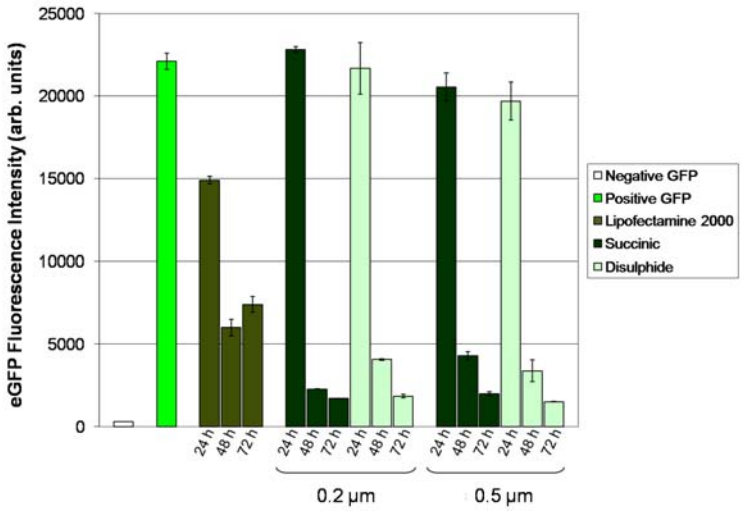

Graph 6.6. EGFP Silencing in HeLa Cells. Reduction in EGFP fluorescence in HeLa-EGFP cells after 24, 48 and 72 hours after treatment 0.2 and 0.5 µm microspheres with siRNA coupled *via* amide (succinic) ((**6.3.3**) and (**6.3.2**) respectively) or disulphide linkages ((**6.6.2**) and (**6.6.1**) respectively). A positive control was established with Lipofectamine™ 2000 (28 nM). 'Negative GFP' refers to HeLa cells that do not express EGFP. 'Positive GFP' refers to untreated HeLa-EGFP cells.

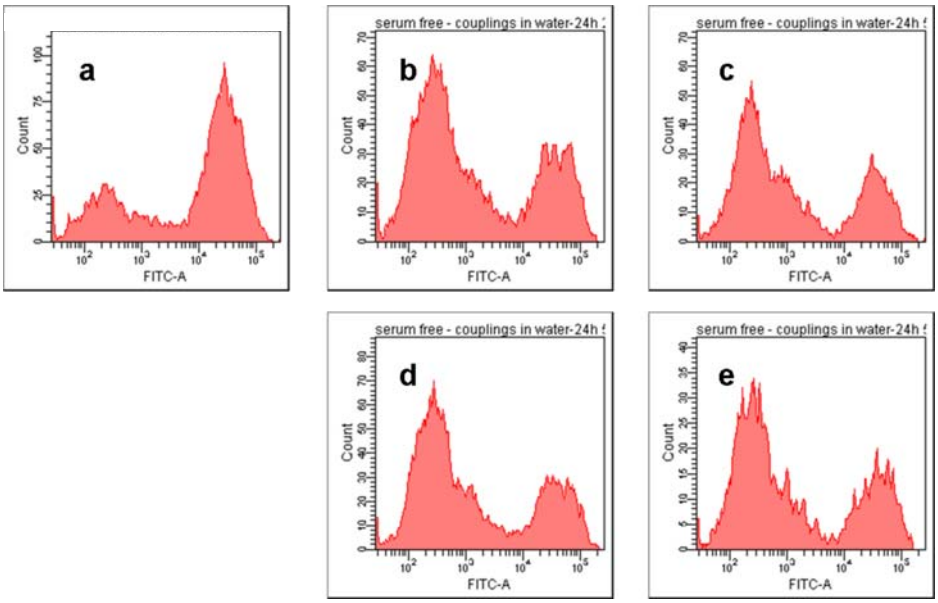

Figure 6.11. EGFP Silencing in HeLa Cells. FACS histograms of HeLa-EGFP cells after 72 hours**, a.** Untreated cells; **b.** Cells treated with 0.2 µm microspheres with siRNA *via* an amide linkage (**6.3.3**); **c.** Cells treated with 0.2 µm microspheres with siRNA *via* a disulphide linkage (**6.7.2**); **d.** Cells treated with 0.5 µm microspheres with siRNA *via* an amide linkage (**6.3.2**); **e.** Cells treated with 0.5 µm microspheres with siRNA *via* a disulphide linkage (**6.7.1**).

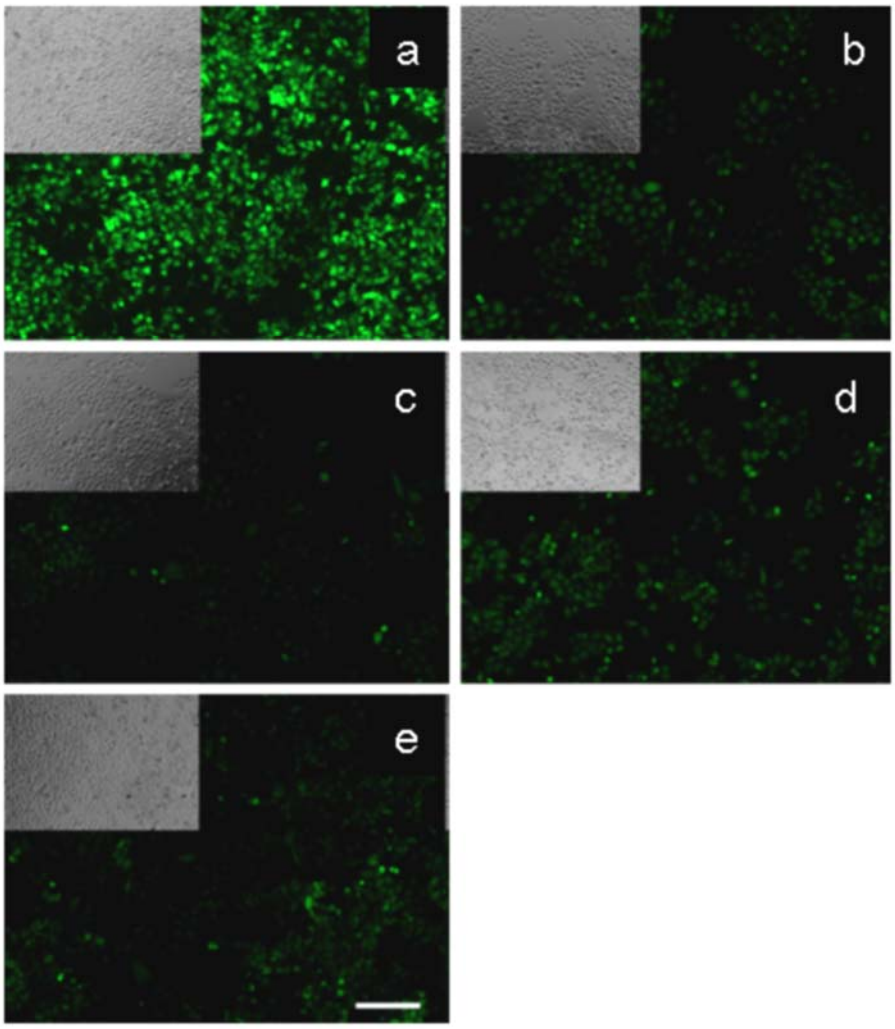

Figure 6.12. Microscopy of Gene Silencing. HeLa-EGFP cells after 72 h. **a.** untreated control cells; **b.** incubated in the presence of 0.2 μm amide-siRNA microspheres (**6.3.3**); **c.** incubated in the presence of 0.2 μm disulphide-siRNA microspheres (**6.6.2**); **d.** incubated in the presence of 0.5 μm amide-siRNA microspheres (**6.3.2**); **e.** in the presence of 0.5 μm disulphide-siRNA microspheres (**6.6.1**). Scale bar is 350 μm. Inset are phase contrast images, showing approximately 70 – 80% cell confluency. Microsphere concentration was 86 μg/mL.

6.4.3. Controls for Gene Silencing

In order to demonstrate the significance of these results, several controls were additionally established to demonstrate that the knockdowns obtained were true and not due to a secondary effect resulting in EGFP fluorescence reduction. These included siRNA not complementary to EGFP mRNA lipofected with Lipofectamine™ 2000 and also beadfected with 0.2 and 0.5 μm microspheres, beads without siRNA and siRNA (GFP-1) without a carrier system (**Graph 6.7**).

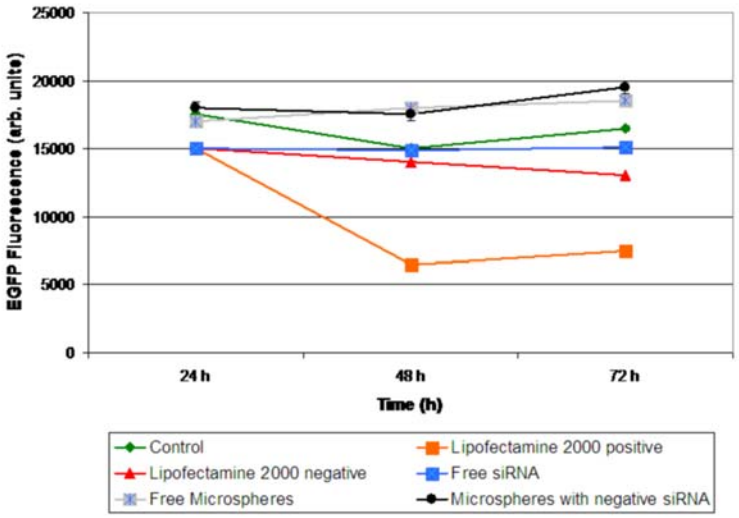

Graph 6.7. Gene Silencing Controls. EGFP fluorescence intensity following addition of siRNA (GFP-1) lipofected with Lipofectamine™ 2000 ('Lipofectamine 2000 positive'), siRNA (not for EGFP silencing) lipofected with Lipofectamine™ 2000 ('Lipofectamine 2000 negative'), siRNA (GFP-1) without a carrier system ('Free siRNA'), microspheres without siRNA ('Free microspheres') and microspheres loaded with siRNA that should not cause EGFP silencing ('Microspheres with negative siRNA'). In each case (as appropriate) 86 µg/mL of microspheres were added to cell cultures and the siRNA concentration was 28 nM. 'Control' refers to untreated HeLa-EGFP cells.

Excluding those employing Lipofectamine™ 2000, none of the controls showed an appreciable decrease in EGFP fluorescence intensity from the control cells (untreated HeLa-EGFP cells). In the case of Lipofectamine™ 2000, the positive control (lipofecting siRNA GFP-1) showed the expected reduction in EGFP, which was optimal after 48 hours. However, the negative control (lipofecting siRNA not complementary to EGFP mRNA) also caused a decrease in EGFP expression by approximately 20%. In contrast, siRNA not targeted against EGFP and beadfected did not result in any decrease in EGFP fluorescence. This suggests that toxicity associated to Lipofectamine™ 2000 may have resulted in some non-specific reduction in EGFP expression.

6.5. Gene Silencing of EGFP in Embryonic Stem Cells

Further to the successful gene silencing of EGFP observed in HeLa cells, the capability of siRNA microspheres to beadfect ES cells with siRNA for GFP knockdown was examined.

6.5.1. Beadfection of ES Cells with *Labelled* siRNA

ES-EGFP cells (expressing EGFP on their membrane) were analysed for their uptake of siRNA laden microspheres using 0.2 (**6.3.3**) and 0.5 μm (**6.3.2**) TAMRA siRNA microspheres. Assessment of uptake was determined qualitatively by microscopy (**Figure 6.13**).

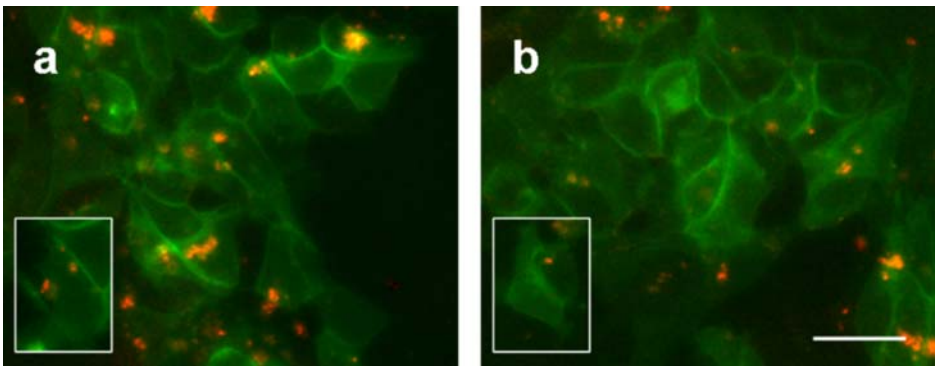

Figure 6.13. TAMRA-siRNA in ES-EGFP Cells. Uptake of TAMRA siRNA microspheres, (**6.3.2**) and (**6.3.3**), in ES-EGFP cells after 24 hours: **a.** 0.5 μm; **b.** 0.2 μm. Inset are magnifications. Bead Concentration: 86 μg/mL. Scale bar is 50 μm.

Uptake was deemed successful, although appeared less prevalent than in HeLa-EGFP cells. Subsequently, following beadfection with TAMRA siRNA microspheres, EGFP expression was assessed by flow cytometry (**Figure 6.14**) and was observed to be decreased after 48 – 72 hours by a maximum of 50% for both diameters of microsphere (0.2 and 0.5 μm). Similar to HeLa cells, this result indicates that it is not essential that the siRNA is disengaged from the microsphere as the RISC is able to select the (non-covalently bound) anti-sense strand and dissociate it from the bead.

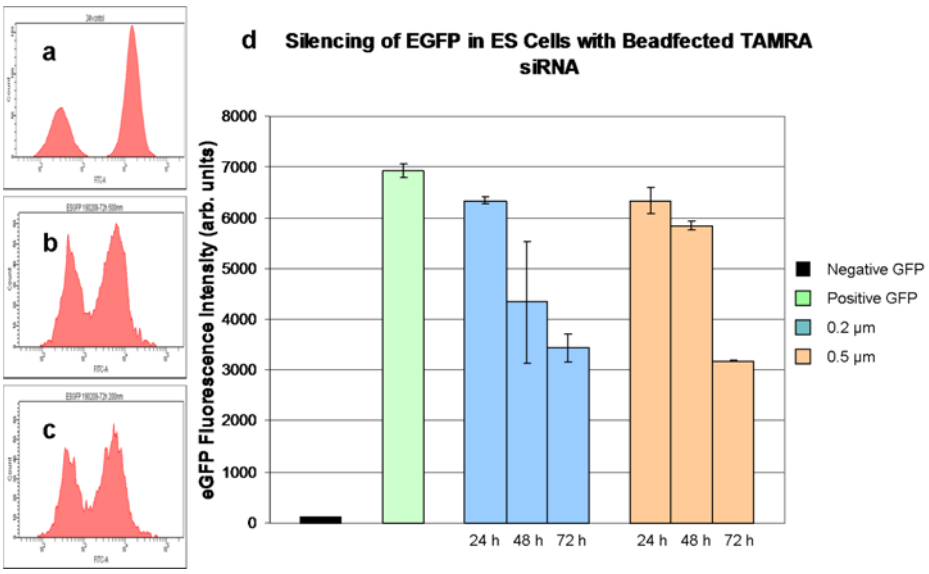

Figure 6.14. Gene Silencing with TAMRA-siRNA Microspheres. *Left:* Flow cytometry histograms after 72 hours **a.** untreated control cells; **b.** cells treated with 0.5 µm (**6.3.2**) TAMRA siRNA microspheres; **c.** cells treated with 0.2 µm (**6.3.3**) TAMRA siRNA microspheres; **d.** Decrease in EGFP fluorescence intensity after 24, 48 and 72 hours as analysed by flow cytometry, following treatment with 0.5 (**6.3.2**) or 0.2 µm (**6.3.3**) TAMRA siRNA microspheres. Microspheres were added to give a siRNA concentration of 28 nM (86 µg/mL microspheres). 'Negative GFP' are untreated ES cells; 'Positive GFP' are untreated ES-EGFP cells.

6.5.2. Beadfection of ES Cells with *Unlabelled* siRNA

ES-EGFP cells were additionally beadfected with unlabelled siRNA microspheres (with succinic (**6.3.2**), (**6.3.3**) and disulphide (**6.6.1**), (**6.6.2**) linkages) and protein expression measured over 24 – 72 hours. The effect on EGFP expression was analysed by flow cytometry and microscopy (**Figure 6.15-6.16, Graph 6.8**).

EGFP silencing with unlabelled siRNA mediated by microspheres was successful in embryonic stem cells (up to 60%) and more prevalent than with the use of TAMRA labelled siRNA as expected. In general, disulphide-siRNA microspheres appeared to be more efficient than amide-siRNA microspheres, suggesting that in the case of stem cells cleavage of the siRNA from the delivery device is important, although not essential. In addition, 0.5 µm microspheres appeared to more efficiently silence EGFP in stem cells than 0.2 µm microspheres. However, this may be due to the increased quantity of siRNA coupled to 0.5 µm microspheres (*ca* 13,000 molecules) compared to 0.2 µm microspheres (*ca* 800 molecules), or may be due to a better uptake of 0.5 µm siRNA microspheres over 0.2 µm microspheres.

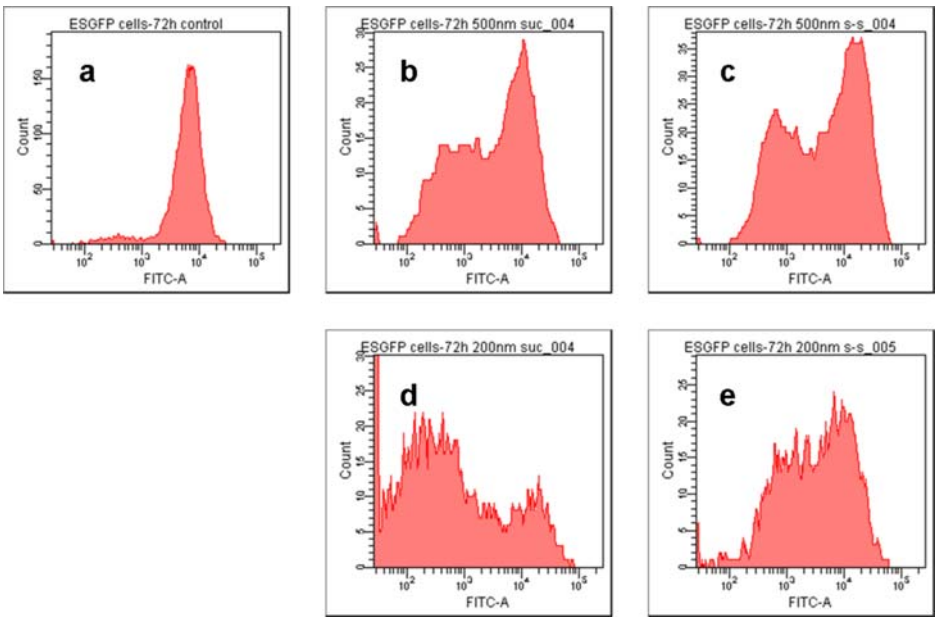

Figure 6.15. EGFP Silencing in ES-EGFP Cells. FACS histograms of ES-EGFP cells after 72 hours: **a.** untreated cells; **b.** 0.5 µm (**6.3.2**) amide-siRNA microspheres; **c.** 0.5 µm (**6.6.1**) disulphide-siRNA microspheres; **d.** 0.2 µm (**6.3.3**) amide-siRNA microspheres; **e.** 0.2 µm (**6.6.2**) disulphide-siRNA microspheres. Microsphere concentration was 86 µg/mL.

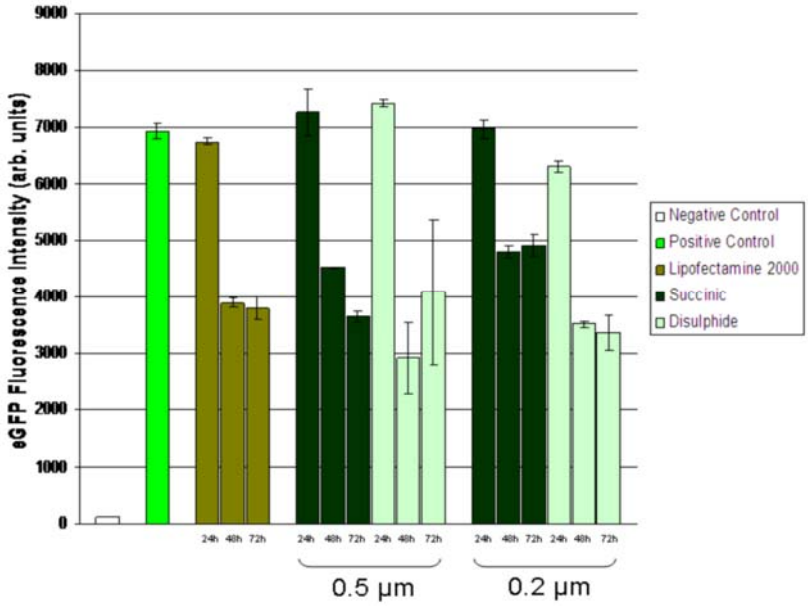

Graph 6.8. EGFP Silencing in ES-EGFP Cells. EGFP fluorescence in mouse embryonic stem cells after 24, 48 and 72 hours treated with 0.5 and 0.2 µm amide (succinic)/disulphide microspheres. 'Negative Control' are untreated cells that do not express EGFP. 'Positive Control' are untreated ES-EGFP cells. Microsphere concentration was 86 µg/mL.

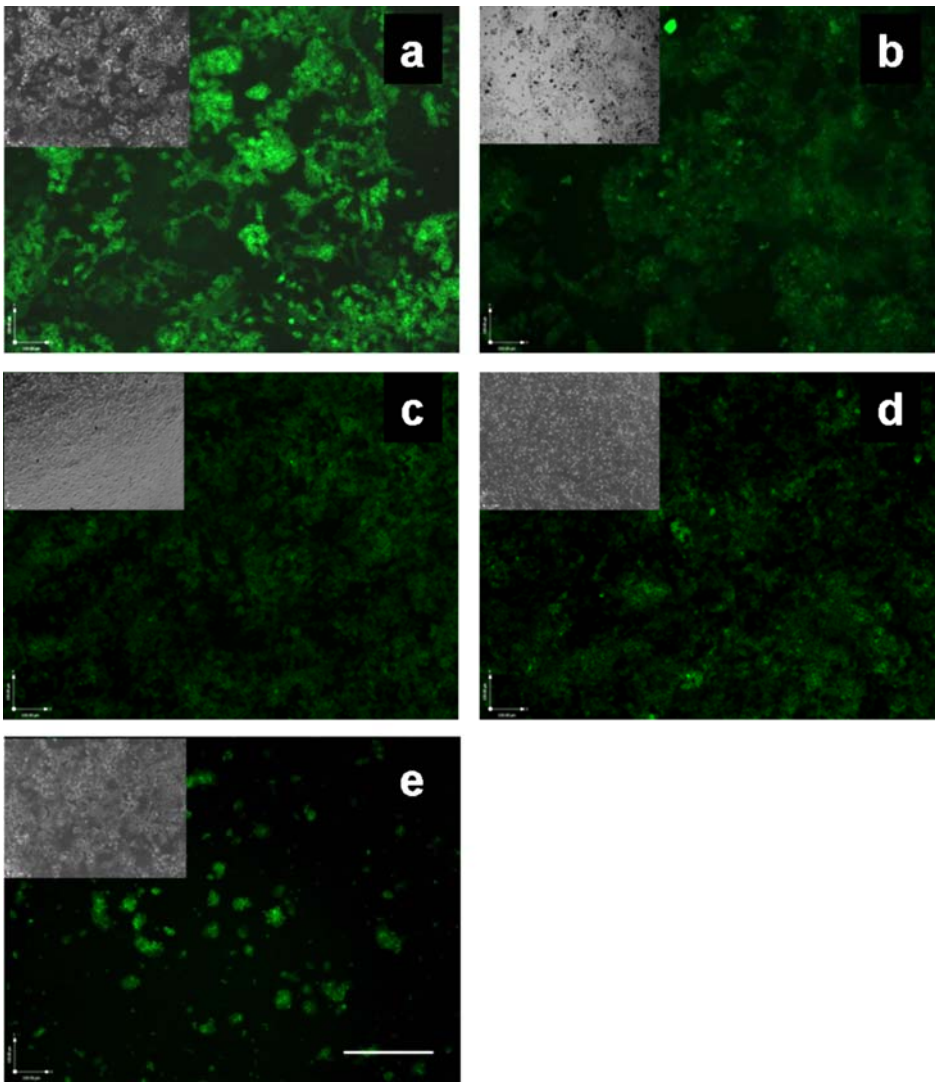

Figure 6.16. Microscopy of Gene Silencing. ES-EGFP cells after 72 h. **a.** untreated control cells; **b.** incubated in the presence of 0.2 µm succinic-siRNA microspheres (**6.3.3**); **c.** incubated in the presence of 0.2 µm disulphide-siRNA microspheres (**6.6.2**); **d.** incubated in the presence of 0.5 µm succinic-siRNA microspheres (**6.3.2**); **e.** incubated in the presence of 0.5 µm disulphide-siRNA microspheres (**6.6.1**). Scale bar is 100 µm. Inset are phase contrast images, showing approximately 70 – 80% cell confluency. Microsphere concentration was 86 µg/mL.

In the case of ES-EGFP cells, gene silencing with microspheres was comparable with the silencing achieved with commercially available lipofection products (**Graph 6.8**).

6.5.3. Controls for Gene Silencing

As with HeLa-EGFP cells, several controls were established to ensure the EGFP

silencing achieved was a true result and not an artefact of some unspecific effect. As such, ES-EGFP cells were incubated with siRNA without a carrier system, siRNA complementary and non-complementary to EGFP lipofected (Lipofectamine™ 2000), siRNA non-complementary to EGFP beadfected and microspheres without siRNA (**Graph 6.9**). It was noted that, as with HeLa-EGFP cells, Lipofectamine™ 2000 as a carrier system caused some decrease in GFP expression itself. However, this was seen to recover after 48 – 72 hours. All other controls did not affect GFP expression.

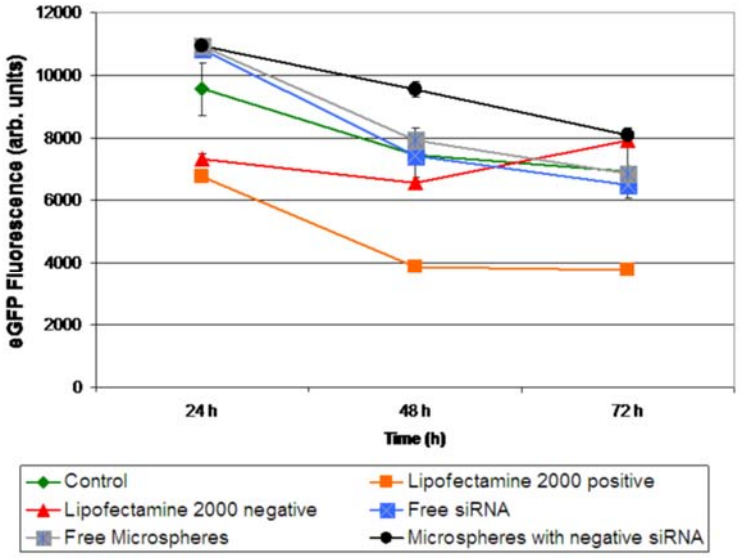

Graph 6.9. Controls of Gene Silencing. EGFP fluorescence intensity following addition of siRNA (GFP-1) lipofected with Lipofectamine™ 2000 ('Lipofectamine 2000 positive'), siRNA (not for EGFP silencing) lipofected with Lipofectamine™ 2000 ('Lipofectamine 2000 negative'), siRNA (GFP-1) without a carrier system ('Free siRNA'), microspheres without siRNA ('Free microspheres') and microspheres loaded with siRNA that will not cause EGFP silencing ('Microspheres with negative siRNA'). In each case, as appropriate, 86 μg/mL microspheres were added to cell cultures and the siRNA concentration was 28 nM.

6.6. A Dual-Functionalised System

6.6.1. Silencing of EGFP in HeLa Cells by Selection

Although the reduction in GFP intensity was clear with microspheres, it was considered that a more accurate assessment of the knockdown would be to obtain a system where the beadfected cells could be assessed independently from non-

beadfected cells. In this manner, cells containing siRNA could be assessed independently from cells that did not contain siRNA.

To this affect, a dual-labelled system was investigated. Here, lysine was employed to allow multi-functionalisation of the microspheres with a fluorophore distinguishable from GFP (Cy5) and siRNA. This system allowed for functionality, for example siRNA, but also meant the microsphere could be tracked *via* the Cy5 label (**Scheme 6.4**).

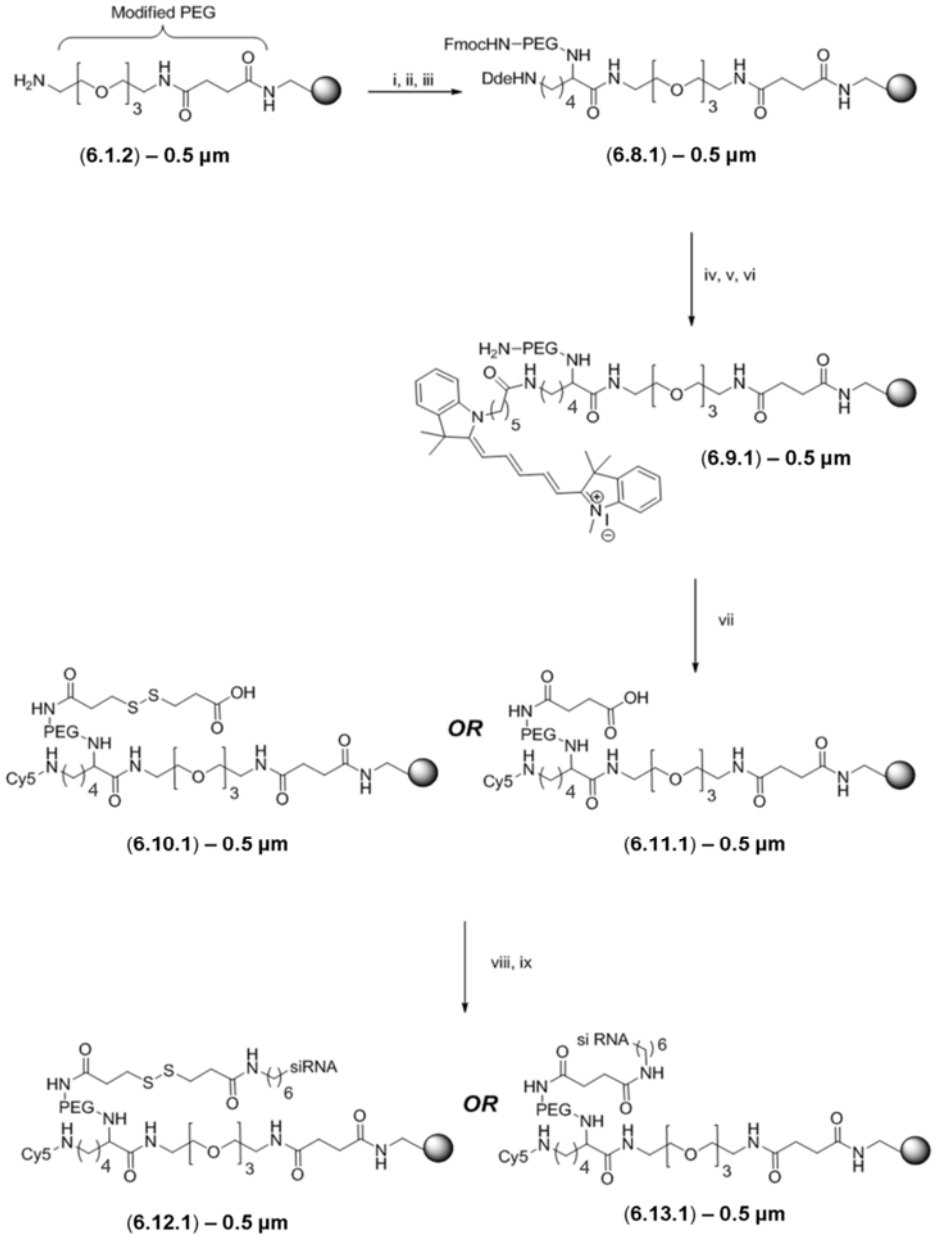

Scheme 6.4. Dual-Functionalisation. Preparation of dual-labelled 0.5 µm Cy5-co-siRNA microspheres (**6.12.1**) and (**6.13.1**).

(i). 10 eq. Fmoc-Lys-(Dde)-OH, 10 eq. HOBt, 10 eq. DIC, DMF, 18 h, 25 ºC; (ii). 20% piperidine/DMF, 3 × 20 min, 25 ºC; (iii). 10 eq. Fmoc-PEG-OH, 10 eq. HOBt, 10 eq. DIC, DMF, 18 h, 25 ºC; (iv). Hydroxylamine.HCl, imidazole, NMP, 1 h, 25 ºC; (v). 5 eq. Carboxylated-Cy5, 5 eq. HOBt, 5 eq. DIC, DMF, 18 h, 25 ºC; (vi). 20% piperidine/DMF, 3 × 20 min, 25 ºC; (vii). 10 eq. Succinic anhydride, 10 eq. DIPEA, 18 h, 25 ºC ***or*** 10 eq. Dithiodipropionic acid, 10 eq. HOBt, 10 eq. DIC, DMF, 18 h, 25 ºC; (viii). 10 eq. EDAC, MES (pH 5.5), 2 h, 25 ºC; ix. amino-siRNA, sterile RNase Free water, 24 h, 25 ºC.

Thus, HeLa-EGFP cells were treated with Cy5-co-siRNA 0.5 μm microspheres with both the cleavable (disulphide) (**6.12.1**) and non-cleavable (succinic) (**6.13.1**) forms. EGFP silencing was analysed after 24, 48 and 72 hours by flow cytometry (**Graph 6.10**) selecting those cells positive for Cy5 fluorescence and, hence, beadfected cells containing siRNA. Gene silencing was observed after 24 hours where EFGP was between 30% (disulphide) and 40% (succinic) reduced. This knockdown was more prevalent at 48 and 72 hours where reductions of up to approximately 90% were noted in both the cases of amide (succinic) and disulphide microspheres.

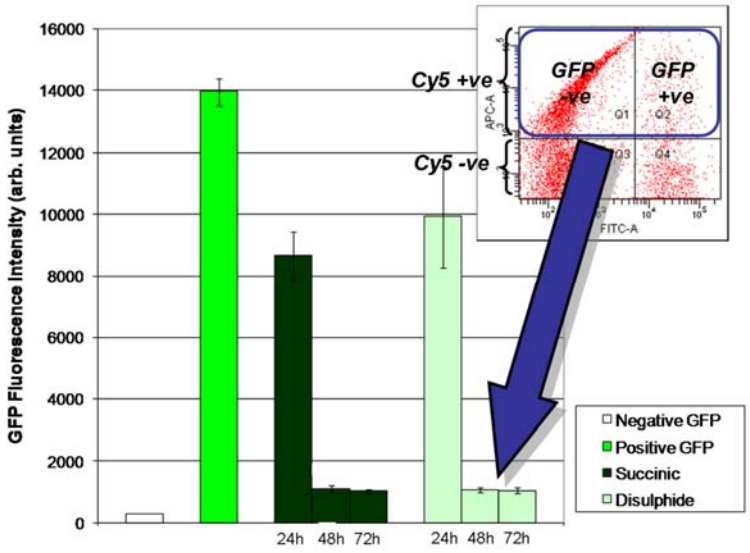

Graph 6.10. Cell Selection. GFP Intensity in HeLa-EGFP cells after 24, 48 and 72 h incubation with Cy5-co-siRNA microspheres ((**6.12.1**) and (**6.13.1**)) as found by flow cytometry (inset: FACS dot plot). 'Negative GFP' refers to HeLa cells not expressing EGFP. 'Positive GFP' refers to untreated HeLa-EGFP cells. Microsphere concentration was 86 μg/mL.

EGFP gene silencing was confirmed by confocal microscopy where cells containing microspheres (**Figure 6.27,** *white arrows*) were seen to be negative for EGFP expression.

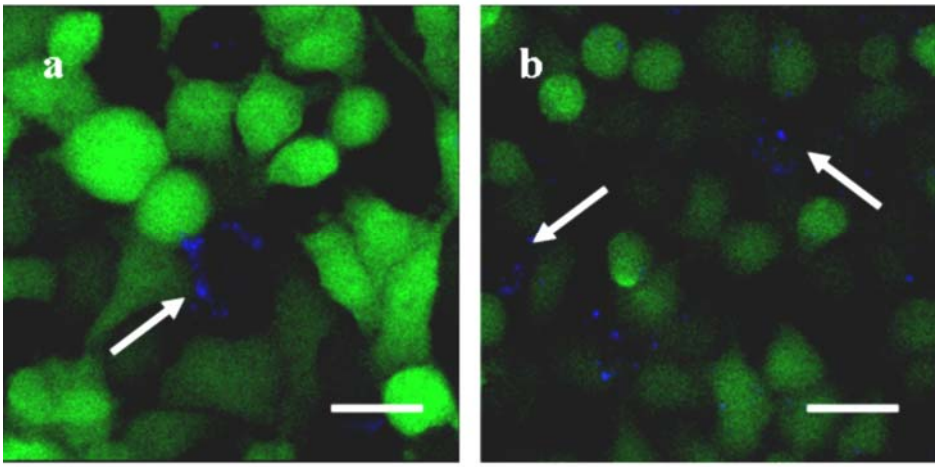

Figure 6.17. Microscopy. HeLa-EGFP cells beadfected with dual functionalised microspheres (86 µg/mL): **a.** HeLa-EGFP cells incubated in the presence of Cy5-co-siRNA succinic 0.5 µm microspheres (**6.13.1**) after 72 h. Scale bar is 50 µm; **c.** HeLa-EGFP cells incubated in the presence of Cy5-co-siRNA disulphide 0.5 µm microspheres (**6.12.1**) after 72 h. Scale bar is 60 µm.

Using this system, a reduction in EGFP expression could be detected after 24 hours, where when using the unlabelled system a decrease in fluorescence intensity could not be observed after such a short time and was only extensively observed after 48 – 72 hours.. Presumably, this is due to a poorer uptake after 24 hours resulting in the knockdown signal being 'diluted' by un-beadfected cells and thus renders it undetectable.

6.6.2. Uptake of siRNA-Laden Microspheres in HeLa Cells

In addition to allowing for a more accurate assessment of the EGFP knockdown, the Cy5-co-siRNA microsphere system also allowed quantification of the uptake of microspheres when they were loaded with siRNA (**Graph 6.11**).

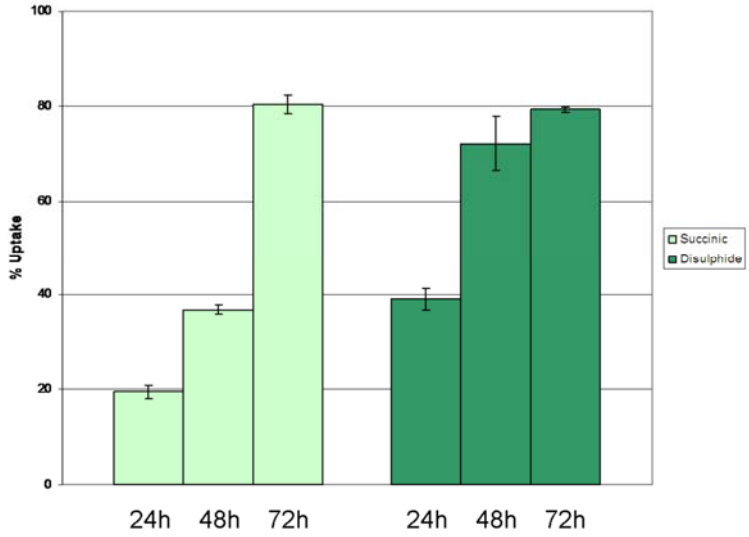

Graph 6.11. siRNA Microspheres. Uptake of Cy5-co-siRNA 0.5 µm microspheres, (**6.12.1**) and (**6.13.1**), in HeLa-EGFP cells after 24, 48 and 72 hours incubation. Microsphere concentration was 86 µg/mL.

Uptake was as much as 80% after 72 hours, but siRNA coupled microspheres did show a slower uptake than microspheres without siRNA. However, this result was to be expected given the negatively charged nature of siRNA, which will inherently repel the microsphere from the negatively charged phosphate head-groups of the lipid bilayer.

6.7. Conclusions

In conclusion, green fluorescent protein expressed in human cervical cancer (HeLa) and mouse embryonic stem cells was successfully silenced using siRNA covalently coupled to 0.5 and 0.2 µm microspheres *via* cleavable and non-cleavable linkers. Microspheres showed no apparent toxicity at appropriate concentrations, even after 72 hours incubation with cells. In addition, an improved system employing dual Cy5-co-siRNA labelled 0.5 µm microspheres allowed independent evaluation of only those cells that had been beadfected with siRNA, yielding much more accurate knockdown data. This system also allowed for a truer determination of siRNA-laden microsphere uptake, which was found to approach 80% after 72 hours.

In consideration that microspheres were capable of delivering siRNA efficiently to two diverse cell lines, without toxicity whilst yielding prolonged protein silencing, this indicates that these particles are particularly applicable to the efficient delivery of exogenous cargos, such as siRNA.

Chapter 7: *Experimental Section*

7.1. General Information

^{1}H-NMR and **^{13}C-NMR** were recorded at 250 MHz and 63 MHz respectively on a Bruker ARX-250 system. Chemical shifts (δ) are quoted in ppm and were referenced to residual non-deuterated solvent. **Electrospray mass spectra** were recorded using a VG Platform Quadrupole Electrospray Ionisation mass spectrometer. Only major peaks (*m/z*) are shown with their intensity to the base peak. **HPLC** analysis was performed on an Agilent Technologies 1100 modular HPLC system with detection by U.V. absorbance. Elution was made with Solvent A (0.1% TFA in deionised water) and Solvent B (0.042% TFA in acetonitrile) and the method (Supelco Discovery) was as follows: the material under investigation was eluted through a C-18 column (50 mm × 2.1 mm × 5 μm) at 1 mL/min with a gradient of 10% Solvent B/90% Solvent A to 90% Solvent B/10% Solvent A over 3 min, followed by 2 min isocratic at 90% Solvent B/10% Solvent A. Spectra were recorded at 254 nm, unless otherwise stated. **IR** spectra were recorded on a Bruker Tensor 27 with a golden-gate accessory on solid samples. The following abbreviations were used to denote peak morphology: s (strong), m (medium), w (weak) and b (broad). **Melting points** were determined on an electrothermal hot stage apparatus. **Laser diffractometry** analysis of microspheres and microparticles was carried out on a Beckman Coulter LS 230 in deionised water. **UV/Vis spectrophotometry** was performed on an Agilent 8453 spectrophotometer using a 60% EtOH blank and recording absorbance at 570 nm for quantitative ninhydrin tests and a 20% piperidine/DMF blank measuring absorbance at 302 nm for Fmoc tests. **Scanning electron microscopy** (**SEM**) and **Energy dispersive X-ray** (**EDX**) analysis were performed on a Philips XL30CP with PGT Spirit X-ray analysis for EDX. 0.2 μm microspheres (**2.12**) and 0.3 μm magnetic microspheres (**4.1**) were analysed on a Jeol JSM 5600. **Cell experiments** were carried out in a HERAsafe KS 18 class II negative-flow cabinet from Heraeus. **Cell cultures** were performed in a HERAcell 150 incubator from Heraeus. **Flow cytometry** was performed on a BD Biosciences FACSAria® system using the BD

FACSDiva software for analysis or a DakoCytomation CyAn™ ADP system with Summit software for analysis. **Cell viability** was assessed using a Bio-Rad microplate reader (Version 1.15) measuring absorbance at 570 nm. **Fluorescence Spectrofluorometry** was carried out on a FluoroMax system and the data analysed using Microsoft Excel. **Real-Time microscopy** was performed on a DeltaVision microscope equipped with an incubation chamber (37 ºC/5% CO_2). **Microscopy** and **Confocal microscopy** were performed on a Zeiss Axiovert 200M pseudo confocal microscope with a 100 W Hg lamp or a Leica Inverted Confocal Microscope with a DM IRE2 microscope stand and analysed using Improvision Volocity acquisition software. **Magnetic sublimations** were performed with a neodymium magnetic separator from Bang's Laboratories. ***In vivo* imaging** was performed on a Kodak FX-PRO Reflectance system using multi-spectral un-mixing software. **Histology** was performed on cryostat sections using a Zeiss Axiovert S100 inverted microscope.

Carboxylated Cy5 and Cy7 fluorophores, Fmoc-amino carboxy-poly(ethylene glycol) (Fmoc-PEG-OH) and Fmoc(Dde)-Lysine-OH were from the Bradley and Sánchez-Martín groups.

7.2. General Methods

7.2.1. Monomer Preparation

Prior to use, styrene (50 mL, Sigma-Aldrich) and DVB (50 mL, Sigma-Aldrich) were treated with 25% aq. NaOH (2 × 100 mL, then 2 × 50 mL) and washed with deionised water (2 × 100 mL, then 2 × 50 mL). The monomers were dried over $MgSO_4$, filtered and stored at 4 ºC until their use.

7.2.2. Microsphere Washings

For microsphere preparation, see the Experimental to Chapter 2.

After precipitation from the polymerisation mixture (70 mL), microspheres were isolated by centrifugation (**Table 7.1**) and washed sequentially with methanol (2 × 50 mL) and deionised water (2 × 50 mL). Where polymerisation were performed on a Radley carousel (reaction volume: 5 mL) microspheres were washed with methanol (2 × 5 mL) and deionised water (2 × 5 mL). Finally, microspheres were stored in deionised water at 4 ºC. Prior to on-bead reactions, the microspheres were isolated by centrifugation and washed in the solvent of the reaction (3 × 1 mL).

Microsphere	*Centrifugal Speed (rpm)*	*Time (minutes)*
2.6.1	**8500**	**2**
2.6.2	**8500**	**7**
2.6.3	**8500**	**26**
2.6.4	**8500**	**78**
2.7.2	**13000**	**34**
2.8	**13000**	**17**
2.9	**13000**	**5**
2.10	**13000**	**3**
2.11	**13000**	**360***
2.12	**13000**	**240**

Table 7.1. Centrifugal speeds and time of centrifugation for polystyrene microspheres.[204] * **2.11** was centrifuged in 1 mL aliquots.

7.2.3. Solid Content of Bead Suspension

A known volume of the suspension of microspheres in deionised water was placed in a (pre-weighed) petri-dish, covered with aluminium foil and dried under vacuum at

50 ºC for 18 hours. The sample was weighed and the solid content ascertained as according to **Equation 7.1**.

$$\% \text{ solid content (sc)} = (m / V_s) \times 100$$

Equation 7.1. Analysis of microsphere solid content of suspension (% sc), where 'm' is the mass of microspheres recovered (g) and 'V_s' is the volume of the suspension dried (mL).[204]

7.2.4. Preparation of Samples for Particle Size Distribution

Microspheres (200 µL, 2% sc) were suspended in 2% polyoxyethylenesorbitan monolaurate in deionised water (200 µL) and sonicated (20 min). Microspheres in solution were then added, in a drop-wise manner, to a LS 230 laser diffractometer chamber as according to the manufacturer's instructions.

7.2.5. Preparation of Samples for Scanning Electron Microscopy and EDX

Microspheres (25 µL, 2% sc) were dried on carbon-coated stubs under vacuum (50 ºC, 5 hours) and gold coated by sputtering (approximately 20 nm layer) prior to analysis.

7.2.6. Preparation of Samples for Elemental Analysis

Microspheres (100 µL, 2% sc) were spread over a petri-dish, covered with aluminium foil and dried under vacuum (50 ºC, 5 hours). Dried microspheres (> 1 mg) were analysed for their carbon, hydrogen and nitrogen content.

7.2.7. Qualitative Ninhydrin Test

Microspheres were suspended in methanol (25 µL, 2% sc) and solid particles obtained by centrifugation. To this, ninhydrin reagent A (10 µL) and ninhydrin reagent B (5 µL) (see below) were added and sonicated (1 min) before heating to 100 ºC for 3 min. A blue colour was indicative of a positive result (free amines) and a yellow colour indicated a negative result (no free amines).

7.2.8. Quantitative Ninhydrin Test

Microspheres were suspended in methanol (150 µL, 2% sc) and solid particles obtained by centrifugation. To this, ninhydrin reagent A (6 drops) and ninhydrin

reagent B (2 drops) (see below) were added and sonicated (1 min) before heating to 100 ºC for 3 min. After this time, 60% aq. ethanol (0.4 mL) was added and the suspension sonicated (1 min) before centrifugation. The supernatant was collected and the solid microspheres were washed with 60% aq. ethanol (2 × 0.4 mL), collecting the supernatant after each wash. The supernatants were combined and the absorbance measured at 570 nm. The amine loading on microspheres was found from **Equation 7.2.**

$$\text{Loading } (\mu\text{molg}^{-1}) = (A_{570} \times V) / (\varepsilon_{570} \times m) \times 1{\times}10^{6}$$

Equation 7.2. Analysis of amine loading, where 'A_{570}' is the absorbance of the supernatant measured at 570 nm, 'V' is the volume of the measured solution (mL), 'ε_{570}' is the molar extinction coefficient at 570 nm (15000 $M^{-1}cm^{-1}$) and 'm' is the mass of microspheres analysed (mg).[204]

Ninhydrin Reagent A

Solution 1: Phenol (40 g) was dissolved in ethanol (10 mL) with gentle warming before stirring over Amberlite mixed-bead resin MB-3 (4 g) for 45 min. The solution was obtained by filtration.

Solution 2: Potassium cyanide (65 mg) was dissolved in deionised water (100 mL) and an aliquot (2 mL) of this solution was diluted with pyridine (38 mL, freshly distilled from ninhydrin) and stirred over Amberlite mixed-bead resin MB-3 (4 g). The solution was obtained by filtration and added to 'Solution 1', yielding 'Reagent A'.

Ninhydrin Reagent B

Ninhydrin (2.5 g) was dissolved in ethanol (50 mL), yielding 'Reagent B'.

7.2.9. Fmoc Loading Test

Microspheres (100 µL, 2% sc) were washed with DMF (**Section 7.2.2**) and suspended in DMF (50 µL) prior to the addition of Fmoc-Ahx-OH (10 eq.) pre-activated with DIC (10 eq.) and HOBt (10 eq.) in DMF (50 µL). The microspheres were mixed on a rotary wheel at 25 ºC for 18 hours prior to sequential washing with DMF (3 × 100 µL). Microspheres were treated with 20% piperidine/DMF (200 µL, 3 × 20 min) and washed with DMF (3 × 200 µL), collecting the supernatants after each

wash. The supernatants were combined and the absorbance recorded at 302 nm. The amine loading on microspheres was determined from **Equation 7.3.**

$$\text{Loading } (\mu\text{molg}^{-1}) = (A_{302} \times V) / (\varepsilon_{302} \times m) \times 1{\times}10^{6}$$

Equation 7.3. Analysis of amine loading, where 'A_{302}' is the absorbance of the supernatant measured at 302 nm, 'V' is the volume of the measured solution (mL), 'ε_{302}' is the molar extinction coefficient at 302 nm (7800 $M^{-1}cm^{-1}$) and 'm' is the mass of microspheres analysed (mg).[206]

7.2.10. Purification of Magnetic Microspheres

Following polymerisations (see Experimental to Chapter 4), microspheres were washed as described in **Section 7.2.2** and treated with 2 M aq. HCl (5 mL, 2 × 10 min). Microspheres were subsequently washed with deionised water (2 × 5 mL) and purified by magnetic sublimation using a neodymium magnetic separator.

7.2.11. Magnetic Hysteresis Loop Analysis

Microspheres (100 μL, sc 2%) were dried under vacuum in a petri-dish covered in aluminium foil at 50 ºC for 18 hours. Analysis was performed on 1 mg of solid microspheres at 300 K and compared to 1 mg of iron (III) oxide nanopowder at 300 K.

7.2.12. Cell Culture

All cells were cultured in the appropriate culture medium at 37 ºC/5% CO_2 (Dulbecco's Modified Eagle Medium (DMEM, Sigma-Aldrich) for RAW264, HEK293T, B16F10 and L929 and Roswell Park's Memorial Institute (RPMI-1640, Sigma-Aldrich) medium for HeLa, HeLa-EGFP, K562 and Jurkat) supplemented with 10% foetal bovine serum (FBS, Biosera), 100 U/mL penicillin and streptomycin and 4 mM L-glutamine (Gibco). E14t2g cells[207] were grown in Glasgow's Modified Eagle Medium (GMEM, Sigma-Aldrich) supplemented with 10% FBS, 0.25% sodium bicarbonate (Gibco), 0.1% non-essential amino acids (Gibco), 2 mM L-glutamine (Gibco), 1 mM sodium pyruvate (Gibco), 0.1 mM β-mercaptoethanol (Gibco) and 100 U/mL Leukaemia Inhibitory Factor (LIF, Gibco). Cells were cultured in T-75 flasks (Nunc) until 70 – 80% confluency (E14 cells were cultured in a T-25 flask coated with 0.1% gelatine/PBS). At this time (for adherent cell lines),

the old growth media was removed and the cells were washed with PBS (10 mL) and harvested *via* trypsination (trypsin/EDTA, Gibco) (1 mL) at 37 ºC. The detached cells were collected in fresh growth media (4 mL) and diluted to the appropriate cell density for experiments in fresh growth media. An aliquot was re-seeded to a T-75 flask for re-growth.

In the case of suspension cells, the cells were collected from the T-75 flask by pipette and isolated by centrifugation (1200 rpm, 4 min), washed with PBS (10 mL) and finally diluted to the appropriate cell density for experiments in fresh growth media.

7.2.13. Haemocytometry

Cell densities were determined by haemocytometry. An aliquot (10 µL) of cells detached from a T-75 flask and collected in growth media (total volume: 5 mL) was mixed with 0.2% trypan blue (40 µL, Sigma-Aldrich) and pipetted into a Bright Line™ haemocytometer (an etched glass device with an H-shaped moat forming two cell-counting areas (with 4 quadrants in each area), with surface features enhanced by Neubauer rulings, Sigma-Aldrich). Cell concentrations and the densities required for experiments were determined by **Equations 7.4** and **7.5** respectively.

$$\text{Concentration (cell/mL)} = (N / Q) \times 5\times10^{4}$$

Equation 7.4. Concentration of cell/mL by haemocytometry, where 'N' is the total number of cells counted and 'Q' is the number of quadrants counted.

$$V_{Exp}\,(mL) = (V_{Tot} \times C_{Well}) \times (1000 / V_{Well}) / C_{Tot}$$

Equation 7.5. Volume of cells detached from T-75 flask (V_{Exp}) required in an experiment a total medium volume of V_{Tot} and a concentration per well of C_{Well}. V_{Well} is the volume required per well and C_{Tot} is the concentration of cells/mL as calculated in **Equation 7.4.**

7.2.14. Beadfection of Adherent Cell Lines

Cells were suspended to the appropriate cell density in fresh growth media before seeding onto polystyrene well-plates (Nunc). Cells were incubated (37 ºC/5% CO_2) for 24 hours to allow adhesion.

Separately, microspheres were dispersed in fresh growth media to a concentration of 86 µg/mL unless otherwise stated. The old media was removed from cells and

replaced with fresh media containing microspheres. Cells were incubated in the presence of microspheres (37 ºC/5% CO_2) for 6 – 24 hours (unless otherwise stated) prior to analysis.

7.2.15. Beadfection of Suspension Cell Lines

Cells were suspended to the appropriate cell density in fresh growth media before seeding onto polystyrene well-plates (Nunc). Microspheres were added to cells to give a concentration of 86 μg/mL (unless otherwise stated). Cells were incubated in the presence of microspheres (37 ºC/5% CO_2) for 6 – 24 hours (unless otherwise stated) prior to analysis.

7.2.16. Flow Cytometry

In preparation for flow cytometric analysis, the old media was removed from cell cultures and the cells were washed with PBS and harvested by trypsination at 37 ºC (trypsin/EDTA). Detached cells were collected in growth media and the cell pellet collected by centrifugation (1200 rpm, 4 min). Cells were re-suspended in 2% FBS/PBS or 0.2% trypan blue/HBSS (where extracellular quenching of fluorescein was desired) (minimum 300 μL). Samples were analysed by flow cytometry according to the fluorophores under investigation (**Table 7.2**) using the BD Biosciences FACSDiva software. Untreated cells were defined as having 0% uptake.

Lasers	*Band Pass Filters*
488 nm Coherent® Sapphire™ solid state	515 - 545 nm (Fluorescein or EGFP) 564 - 606 nm (Rhodamine B or TAMRA) 675 - 715 nm or 665 - 685 nm (Propidium Iodide)
633 nm JDS Uniphase™ HeNe air-cooled	650 - 670 nm (Cy5 or Trypan blue) 750 - 810 nm (Cy7)
407 nm Point Source violet solid state	515 - 545 nm (Dansyl)

Table 7.2. BD Biosciences FACSAria® system specifications (lasers and band pass filters) and corresponding fluorophores.

7.2.17. Toxicity Assays

Cells were cultured as described (**Section 7.2.13**) and seeded onto a 96-well plate at

a density of 1×10^4 cells/well (volume per well: 100 µL). The last row of the well-plate was used as a blank (no cells seeded). Cells were incubated (37 ºC/5% CO_2) for 24 hours prior to beadfection (**Sections 7.2.15** and **7.2.16**) at concentrations of 75 and 150 µg/mL. After 24 hours (unless otherwise stated), the old media was removed and replaced with fresh phenol red-free culture media (supplemented as described in **Section 7.2.13**) (90 µL) and 3-(4,5-dimethylthiazol-2-yl)-2,5-diphenyltetrazolium bromide (MTT, Sigma-Aldrich) (10 µL). Cells were incubated for 5 hours at 37 ºC/5% CO_2. After this time, MTT solubilising solution (10% Triton-X, 0.1 N HCl in isopropanol) (100 µL) was added and the 96-well plate was gently shaken for 5 hours. Absorbance was measured at 570 nm. Untreated cells were considered to be 100% viable and cell viability was calculated from **Equation 7.6.**

$$\% \text{ Viable Cells} = (Abs_{Exp} / Abs_{Cont}) \times 100$$

Equation 7.6. Viability of cells by MTT assays, where 'Abs_{Exp}' refers to the absorbance at 570 nm of cells treated with microspheres and 'Abs_{Cont}' refers to the absorbance at 570 nm of untreated control cells.

7.2.18. Microscopy and Cell Staining

Cells were cultured and beadfected as described in **Sections 7.2.13, 7.2.15** and **7.2.16**. In preparation for microscopy, cells were washed with PBS and, if no staining was required (see below), microscopy was directly performed in 2% FBS/PBS or 0.2% trypan blue/HBSS.

Nuclei Staining with Hoechst 33342

Following washing with PBS, cells were treated with Hoechst 33342 (1 µg/mL, Sigma-Aldrich) for 10 min at 25 ºC. Cells were washed three times with PBS. Microscopy was performed in 2% FBS/PBS.

Cellular Fixation

PBS washed cells were fixed with 3% *para*-formaldehyde (20 min, 25 ºC) and washed three times with PBS. Microscopy was performed in PBS.

Actin Filament Staining with AlexaFluor®-568 Phalloidin

Fixed cells were treated with AlexaFluor®-568 phalloidin (1 U/mL, Invitrogen) for 15 min at 25 ºC. Cells were washed with PBS three times prior to microscopy. Microscopy was performed in PBS.

7.3. Experimental for Chapter 2

7.3.1. Preparation of 4-Vinylbenzyl Phthalimide (**2.5**)

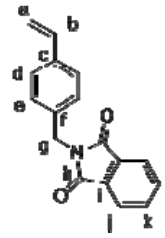

(2.5)

In a typical experiment, 4-vinylbenzyl chloride (21.1 mL, 0.15 mol, Sigma-Aldrich) was dissolved in DMF (75 mL) with potassium phthalimide (27.8 g, 0.15 mol, Sigma-Aldrich) and stirred (350 rpm) for 15 hours at 50 ºC. After this time, the solution was poured into sodium hydroxide (1.5 mol dm^{-3}, 1500 mL), facilitating precipitation of the crude product, which was isolated by vacuum filtration. The solid was dissolved in ethyl acetate (300 mL) and the solvent removed *in vacuo.* The pure product was obtained following re-crystallisation from methanol, vacuum filtration and drying of the resulting colourless crystals under vacuum.

Mass Yield: 27.4 g

% Yield: 70%

Mp: 100 ºC (Lit.[208] 107 – 108 ºC)

Rf: (Hexane:EtOAc, 3:1) 0.48

HPLC: (S50D, λ = 220 nm) 98% pure, retention time 4.07 min

IR: 1700 cm^{-1} (m)

Mass Spectrometry: (ES, MeOH) *m/z* 286 (100%, $[M + Na^+]$), 318 (15%, $[M + Na^+ + MeOH]^+$)

^{1}H-NMR: ($CDCl_3$, 250 MHz) δ (ppm): 4.75 (s, 2H, H-g), 5.15 (d, 1H, J = 11.8 Hz, H-a_{cis}), 5.64 (d, 1H, J = 18.5 Hz, H-a_{trans}), 6.60 (dd, 1H, J = 11.8, 18.5 Hz, H-b), 7.28 (d, 2H, J = 8.5 Hz, H-d), 7.33 (d, 2H, J = 8.5 Hz, H-e), 7.63 (dd, 2H, J = 2.9, 5.5 Hz, H-k), 7.77 (dd, 2H, J = 3.1, 5.3 Hz, H-j)

^{13}C-NMR: ($CDCl_3$, 63 MHz) δ (ppm): 41.7 (C-g), 114.5 (C-a), 123.7 (C-j), 126.9 (C-d), 129.2 (C-e), 132.5 (C-i), 134.4 (C-k), 136.2 (C-f), 136.7 (C-b), 137.6 (C-c), 168.4 (C-h)

7.3.2. Preparation of 4-Vinylbenzyl Amine, (**2.3.1**)

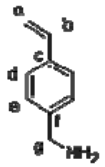

(2.3.1)

In a typical experiment, 4-vinylbenzyl phthalimide (6.4 g, 0.024 mol) was suspended in nitrogen-purged ethanol (34 mL) and heated to reflux under nitrogen for 30 min. Hydrazine hydrate (2.3 mL, 0.05 mol, Sigma-Aldrich) was added *via* a self-equilibrating dropping funnel and the reaction mixture was stirred for 3 hours. After this time, the by-product was removed by vacuum filtration and the filtrates were concentrated *in vacuo*. The resulting crude product was treated with aqueous potassium hydroxide (1.5 mol dm^{-3}, 50 mL) and extracted with diethyl ether (3 × 50 mL). The organic fractions were combined and washed with 2% potassium carbonate (50 mL) before drying over magnesium sulphate and concentrated *in vacuo* to give an orange oil.

Mass Yield: 1.7 g

% Yield: 52%

Rf: (Diethyl ether) 0.24

HPLC: (S50D, λ = 220 nm) 100% pure, retention time 2.24 min

IR: 2975 cm^{-1} (m, b)

Mass Spectrometry: (ES, MeOH) *m/z* 117 (100%, $[M - NH_2]^+$), 134 (12%, $[M + H]^+$)

^{1}H-NMR: ($CDCl_3$, 250 MHz) δ (ppm): 3.70 (s, 2H, H-g), 5.10 (d, 1H, J = 10.9 Hz, H-a_{cis}), 5.55 (d, 1H, J = 17.6 Hz, H-a_{trans}), 6.53 (dd, 1H, J = 10.9, 17.6 Hz, H-b), 7.10 (d, 2H, J = 8.2 Hz, H-d), 7.20 (d, 2H, J = 8.1 Hz, H-e)

^{13}C-NMR: ($CDCl_3$, 63 MHz) δ (ppm): 46.5 (C-g), 113.8 (C-a), 126.8 (C-d), 127.6 (C-e), 136.6 (C-f), 136.9 (C-b), 143.2 (C-c).

7.3.3. Preparation of 4-Vinylbenzyl Amine.HCl, (**2.3.2**)

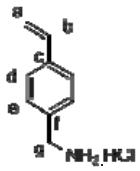

(2.3.2)

In a typical experiment, 4-vinylbenzyl amine (1.7 g, 0.01 mol) was dissolved in diethyl ether (150 mL) and acidic isopropanol (HCl, 6N) was added drop-wise at 0 ºC until salt precipitation was complete. The hydrochloride salt was collected by vacuum filtration and dried under vacuum. Commonly, the free amine (**2.3.1**) was not isolated and vinylbenzylamine.HCl was precipitated directly, as above.

Mass Yield: 0.8 g

% Yield: 46%

Mp: 180 ºC (Lit.[209] 160 – 170 ºC)

Rf: (Diethyl ether) 0.095

HPLC: (S50D, λ = 220 nm) 100% pure, retention time 2.30 min

IR: 2975 cm^{-1} (m, b)

Mass Spectrometry: (ES, MeOH) *m/z* 117 (100%, $[M - NH_3Cl]^+$), 134 (16%, $[M - Cl]^+$)

^{1}H-NMR: (D_2O, 250 MHz) δ (ppm): 4.30 (s, 2H, H-g), 5.50 (d, 1H, J = 10.2 Hz, H-a_{cis}), 6.03 (d, 1H, J = 17.0 Hz, H-a_{trans}), 6.94 (dd, 1H, J = 10.2, 17.0 Hz, H-b), 7.55 (d, 2H, J = 8.2 Hz, H-d), 7.70 (d, 2H, J = 8.2 Hz, H-e)

^{13}C-NMR: (D_2O, 63 MHz) δ (ppm): 43.2 (C-g), 115.7 (C-a), 127.2 (C-d), 129.6 (C-e), 132.4 (C-f), 136.3 (C-b), 138.6 (C-c)

7.3.4. Preparation of Microspheres with Varying Molecular Weight PVP, (**2.6.1**) – (**2.6.4**)

(2.6.1) – (2.6.4)

In a typical polymerisation, poly(vinyl pyrrolidone) (PVP, M_w 10,000, 29,000, 40,000 and 360,000; 70 µmol, 0.2 mol% with regards to styrene, Sigma-Aldrich) was dissolved in nitrogen-purged ethanol (70 mL). To this, nitrogen-purged styrene (3.7 mL, 32 mmol, 1 eq.) with divinylbenzene (DVB; 0.06 mL, 0.4 mmol, 1.3 mol% with regards to styrene), vinylbenzylamine.HCl (VBAH; 0.16 g, 0.9 mmol, 2.8 mol% with regards to styrene) and 2,2′-Azobis(2-methylpropionitrile) (AIBN; 0.1 g, 0.6 mmol, 1.9 mol% with regards to styrene, Sigma-Aldrich) were added and the resultant mixture stirred (350 rpm) at 25 ºC under nitrogen. After 2 hours, the temperature was increased to 70 ºC and the reaction stirred (350 rpm) under nitrogen at this temperature for 18 hours, facilitating the precipitation of microspheres. The reaction mixture was allowed to cool before microspheres were collected by centrifugation (**Table 7.1**) and washed with methanol (2 × 50 mL) and deionised water (2 × 50 mL). Microspheres were stored in deionised water at 4 ºC.

Microsphere	*Yield*	*Size Distribution*	*Amine Loading*	*Elemental Analysis*
2.6.1	0.7 g (20%)	Mean: 3.3 µm S.D.: 2.6 µm C.V.: 79%	25 µmolg^{-1} (Fmoc: 21 µmolg^{-1})	C 92.2, H 7.7, N 0.4 (Loading: 0.29 mmolg^{-1})
2.6.2	1.7 g (48%)	Mean: 1.4 µm S.D.: 0.6 µm C.V.: 44%	16 µmolg^{-1} (Fmoc: 15 µmolg^{-1})	C 92.0, H 5.5, N 0.3 (Loading: 0.21 mmolg^{-1})
2.6.3	3.2 g (90%)	Mean: 0.7 µm S.D.: 0.4 µm C.V.: 59%	9 µmolg^{-1} (Fmoc: 8 µmolg^{-1})	C 91.5, H 8.1, N 0.2 (Loading: 0.14 mmolg^{-1})
2.6.4	2.8 g (78%)	Mean: 0.4 µm S.D.: 0.2 µm C.V.: 39%	29 µmolg^{-1} (Fmoc: 28 µmolg^{-1})	C 89.2, H 7.4, N 0.6 (Loading: 0.43 mmolg^{-1})

Table 7.3. Microspheres Prepared with Varying PVP M_w. Yield, size distribution (by laser diffractometry), amine loading (by quantitative ninhydrin test, Fmoc test results are included in parentheses) and elemental analysis of (**2.6.1**), (**2.6.2**), (**2.6.3**) and (**2.6.4**).

7.3.5. Preparation of Microspheres and the Addition of Water, (**2.7.1**) – (**2.7.3**)

Polymerisations were performed in a 12-tube Radley carousel fitted with a water condenser and nitrogen inlet valves.

In a typical polymerisation, poly(vinyl pyrrolidone) (M_w 40,000; 0.2 g, 5 μmol, 0.2 mol% with regards to styrene) was dissolved in nitrogen-purged ethanol : deionised water (94:6, 97:3 and 92:8, 5 mL). To this, nitrogen-purged styrene (0.3 mL, 2.6 mmol, 1 eq.) with DVB (4.3 μL, 29 μmol, 1.3 mol% with regards to styrene), VBAH (0.01 g, 64 μmol, 2.8 mol% with regards to styrene) and AIBN (7 mg, 43 μmol, 1.9 mol% with regards to styrene) were added and the resultant mixture stirred (350 rpm) at 25 ºC under nitrogen. After 2 hours, the temperature was increased to 70 ºC and the reaction stirred (350 rpm) under nitrogen at this temperature for 18 hours, facilitating the precipitation of microspheres. The reaction mixture was allowed to cool before microspheres were collected by centrifugation (**Table 7.1**) and washed with methanol (2 × 10 mL) and deionised water (2 × 10 mL). Microspheres were stored in deionised water at 4 ºC.

Microsphere	*Yield*	*Size Distribution*	*Amine Loading*	*Elemental Analysis*
2.7.1	0.1 g (36%)	Mean: 0.4 μm S.D.: 0.07 μm C.V.: 17%	28 μmolg^{-1} (Fmoc: 24 μmolg^{-1})	/
2.7.2	0.16 g (57%)	Mean: 0.5 μm S.D.: 0.07 μm C.V.: 14%	29 μmolg^{-1} (Fmoc: 23 μmolg^{-1})	C 91.1, H 7.9, N 0.3 (Loading: 0.21 mmolg^{-1})
2.7.3	0.15 g (54%)	Mean: 0.4 μm S.D.: 0.06 μm C.V.: 15%	16 μmolg^{-1} (Fmoc: 12 μmolg^{-1})	/

Table 7.4. Microspheres Prepared with Varying PVP M_w. Yield, size distribution (by laser diffractometry), amine loading (by quantitative ninhydrin test, Fmoc test results are included in parentheses) and elemental analysis of (**2.7.1**), (**2.7.2**) and (**2.7.3**).

7.3.6. Preparation of Microspheres and the Addition of *n*-Butanol, (**2.8**)

Polymerisations were performed as shown in **Section 7.3.5** forming microspheres (**2.7.1**) – (**2.7.3**). However, ethanol : *n*-butanol (98:2, 5 mL) was used as the polymerisation solvent.

Yield: 0.07 g (25%).

Size Distribution (by laser diffractometry): Mean 0.7 µm, S.D. 0.1 µm, C.V. 13%.

Amine Loading (quantitative ninhydrin test): 8.7 $\mu molg^{-1}$.

Amine Loading (Fmoc test): 7.8 $\mu molg^{-1}$.

Elemental Analysis: C 92.1, H 7.4, N 0.4 (Amine Loading: 0.29 $mmolg^{-1}$).

7.3.7. Preparation of Microspheres and the Addition of Dimethoxyethane, (**2.9**)

Polymerisations were performed as shown in **Section 7.3.5** forming microspheres (**2.7.1**) **–** (**2.7.3**). However, ethanol : dimethoxyethane (98:2, 5 mL) was used as the polymerisation solvent.

Yield: 0.1 g (36%).

Size Distribution (by laser diffractometry): Mean 1.4 µm, S.D. 0.4 µm, C.V. 31%.

Amine Loading (quantitative ninhydrin test): 5.0 $\mu molg^{-1}$.

Amine Loading (Fmoc test): 5.0 $\mu molg^{-1}$.

Elemental Analysis: C 91.4, H 7.8, N 0.5 (Amine Loading: 0.36 $mmolg^{-1}$).

7.3.8. Preparation of Microspheres and the Addition of Toluene, (**2.10**)

Polymerisations were performed as shown in **Section 7.3.5** forming microspheres (**2.7.1**) **–** (**2.7.3**). However, ethanol : toluene (96:4, 5 mL) was used as the polymerisation solvent.

Yield: 0.1 g (36%).

Size Distribution (by laser diffractometry): Mean 1.8 µm, S.D. 0.3 µm, C.V. 16%.

Amine Loading (quantitative ninhydrin test): 6.7 $\mu molg^{-1}$.

Amine Loading (Fmoc test): 6.0 $\mu molg^{-1}$.

Elemental Analysis: C 91.5, H 8.1, N 0.5 (Amine Loading: 0.36 $mmolg^{-1}$).

7.3.9. Preparation of Microspheres by Emulsion Polymerisation, (**2.11**) – (**2.12**)

In a typical polymerisation, styrene (0.3 mL, 2.6 mmol, 1 eq.), DVB (7.3 µL, 50.7 µmol, 2 mol% with regards to styrene), VBAH (8.7 mg, 65 µmol, 2.5 mol% with regards to styrene) and magnesium sulphate (1 mg, 8.3 µmol, 0.3 mol% with regards to styrene) were emulsified in boiled nitrogen-purged deionised water (cooled to 25 ºC, 5 mL). The mixture was bubbled with nitrogen and stirred (350 rpm) at 25 ºC for 30 min before being heated to 80 ºC and stirred under nitrogen for 20 min. After this time, 2,2'-Azobis-2-methyl propionamide (V-50, 4 mg, 14 µmol, 0.6 mol% with regards to styrene, Sigma-Aldrich) was added in deionised water (50 µL) and the emulsification stirred (350 rpm) at 80 ºC under nitrogen for 1 hour (**2.11**) and 2 hours (**2.12**). The reaction mixture was allowed to cool before microspheres were collected by centrifugation (**Table 7.1**) and washed with methanol (2 × 10 mL) and deionised water (2 × 10 mL). Microspheres were stored in deionised water at 4 ºC.

Microsphere	*Yield*	*Size Distribution*	*Amine Loading*	*Elemental Analysis*
2.11	0.1 g (34%)	Mean: 0.1 µm S.D.: 0.02 µm C.V.: 14%	16 µmolg^{-1} (Fmoc: 15 µmolg^{-1})	C 88.9, H 8.1, N 0.7 (Loading: 0.50 mmolg^{-1})
2.12	0.1 g (34%)	Mean: 0.25 µm S.D.: 0.06 µm C.V.: 25%	17 µmolg^{-1} (Fmoc: 16 µmolg^{-1})	C 91.0, H 0.4, N 1.0 (Loading: 0.71 mmolg^{-1})

Table 7.5. Microspheres Prepared with Varying PVP M_w. Yield, size distribution (by laser diffractometry), amine loading (by quantitative ninhydrin test, Fmoc test results are included in parentheses) and elemental analysis of (**2.11**) and (**2.12**).

7.3.10. Preparation of Aminohexanoic-Microspheres, (**2.13) – (2.15**)

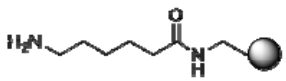

(2.13) – (2.15)

0.2 (**2.12**), 0.5 (**2.7.2**) and 2 µm (**2.10**) amino functionalised microspheres (1 mL, solid content: 2%, 16.7, 29 and 6.7 µmolg^{-1} respectively, 1 eq.) were washed in dimethylformamide (DMF, 3 × 1 mL) and suspended in DMF (0.5 mL). Separately,

Fmoc-aminohexanoic acid (10 eq., see **Table 7.6**, Iris Biotech GmbH) was dissolved in DMF (0.5 mL) with diisopropylcarbodiimide (DIC, 10 eq., see **Table 7.6**, Sigma-Aldrich) and mixed for 10 min at 25 ºC before the addition of 1-hydroxybenzotriazole hydrate (HOBt, 10 eq., see **Table 7.6**) and mixed for 10 min at 25 ºC. The solution was then added to amino microspheres (**2.12, 2.7.2** and **2.10**) and the suspension mixed on a rotary-wheel at 25 ºC for 18 hours. The resultant microspheres were washed with DMF (3 × 1 mL), methanol (3 × 1 mL) and deionised water (3 × 1 mL) and reaction completion was confirmed by a negative qualitative ninhydrin test. Fmoc deprotection was carried out on microspheres washed with DMF (3 × 1 mL) with 20% piperidine/DMF (1 mL), requiring 3 cycles of 20 min to afford deprotection (as evidenced by qualitative and quantitative ninhydrin test). Microspheres were washed sequentially with DMF, methanol and deionised water yielding **2.13** (0.2 μm), **2.14** (0.5 μm) and **2.15** (2 μm). Aminohexanoic-microspheres were stored in deionised water at 4 ºC.

Diameter (μm)	*Amine Loading (μmolg^{-1})*	*Fmoc-Ahx-OH*	*DIC*	*HOBt*
0.2	16.7	1.2 mg (3.4 μmol)	0.5 μL (3.4 μmol)	0.5 mg (3.4 μmol)
0.5	29	2 mg (5.7 μmol)	0.9 μL (5.7 μmol)	0.8 mg (5.7 μmol)
2	6.7	0.5 mg (1.4 μmol)	0.2 μL (1.4 μmol)	0.2 mg (1.4 μmol)

Table 7.6. Quantities of Fmoc-aminohexanoic acid (Fmoc-Ahx-OH), DIC and HOBt used for couplings with 0.2, 0.5 and 2 μm microspheres. Reagents were used in a 10 equivalent excess over microsphere loadings.

Amine Loading (quantitative ninhydrin test): **2.13:** 16 μmolg^{-1}; **2.14:** 23 μmolg^{-1}; **2.15:** 6.0 μmolg^{-1}.

7.3.11. Preparation of Fluorescein-Microspheres, (**2.16) – (2.18**)

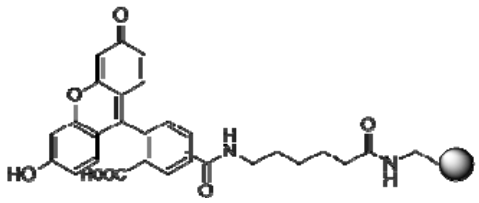

(2.16) – (2.18)

0.2 (**2.13**), 0.5 (**2.14**) and 2 μm (**2.15**) aminohexanoic-microspheres (1 mL, solid content: 2%, 16.0, 23.0 and 6.0 μmolg^{-1} respectively, 1 eq.) were washed in dimethylformamide (DMF, 3 × 1 mL) and suspended in DMF (0.5 mL). Separately, 5(6)-carboxyfluorescein (10 eq., see **Table 7.7**, Sigma-Aldrich) was dissolved in DMF (0.5 mL) with (Benzotriazol-1-yloxy)tripyrrolidinophosphonium hexafluorophosphate (PyBOP, 10 eq., see **Table 7.7**, GL Biochem (Shanghai)), HOBt (10 eq., see **Table 7.7**) and diisopropylethylamine (DIPEA, 10 eq., see **Table 7.7**) and mixed for 1 min prior to addition to microspheres (**2.13 – 2.15**). The suspension was mixed on a rotary-wheel at 25 ºC for 18 hours. The resultant microspheres were washed with DMF (3 × 1 mL), methanol (3 × 1 mL) and deionised water (3 × 1 mL) and reaction completion was confirmed by a negative qualitative ninhydrin test, yielding **2.16** (0.2 μm), **2.17** (0.5 μm) and **2.18** (2 μm). Fluorescein-microspheres were stored in deionised water at 4 ºC.

Diameter (μm)	*Amine Loading (μmolg^{-1})*	*5(6)-Carboxyfluorescein*	*PyBOP*	*HOBt*	*DIPEA*
0.2	16.0	1.2 mg (3.2 μmol)	1.7 mg (3.2 μmol)	0.4 mg (3.2 μmol)	0.6 μL (3.2 μmol)
0.5	23	1.7 mg (4.6 μmol)	2.4 mg (4.6 μmol)	0.6 mg (4.6 μmol)	0.8 μL (4.6 μmol)
2	6.0	0.5 mg (1.2 μmol)	0.6 mg (1.2 μmol)	0.2 mg (1.2 μmol)	0.2 μL (1.2 μmol)

Table 7.7. Quantities of 5(6)-carboxyfluorescein, PyBOP, HOBt and DIPEA used for couplings with 0.2, 0.5 and 2 μm microspheres. Reagents were used in a 10 fold excess over microsphere loadings.

7.3.12. Cellular Uptake of Fluorescein-Microspheres, (**2.16) – (2.18**)

Cells were seeded onto a 24-well plate at a density of 3 × 10^4 cells/well (volume of culture media per well: 350 μL). After 24 hours, beadfections were carried out according to the general procedures using 86 μg/mL and analysis of uptake made after 6, 12 and 24 hours incubation by flow cytometry in 0.2% trypan blue/HBSS (general procedures).

7.3.13. Microscopy of Beadfected Cells

Cells were seeded onto a 12-well plate at a density of 6 × 10^4 cells/well (volume of culture media per well: 800 μL). After 24 hours, beadfections were carried out

according to the general procedures using 86 μg/mL and microscopy performed after 24 hours (general procedures). Cells were fixed and stained with AlexaFluor-568 phalloidin and Hoechst 33342 and imaged in 2% FBS/PBS on a Zeiss Axiovert 200 M pseudo-confocal microscope.

7.3.14. Concentration Dependence on Uptake

Beadfections and flow cytometry were carried out as according to the general procedures using 30, 60 and 86 μg/mL and analysis performed after 24 hours.

7.3.15. Extracellular Quenching of Beadfected B16F10 Cells

Beadfections were carried out as according to the general procedures with (**2.16**), (**2.17**) and (**2.18**) at a concentration of 86 μg/mL. After 10 min, 30 min, 1 hour, 3 hours, 6 hours, 12 hours and 24 hours cells were analysed *via* flow cytometric analysis in 2% FBS/PBS or 0.2% trypan blue/HBSS. Microscopy was performed as described in the general procedures after 24 hours and after 30 min in 2% FBS/PBS, then 0.2% trypan blue/HBSS and the fluorescence output of the images compared.

7.3.16. Serum-Free Cellular Uptake

Cell cultures and beadfections were carried out as according to the general procedures. However, cells were incubated in the appropriate culture media without supplementation with foetal bovine serum. Analysis of uptake was made after 6 and 24 hours by flow cytometry as described in the general procedures.

7.3.17. In Vivo

Animal studies were carried out at the Queen's Medical Research Institute, Centre of Inflammation, Little France, Edinburgh by Dr. K. Dhaliwal under licence from the Animal Scientific Procedure Division of the Home Office, London, U.K.

Cy7 labelled microspheres were sterilised by UV and a single intravenous injection of Cy7 microspheres (tail vein injection, 30 μg) was made into a 6 week old mouse and after 4 hours whole body optical imaging was performed using multi-spectral un-mixing software to determine the fluorescence emissions.

7.4. Experimental for Chapter 3

7.4.1. Preparation of Cy5-Microspheres (**3.4) – (3.6**)

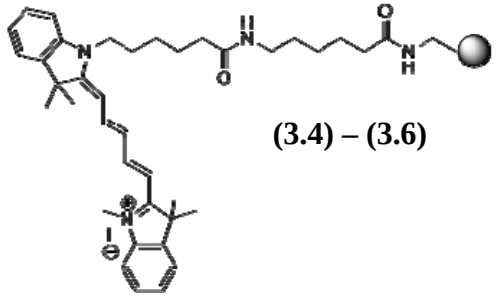

(3.4) – (3.6)

0.2 (**3.4**), 0.5 (**3.5**) and 2 μm (**3.6**) Cy5-labelled microspheres were prepared in the same manner as carboxyfluorescein microspheres (**Sections 7.3.10** and **7.3.11**) using carboxylated Cyanine 5 (5 eq.) in place of 5(6)-carboxyfluorescein.

7.4.2. Chemical Inhibition of Uptake of (**2.16**), (**2.17**) and (**2.18**)

Cell cultures and beadfections were carried out as described in the general procedures, seeding cells onto a 24-well plate at a density of 3×10^4 cells/well (well volume: 350 μL) using 86 μg/mL of (**2.16**), (**2.17**) and (**2.18**). Analysis was carried out after 3 hours by flow cytometry (general procedures). Controls were established with untreated cells and cells treated with microspheres in the absence of chemical inhibitors. Additional analysis was carried out by microscopy in 0.2% trypan blue/HBSS as described in the general procedures (using a Zeiss Axiovert 200M pseudo-confocal microscope). Microscopy of cytochalasin D-treated cells was carried out in PBS following staining with Hoechst 33342, fixation in *para*-formaldehyde and staining with AlexFluor®-568 phalloidin (as according to the general procedures).

ATP Depletion

E14, HEK293T, L929, HeLa and B16F10 cells were treated with sodium azide (20 mM, Sigma-Aldrich) in serum-free culture media for 1 hour prior to beadfection.

Cholesterol Depletion

B16F10 cells were treated with mβ-cyclodextrin (10 mM, Sigma-Aldrich) and lovastatin (1 μg/mL, Tocris Cookson) in serum-free culture media for 1 hour prior to beadfection.

Caveolae-Mediated Endocytosis Inhibition

B16F10 cells were treated with filipin III (5 μg/mL, Sigma-Aldrich) or genistein (200 μM, Sigma-Aldrich) in serum-free culture media for 1 hour prior to beadfection.

Clathrin-Mediated Endocytosis Inhibition

B16F10 cells were treated with chlorpromazine (10 μg/mL, Sigma Aldrich) in serum-free culture media for 1 hour prior to beadfection. Alternatively, cells were washed (3 × 350 μL) and incubated under potassium depleted conditions *via* a potassium-free buffer (140 mM NaCl, 20 mM Hepes, 1 mM $CaCl_2$, 1 mM $MgCl_2$, 1 mg/mL D-glucose, pH 7.4).

Macropinocytosis Inhibition

B16F10 cells were treated with cytochalasin D (10 μM, Tocris Cookson) or dimethylamiloride (DMA, 10 μM, Sigma-Aldrich) in serum-free culture media for 1 hour prior to beadfection.

Inhibition of Membrane Ruffling

B16F10 cells were seeded at a high density (6×10^4 cell/well) and grown to approximately 100% confluency prior to beadfection (86 μg/mL). A control was established where cells were grown to approximately 50% confluency (seeding 3×10^4 cell/well) and beadfected with 43 μg/mL microspheres. Analysis of uptake was performed after 6 hours.

Microtubule Polymerisation Inhibition

B16F10 cells were treated with nocodazole (10 μg/mL, Tocris Cookson) in serum-free culture media for 1 hour prior to beadfection.

7.4.3. Toxicity Assays

MTT toxicity assays were carried out as according to the general procedures. Cells were pre-treated with chemical inhibitors (for 1 hour) prior to beadfection (86 μg/mL) and incubations were run over 3 hours before analysis.

7.4.4. Real-Time Microscopy

Cells (grown on 24 mm glass coverslips at a density of 1×10^5 cells/coverslip) were stained with FM4-64 (5 μg/mL, Invitrogen) in ice cold HBSS (without magnesium or calcium) for 1 min. After this time, the staining solution was removed and fresh phenol red-free media was added containing 0.5 μm fluorescein-microspheres (**2.17**) (43 μg/mL). The glass coverslip was mounted on a DeltaVision RT microscope fitted with an incubation chamber (37 ºC/5% CO_2) and cells were imaged confocally (100 nm slices) repeatedly over 30 min. Fluorescein-microspheres were excited using a 490/20nm excitation filter and collecting emission using a 528/38 nm band-pass filter and FM4-64 was excited using a 555/28 nm excitation filter and collecting emission using a 617/73 nm band-pass filter.

7.4.5. Lysosomal Staining

Cells (grown on 24 mm glass coverslips at a density of 1×10^5 cells/coverslip) were beadfected with Cy5-microspheres ((**3.4**) – (**3.6**), 86 μg/mL) added in fresh media and incubated with cells for 12 hours. After this time, the old media was removed and the beadfected cells were washed with PBS (1 mL) prior to the addition of LysoTracker Red DND-99 (50 pM, 1 mL, Invitrogen). Cells were incubated for a further 2 hours (37 ºC/5% CO_2) before washing with PBS (1 mL). Glass slides were mounted on a Leica inverted confocal microscope in 2% FBS/PBS. Cy5-microspheres were excited with a 633 nm red diode laser and emission collected at 640 – 700 nm. LysoTracker Red DND-99 was excited using a 543 nm HeNe laser and emission collected at 580 – 600 nm. Positive controls were established in the same manner using BODIPY-LacCer (5 μM) and FITC-transferrin (70 μg/mL).

7.4.6. Uptake of BODIPY-LacCer and FITC-Transferrin

B16F10 cells were seeded to a 24-well plate at a density of 3×10^4 cells/well (volume of culture media per well: 350 μL).

After 24 hours, the old media was removed and replaced with fresh media containing sodium azide (20 mM). Cells were incubated at 37 ºC/5% CO_2 for 1 hour prior to the addition of BODIPY-LacCer (5 μM, Invitrogen) or FITC-Transferrin (70 μg/mL, Invitrogen) (controls were established with untreated cells and cells treated with LacCer or transferrin but not treated with any chemical inhibitors). Cells were incubated for a further 2 hours. After this time the old media was removed and cells incubated with LacCer were washed with 1% bovine serum albumin (BSA) in PBS (2 × 200 μL) and cells incubated with transferrin were washed with an acidic buffer (pH 5.0, 2 × 200 μL). Cells were washed with PBS and trypsinised in the usual manner and re-suspended for flow cytometry in 2% FBS/PBS. Untreated cells were considered to have an uptake of 0%.

A similar procedure was used adding mβ-cyclodextrin (10 mM) and lovastatin (1 μg/mL) for cholesterol depletion. Uptake of transferrin was additionally analysed under clathrin-mediated endocytosis inhibition using chlorpromazine (10 μg/mL) and potassium depletion (see general procedures). Uptake of LacCer was analysed under caveolae-mediated endocytosis inhibition using filipin III (5 μg/mL) and genistein (200 μM).

7.4.7. Temperature Dependence on Uptake

B16F10 cells were seeded onto a 24-well plate at a density of 3×10^4 (volume of culture media per well: 350 μL).

After 24 hours, the old media was removed and replaced with fresh media containing fluorescein-microspheres ((**2.16**) – (**2.18**), 86 μg/mL). Cells were incubated for 3 hours at 37, 20 or 4 ºC prior to washing, trypsination and flow cytometry as described in the general procedures. Microscopy of the cells was performed in 2% FBS/PBS as described in the general procedures.

7.4.8. Scanning Electron Microscopy of Beadfected Cells

B16F10 cells were seeded onto a 24 mm glass coverslip at a density of 2×10^5 cells/well (volume of culture media per well: 1.5 mL).

After 24 hours, the old media was removed and replaced with fresh media containing 2 μm fluorescein-microspheres, (**2.18**) (86 μg/mL). After 2, 6 and 24 hours cells were washed with PBS (1 mL) and fixed with 2.5% glutaraldehyde in 0.1 M cacodylate buffer (pH 7.4, 1 mL) at room temperature for 2 hours. After washing with 0.1 M cacodylate buffer (2 × 1 mL), the cells were post-fixed with 1% osmium tetroxide (1 mL) for 1 h at room temperature, dehydrated through graded ethanol (50, 70, 90 and 100%) and critical point dried in CO_2. The glass coverslips were mounted onto carbon-coated stubs and gold coated by sputtering prior to analysis by SEM.

7.4.9. Membrane Leakage to Propidium Iodide

Cells were seeded onto a 24-well plate at a density of 3×10^4 cells/well (volume of culture media per well: 350 μL).

After 24 hours, the old media was removed and replaced with fresh media containing Cy5-microspheres ((**3.4**) – (**3.6**), 86 μg/mL) and propidium iodide (14 μg/mL, Sigma-Aldrich). After 3 hours, the old media was removed and the cells were washed and harvested for flow cytometric analysis in 2% FBS/PBS (general procedures). Controls were established with untreated cells, cells treated only with Cy5 microspheres, cells treated with only propidium iodide (for 3 hours and for 30 min), cells treated with Cy5-microspheres for 3 hours followed by propidium iodide for 30 min and cells treated with BODIPY-LacCer and propidium iodide.

Microscopy was performed on cells as according to the general procedures in 2% FBS/PBS exciting Cy5-microspheres with a red diode 633 nm laser and collecting emission at 640 – 700 nm. Propidium iodide was excited with an argon 488 nm laser and emission collected at 562 – 588 nm.

7.4.10. Membrane Leakage to Trypan Blue

Cultures were performed replacing propidium iodide with trypan blue (6 μg/mL) and fluorescein-microspheres is replace of Cy5-microspheres. Controls were established as for propidium iodide.

Microscopy was performed on cells washed with PBS in 2% FBS/PBS exciting Fluorescein-microspheres with an argon ion 488 nm laser and collecting emission at 510 – 530 nm. Trypan blue was excited with a red diode 633 nm laser and collecting emission at 640 – 700 nm.

7.5. Experimental to Chapter 4

7.5.1 Preparation of Magnetic Microspheres, (**4.1**)

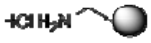

(4.1)

Polymerisations were performed on a 12-tube Radley carousel fitted with a water condenser and nitrogen inlet valves.

In a typical polymerisation, PVP (M_w 360,000; 1.8 g, 5 μmol, 0.2 mol% with regards to styrene) was dissolved in nitrogen-purged ethanol : deionised water (93:7, 5 mL). Iron oxide nanopowder (Fe_2O_3, 8.2 mg, 52 μmol, 2 mol% with regards to styrene, Sigma-Aldrich) was dispersed in the solution by sonication (10 min). To this, nitrogen-purged styrene (0.3 mL, 2.6 mmol, 1 eq.) with DVB (4.3 μL, 29 μmol, 1.3 mol% with regards to styrene), VBAH (8.7 mg, 64 μmol, 2.8 mol% with regards to styrene) and AIBN (7 mg, 43 μmol, 1.9 mol% with regards to styrene) were added and the resultant mixture stirred (350 rpm) at 25 ºC under nitrogen. After 2 hours, the temperature was increased to 70 ºC and the reaction stirred (350 rpm) under nitrogen at this temperature for 18 hours, facilitating the precipitation of the microspheres. The reaction mixture was allowed to cool before microspheres were collected by centrifugation (**Table 7.1**) and were washed and purified according to the general procedures. Magnetic microspheres were stored in deionised water at 4 ºC.

Yield: 0.03 g (11%).

Size Distribution (by laser diffractometry): Mean 0.3 μm, S.D. 0.06 μm, C.V. 19%.

Amine Loading (quantitative ninhydrin test): 9.5 $\mu molg^{-1}$.

Amine Loading (Fmoc test): 5.3 $\mu molg^{-1}$.

Elemental Analysis: C 90.8, H 7.7, N 0.6 (Amine Loading: 0.43 $mmolg^{-1}$).

7.5.2. Preparation of Magnetic Microspheres, (4.2) by PVP 40,000

Polymerisations were performed as according to **Section 7.5.1** using PVP with a molecular weight of 40,000 (0.2g, 5 μmol, 0.2 mol% with regards to styrene).

Yield: 0.03 g (11%).

Size Distribution (by laser diffractometry): Mean 2.0 μm, S.D. 2.0 μm, C.V. 92%.

Amine Loading (quantitative ninhydrin test): 4.9 $\mu molg^{-1}$.

Amine Loading (Fmoc test): 4.3 $\mu molg^{-1}$.

Elemental Analysis: C 61.5, H 3.2, N 0.3 (Amine Loading: 0.21 $mmolg^{-1}$).

7.5.3. Preparation of Magnetic Microspheres, (**4.3**) by DVB Post-Addition

Polymerisations were performed as according to **Section 7.5.1** using PVP with a molecular weight of 40,000 (0.2g, 5 μmol, 0.2 mol% with regards to styrene) and adding DVB (4.3 μL, 29 μmol, 1.3 mol% with regards to styrene) after heating to 70 ºC and stirring at this temperature until a very faint opaque solution resulted.

Yield: 0.13 g (46%).

Size Distribution (by laser diffractometry): Mean 1.6 μm, S.D. 1.1 μm, C.V. 66%.

Amine Loading (quantitative ninhydrin test): 18.3 $\mu molg^{-1}$.

Amine Loading (Fmoc test): 18.0 $\mu molg^{-1}$.

Elemental Analysis: C 90.6, H 7.5, N 0.5 (Amine Loading: 0.36 $mmolg^{-1}$).

7.5.4. Preparation of Aminohexanoic-Magnetic Microspheres, (**4.4) – (4.6**)

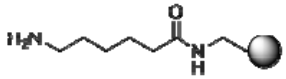

(4.4) – (4.6)

Aminohexanoic-magnetic microspheres were prepared from (**4.1**), (**4.3**) and (**4.2**) as according to **Section 7.3.10**, yielding (**4.4**), (**4.5**) and (**4.6**) respectively. Aminohexanoic-microspheres were stored in deionised water at 4 ºC.

Amine Loading (quantitative ninhydrin test): **(4.4)**: 9.0 μmolg^{-1}; (**4.5)**: 17.9 μmolg^{-1}; (**4.6)**: 4.3 μmolg^{-1}.

7.5.5. Preparation of Fluorescein-Magnetic Microspheres, (**4.7) – (4.9**)

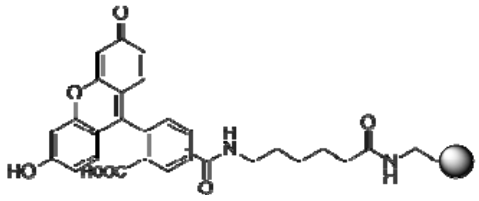

(4.7) – (4.9)

Fluorescein labelled magnetic microspheres were prepared from aminohexanoic magnetic microspheres (**4.4**), (**4.5**) and (**4.6**), yielding (**4.7**), (**4.8**) and (**4.9**) respectively as according to **Section 7.3.11**. Fluorescein-microspheres were stored in deionised water at 4 ºC.

7.5.6. Biased Cellular Movement

Petri-Dish

HEK293T cells were cultured (in a 6-well plate at a density of 2 × 10^5 cell/well) and beadfected with (**4.8**) fluorescein microspheres (general procedures). After 24 hours, cells were washed with PBS (1 mL) and harvested *via* trypsination (trypsin/EDTA, 100 μL). Detached cells were collected in growth media (900 μL) and the cell pellet obtained by centrifugation (1200 rpm, 4 min). Cells were re-suspended in growth media (DMEM, 1 mL) and sorted based on their beadfection with fluorescein microspheres using a BD Biosciences FACSAria® system. Beadfected cells were collected in a sorting chamber containing growth media and isolated after sorting by

centrifugation (1200 rpm, 4 min). Beadfected cells were re-suspended in growth media (2 mL) and seeded to a petri-dish (35 mm diameter) over a neodymium disc magnet (1 cm diameter). Beadfected cells were incubated over the magnet at 37 ºC/5% CO_2 for 24 hours. After this time, microscopy was performed at random positions close to (< 5 mm) and far from (> 2 cm) the magnet.

Magnetic Sublimation of Cells

HEK293T cells were cultured, beadfected and sorted as described above. After sorting, cells were collected by centrifugation (1200 rpm, 4 min) and re-suspended in 2% FBS/PBS (1 mL) with a cell density of approximately 6×10^6 cell/mL. The cell suspension was transferred to a 1.5 mL eppendorf and placed in a neodymium magnetic separator. Attraction of the beadfected 'magnetic' cells to the external magnet was filmed using a Fujifilm Finepix 9.0 Megapixels camera.

7.6. Experimental for Chapter 5

7.6.1. Preparation of Particles by Addition of Diethylketone, (**5.1**)

Polymerisations were carried out according to **Section 7.3.5.** However, precipitation of particles was from ethanol : diethylketone (98:2, 5 mL).

Yield: 0.09 g (32%).

Size Distribution (by laser diffractometry): Mean 2.3 μm, S.D. 0.9 μm, C.V. 40%.

Amine Loading (quantitative ninhydrin test): 7.1 $\mu molg^{-1}$.

Amine Loading (Fmoc test): 7.0 $\mu molg^{-1}$.

Elemental Analysis: C 91.8, H 4.4, N 0.3 (Amine Loading: 0.21 $mmolg^{-1}$).

7.6.2. Preparation of Particles by Addition of Isopropyl Alcohol, (**5.2**)

Polymerisations were carried out as above with precipitation from ethanol : IPA (98:2, 5 mL).

Yield: 0.14 g (50%).

Size Distribution (by laser diffractometry): Mean 1.8 μm, S.D. 0.3 μm, C.V. 16%.

Amine Loading (quantitative ninhydrin test): 9.2 $\mu molg^{-1}$.

Amine Loading (Fmoc test): 9.0 $\mu molg^{-1}$.

Elemental Analysis: C 91.8, H 7.8, N 0.5 (Amine Loading: 0.36 $mmolg^{-1}$).

7.6.3. Preparation of Particles of Addition of Tetrahydrofuran, (**5.3**)

Polymerisations were carried out as above with precipitation from ethanol : THF (95:5, 5 mL).

Yield: 0.1 g (36%).

Size Distribution (by laser diffractometry): Mean 1.6 μm, S.D. 0.3 μm, C.V. 21%.

Amine Loading (quantitative ninhydrin test): 5.2 $\mu molg^{-1}$.

Amine Loading (Fmoc test): 4.9 μmolg^{-1}.

Elemental Analysis: C 91.1, H 7.7, N 0.5 (Amine Loading: 0.36 mmolg^{-1}).

7.6.4. Preparation of Particles by Addition of 1,4-Dioxane, (**5.4**) – (**5.14**)

Polymerisations were carried out as above with precipitation from ethanol : 1,4-dioxane (99.5:0.5 – 90:10, 5 mL). Addition of 5% dioxane in ethanol facilitated precipitation of micro-doughnuts (**5.9**).

Microsphere	*Yield*	*Size Distribution*	*Amine Loading*	*Elemental Analysis*
5.4	0.12 g (43%)	Mean: 5.5 μm S.D.: 7.8 μm C.V.: 141%	8 μmolg^{-1}	/
5.5	0.06 g (21%)	Mean: 1.7 μm S.D.: 1.2 μm C.V.: 71%	16 μmolg^{-1}	/
5.6	0.07 g (25%)	Mean: 2.1 μm S.D.: 0.5 μm C.V.: 22%	9 μmolg^{-1}	/
5.7	0.07 g (25%)	Mean: 6.3 μm S.D.: 13.7 μm C.V.: 218%	15 μmolg^{-1}	/
5.8	0.1 g (36%)	Mean: 1.6 μm S.D.: 0.3 μm C.V.: 24%	9 μmolg^{-1}	/
5.9	0.19 g (68%)	Mean: 4.8 μm S.D.: 10.8 μm C.V.: 227%	10 μmolg^{-1} (Fmoc: 9 μmolg^{-1})	C 92.4, H 7.4, N 0.3 (Loading: 0.21 mmolg^{-1})
5.10	0.07 g (25%)	Mean: 2.0 μm S.D.: 0.5 μm C.V.: 24%	6 μmolg^{-1}	/
5.11	0.08 g (29%)	Mean: 9.1 μm S.D.: 12.5 μm C.V.: 137%	10 μmolg^{-1}	/
5.12	0.19 g (68%)	Mean: 1.2 μm S.D.: 1.0 μm C.V.: 83%	6 μmolg^{-1}	/
5.13	0.09 g (32%)	Mean: 1.4 μm S.D.: 0.5 μm C.V.: 34%	7 μmolg^{-1}	/
5.14	0.15 g (54%)	Mean: 1.3 μm S.D.: 0.6 μm C.V.: 46%	6 μmolg^{-1}	/

Table 7.8. Micro-Doughnut Preparation. Yield, size distribution (by laser diffractometry), amine loading (by quantitative ninhydrin test, Fmoc test results are included in parentheses) and elemental analysis of (**5.4**) - (**5.14**). (**5.9**) are micro-doughnuts.

7.6.5. Preparation of Aminohexanoic Micro-Doughnuts, (**5.15**)

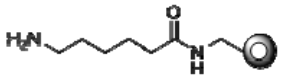

(5.15)

Aminohexanoic micro-doughnuts (**5.15**) were prepared from (**5.9**) in the same manner as aminohexanoic microspheres (**Section 7.3.10**). Aminohexanoic-micro-doughnuts were stored in deionised water at 4 ºC.

Amine Loading (quantitative ninhydrin test): 9.0 μmolg^{-1}.

7.6.6. Preparation of Fluorescein, Rhodamine B and Cy7 Micro-doughnuts, (**5.16**) – (**5.18**)

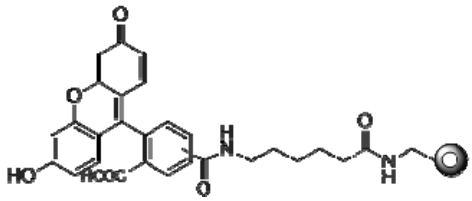

(5.16)

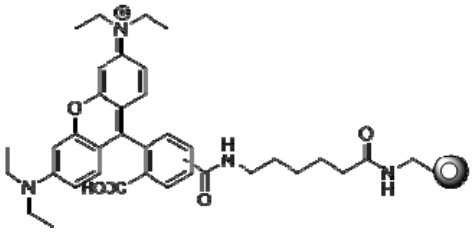

(5.17)

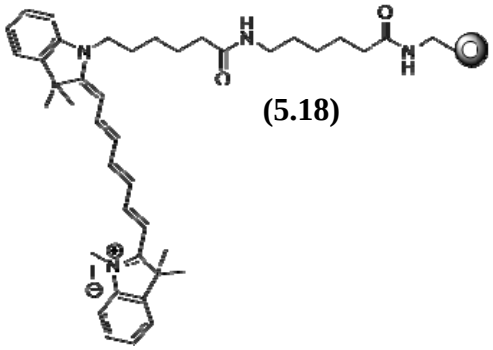

(5.18)

Fluorescein, rhodamine B and Cy7 micro-doughnuts (**5.16**), (**5.17**) and (**5.18**) respectively were prepared from (**5.15**) in the same manner as fluorescein microspheres (**Section 7.3.11**).

7.6.7. Preparation of Dansyl Microspheres

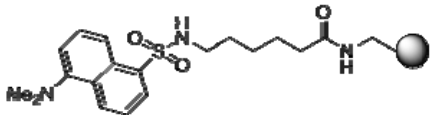

0.5 μm aminohexanoic microspheres (**2.14**) (1 mL, solid content: 2%, 23.0 μmolg^{-1}) were washed in dimethylformamide (DMF, 3 × 1 mL) and suspended in DMF (0.5 mL). Separately, dansyl-chloride (1.2 mg, 4.6 μmol, 10 eq., Sigma-Aldrich) was dissolved in DMF (0.5 mL) with DIPEA (0.8 μL, 4.6 μmol, 10 eq.) and mixed for 1 min prior to addition to microspheres (**2.14**). The suspension was mixed on a rotary-wheel at 25 ºC for 18 hours. The resultant microspheres were washed with DMF (3 × 1 mL), methanol (3 × 1 mL) and deionised water (3 × 1 mL) and reaction completion was confirmed by a negative qualitative ninhydrin test. Dansyl-microspheres were stored (in foil) in deionised water at 4 ºC.

7.6.8. Doughnut-Fection of Cells

Doughnut-fections were carried out in a similar manner to beadfections (general procedures), using 86 μg/mL fluorescein micro-doughnuts and performing incubations over 6, 12 and 24 hours prior to analysis by flow cytometry (in 0.2% trypan blue/HBSS) as described in the general procedures.

7.6.9. Microscopy of Doughnut-fected Cells

Microscopy and staining of doughnut-fected cells was carried out as according to the general procedures in 2% FBS/PBS using a Leica inverted confocal microscope.

In the case of multiplexing assays, cells were imaged by confocal microscopy exciting rhodamine B doughnuts with a 543 nm HeNe laser and collecting emission at 560 nm – 650 nm, exciting dansyl microspheres with a 405 nm laser and collecting emission at 450 nm – 550 nm and exciting Cy5 microspheres with a 633 nm red diode laser and collecting emission at 650 nm – 700 nm.

7.6.10. Micro-doughnut Multiplexing

HEK293T and B16F10 cells were cultured in DMEM as described in the general procedures. Cells were seeded at a density of 3×10^4 cell/well to a 24-well plate. After 24 hours, HEK293T cells were beadfected with 0.5 μm Cy5 microspheres (86 μg/mL) and B16F10 cells were beadfected with 0.5 μm dansyl microspheres (86 μg/mL). Cells were incubated with microspheres (37 ºC/5% CO_2) for 24 hours. After this time the cells were sorted based on their Cy5 or dansyl fluorescence collecting only beadfected cells. These cells (approximately 1×10^5) were isolated by centrifugation and mixed in DMEM growth media (1.5 mL) before seeding at a density of 3×10^4 to a 24-well plate. After 24 hours, 0.5 μm fluorescein microspheres (**2.17**) (86 μg/mL) or rhodamine micro-doughnuts (**5.17**) (86 μg/mL) were added to mixed cell cultures and incubated for a further 24 hours. After this time, analysis was made by flow cytometry (general procedures) to determine uptake of (**2.17**) and (**5.17**) by HEK293T (Cy5 positive) and B16F10 (dansyl positive) cells.

7.6.11. *In Vivo* Doughnut-fection

All animal studies (including histology) were carried out at the Queen's Medical Research Institute, Centre of Inflammation, Little France, Edinburgh by Dr. K. Dhaliwal.

Cy7 labelled micro-doughnuts (**5.18**) were sterilised by UV prior to animal studies and all animal experiments were undertaken with an approved licence from the Animal Scientific Procedure Division of the Home Office, London, U.K.

A single intravenous injection of Cy7 micro-doughnuts (tail vein injection, 30 μg) was made into a 6 week old mouse and after 4 hours whole body optical imaging was performed using multi-spectral un-mixing software to determine the fluorescence emissions. Cy7 micro-doughnuts were artificially coloured yellow. Chlorophyll was administered orally to show gut location.

7.6.12. Histology of Doughnut-fected Liver

After 4 hours of *in vivo* doughnut-fection, the liver was excised from the animal and frozen over solid carbon dioxide. The frozen organ was then thinly sliced into 5 – 10 μm sections, which were mounted onto glass microscope slides and imaged.

7.7. Experimental for Chapter 6

7.7.1. siRNA Sequences

Three unfunctionalised siRNA sequences (Qiagen) were lipofected (Lipofectamine™ 2000, Invitrogen) for EGFP gene silencing assessment. siRNA sequences (GFP-1 and negative) were subsequently purchased functionalised with an amine (*via* a C-6 linker, Microsynth) at the 5' end of the sense strand to facilitate coupling to microspheres. In the case of TAMRA siRNA, the fluorophore was located on the 5' end of the anti-sense strand (Dharmacon).

GFP Sequence	*Sense (5' → 3')*	*Anti-Sense (5' → 3')*
Negative	GUG AAA ACC AGG ACA AAA GUU	CUU UUG UCC UGG UUU UCA CUU
GFP-1	GCU GAC CCU GAA GUU CAU CUU	GAU GAA CUU CAG GGU CAG CUU
GFP-2	CGA GCA CGA CUU CUU CAA GUU	CUU GAA GAA GUC GUG CUG CUU
GFP-3	GCA AGC UGA CCC UGA AGU UCA UUU	AUG AAC UUC AGG GUC AGC UUG CUU

Table 7.9. siRNA sequences for EGFP gene silencing. 'Negative' refers to scrambled siRNA, with no homology to the target sequence.

7.7.2. Lipofection with Lipofectamine™ 2000

HeLa-EGFP and ES-EGFP cells were seeded in the appropriate growth media to 24-well plates (ES-EGFP cells required plates gelatinised with 0.1% gelatine/PBS) at a density of 3×10^4 cell/well (well volume: 350 μL).

For each well, Lipofectamine™ 2000 (1 μL) was incubated in PBS (50 μL) at 25 ºC for 5 min. It was then added to siRNA (20 pmol) in PBS (50 μL) and incubated at 25 ºC for 20 min.

After 24 hours, the old media was removed from the cells and replaced with fresh serum- and antibiotic-free media (250 μL) containing siRNA treated with Lipofectamine™ 2000 in PBS (100 μL). After 24 – 72 hours cells were washed, harvested by trypsination and prepared for flow cytometric analysis as described in the general procedures.

7.7.3. Controls for Gene Silencing

As well as lipofecting cells with siRNA delivered by Lipofectamine™ 2000, several other controls were established:

HeLa-EGFP and ES-EGFP cells were seeded in the appropriate growth media to 24-well plates (ES-EGFP cells required plates gelatinised with 0.1% gelatine/PBS) at a density of 3×10^4 cell/well (well volume: 350 μL).

After 24 hours, the old media was removed and replaced with fresh serum-free and antibiotic-free media containing scrambled siRNA lipofected with Lipofectamine™ 2000 (as **Section 7.7.2**), siRNA (GFP-1) alone, microspheres conjugated to scrambled siRNA (86 μg/mL, 28 nM siRNA) and microspheres alone (86 μg/mL). Analysis of EGFP expression was made by flow cytometry (general procedures) and compared to untreated cells.

7.7.4. Preparation of PEG Microspheres, (**6.1.1) – (6.1.3**)

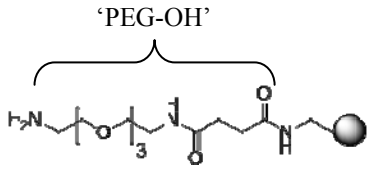

(6.1.1) – (6.1.3)

In a typical reaction, Fmoc-PEG-OH (10 eq. see **Table 7.10**) was activated with DIC (10 eq. see **Table 7.10**) in DMF (0.5 mL) for 10 min at 25 ºC, followed by HOBt (10 eq. see **Table 7.10**) for 10 min at 25 ºC. The resulting solution was added to (**2.10**), (**2.72**) and (**2.12**) suspended in DMF (0.5 mL, 4% sc). The resulting suspension was mixed on a rotary wheel at 25 ºC for 18 hours. After this time, the microspheres were washed with DMF (3 × 1 mL), methanol (3 × 1 mL), deionised water (3 × 1 mL) and finally DMF (3 × 1 mL). Fmoc deprotection was achieved by treating microspheres with 20% piperidine/DMF (1 mL, 3 × 20 min). Microspheres were washed sequentially with DMF, methanol and deionised water, yielding 0.2 (**6.1.3**), 0.5 (**6.1.2**) and 2 μm (**6.1.1**) PEGylated microspheres. Microspheres were stored in deionised water at 4 ºC.

Diameter (µm)	*Amine Loading (µmolg^{-1})*	*Fmoc-PEG-OH*	*DIC*	*HOBt*
0.2	16.7	1.7 mg (3.4 µmol)	0.5 µL (3.4 µmol)	0.5 mg (3.4 µmol)
0.5	29	2.9 mg (5.7 µmol)	0.9 µL (5.7 µmol)	0.8 mg (5.7 µmol)
2	6.7	0.7 mg (1.4 µmol)	0.2 µL (1.4 µmol)	0.2 mg (1.4 µmol)

Table 7.10. Quantities of Fmoc-PEG-OH, DIC and HOBt used for coupling with the 0.2, 0.5 and 2 µm microspheres. Reagents were used in a 10 equivalent excess over microsphere loadings.

7.7.5. Preparation of PEG-Succinic Microspheres, (**6.2.1) – (6.2.3**)

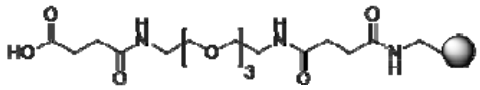

(6.2.1) – (6.2.3)

In a typical reaction, succinic anhydride (10 eq. see **Table 7.11**) and DIPEA (10 eq. see **Table 7.11**) in DMF (0.5 mL) were added to either (**6.1.1**), (**6.1.2**) or (**6.1.3**) suspended in DMF (0.5 mL, 4% sc). The resulting suspension was mixed on a rotary wheel at 25 ºC for 18 hours. After this time, the microspheres were washed with DMF (3 × 1 mL), methanol (3 × 1 mL) and deionised water (3 × 1 mL), yielding 0.2 (**6.2.3**), 0.5 (**6.2.2**) and 2 µm (**6.2.1**) succinic microspheres. Microspheres were stored in deionised water at 4 ºC.

Diameter (µm)	*Amine Loading (µmolg^{-1})*	*Succinic Anhydride*	*DIPEA*
0.2	16.7	0.3 mg (3.4 µmol)	0.3 µL (1.8 µmol)
0.5	29	0.6 mg (5.7 µmol)	0.6 µL (3.6 µmol)
2	6.7	0.1 mg (1.4 µmol)	0.2 µL (1.2 µmol)

Table 7.11. Quantities of succinic anhydride and DIPEA used for couplings with 0.2, 0.5 and 2 µm microspheres. Reagents were used in a 10 equivalent excess over microsphere loadings.

7.7.6. Preparation of PEG-Disulphide Microspheres, (**6.4.1) – (6.4.2**)

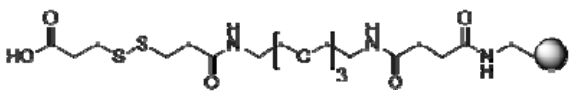

(6.4.1) – (6.4.2)

Carboxyethyldisulphide (10 eq. see **Table 7.12**) was activated with DIC (10 eq. see **Table 7.12**) in DMF (0.5 mL) for 10 min at 25 ºC, followed by HOBt (10 eq. see **Table 7.12**) for 10 min at 25 ºC. The resulting solution was added to (**6.1.2**) or (**6.1.3**) suspended in DMF (0.5 mL, 4% sc). The resulting suspension was mixed on a rotary wheel at 25 ºC for 18 hours. After this time, the microspheres were washed with DMF (3 × 1 mL), methanol (3 × 1 mL) and deionised water (3 × 1 mL), yielding 0.2 (**6.4.2**) and 0.5 µm (**6.4.1**) disulphide microspheres. Microspheres were stored in deionised water at 4 ºC.

Diameter (µm)	*Amine Loading (µmolg⁻¹)*	*Carboxy ethyldisulphide*	*DIC*	*HOBt*
0.2	16.7	0.7 mg (3.4 µmol)	0.5 µL (3.4 µmol)	0.5 mg (3.4 µmol)
0.5	29	1.2 mg (5.7 µmol)	0.9 µL (5.7 µmol)	0.8 mg (5.7 µmol)

Table 7.12. Quantities of carboxyethyldisulphide, DIC and HOBt used for couplings with 0.2 and 0.5 µm microspheres. Reagents were used in a 10 equivalent excess over microsphere loadings.

7.7.7. siRNA Coupling to Microspheres, (**6.3.2**), (**6.3.3**), (**6.6.1**) or (**6.6.2**)

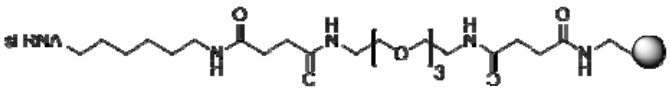

(6.3.2) – (6.3.3)

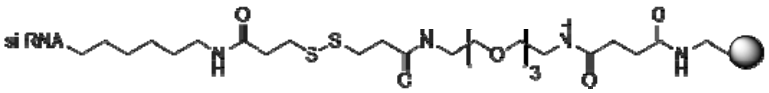

(6.6.1) – (6.6.2)

Succinic and disulphide microspheres (100 µL, 2% sc) (**6.2.1**), (**6.2.2**), (**6.2.3**), (**6.4.1**) and (**6.4.2**) were isolated by centrifugation and washed with MES buffer (pH 5.5, 3 × 100 µL) before activation with EDAC.HCl (10 eq., Sigma-Aldrich) in MES (100 µL) for 2 hours. Microspheres were isolated by centrifugation and treated with RNase Zap™ solution (100 µL, Ambion) before being transferred to an RNase-free eppendorf and washed with RNase-free deionised water (100 µL). siRNA (GFP-1, 1 nmol) was added to microspheres in RNase-free PBS (100 µl) and shaken at 25 ºC for 24 hours. After this time siRNA-microspheres were isolated by centrifugation, yielding 0.5 (**6.3.2**), 0.2 µm (**6.3.3**) succinic siRNA microspheres and 0.5 (**6.6.1**), 0.2

μm (**6.6.2**) disulphide-siRNA microspheres, stored in RNase-free deionised water at 4 ºC.

7.7.8. Analysis of siRNA Loading on Microspheres

0.2 (**6.1.3**) and 0.5 μm (**6.1.2**) succinic microspheres (100 μL, 3% sc) were loaded with TAMRA-labelled siRNA as according to **Section 7.7.7**, yielding 0.2 (**6.3.3**) and 0.5 μm (**6.3.2**) siRNA microspheres. Following coupling, siRNA microspheres were obtained by centrifugation and washed with RNase-free deionised water (100 μL) and the supernatant collected and analysed by spectrofluorometry (excitation: 540 nm, emission collected over 560 – 700 nm).

Calibration solutions of TAMRA-labelled siRNA in RNase-free deionised water were prepared at concentrations of 0.25, 0.15, 0.1 and 0.05 μM and analysed by spectrofluorometry.

The emission maximum was found at 580 nm and the fluorescence intensity at this wavelength was plotted against the solution siRNA concentration, giving a linear relationship. From this the concentration of siRNA present in supernatants collected from (**6.3.2**) and (**6.3.3**) was calculated and found to be 0.3 and 0.4 μM respectively. Given that 1 nmol of siRNA was originally added to microspheres, this allows the concentration of siRNA on the microspheres to be calculated as follows:

The 0.2 μm bead-siRNA supernatant contained 4×10^{-11} moles of siRNA and the 0.5 μm bead-siRNA supernatant 3×10^{-11} mol of siRNA. A total of 1×10^{-9} moles siRNA was added to the beads originally thus the 0.2 μm beads must have retained 9.6×10^{-10} moles siRNA (96% of siRNA coupled to microspheres) and the 0.5 μm beads must have retained 9.7×10^{-10} moles siRNA (97% of siRNA coupled to microspheres).

The number of beads per gram of solid can be calculated by **Equation 7.7**.

$$\text{Number of beads/g} = 6 \times 10^{12} / (\pi \times \rho \times d^3)$$

Equation 7.7. Number of microspheres per gram of solid, where 'ρ' is the density of the microspheres (1.0 g/mL for polystyrene microspheres) and 'd' is the diameter of the microspheres.[204]

0.2 µm siRNA Microspheres

In the case of 0.2 µm microspheres, there are 2.4×10^{14} beads/g and in a 100 µL aliquot (solid content of 3%, as used in the siRNA couplings) there was 3 mg of beads. This equates to 7.2×10^{11} beads, therefore each bead holds, on average, 1.3×10^{-21} moles of siRNA, which equates to 783 molecules of siRNA per bead.

In a typical culture where 86 µg/mL microspheres (or 2.1×10^{10} beads/mL) are added to cells, 1.3×10^{-21} moles of siRNA per bead equates to 9.4×10^{-12} moles siRNA per culture. Given the cell culture volume is 350 µL, this gives a concentration of 2.7×10^{-8} moldm^{-3}.

0.5 µm siRNA Microspheres

In the case of 0.5 µm microspheres, there are 1.5×10^{13} beads/g and in a 100 µL aliquot at a solid content of 3% (as used in the siRNA couplings) this equates to 3 mg of beads. This equates to 4.5×10^{10} beads, therefore each bead holds, on average, 2.2×10^{-20} moles of siRNA, which equates to 13,244 chains of siRNA per bead.

In a typical culture where 86 µg/mL (or 1.3×10^{9} beads/mL) microspheres are added to cells, 2.2×10^{-20} moles of siRNA per bead equates to 1.0×10^{-11} moles siRNA per culture. Given then cell culture volume is 350 µL, this gives a concentration of 2.8×10^{-8} moldm^{-3}.

7.7.9. siRNA stability on Microspheres

siRNA microspheres (**6.3.2**) and (**6.3.3**) were incubated (37 ºC/5% CO_2) in complete growth media, serum-free media, phenol red- and serum-free media and PBS (pH 7.4) for 30 min to 24 hours. Microspheres were collected by centrifugation and analysed for TAMRA fluorescence by flow cytometry in RNase-free PBS and compared to untreated TAMRA siRNA microspheres.

7.7.10. Preparation of PEG-Fluorescein (Succinic/Disulphide) Microspheres (**6.5.1**), (**6.5.2**), (**6.7.1**), (**6.7.2**)

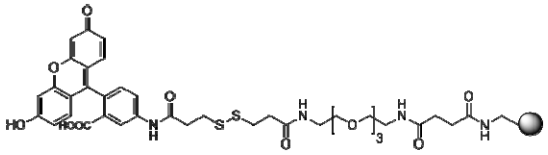

(6.5.1) – (6.5.2)

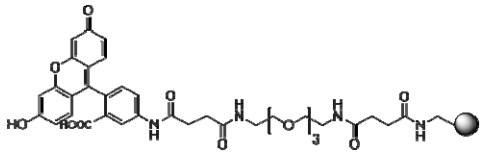

(6.7.1) – (6.7.2)

Succinic and disulphide microspheres (1 mL, 2% sc) (**6.2.2**), (**6.2.3**), (**6.4.1**) and (**6.4.2**) were isolated by centrifugation and washed with DMF (3 × 1 mL) before being suspended in DMF (0.5 mL). To these, DIC (10 eq. see **Table 7.13**) and HOBt (10 eq. see **Table 7.13**) were added in DMF (0.5 mL) and the resulting suspension mixed on a rotary wheel for 5 hours at 25 ºC. After this time, fluoresceinamine (10 eq. see **Table 7.13**) was added and the suspension mixed in the dark at 25 ºC for 18 hours. Microspheres were washed with DMF (3 × 1 mL), methanol (3 × 1 mL) and deionised water (3 × 1 mL) and finally stored in deionised water at 4 ºC, yielding 0.2 (**6.5.2**) and 0.5 µm (**6.5.1**) disulphide-FAM and 0.2 (**6.7.2**) and 0.5 µm (**6.7.1**) succinic-FAM microspheres.

Diameter (µm)	*Amine Loading ($\mu mol g^{-1}$)*	*Fluoresceinamine*	*DIC*	*HOBt*
0.2	16.7	1.2 mg (3.4 µmol)	0.5 µL (3.4 µmol)	0.5 mg (3.4 µmol)
0.5	29	2.0 mg (5.7 µmol)	0.9 µL (5.7 µmol)	0.8 mg (5.7 µmol)

Table 7.13. Quantities of fluoresceinamine, DIC and HOBt used for couplings with 0.2 and 0.5 µm microspheres. Reagents were used in a 10 equivalent excess over microsphere loadings.

7.7.11. Disulphide Cleavage with Glutathione and DTT

(**6.5.1**) and (**6.5.2**) disulphide-FAM microspheres were treated with glutathione (Sigma-Aldrich) (10 mM) or dithiothreitol (DTT, Sigma-Aldrich) (10 mM) in PBS (pH 7.4) for 1, 6 and 24 hours. Cleavage was assessed *via* the reduction in fluorescence intensity of the microspheres compared to untreated control beads by flow cytometry (in PBS). (**6.7.2**) and (**6.7.1**) succinic-FAM microspheres were additionally treated with glutathione and DTT as controls.

7.7.12. Preparation of Lysine Microspheres, (**6.8.1**)

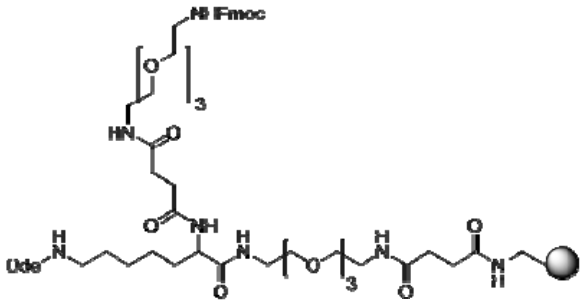

(6.8.1)

PEGylated 0.5 µm microspheres (1 mL, 2% sc) (**6.1.2**) were washed with DMF (3 × 1 mL) and re-suspended in DMF (0.5 mL) prior to addition of orthogonally protected Fmoc-Lysine(Dde)-OH (3.0 mg, 5.7 µmol, 10 eq.) pre-activated with DIC (0.9 µL, 5.7 µmol, 10 eq.) (10 min, 25 ºC) and HOBt (0.8 mg, 5.7 µmol, 10 eq.) (10 min, 25 ºC) in DMF (0.5 mL). The resulting suspension was mixed on a rotary wheel for 18 hours at 25 ºC. Microspheres were obtained by centrifugation and subsequently washed with DMF (3 × 1 mL), methanol (3 × 1 mL), deionised water (3 × 1 mL) and finally DMF (3 × 1 mL). Fmoc deprotection was facilitated in 20% piperidine/DMF (1 mL, 3 × 20 min), yielding free amino residues, which were PEGylated as described in **Section 7.7.4**, yielding (**6.8.1**). PEG residues were *not* Fmoc deprotected at this stage.

7.7.13. Preparation of Cy5 Lysine (Disulphide/Succinic) Microspheres, (**6.10.1**), (**6.11.1**)

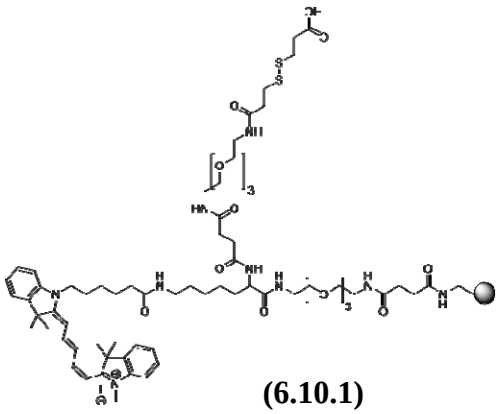

(6.10.1)

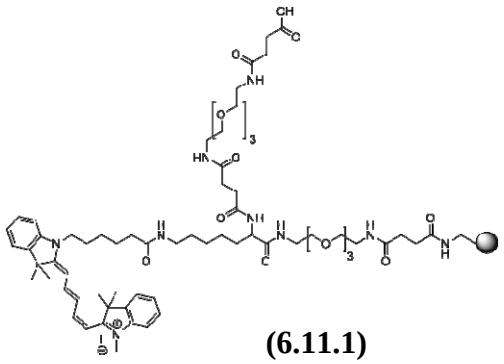

(6.11.1)

(**6.8.1**) Lysine microspheres (1 mL, sc 2%) were washed with DMF (3 × 1 mL) and suspended in DMF (0.5 mL) before treatment with hydroxylamine.HCl (0.4 mmol) and imidazole (0.3 mmol) in NMP for 1 hour at 25 ºC to afford Dde deprotection. At

this time, microspheres were washed sequentially with methanol and then returned to DMF (0.5 mL). Cy5 (1.8 mg, 2.9 µmol, 5 eq.) in DMF (0.5 mL) activated with PyBOP (1.5 mg, 2.9 µmol, 5 eq.), HOBt (0.4 mg, 2.9 µmol, 5 eq.) and DIPEA (0.5 µL, 2.9 µmol, 5 eq.) was added to microspheres and the resulting suspension mixed on a rotary wheel for 18 hours at 25 ºC. Microspheres were washed sequentially with DMF (3 × 1 mL), methanol (3 × 1 mL), deionised water (3 × 1 mL) and DMF (3 × 1 mL). Fmoc deprotection of the PEG residue was subsequently achieved by treatment of microspheres with 20% piperidine/DMF (1 mL, 3 × 20 min) followed by washing with DMF, methanol and deionised water as previous, yielding (**6.9.1**). Microspheres were returned to DMF (0.5 mL) and coupled with succinic anhydride (see **Section 7.7.5**) yielding (**6.11.1**) or carboxyethyldisulphide (see **Section 7.7.6**) yielding (**6.10.1**). Microspheres were stored in deionised water.

7.7.14. siRNA Coupling for Dual Functionalised Microspheres, (**6.12.1**), (**6.13.1**)

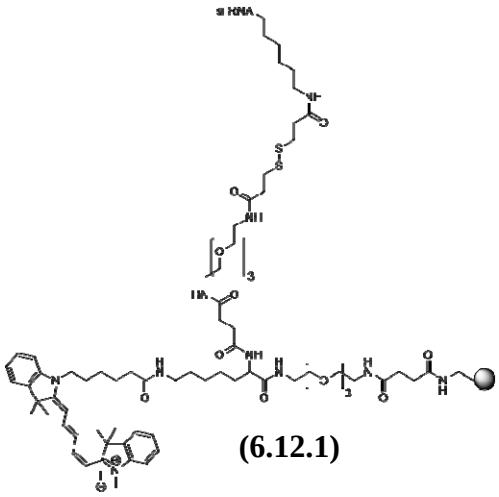

(6.12.1)

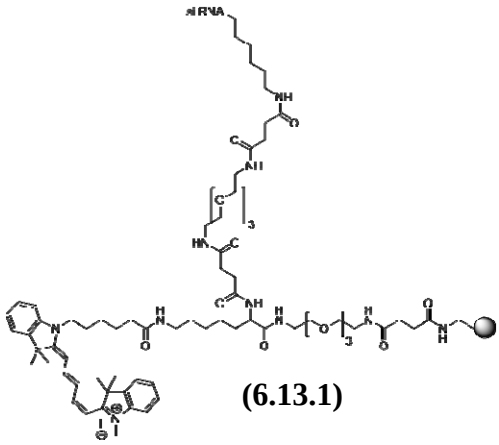

(6.13.1)

(**6.10.1**) and (**6.11.1**) (2 × 0.5 mL, 2% sc) were washed with MES buffer (pH 5.5, 3 × 0.5 mL) and re-suspended in MES (250 µL). Microspheres were activated with EDAC.HCl (1.1 mg, 5.7 µmol, 10 eq.) in MES (250 µL) for 2 hours prior to the addition of siRNA (GFP-1, 1 nmol) as according to **Section 7.7.7**, yielding disulphide (**6.12.1**) and succinic (**6.13.1**) Cy5-co-siRNA microspheres.

7.7.15. Disulphide Cleavage in HeLa Cells

Cells were seeded to a 24-well plate at a density of 3×10^4 cell/well and beadfected as described in the general procedures with (**6.5.1**) and (**6.5.2**) disulphide-FAM

microspheres (86 μg/mL). Cells were imaged by microscopy as according to the general procedures after 6, 12 and 24 hours on a Zeiss Axiovert 200M pseudo-confocal microscope in 2% FBS/PBS.

7.7.16. Microscopy of Gene Silencing and Cell Staining

Assessment of GFP silencing by microscopy was made in 2% FBS/PBS as according to the general procedures after 24, 48 and 72 hours. Staining of cells with Hoechst 33342 and AlexaFluor®-568 phalloidin was achieved as according to the general procedures.

7.7.17. Toxicity of (**6.3.2**), (**6.3.3**), (**6.6.1**) and (**6.6.2**) by MTT Assays

Toxicity assays with MTT were carried out as according to **Section 7.2.18** using 43 and 86 μg/mL of microspheres and analysis was performed after 72 hours.

7.7.18. Beadfection of Cells for Gene Silencing

Beadfections with siRNA microspheres were carried out as according to the general procedures. However, siRNA microspheres were added to cells in serum-free media, which was exchanged for complete growth media after 24 hours. Analysis of EGFP expression was made after 24, 48 and 72 hours by flow cytometry and by microscopy (general procedures).

7.7.19. Beadfection of Cells with Cy5-co-siRNA Microspheres for Gene Silencing

Beadfections were carried out as according to the general procedure.

Analysis of EGFP expression was made after 24, 48 and 72 hours by flow cytometry selecting only those cells that were positive for Cy5 (i.e. beadfected cells). Analysis was additionally made by confocal microscopy using a Leica confocal microscope, exciting EGFP with a 488 nm argon laser and collecting emission at 500 nm – 560 nm. Cy5 was excited with 633 nm red diode laser and emission collected at 640 nm – 700 nm.

References

[1] C. Adrian, M. Hogben, *The Physiologist,* **1960,** *3,* 56 – 62: Movement of material across cell membranes.

[2] E. Gorter, F. Grendel, *J. Exp. Med.,* **1925,** *41,* 439 – 443: On bimolecular layers of lipoids on the chromocytes of the blood.

[3] H. Lodish, A. Berk, L.S. Zipursky, P. Matsudaira, D. Baltimore, J. Darnell, *Molecular Cell Biology,* **2000,** *4th Edition,* W.H. Freeman and Company, New York: Transport across cell membranes.

[4] A. Hodgkin, A. Huxley, *J. Physiol.,* **1952,** *116*, 449 – 472: Currents carrier by sodium and potassium ions through the membrane of the giant axon of Loligo.

[5] Z. Sands, A. Grottesi, M.S.P. Sansom**,** *Curr. Biol.,* **2005,** *15,* R44 – 47: Voltage-gated ion channels.

[6] R.M. Stroud, M.P. McCarthy, M. Shuster, *Biochem.,* **1990,** *29,* 11009 – 11023: Nicotinic acetylcholine receptor superfamily of ligand-gated ion channels.

[7] a. S.D. Conner, S.L. Schmid, *Nature,* **2003**, *422*, 37 – 44: Regulated portals of entry into the cell; b. H.J. Hamburger, *Nature,* **1915**, *96,* 19 – 23: Researches on phagocytosis.

[8] A. Policard, M. Bessis, *Nature,* **1962**, *194,* 110 – 111: Micropinocytosis and rhopheocytosis.

[9] J.L. Goldstein, R.G.W. Anderson, M.S. Brown, *Nature,* **1979**, *279,* 679 – 685: Coated pits, coated vesicles, and receptor-mediated endocytosis.

[10] F.M. Brodsky, C.Y. Chen, C. Knuehl, M.C. Towler, D.E. Wakeham, *Annu. Rev. Cell Dev. Biol.,* **2001**, 17*,* 517 – 568: Biological basket weaving: formation and function of clathrin-coated vesicles.

[11] R.G. Anderson, *Annu. Rev. Biochem.,* **1998,** *67*, 199 – 225: The caveolae membrane system.

[12] L.-H. Wang, K.G. Rothberg, R.G.W. Anderson, *J. Cell. Biol.,* **1993**, *123,* 1107 – 1117: Mis-assembly of clathrin lattices on endosomes reveals a regulatory switch for coated pit formation.

[13] R.P. Haugland, Handbook of Fluorescent Probes and Research Products, **2002,** 9th Edition, Molecular Probes.

[14] L. Johannes, C. Lamaze, *Traffic,* **2002,** *3,* 443 – 451: Clathrin-dependent or not: Is it still the question.

[15] M. Mano, C. Teodósio, A. Paiva, S. Simões, M.C. Pedroso De Lima, *Biochem. J.,* **2005,** *390,* 603 – 612: On the mechanisms of the internalization of S413-PV cell-penetrating peptide.

[16] J.A. Fischer, S.H. Eun, B.T. Doolan, *Annu. Rev. Cell Dev. Biol.,* **2006,** *22*, 181 – 206: Endocytosis, Endosome Trafficking, and the Regulation of *Drosophila* Development.

[17] J.C. Weaver, Y.A. Chizmadzhev, *Bioelectrochem. Bioenerg.,* **1996,** *41,* 135 – 160: Theory of electroporation: A review.

[18] H. Schneckenburger, A. Hendinger, R. Sailer, W.S.L. Strauss, M. Schmitt, *J. Biomed. Opt*., **2002,** *7,* 410 – 416: Laser-assisted optoporation of single cells.

[19] A. Iritani, *Mol. Reprod. Dev.,* **1991,** *28,* 199 – 207: Micromanipulation of gametes for in vitro assisted fertilization.

[20] M.R. Prausnitz, V.G. Bose, R. Langer, J.C. Weaver, *Proc. Nat. Acad. Sci.,* **1993,** *90,* 10504 – 10508: Electroporation of mammalian skin: a mechanism to enhance transdermal drug delivery.

[21] S. Mehier-Humbert, R.H. Guy**,** *Adv. Drug Delivery Rev.,* **2005,** *57,* 733 – 753: Physical methods for gene transfer: Improving the kinetics of gene delivery into cells.

[22] W.C. Heiser, *Methods Mol. Biol.,* **2000**, *130,* 117 – 134: Optimizing electroporation conditions for the transformation of mammalian cells.

[23] I. Walev, S. Chakrit Bhakdi, F. Hofmann, N. Djonder, A. Valeva, K. Aktories, S. Bhakdi *Proc. Nat. Acad. Sci. U.S.A.,* **2001***, 98,* 3185 – 3190: Delivery of proteins into living cells by reversible membrane permeabilization with streptolysin-O.

[24] A. Thompson, S.P. Halbert, U. Smith, *J. Exp. Med.,* **1970,** *131,* 745 – 764: The toxicity of streptolysin-O for beating mammalian heart cells in tissue cultures.

[25] H. Brooks, B. LeBleu, E. Vives, *Adv. Drug Delivery Rev.,* **2005,** *57,* 559 – 577: Tat peptide-mediated cellular delivery: Back to basics.

[26] M. Zhao, R. Weissleder, *Med. Res. Rev.,* **2004,** *24,* 1 – 12: Intracellular cargo delivery using tat peptide and derivatives.

[27] S. Ruben, A. Perkins, R. Purcell, K. Joung, R. Sia, R. Burghoff, W.A. Haseltine, C.A. Rosen, *J. Virol.,* **1989,** *63,* 1 – 8: Structural and functional characterisation of human immunodeficiency virus tat protein.

[28] E. Vives, P. Brodlin, B. LeBleu, *J. Biol., Chem.,* **1997,** *272,* 16010 – 16017: A truncated HIV-1 tat protein basic domain rapidly translocates through the plasma membrane and accumulates in the cell nucleus.

[29] D.S. Youngblood, S.A. Hatlevig, J.N. Hassinger, P.L. Iversen, H.M. Moulton**,** *Bioconj. Chem.,* **2007,** *18,* 50 – 60: Stability of Cell-Penetrating Peptide−Morpholino Oligomer Conjugates in Human Serum and in Cells.

[30] R. Fraley, S. Subramani, P. Berg, D. Papahadjopolous, *J. Biol. Chem*., **1980,** *255,* 10431 – 10435: Introduction of liposome-encapsulated SV40 DNA into cells.

[31] A.F. Odell, D.F. Van Helden, J.L. Scott**,** *J. Biol. Chem.,* **2008,** *283,* 4395 – 4407: The spectrin cytoskeleton influences the surface expression and activation of human transient receptor potential channel 4 channels.

[32] B. Wang, Y.B. Chen, O. Ayalon, J. Bender, A. Garen**,** *Proc. Net. Ac. Sci. USA,* **1999,** *96,* 1627 – 1632: Human single-chain Fv immunoconjugates targeted to a melanoma-associated chondroitin sulphate proteoglycan mediate specific lysis of human melanoma cells by natural killer cells and complement.

[33] Z.Y. Du, R.Y. Qin, W. Xia, R. Tian, M. Kumar**,** *World J. Gastroenterol.,* **2005,** *11,* 516 – 520: Gene transfer of somatostatin receptor type 2 by intratumoral injection inhibits established pancreatic carcinoma xenografts.

[34] H. Lv, S. Zhang, B. Wang, S. Cui, J. Yan**,** *J. Contr. Rel.,* **2006,** *114,* 100 – 109: Toxicity of cationic lipids and cationic polymers in gene delivery.

[35] N.W. Kam, T.C. Jessop, P.A. Wender, H.J Dai, *J. Am. Chem. Soc.,* **2004,** *126,* 6850 – 6851: Nanotube Molecular Transporters: Internalization of Carbon Nanotube−Protein Conjugates into Mammalian Cells.

[36] N.W. Kam, H. Dai, *J. Am. Chem. Soc.,* **2005,** *127,* 6021 – 6026: Carbon nanotubes as intracellular protein transporters: Generality and biological functionality.

[37] D. Pantarotto, J.-P. Briand, M. Prato, A. Bianco, *Chem. Commun.,* **2004,** *1,* 16 – 17: Translocation of bioactive peptides across cell membranes by carbon nanotubes.

[38] N.W. Kam, Z. Liu, H. Dai, *J. Am. Chem. Soc.,* **2005,** *127,* 12492 – 12493: Functionalization of carbon nanotubes via cleavable disulphide bonds for efficient delivery of siRNA and potent gene silencing.

[39] J.M. Wörle-Knirsch, K. Pulskamp, H. F. Krug, *Nano Lett.,* **2006,** *6,* 1261 – 1268: Oops they did it again! Carbon nanotubes hoax scientists in viability assays.

[40] F. Belavoine, P. Schultz, C. Richard, V. Mallouh, T. W. Ebbesen, C. Mioskowski, *Angew. Chem., Int. Ed.*, **1999**, *38*, 1912 – 1915: Helical Crystallization of Proteins on Carbon Nanotubes: A First Step towards the Development of New Biosensors.

[41] C.M. Tseng, Y.Y. Lu, M.S. El-Aasser, J.W. Vanderhoff, *J. Polym. Sci. Part A. Polym. Chem.,* **1986,** *24,* 2995 – 3007: Uniform polymer particles by dispersion polymerisation in alcohol.

[42] T. Delair, V. Marguet, C. Pichot, B. Mandrad, *Colloid Polym. Sci.,* **1994,** *272,* 962 – 970: Synthesis and characterization of cationic amino functionalized polystyrene latexes.

[43] J.-W. Kim, K.-D. Suh, *Colloid Polym. Sci.,* **1998,** *276,* 870 – 878: Highly monodispersed crosslinked polystyrene microparticles by dispersion polymerisation.

[44] M. Munzer, Trommsdorff, G. Rohem, **1977**, Suspension polymerization. In C. E. Shildknecht, I. Skeist, *Polymerization processes*. New York: Wiley.

[45] A.J. Paine, J. McNulty, *J. Polym. Sci. Part A Polym. Chem.,* **1990,** *28,* 2569 – 2574: A comment on the paper "uniform polymer particles by dispersion polymerisation in alcohol" by C.M. Tseng, Y.Y. Lu, M.S. El-Aasse and J.W. Vanderhoff [J. polym. sci. polym. chem.. Ed 24, 2995 (1986)].

[46] Y. Itoh, N. Mizuki, T. Shimada, F. Azuma, M. Itakura, K. Kashiwase, E. Kikkawa, J.K. Kulski, M. Satake, H. Inoko, *Immunogen.,* **2005,** *57,* 717 – 729: High-throughput DNA typing of HLA-A, -B, -C, and -DRB1 loci by a PCR–SSOP–Luminex method in the Japanese population.

[47] a. J.A. Steinkamp, J.S. Wilson, G.C. Saunders, C.C. Stewart, *Science,* **1982,** *215,* 64 – 66: Phagocytosis: Flow cytometric quantitation with fluorescent microspheres; b. D.A.A. Vignali, *J. Immunol. Methods,* **2000,** *243,* 243 – 255: Multiplexed particle-based flow cytometric assays.

[48] a. Y. Zhang, A.O. Eniola, D.J. Graves, D.A. Hammer, *Langmuir,* **2003,** *19,* 6905 – 6911: Specific adhesion of micro sized colloids to surfaces mediated by hybridizing DNA chains; b. P.H. Rogers, E. Michel, C.A. Bauer, S. Vanderet, D. Hansen, B.K. Roberts, A. Calvez, J.B. Crews, K.O. Lau, A. Wood, D.J. Pine, P.V. Schwartz, *Langmuir,* **2005,** *21,* 5562 – 5569: Selective controllable and reversible aggregation of polystyrene latex microspheres via DNA hybridization.

[49] J.A. Delmonico, Old Western Paints Inc., US Patent: 4623390, November 1986: Insulating paint for interior and exterior of buildings and method of making same.

[50] T. Martin, I.I.I. Hogan, Daubert Chemical Company Inc., US Patent 6207730, March 2001: Epoxy and microsphere adhesive composition.

[51] X.Z. Li, H. Liu, L.F. Cheng, H.J. Tong, *Environ. Sci. Technol.,* **2003,** *37,* 3989 – 3994: Photocatalytic oxidation using a new catalyst – TiO_2 microspheres for water and wastewater treatment.

[52] M.L. Schlossman, **1997,** *3*, Chemistry and Manufacture of Cosmetics, Culinary and Hospitality Industry Publications Services.

[53] Y. He, X. Yu, Tianliang Li, L. Yan, B. Yang**,** *Powder Technol.,* **2006,** *166,* 72 – 76: Preparation of CeO_2/ZnO nanostructured microspheres and their catalytic properties.

[54] I. Radomska-Galant, T. Basinska, *Biomater.,* **2003,** *4,* 1848 – 1855: Poly(styrene/α-tert-butoxy-ω-vinylbenzylpolyglycidol) microspheres for immunodiagnostics. Principle of a novel latex test based on combined electrophoretic mobility and particle aggregation measurements.

[55] S. Freiberg, X.X.Zhu, *Int. J. Pharm.,* **2004,** *282,* 1 – 18: Polymer microspheres for controlled drug release.

[56] D.W. Grainer, *Adv. Drug Deliv. Rev.,* **2003,** *55,* 311 – 313: Biomedical micro- and nanotechnology.

[57] I. Piirma, **1985,** Colloids In: H.F. Mark, N.M. Bikales, C.G. Overberger, G. Menges, J.I. Kroschwitz, Encyclopaedia of polymer science and engineering, 2nd Edition, John Wiley and sons, Mew York, 125 – 130.

[58] a. K.E.J. Barrett, **1975,** Dispersion Polymerisation in Organic Media, Wiley, London; b. H.D.H. Strover, K. Li, **1996,** 1900 – 1905: Dispersion polymerisation. In: Polymer materials encyclopaedia. CRC Press, Boca Raton.

[59] J.M. Weissman, H.B. Sunkara, A.S. Tee, S.A. Asher, *Science,* **1996,** *274,* 959 – 965: Thermally switchable periodicities and diffraction from mesoscopically ordered materials.

[60] Y. Ogawa, M. Yamamoto, H. Okada, T. Yashiki, T. Shimamoto, *Chem. Pharm. Bull.,* **1988,** *36,* 1095 – 1103: A new technique to efficiently trap leuprolide acetate into microcapsules or polylactic acid or copoly-(lactic/glycolic) acid.

[61] J.K. Vasir, K. Tambwekar, S. Garg, *Int. J. Pharm.,* **2003,** *255,* 13 – 32: Bioadhesive microspheres as a controlled drug delivery system.

[62] U. Edlund, A.-C. Albertsson, *Adv. Polym. Sci.,* **2002,** *157,* 67 – 112: Degradable polymer microspheres for controlled drug delivery.

[63] R. Bodmeier, H. Chen, *J. Pharm. Pharmacol.,* **1988,** *40,* 754 – 757: Preparation of biodegradable poly(lactide) microparticles using a spray drying technique.

[64] J.A. Steinkamp, J.S. Wilson, G.C. Saunders, C.C. Stewart, *Science*, **1982,** *215,* 64 – 66: Phagocytosis: Flow cytometric quantitation with fluorescent microspheres.

[65] M.K. Pratten, J.B. Lloyd, *Biochim. Biophys. Acta,* **1986,** *881,* 307 – 313: Pinocytosis and phagocytosis: The effects of size of a particulate substrate on its mode of capture by rat peritoneal macrophages cultured *in vitro.*

[66] K. Ng, K.A. Stringer, Z. Cohen, R. Serravo, B. Tian, J.D. Meyer, R. Falk, T. Randolph, M.C. Manning, D.C. Thompson, *Int. J. Pharma.,* **1998,** *170,* 41 – 49: Alveolar macrophage cell line is not activated by exposure to polymeric microspheres.

[67] R.M. Sánchez-Martín, M. Cuttle, S. Mittoo, M. Bradley, *Angew. Chem. Int. Ed.,* **2006,** *45,* 5472 – 5474: Microsphere-Based Real-Time Calcium Sensing.

[68] M. Bradley, L. Alexander, K. Duncan, M. Chennaoui, A.C. Jones, R.M. Sánchez-Martín, *Bioorg. Med. Chem. Lett.,* **2008,** *18,* 313 – 317: pH sensing in living cells using fluorescent microspheres.

[69] B. Khodorov, O. Valkina, V. Turovetsky, *FEBS Lett*., **1994**, *341*, 125 - 127: Mechanisms of stimulus-evoked intracellular acidification in frog nerve fibres.

[70] K. Tokuoka, M. Senna, H. Kuno, *J. Mater. Sci.,* **1986,** *21,* 493 – 496: Preparation of inorganic/polymeric composite microspheres by direct suspension polymerisation.

[71] Reference 45 and A.J. Paine, J. McNulty, *J. Polym. Sci. Part A Polym. Chem.,* **1990,** *28,* 2569 – 2574: A comment on the paper "uniform polymer particles by dispersion polymerisation in alcohol" by C.M. Tseng, Y.Y. Lu, M.S. El-Aasse and J.W. Vanderhoff [J. polym. sci. polym. chem.. Ed 24, 2995 (1986)].

[72] Reference 44 and F.H. Winslow, W. Matreyek, *Industrial and Engineering Chemistry*, **1951**, *43*, 1108 – 1112: Particle size in suspension polymerisation.

[73] G. Wang, M. Li, X. Chen, *J. Appl. Polym. Sci.,* **1997,** *65,* 789 – 794: Inverse Suspension Polymerisation of Sodium Acrylate.

[74] W.S Lyoo, J.W. Kwak, J.H. Yeumb, Y.C. Ji, C.J. Lee, S.K. Noh, *J. Poly. Sci. Part A Polym. Chem.,* **2005,** *43,* 789 – 800: Preparation of ultrahigh-molecular-weight syndiotactic poly(vinyl pivalate) monodisperse microspheres by low-temperature suspension polymerisation of vinyl pivalate.

[75] C. Ober, K. Lok, *Macromole.,* **1987,** *20,* 268 – 273: Formation of large monodisperse copolymer particles by dispersion polymerisation.

[76] Q. Ye, Z. Zhang, H. Jia, W. He, X. Ge, *J. Colloid Interface Sci.,* **2002,** *253,* 279 – 284: Formation of Monodisperse Polyacrylamide Particles by Radiation-Induced Dispersion Polymerisation: Particle Size and Size Distribution.

[77] A.J. Paine, *J. Colloid Interface Sci.,* **1990,** *138,* 157 – 169: Dispersion polymerisation of styrene in polar solvents : I. Grafting mechanism of stabilization by hydroxypropyl cellulose.

[78] A. Paine, Y. Deslander, P. Gerroir, B. Henrissat, *J. Colloid Interface Sci.,* **1990,** *138,* 170 – 181: Dispersion polymerisation of styrene in polar solvents : II. Visualization of surface layers of steric stabiliser on dispersion-polymerised and precipitated polystyrene latex particles by transmission electron microscopy.

[79] D. Napper, *J. Colloid Interface Sci.,* **1977,** *58,* 390 – 407: Steric stabilisation.

[80] H. Bamnolker, S. Margel, *J. Polym. Sci. Part A Polym. Chem.,* **1996,** *34,* 1857 – 1871: Dispersion polymerisation of styrene in polar solvents: Effects of reaction parameters on microsphere surface composition and surface properties, size and size distribution and molecular weight.

[81] Y.-Y. Yang, T.-S. Chung, X.-L. Bai, W.-K. Chan, *Chem. Eng. Sci.,* **2000,** *55,* 223 – 2236: Effect of preparation conditions on morphology and release profiles of biodegradable polymeric microspheres containing protein fabricated by double-emulsion method.

[82] R. Jalil, J.R. Nixon, *J. Microencapsul.,* **1990,** *7,* 25 – 39: Microencapsulation using poly(L-lactic acid) II: Preparative variables affecting microcapsule properties.

[83] D. Horák, B. Rittich, A. Španová, *Prog. Colloid Polym. Sci.,* **2004,** *124,* 77 – 81: Effect of reaction parameters on properties of dispersion-polymerised hydrophilic microspheres as supports for immobilization of proteins.

[84] A.J. Paine, W. Luymes, J. McNulty, *Macromole.,* **1990,** *23,* 3104 – 3109: Dispersion polymerisation of styrene in polar solvents. 6. Influences of reaction parameters on particle size and molecular weight in poly (N-vinylpyrrolidone)-stablized reactions.

[85] J.-X. Huang, X.-Y. Yuan, X.-L. Yu, H.-T. Zhang, *Polym. Int.,* **2003,** *52,* 819 – 826: Dispersion copolymerisation of methyl methacrylate and acrylic acid in polar media: Effect of reaction parameters on the particle size distribution of the copolymer microspheres.

[86] H. Bamnolker, S. Margel, *J. Polym. Sci. Part A Polym. Chem.,* **1996,** *34,* 1857 – 1871: Dispersion polymerisation of styrene in polar solvents: Effects of reaction parameters on microsphere surface composition and surface properties, size and size distribution and molecular weight.

[87] L.I. Gabaston, R.A. Jackson, S.P. Armes, *Macromole*., **1998,** *31*, 2883 – 2888: Living Free-Radical Dispersion Polymerisation of Styrene.

[88] B. Yan, Analytical methods in combinatorial chemistry, **1999**, CRC Press, pg. 131.

[89] G.S. Whitby, M. Katz, *Ind. Eng. Chem.,* **1933,** *25,* 1338 – 1348: Synthetic rubber.

[90] A.G. Farbenfabrik, German Patent 250690 (Sept 12 1909).

[91] M. Luther, C. Heuck, Polymerizing butadiene hydrocarbons, German Patent 558890 (Jan 8 1927).

[92] W.V. Smith, R.H. Ewart, *J. Chem. Phys.,* **1948,** *16,* 592 – 599: Kinetics of Emulsion Polymerisation.

[93] W.D. Hawkins, *J. Am. Chem. Soc.,* **1947,** *69,* 1428 – 1444: A General Theory of the Mechanism of Emulsion Polymerisation.

[94] R.G. Gilbert, Emulsion Polymerisation: a mechanistic approach, **1996,** Academic Press, London.

[95] R.M. Sánchez-Martín, M. Muzerelle, N. Chitkul, S.E. How, S. Mittoo, M. Bradley, *ChemBioChem,* **2005,** *6,* 1341 – 1345: Bead-Based Cellular Analysis, Sorting and Multiplexing.

[96] M.J. Evans, M.H. Kaufman, *Nature,* **1981***, 292***,** 154 – 156: Establishment in culture of pluripotential cells from mouse embryos.

[97] G.R. Martin, *Proc. Nat. Ac. Sci. USA,* **1981,** *78,* 7634 – 7638: Isolation of a pluripotent cell line from early mouse embryos cultured in medium conditioned by teratocarcinoma stem cells.

[98] A.G. Smith, *Annual review of cell and developmental biology*, **2001,** 17**,** 435 – 462: Embryo-derived stem cells: Of mice and men.

[99] S. Chen, A. Choo, N.D. Wang, H.P. Too, S.K. Oh, *Biotechnol. let.,* **2007,** *29,* 261 – 265: Establishing efficient siRNA knockdown in mouse embryonic stem cells.

[100] S. McLenachan, J.P. Sarsero, P.A. Ioannou, *Genomics,* **2007,** *89,* 708 – 720: Flow-cytometric analysis of mouse embryonic stem cell lipofection using small and large DNA constructs.

[101] V.L. Mosiman, B.K. Patterson, L. Canterero, C.L. Goolsby, *Cytometry Part B: Clinical Cytometry,* **1997**, *30,* 151 – 156: Reducing cellular autofluorescence in flow cytometry: An in situ method.

[102] G. Zhang, V. Gurtu, T.H. Smith, P.Nelson, S.R. Kain, *Biochem. Biophys. Res. Commun*., **1997**, *236*, 126 – 129: A Cationic Lipid for Rapid and Efficient Delivery of Plasmid DNA into Mammalian Cells.

[103] R.M. Sánchez-Martín, L.M. Alexander, M. Bradley, *Annals New York Ac. Sci.,* **2008,** *1130,* 207 – 217: Multifunctionalised Biocompatible Microspheres for Sensing.

[104] T. Mosmann, *J. Immunol. Methods*, **1983**, *65*, 55-63: Rapid colorimetric assay for cellular growth and survival: application to proliferation and cytotoxicity assays.

[105] A. L. Politoff, S. J. Socolar, W. R. Loewenstein, *J. Gen. Physiol.,* **1969,** *53,* 498 – 515: Permeability of a cell membrane junction: Dependence on energy metabolism.

[106] D.W. Hilgemann, *Annu. Rev. Physiol.,* **1997,** *59*, 193 – 220: Cytoplasmic ATP-dependent regulation of ion transporters and channels: mechanisms and messengers.

[107] I.S. Zuhorn, U. Bakowsky, E. Polushkin, W.H. Visser, M.C.A. Stuart, J.B.F.N. Engberts, D. Hoekstra*, Molec. Ther.* **2005**, *11,* 801–810: Nonbilayer phase of lipoplex-membrane mixture determines endosomal escape of genetic cargo and transfection efficiency.

[108] Y. Xu, F. C. Szoka, *Biochemistry,* **1996,** *35,* 5616 – 5623: Mechanism of DNA release from cationic liposome/DNA complexes used in cell transfection.

[109] W. Zauner, N.A. Farrow, A.M.R. Haines, *J. Contr. Rel,* **2001,** *71*, 39 – 51: In vitro uptake of polystyrene microspheres: effect of particle size, cell line and cell density.

[110] J. Rejman, V. Oberle, I.S. Zuhorn, D. Hoesktra, *Biochem. J.* **2004,** *377,* 159 – 170: Size-dependent internalisation of particles via the pathways of clathrin- and caveolae-mediated endocytosis.

[111] S.K. Banerji, M.A. Hayes, *Langmuir* , **2007**, *23*, 3305 – 3313: Examination of nonendocytotic bulk transport of nanoparticles across phospholipid membranes.

[112] D. Pantarotto, J. Briand, M. Prato, A. Bianco, *Chem. Commun,* **2004,** *1,* 16 – 17: Translocation of bioactive peptides across cell membranes by carbon nanotubes.

[113] P. Cherukuri, S.M. Bachilo, S.H. Litovsky, R.B. Weisman, *J. Am. Chem. Soc,* **2004,** *126,* 15638 – 15639: Near-Infrared fluorescence microscopy of single-walled carbon nanotubes in phagocytic cells.

[114] S. Akhtar, K.J. Lewis; *Internat. J. Pharm,* **1997,** *151,* 57 – 67: Antisense oligonucleotide delivery to cultured macrophages is improved by incorporation into sustained-release biodegradable polymer microspheres.

[115] a. Y.G. Shellman, D. Ribble, L. Miller, J. Gendall, K. VanBuskirk, D. Kelly, D.A. Norris, R.P. Dellavalle, *Melanoma Res.,* **2005,** *15,* 83 – 89: Lovastatin-induced apoptosis in human melanoma cell lines; b. E.J. Choi, T. Kim, M.-S. Lee, *Life Sci.,* **2007,** *80,* 1403 – 1408: Pro-apoptotic effect and cytotoxicity of genistein and

genistin in human ovarian cancer SK-OV-3 cells; c. M.A. Shenoy, B.B. Singh, *Int J Radiat Biol Relat Stud Phys Chem Med.* **1978**, *34*, 595 – 600: Hypoxic cytotoxicity of chlorpromazine and the modification of radiation response in E. coli B/r.

[116] L.B. Clerch, F. Huijing, *Biochim. Biophys. Acta,* **1972**, *268*, 654 – 662: The role of magnesium in muscle phosphorylase kinase activity.

[117] S.L. Schmid, L.L. Carter, *J. Cell Biol.,* **1990**, *111*, 2307 – 2318: ATP is required for receptor-mediated endocytosis in intact cells.

[118] E.P. Rico, M.R. Senger, M. Fauth, R.D. Dias, M.R. Bogo, C.D. Bonan, *Life Sci.,* **2003,** *73,* 2071 – 2082: ATP and ADP hydrolysis in brain membranes of zebrafish (*Danio rerio*).

[119] D.J. Yamashiro, B. Tycko, S.R. Fluss, F.R. Maxfield, *Cell,* **1984,** *37,* 789 – 800: Segregation of transferrin to a mildly acidic (pH 6.5) *para*-Golgi compartment in the recycling pathway.

[120] R.D. Singh, V. Puri, J.T. Valiyaveettil, D.L. Marks, R. Bittman, R.E. Pagano, *Mol. Biol. Cell,* **2003,** *14,* 3254–3265: Selective caveolin-1-dependent endocytosis of glycosphingolipids.

[121] M.T. Cook, P.J. Hayball, B.F. Nowak, J.D. Hayball, *Dev. Comparative Immunol.,* **2004,** *29,* 703 – 712: The opsonising activity of a pentraxin-like protein isolated from snapper (*Pagrus auratus,* Sparidae) serum.

[122] S. Mayor, S. Sabharanjak, F.R. Maxfield, *EMBO J.,* **1998,** *17,* 4626 – 4638: Cholesterol-dependent retention of GPI-anchored proteins in endosomes.

[123] E.P. Kilsdonk, P.G. Yancey, G.W. Stoudt, F.W. Bangerter, W.J. Johnson, M.C. Phillips and G.H. Rothblat, *J. Biol. Chem.,* **1995**, *270,* 17250 – 17256: Cellular cholesterol efflux mediated by cyclodextrins.

[124] I.S. Zuhorn, R. Kalicharan, D. Hoekstra, *J. Biol. Chem,* **2002**, *277,* 18021 – 18028: Lipoplex-mediated transfection of mammalian cells occurs through the cholesterol-dependent clathrin-mediated pathway of endocytosis.

[125] P.A. Orlandi, P.H. Fishman, *J. Cell Biol.,* **1998**, *141,* 905 – 915: Filipin-dependent inhibition of cholera toxin: Evidence for toxin internalisation and activation through caveolae-like domains.

[126] L. Pelkmans, D. Püntener and A. Helenius, *Science,* **2002**, *296,* 535 – 539: Local actin polymerisation and dynamin recruitment in SV40-induced internalisation of caveolae.

[127] J.-S. Shin, S.N. Abraham, *Microbes and Infection,* **2001**, *3*, 755 – 761: Caveolae as portals of entry for microbes.

[128] X. Sun, V.K. Yau, B.J. Briggs, G.R. Whittaker, *Virology,* **2005,** *338,* 53 – 60: Role of clathrin-mediated endocytosis during vesicular stomatitis virus entry into host cells.

[129] J.W. Murray, A.W. Wolkoff, *Adv. Drug Deliv. Rev.,* **2003**, *55,* 1385 -1403: Roles of the cytoskeleton and motor proteins in endocytic sorting.

[130] J.A. Swanson, C. Watts, *Trends Cell Biol.,* **1995,** *5,* 424 – 428: Macropinocytosis.

[131] J.R. Peterson, T.J. Mitchison, *Chem. Biol.,* **2002,** *9,* 1275 – 1285: Small molecules, big impact: A history of chemical inhibitors and the cytoskeleton.

[132] M.A. West, M.S. Bretscher, C. Watts, *J. Cell Biol.,* **1989,** *109,* 2731 – 2739: Distinct endocytic pathways in epidermal growth factor-stimulated human carcinoma A431 cells.

[133] M. Maniak, *Macropinocytosis in Endocytosis,* **2001,** Edited by M. Marsh. Oxford: Oxford University Press, 78 – 93.

[134] A. Goytain, R.M. Hines, A. El-Husseini, G.A. Quamme, *J Biol Chem,* **2007,** *282,* 8060 – 8068*: NIPA1*(*SPG6*), the basis for autosomal dominant form of hereditary spastic paraplegia, encodes a functional Mg^{2+} transporter.

[135] K.C. Holmes, D. Popp, W. Gebhard, W. Kabsch, *Nature,* **1990,** *347,* 44 – 48: Atomic model of the actin filament.

[136] I. Mellman, *Annu. Rev. Cell Biol.,* **1996,** *12,* 575 – 625: Endocytosis and molecular sorting.

[137] a. T. Enomoto, Y. Asano, *Cell Struct. Funct.,* **1994,** *19,* 227 – 239: Differential Susceptibility of Morphologically TPA-Resistant and -Sensitive Balb/c 3T3 Variants to TPA-Induced Cell Transformation : Relationship to Induction of Membrane Ruffling; b. J. Garrigues, J. Anderson, K.E. Hellström, I. Hellström, *J. Cell Biol.,* **1994,** *125,* 129 – 142: Anti-tumor antibody BR96 blocks cell migration and binds to a lysosomal membrane glycoprotein on cell surface microspikes and ruffled membranes.

[138] S.C. Silverstein, R.M. Steinman and Z.A. Cohn, *Annu. Rev. Biochem.,* **1977,** *46,* 669 – 722: Endocytosis.

[139] J.M. Hall, C.C. Parrish and R.J. Thompson**,** *Biol. Bull.,* **2002**, *202,* 201 – 203: Eicosapentaenoic acid regulates scallop (Placopecten magellanicus) membrane fluidity in response to cold.

[140] D. Bray, *Methods Biotechnol.,* **2000,** *13,* 235 – 243: Critical point drying of biological specimens for Scanning Electron Microscopy.

[141] W.J. Betz, F. Mao and C.B. Smith, *Curr. Opin. Neurobiol.,* **1996**, *6*, 365 – 371: Imaging exocytosis and endocytosis.

[142] D.R. Trollinger, W.E. Cascio and J.J. Lemasters, *Biophys. J.,* **2000**, *79,* 39 – 50: Mitochondrial calcium transients in adult rabbit cardiac myocytes: inhibition by ruthenium red and artefacts caused by lysosomal loading of Ca(2+)-indicating fluorophores.

[143] L. Alexander, S. Pernagallo, A. Livigni, R.M. Sánchez-Martín, J. Brickman, M. Bradley, **2009,** Analysis of microsphere-mediated cellular delivery by chemical, microscopic and gene expression analysis, *Submitted*.

[144] T. Weiser, *J. Neurosci. Methods,* **2004,** *137,* 79 – 85: A novel toxicity-based assay for the identification of modulators of voltage-gated Na^+ channels.

[145] M.F. Cury-Boaventura, R. Gorjaõ, T. Martins de Lima, P. Newsholme, R. Curi, *Life Sci.,* **2006,** *78,* 1448 – 1456: Comparative toxicity of oleic and linoleic acid on human lymphocytes.

[146] M.E. Anderson, *Methods Enzymol.,* **1985**, *113*, 548–553: Determination of glutathione and glutathione disulfide in biological samples.

[147] C.R. Martin, P. Kohli, *Nat. Rev. Drug Discovery,* **2003**, *2*, 29 – 37: The emerging field of nanotube biotechnology.

[148] S. Bucak, D.A. Jones, P.E. Laibinis, T.A. Hatton, *Biotechnol. Prog*. **2003**, *19*, 477 – 484: Protein separations using colloidal magnetic nanoparticles.

[149] Y. Huang, A. Nan, G.M. Rosen, C.S. Winaiski, E. Schneider, P. Isai, H. Ghandehari, *Macromol. Biosci.* **2003**, *3*, 647 – 652: N-(2-Hydroxypropyl)methacrylamide (HPMA) copolymer-linked nitroxides: potential magnetic resonance contrast agents.

[150] E.E. Carpenter, *J. Magn. Magn. Mater.,* **2001,** *225,* 17 – 20: Iron nanoparticles as potential magnetic carriers.

[151] S.J. Son, J. Reichel, B. He, M. Schuchman, S.B Lee, *J. Am. Chem. Soc.,* **2005,** *127,* 7316 – 7317: Magnetic nanotubes for magnetic-field-assisted bioseparation, biointeraction, and drug delivery.

[152] M. Tanase, E.J. Felton, D.S. Gray, A. Hultgren, Mc.s. Chen, D.H. Reich, *Lab Chip,* **2005,** *5,* 598 – 605: Assembly of multicellular constructs and microarrays of cells using magnetic nanowires.

[153] R.S. Haines (International Business Machines Corp), *Ger. Offen.,* **1970,** *GB 12 97, 503.*

[154] C. Bergemann, D. Müller-Schulte, J. Oster, L. à Brassard, A.S. Lübbe, *J. Magn. Magn. Mater.,* **1999,** *194,* 45 – 52: Magnetic ion-exchange nano- and microparticles for medical, biochemical and molecular biological applications.

[155] J.M. Colet, Y. Van Verbeke, R.N. Muller, *Invest. Radiol.,* **1994,** *29 (2),* S223 – S225: Evidence for attachment of magnetic starch microspheres to kupffer cells receptors in excised and perfused rat liver.

[156] J. Lee, M. Senna, *Colloid Polym. Sci.,* **1995,** *273,* 76 – 82: Preparation of monodispersed polystyrene microspheres uniformly coated by magnetite *via* heterogeneous polymerisation.

[157] C. Yang, Y. Guan, J. Xing, J. Liu, G. Shan, Z. An, H. Liu, *AIChE. J.* **2005,** *51,* 2011 – 2015: Preparation of magnetic polystyrene microspheres with a narrow size distribution.

[158] B. I. Haukanes, C. Kvam, *Bio/Technol.,* **1993,** *11,* 60 – 63: Applications of magnetic beads in bioassays.

[159] M.C.F.C. Felinto, D.F. Parra, A.B. Lugao, M.P. Batista, O.Z. Higa, M. Yamaura, R.L. Camilo, M.T.C.P. Ribela, L.C. Sampaio, *Nucl. Instrum. Methods Phys. Res. Sect. B.,* **2005,** *236,* 495 – 500: Magnetic polymeric microspheres for protein adsorption.

[160] X. Liu, Y. Guan, R. Shen, H. Liu, *J. Chromatogr. B.,* **2005,** *822,* 91 – 97: Immobilization of lipase onto micron-sized magnetic beads.

[161] Miltenyi Biotec: MACS & more, **2002**, *6*, 1 – 16: Immunoprecipitation with μMACS protein A and protein G microbeads.

[162] M. Reyes, T. Lund, T. Lenvik, D. Aguiar, L. Koodie, C.M. Verfaillie, *Blood,* **2001,** *98,* 2615 – 2628: Purification and ex vivo expansion of postnatal human marrow mesodermal progenitor cells.

[163] B. Sinclair, *Scientist,* **1998,** *12,* 17 – 23: To bead or not to bead: applications of magnetic bead technology.

[164] Y. Less, J. Rho, B. Jung, *J. Appl. Polym. Sci.,* **2003,** *89,* 2058 – 2067: Preparation of magnetic ion-exchange resins by the suspension polymerisation of styrene with magnetite.

[165] P.H. Wang, C.Y. Pan, *Eur. Polym. J.,* **2000,** *36,* 2297 – 2300: Polymer metal composite microspheres: Preparation and characterization of poly(St-co-AN)Ni microspheres.

[166] J. Ugelstad, T. Ellingsen, A. Berge, B. Helgee, *PCT Int. Appl*., **1983**, WO 83 03, 920.

[167] D. Horák, *J. Polym. Sci. Part A. Polym. Chem.,* **2001,** *39,* 3707 – 3715: Magnetic polyglycidylmethacrylate microspheres by dispersion polymerisation.

[168] J. Zhang, X. Ding, Y. Peng, W. Mang, *Polym. Int.,* **2002,** *51,* 617 – 621: Magnetic polymer microsphere with photoconductivity: preparation and characterization of iron(III) phthalocyanine covalently bonded on to polystyrene microsphere surface.

[169] X. Liu, X. Ding, Z. Zheng, Y. Peng, X. Long, X. Wang, A.S.C. Chan, C.W. Yip, *J. Appl. Polym. Sci.,* **2003,** *90,* 1879 – 1884: Synthesis of novel magnetic polymer microspheres with amphiphilic structure.

[170] K. Cao, J. Yu, B-G. Li, B-F. Li, Z-R. Pan, *Chem. Eng. J.,* **2000,** *78,* 211 – 215: Micron-size uniform poly(methyl methacrylate) particles by dispersion polymerisation in polar media: 1. Particle size and particle size distribution.

[171] A. Pich, S. Bhattacharya, A. Ghosh, H.-J.P. Adler, *Polym.,* **2005,** *46,* 4596 – 4603: Composite magnetic particles: 2. Encapsulation of iron oxide by surfactant-free emulsion polymerisation.

[172] Y. Tabata, Y. Ikada, *Biomater.* **1988,** *9,* 356 – 362: Composite magnetic particles: 2. Encapsulation of iron oxide by surfactant-free emulsion polymerisation.

[173] D.A.A. Vignali, *J. Immunol. Methods,* **2000,** *243,* 243 – 255: Multiplexed particle-based flow cytometric assays.

[174] P.H. Rogers, E. Michel, C.A. Bauer, S. Vanderet, D. Hansen, B.K. Roberts, A. Calvez, J.B. Crews, K.O. Lau, A. Wood, D.J. Pine, P.V. Schwartz, *Langmuir,* **2005,** *21,* 5562 – 5569: Selective, Controllable, and Reversible Aggregation of Polystyrene Latex Microspheres via DNA Hybridization.

[175] J.W. Kim, B.S. Kim, K.D. Suh, *Colloids Polym. Sci.,* **2000,** *278,* 591 – 594 : Monodisperse micron-sized cross-linked polystyrene particles. VI. Understanding of nucleated particle formation and particle growth.

[176] Y. Deng, C. Wang, X. Shen, W. Yang, L. Jin, H. Gao, S. Fu, *Chem. Eur. J.,* **2005,** *11,* 6006 – 6013: Preparation, Characterization, and Application of Multistimuli-Responsive Microspheres with fluorescence-labeled magnetic cores and thermoresponsive shells.

[177] H.T. Zhang, J.X. Huang, B.B. Jiang, *J. Appl. Polym. Sci.,* **2002,** *85,* 2230 – 2238: Kinetics of polymerisation and particle stabilization mechanism on dispersion copolymerisation of styrene and divinylbenzene.

[178] A. Pich, S. Bhattacharya, A. Ghush, H.-J.P. Adler, *Polymer,* **2005**, *46,* 4596 – 4603: Composite magnetic particles: II. Encapsulation of iron oxide by surfactant-free emulsion polymerisation.

[179] Y.E. Korchev, J. Gorelik, M.J. Lab, E.V. Sviderskaya, C.L. Johnston, C.R. Coombes, I. Vodyanoy, C.R.W. Edwards, *Biophys. J*., **2000**, *78,* 451 – 457: Cell volume measurement using scanning ion conductance microscopy.

[180] M. Margulies, M. Egholm, W.E. Altman, S. Attiya, J.S. Bader, L.A. Bemben, J. Berka, M.S. Braverman, Y.-J. Chen, Z. Chen, S.B. Dewell, L. Du, J.M. Fierro, X.V. Gomes, B.C. Godwin, W. He, S. Helgesen, C.H. Ho, G.P. Irzyk, S.C. Jando, M.L.I. Alenquer, T.P. Jarvie, K.B. Jirage, J.-B. Kim, J.R. Knight, J.R. Lanza, J.H. Leamon, S.M. Lefkowitz, M. Lei, J. Li, K.L. Lohman, H. Lu, V.B. Makhijani, K.E. McDade, M.P. McKenna, E.W. Myers, E. Nickerson, J.R. Nobile, R. Plant, B.P. Puc, M.T. Ronan, G.T. Roth, G.J. Sarkis, J.F. Simons, J.W. Simpson, M. Srinivasan, K.R. Tartaro, A. Tomasz, K.A. Vogt, G.A. Volkmer, S.H. Wang, Y. Wang, M.P. Weiner, P. Yu, R.F. Begley, J.M. Rothberg, *Nature,* 2005, **437,** 376 – 380 : Genome sequencing in microfabricated high-density picolitre reactors.

[181] Y. Itho, N. Mitzuki, T. Shimada, F. Azuma, M. Itakura, K. Kashiwase, E. Kikkawa, J.K. Kulski, M. Satake, H. Inoko, *Immunogen.,* **2005**, *57***,** 717 – 729 : High-throughput DNA typing of HLA-A, -B, -C, and -DRB1 loci by a PCR–SSOP–Luminex method in the Japanese population.

[182] F. Wang, C. Wang, *J. Contr. Rel.,* **2002**, *81***,** 263 - 280: Sustained release of etanidazole from spray dried microspheres prepared by non-halogenated solvents.

[183] J. Xie, J. Marijnissen, C. Wang, *Biomater.,* **2006**, *27,* 3321 - 3332: Microparticles developed by electrohydrodynamic atomization for the local delivery of anticancer drug to treat C6 glioma in vitro.

[184] L.A Connal, G.G. Qiao, *Soft Matter*, **2007**, *3*, 837 - 839: Honeycomb coated particles: porous doughnuts, golf balls and hollow porous pockets.

[185] H.A. Wege, A.K.F. Dyab, O.D. Velev, V.N. Paunov, *Phys. Chem. Chem. Phys.,* **2007**, *9,* 6300 – 6303: Fabrication of magnetically-functionalised lens- and donut-shaped microparticles by a surface-formation technique.

[186] L.N. Ding, T. Lee, C.H. Wang, *J. Control. Rel.,* **2005**, *102,* 395 – 413: Fabrication of monodispersed Taxol-loaded particles using electrohydrodynamic atomization.

[187] G. Widawski, M. Rawiso, B. Francois, *Nature,* **1994**, *369,* 387 – 389: Self-organised honeycomb morphology of star-polymer polystyrene films.

[188] R.M. Sanchez-Martin, L. Alexander, M. Muzerelle, J.M. Cardenas-Maestre, A. Tsakiridis, J. Brickman, M. Bradley, *ChemBioChem,* **2009,** Microsphere mediated protein delivery into cells*, In Press*.

[189] A. Fire, S. Xu, M.K. Montgomery, S.A. Kostas, S.E. Driver, C.C. Mello, *Nature,* **1998,** *391,* 806 – 811: Potent and specific genetic interference by double-stranded RNA in *Caenorhabditis elegans.*

[190] S.M. Elbashir, J. Harborth, W. Lendeckel, A. Yalcin, K. Weber, T. Tuschl, *Nature,* **2001,** *411,* 494 – 498: Duplexes of 21-nucleotide RNAs mediate RNA interference in cultured mammalian cells.

[191] A.J. Hamilton, D.C. Baulcombe, *Science,* **1999,** *286 (5441),* 950 – 952: A species of small anti-sense RNA in posttranscriptional gene silencing in plants.

[192] J. Hong, N. Wei, A. Chalk, J. Wang, Y. Song, F. Yi, R.-P. Qiao, E.L.L. Sonnhammer, C. Wahlestedt, Z. Liang, Q. Du, *Biochem. Biophys. Res. Commun.,* **2008,** *368,* 703 – 708: Focusing on RISC assembly in mammalian cells.

[193] D.S. Schwartz, G. Hutvagner, T. Du, Z. Xu, N. Aronin, P.D. Zamore, *Cell,* **2003,** *115,* 199 – 208: Asymmetry in the assembly of the RNAi enzyme complex.

[194] S. Schubert. A. Grunweller, V.A. Erdmann, J. Kurreck, *J. Mol. Biol.,* **2005,** *348,* 883 – 893: Local RNA target structure influences siRNA efficacy: systematic analysis of intentionally designed binding regions.

[195] D.M. Dykxhoorn, C.D. Novina, P.A. Sharp, *Nat. Rev. Mol. Cell Biol,* **2003,** *4,* 457 - 467: Killing the messenger: Short RNAs that silence gene expression.

[196] E.W. Song, P. C. Zhu, S. K. Lee, D. Chowdhury, S. Kussman, D. M. Dykxhoorn, Y. Feng, D. Palliser, D. B.Weiner, P. Shankar, W. A. Marasco, J. Lieberman, *Nat. Biotechnol*. **2005**, *23*, 709 – 717: Antibody mediated *in vivo* delivery of small interfering RNAs via cell-surface receptors.

[197] S. Sabbioni, E. Callegari, M. Manservigi, R. Argnani, A. Corallini, M. Negrini, R. Manservigi, *Gene Therapy*, **2007**, *14*, 459 – 464: Use of herpes simplex virus type 1-based amplicon vector for delivery of small interfering RNA.

[198] Z. Liu, M. Winters, M. Holodniy, H. Dai, *Angew. Chem. Int. Ed.* **2007,** *46,* 2023 - 2027: siRNA delivery into human T cells and primary cells with carbon-nanotube transporters.

[199] A.S. Arnold, Y.L. Tang, K. Qian, L. Shen, V. Valencia, M.I. Phillips, Y.C. Zhang, *J. Hypertens.* **2007,** *25,* 197 – 205: Specific [beta]1-adrenergic receptor silencing with small interfering RNA lowers high blood pressure and improves cardiac function in myocardial ischemia.

[200] C. M. Sayes, F. Liang, J. L. Hudson, J. Mendez, W. H. Guo, J. M. Beach, V. C. Moore, C. D. Doyle, J. L. West, W. E. Billups, K. D. Ausman and V. L. Colvin, *Toxicology Letters,* **2006,** *161*, 135-142: Functionalization density dependence of single-walled carbon nanotubes cytotoxicity in vitro.

[201] D.H. Kim, M.A. Behlke, S.D. Rose, M. Chang, S. Choi, J. Rossi, *Nat. Biotechnol.,* **2005**, *23*, 222 – 226: Synthetic dsRNA Dicer substrates enhance RNAi potency and efficacy.

[202] N.J. Caplen, S. Parrish, F. Imani, A. Fire, R.A. Morgan, *Proc. Nat. Ac. Sci. USA,* **2001,** *98,* 9742 – 9747: Specific inhibition of gene expression by small double-stranded RNAs in invertebrate and vertebrate systems.

[203] K. Wang, C. Wang, F. Xiao, H. Wang, Z. Wu, *J. Biol. Chem.,* **2008,** *283,* 34029 – 34036: JAK2/STAT2/STAT3 are required for myogenic differentiation.

[204] Bang's Laboratories, Technical Note, **2001**.

[205] A. Järve, J. Müller, I. Kim, K. Rohr, C. MacLean, G. Fricker, U. Massing, F. Eberle, A. Dalpke, R. Fischer, M.F. Trendelenburg, M. Helm, *Nucleic Acids Res*., **2007**, *e124*: Surveillance of siRNA integrity by FRET imaging.

[206] M. Gude, J. Ryf, P.D. White, *Lett. Pept. Sci.,* **2002,** *9,* 203 – 206: An accurate method for the quantitation of Fmoc-derivatized solid phase supports.

[207] A.G. Smith, M.L. Hooper, *Devel. Biol.,* **1987**, *121,* 1 – 9: Buffalo rat liver cells produce a diffusible activity which inhibits the differentiation of murine embryonal carcinoma and embryonic stem cells.

[208] K. Kobayashi, H. Sumimoto, Y. Ina, *Polym. J.,* **1983,** *15,* 667 – 671: A Carbohydrate-Containing Synthetic Polymer Obtained from *N*-*p*-Vinylbenzyl-D-gluconamide.

[209] G. Wulff, J. Gimpel, J. Feld, I. Hufnagel, *Makromol. Chem.,* **1982,** *183,* 2459 – 2467: Über enzymanalog gebaute polymere, 15. Über die synthese von (R)- und von (S)-1-(4-vinylopohenyl)ethylamin und einiger anderer monomere mit funktionellen gruppen.